The structure of the south-central Taiwan thrust belt

Giovanni Camanni

Institute of Earth Sciences 'Jaume Almera'

Spanish National Research Council

The structure of the south-central Taiwan thrust belt

Ph.D. thesis presented at the Faculty of Geology of the University of Barcelona to obtain the Degree of Doctor in Geology

Ph.D. student:

Giovanni Camanni[1]

Supervisors:

Dr. Dennis Brown[1]

Dr. Joaquina Alvarez-Marron[1]

Tutor:

Prof. Eduard Roca Abella[2]

[1]*Institute of Earth Sciences 'Jaume Almera'*

[2]*Department of Geodynamic and Geophysics of the University of Barcelona*

September 2014

To Maria who, while preparing one of her unforgettable meals years ago, read the future in my eyes,

and to Andrés

"The real voyage of discovery consists not in seeking new landscapes, but in having new eyes"
Marcel Proust

Table of Contents

Abbreviations ..... **vii**

List of figures ..... **viii**

Abstract ..... **ix**

Chapter 1 - Introduction **1**

1.1. Presentation of the thesis 2
1.2. Geological framework 4
1.2.1. The Eurasian margin 4
1.2.2. The Taiwan mountain belt 6
1.3. Objectives 8
1.4. Methodology 9
1.4.1. Field mapping 9
1.4.2. P-wave velocity models 10
1.4.2.1. Data description 10
1.4.2.2. Data processing and usage 11
1.4.3. Earthquake hypocentres and focal mechanisms 12
1.4.3.1. Data description 12
1.4.3.2. Data processing and usage 12
1.4.4. 3D data analysis and visualization 13
1.5. Geology of south-central Taiwan 15
1.5.1. The Western Foothills 15
1.5.2. The Hsuehshan Range 16
1.5.3. The Central Range 17

Chapter 2 - Articles **19**

Presentation of the articles 20
Article 1 - The structure and kinematics of the central Taiwan mountain belt derived from geological and seismicity data 22
Article 2 - The Shuilikeng fault in the central Taiwan mountain belt 48
Article 3 - Basin inversion in central Taiwan and its importance for seismic hazard 63
Article 4 - Structural complexities in a foreland thrust belt inherited from the shelf-slope transition: Insights from the Alishan area of Taiwan 68
Article 5 - The deep structure of south-central Taiwan illuminated by seismic tomography, earthquake hypocentre, and gravity data 87

Chapter 3 - Overall summary **111**

3.1. Summary of results 112
3.1.1. The structure and kinematics of the Shuilikeng Fault 112
3.1.1.1. The Shuilikeng Fault at the surface 112
3.1.1.2. The Shuilikeng Fault at depth 113
3.1.2. Deep structure beneath south-central Taiwan 114
3.1.2.1. Basement-cover interface 114
3.1.2.2. Deep-seated fault systems 115

3.2. Discussion: the influence of variously oriented extensional basement faults inherited from the Eurasian margin on the structural development of the south-central Taiwan thrust belt 117
3.2.1. Introduction to the discussion 117
3.2.2. Inherited faults sub-parallel to the structural grain of south-central Taiwan 118
3.2.3. Inherited faults at an angle to the structural grain of south-central Taiwan 119
3.2.4. Implications for the interpretation of the structure of south-central Taiwan 120
3.3. Conclusions 121

Acknowledgements 123

References cited in the text 125

Appendices 135

Appendix 1 - Geological maps 136
Appendix 2 - Conference abstracts related to the thesis 141

Abbreviations

Faults:

AF = Alenkeng Fault
BF = “B” Fault
ChF = Chaochou Fault
ChyF = Chiayang fault
ChiF = Chinma Fault
ChT = Changhua Thrust
CT = Chelungpu Thrust
GF = Guaosing Fault
LF = Lishan Fault
LvF = Longitudinal Valley Fault
SF = Shenmu Fault
SkF = Shuilikeng Fault
ST = Shuangtung Thrust
TT = Tili Thrust
YF = Yichu Fault

Folds:

CS = Chuangyuan Syncline
GA = Guaosing Anticline
HA = Hsiaoan Anticline
LS = Lileng Syncline
MA = Meitzulin Anticline
TA = Tsukeng Anticline
TiS = Tingkan Syncline
TS = Tachiwei Syncline
TaaS = Taanshan Syncline
TahS = Tahenpingshan Syncline

Institutions:

CGS = Central Geological Survey
CSIC = Consejo Superior de Investigaciones Científicas
CWBSN = Central Weather Bureau Seismic Network
ICTJA = Instituto de Ciencias de la Tierra ‘Jaume Almera’
NTU = National Taiwan University

List of figures

Figure 1.1. *Geodynamic setting of the Taiwan mountain belt*
Figure 1.2. *Sections of the Eurasian continental margin to the west of the Taiwan mountain belt*
Figure 1.3. *Tectonostratigraphic zones and major bounding faults of the Taiwan mountain belt*
Figure 1.4. *Distribution of the stations used to construct the P-wave velocity models used in this study*
Figure 1.5. *Comparison between relocated earthquake hypocentres before and after the collapsing*
Figure 1.6. *Earthquake seismicity datasets used in this thesis visualized using the software Voxler*
Figure 1.7. *Schematic stratigraphy of the geology within the study area*
Figure 1.8. *Geological cross-sections through the study area*

Figure 3.1. *Sketch and photographs of the Shuilikeng Fault*
Figure 3.2. *P-wave velocity model of Wu et al. (2007) from within central Taiwan*
Figure 3.3. *March 27th to April 15th 2013 Nantou sequence hypocentres*
Figure 3.4. *Depth distribution of the basement-cover interface beneath the study area*
Figure 3.5. *Schematic block diagram showing the interpreted deep structure beneath the study area*

Abstract

The Taiwan thrust belt is generally thought to develop above a shallow, through-going basal detachment confined to within the sedimentary cover of the Eurasian continental margin. A number of data sets, however, such as surface geology, earthquake hypocentre, and seismic tomography data among others, suggest that crustal levels below the interpreted location of the detachment are also currently being involved in the deformation. In this thesis, new surface geology data were combined with several available geophysical data sets to find a model for the structure of the south-central part of the thrust belt that takes into account deformation taking place at depth. Results of this thesis indicate that beneath the internal Hsuehshan and Central ranges the structural development of the south-central Taiwan thrust belt is controlled by steeply dipping and deep-penetrating faults that are currently inverting pre-existing basement faults inherited from the Eurasian continental margin. Basement rocks are uplifted along these faults to form a basement culmination in the interior of the thrust belt. Beneath the more external Coastal Plain and Western Foothills, however, most of the deformation appears to be taking place near the basement-cover interface, which is acting as an extensive level of detachment and still preserves the extensional geometry inherited from the Eurasian margin.

Chapter 1 - Introduction

1.1. Presentation of the thesis

This Ph.D. thesis was carried out at the Institute of Earth Sciences 'Jaume Almera' (ICTJA) of the Spanish National Research Council (CSIC) during the years 2010 (November) through to 2014 (September) with the aid of the JAE-Predoc Ph.D. grant by the CSIC, and co-funded by the European Social Fund (ESF). Furthermore, the thesis was also part of a research project on "*Arc-continent collision processes in Taiwan"* (CGL2009-11843 BTE) financed by the Spanish Ministry of Education and Science aimed at studying the deformation of the continental crust during arc-continent collision in Taiwan. This research project was carried out in collaboration with colleagues from the National Taiwan University (NTU), and the Central Geological Survey (CGS) in Taipei (Taiwan). Funding from this research project allowed the Ph.D. student to:

- Carry out three field campaigns of one month each in Taiwan, in collaboration with colleagues from ICTJA, and with the aid of collaborators from CGS;
- Carry out a stay of one month at the Seismological Laboratory of NTU;
- Attend a three-day course on "*Convergent margins and subduction zones: deformation processes at the plate interface*" at the University of Torino (Italy);
- Attend international and national conferences;
- Cover the costs for the publication of the articles.

In addition, the Ph.D. student was granted a scholarship for extended stays given by the CSIC to the holders of a JAE-Predoc grant. This additional funding allowed the student to:

- Carry out a stay of three months at the Seismological Laboratory of NTU.

Results of the work carried out by the Ph.D. student during his thesis have been presented either as poster and oral presentations in a total of eight international and national conferences. These include, among others, the General Assembly of the European Geophysical Union (EGU), the American Geophysical Union (AGU) Fall Meeting, and the International Conference on the Tectonics of Taiwan (TOTIC). Results were also presented as poster presentations in national congresses such as the Annual Meeting of the Italian Group of Structural Geology, and the 8th Geological Congress of Spain. Finally, results of the work carried out during the thesis are included in five original articles that have been either published (4 articles) or under review (1 article) in SCI journals. This thesis is organized as a compilation of these five articles that are presented in a chronological order according to their date of publication. These articles are:

- Brown, D., Alvarez-Marron, J., Schimmel, M., Wu, Y.-M., and Camanni, G. (2012), *The structure and kinematics of the central Taiwan mountain belt derived from geological and seismicity data*. **Tectonics**, v. 31, no. 5, doi: 10.1029/2012TC003156;

- Camanni, G., Brown, D., Alvarez-Marron, J., Wu, Y.-M., and Chen, H.-A. (2014), *The Shuilikeng fault in the central Taiwan mountain belt*. **Journal of the Geological Society, London**, v. 171, p. 117-130, doi: 10.1144/jgs2013-014;

- Camanni, G., Chen, C.-H., Brown, D., Alvarez-Marron, J., Wu, Y.-M., Chen, H.-A., Huang, H.-H., Chu, H.-T., Chen, M.-M., and Chang, C.-H. (2014), *Basin inversion in central Taiwan and its importance for seismic hazard*. **Geology**, v. 42, no. 2, p. 147-150, doi: 10.1130/G35102.1;

- Alvarez-Marron, J., Brown, D., Camanni, G., Wu, Y.-M., and Kuo-Chen, H. (2014), *Structural complexities in a foreland thrust belt inherited from the shelf-slope transition: Insights from the Alishan area of Taiwan.* **Tectonics**, v. 33, no. 7, p. 1322-1339, doi: 10.1002/2014TC003584;

- Camanni, G., Alvarez-Marron, J., Brown, D., Ayala, C., Wu, Y.-M., and Hsieh, H.-H. (under review), *The deep structure of south-central Taiwan illuminated by seismic tomography, earthquake hypocentres, and gravity data*. **Geological Society of America Bulletin**, MS number: B31138.

Following the Article 37 of the guidelines ("*Normativa reguladora del doctorat*" of October 2013) of the University of Barcelona for Ph.D. thesis presented as a compilation of scientific articles, this thesis is divided into three chapters followed by two appendices in which two geological maps from within the study area of the Ph.D. thesis are presented, and the conference abstracts of the poster and oral presentations related to the thesis are listed. This chapter (Chapter 1) is an introductory part to the thesis in which the geological framework of the study area in south-central Taiwan, the main objectives of the thesis, the methodological approach used by the Ph.D. student in his research, and an overview of the geology of the study area are presented. Chapter 2 contains the original articles that include the results of the work carried out by the Ph.D. student during his thesis. The articles are preceded by a presentation of them in which it is specified their content and how they link to each other. Each article in Chapter 2, furthermore, is preceded by a page in which, along with the title and the authors of the article, the contributions of the Ph.D. student to the article are clearly specified. Finally, Chapter 3 comprises an extended summary of the thesis, which includes a summary of the results of the work carried out by the Ph.D. student during this thesis, a comprehensive discussion of them, and the overall conclusions of the thesis.

1.2. Geological framework

1.2.1. The Eurasian margin

The active Taiwan mountain belt is located in the island of Taiwan, which lies nearly 180 km off the southeastern coast of mainland China, across the Taiwan Strait (Fig. 1.1). The mountain belt is developing in a complex geodynamic setting defined by two quasi-orthogonal subduction systems in which the Eurasian and the Philippine Sea plates interact. Southwest the mountain belt, the Eurasian Plate is subducting eastward beneath the Philippine Sea Plate at the Manila Trench, and, east of the mountain belt, the Philippine Sea Plate is in turn subducting northward beneath the Eurasian Plate at the Ryukyu Trench (Angelier, 1986; Byrne et al., 2011; Huang et al., 1997; Huang et al., 2000; Huang et al., 2006; Sibuet and Hsu, 2004). Since the study area is located in south-central Taiwan, only the former subduction system, its footwall and its hanging wall are of importance for this thesis.

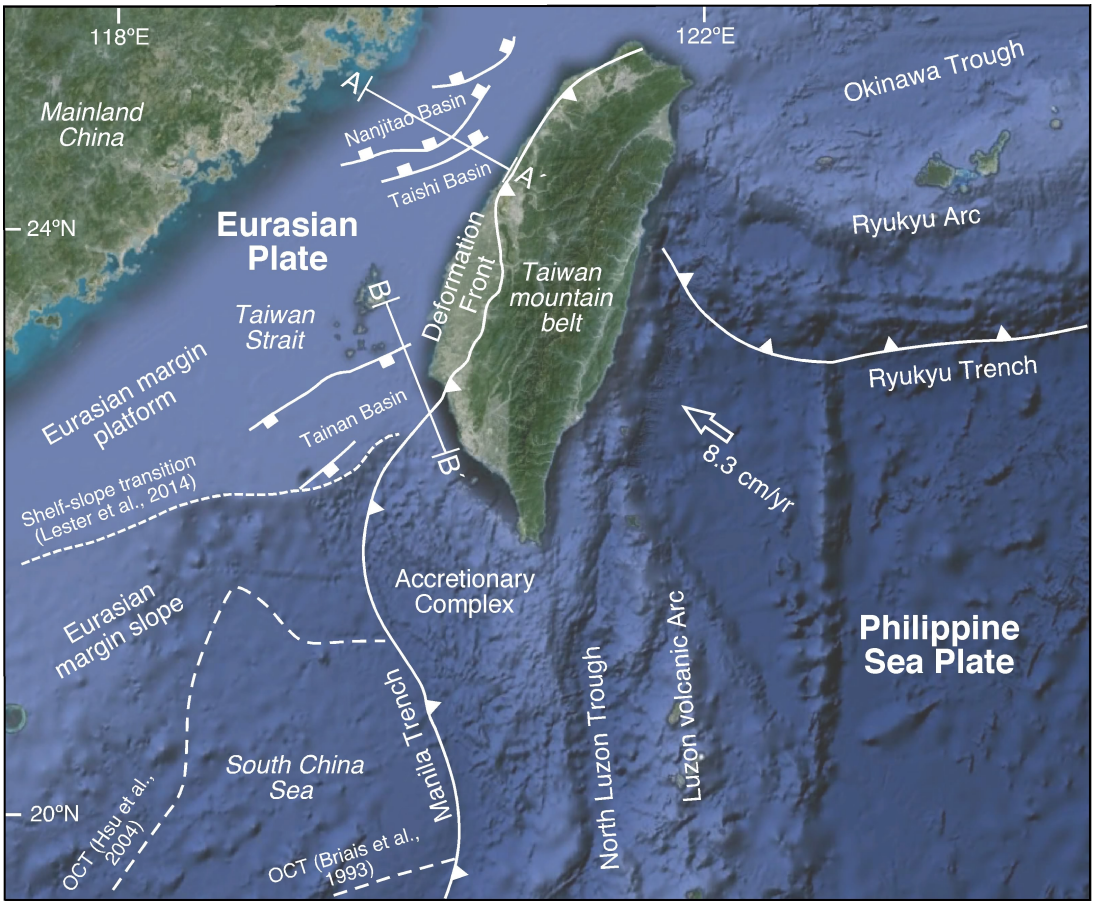

Fig. 1.1. Geodynamic setting of the Taiwan mountain belt. OCT = ocean-continent transition. The convergence vector of 8.3 cm/yr is from Yu et al. (1997). The structures on the Eurasian margin and the location of the deformation front offshore southwestern Taiwan are from Lin et al. (2008); Lin et al. (2003); Yeh et al. (2012). The locations of the sections A-A´ and B-B´, shown in Fig. 1.2, are given.

The tectonic evolution that led to the pre-collisional configuration of the Eurasian Plate margin in the footwall of the Manila Trench can be summarized in a number of significant tectonic events that pre-date the Taiwan orogeny (e.g., Huang et al., 1997; Huang et al., 2000; Huang et al., 2006; Lin et al., 2003). From the oldest to the youngest, these are:

- A phase of Paleocene to Early Oligocene rifting, which resulted in the development of the Eurasian continental margin in this area;

- A phase of Early Oligocene to Middle Miocene sea floor spreading, which resulted in the opening of the South China Sea;
- A phase of Late Oligocene to Miocene extension, which resulted in the development of basins on the outer platform to slope areas of the Eurasian continental margin;
- A phase of intraoceanic subduction of the South China Sea oceanic crust beneath the Philippine Sea Plate since the Early Miocene, which resulted in the development of the Luzon volcanic Arc on the Philippine Sea Plate.

Continuous subduction of the South China Sea oceanic crust beneath the Philippine Sea Plate brought the leading edge of the Eurasian continental margin progressively closer to the Luzon volcanic Arc, and finally determined their oblique collision since the Late Miocene. The Taiwan mountain belt is forming as the result of this oblique arc-continent collision (Byrne et al., 2011; Ho, 1988; Huang et al., 1997; Huang et al., 2000; Huang et al., 2006; Sibuet and Hsu, 2004; Suppe, 1981, 1984; Teng, 1990). At present, the Philippine Sea Plate is moving towards the NW (N49°W) at a rate of c. 8.3 cm/yr relative to a fixed point (Penghu Island) on the Eurasian Plate (Seno, 1977; Yu et al., 1997).

A template for the structure of the Eurasian continental margin, which is currently being involved in the Taiwan orogeny, can be derived from the current structure of the margin to the west and southwest of Taiwan (Fig. 1.1), since this part of the margin is still not involved in the collision with the Luzon volcanic arc. The overall regional structure of this part of the margin is well-known from seismic reflection, boreholes, gravity, and magnetic data (Deng et al., 2012; Hayes and Nissen, 2005; Lester et al., 2012; Lester et al., 2014; Li et al., 2007; Liao et al., 2014; Lin et al., 2008; Lin et al., 2003; McIntosh et al., 2013; Nissen et al., 1995; Pin et al., 2001; Sibuet et al., 2002; Teng and Lin, 2004; Yeh et al., 2012). In these articles, the entire profile of the continental margin has been described, from the full thickness of the continental crust (platform) in the north, to the thinned crust of the slope, towards the ocean-continent transition in the south. The shelf-slope transition is commonly taken to coincide with the 200 m bathymetry contour, whereas there is some uncertainty as to the exact location of the ocean-continent transition (the different interpretations of Briais et al., 1993; Hsu et al., 2004 are given in Fig 1.1). Furthermore, it has been shown that the platform, slope and more distal areas of the margin to the west and southwest of Taiwan are defined by a number of Paleogene-aged, rift-related, roughly NE-oriented basins (Lin et al., 2003). Examples of these Paleogene-aged basins are the Nanjihtao and Taihsi basins (Figs. 1.1 and 1.2) that are located on the platform area of the margin. These basins are mainly filled with Paleogene clastic sediments that can reach up to 6 km in thickness overlain by up to 3 km thick Oligo-Miocene clastic platform sediments (Lin et al., 2003). These sediments are overlain by up to 5 km thick Pliocene-Holocene syn-orogenic sediments derived form the adjacent Taiwan mountain belt. Another example of Paleogene-aged rift-related basins is the Hsuehshan Basin which is interpreted to be a graben or half-graben located on the platform part of the margin(Ho, 1988; Huang et al., 1997; Teng, 1990; Teng and Lin, 2004; Teng et al., 1991), and which is currently involved in the deformation within the Taiwan orogen where it forms the Hsuehshan Range of the mountain belt (see section 1.2.2). According to Teng et al. (1991) and Teng and Lin (2004) this basin was filled with up to 4 km thick Paleogene clastics overlain by up to 5 km of Oligo-Miocene clastic platform sediments.

Importantly for this thesis, Late Oligocene to Miocene extension resulted in the development of the Tainan Basin on the outer platform to slope areas of the margin (Figs. 1.1 and 1.2) (Chen and Yang, 1996; Ding et al., 2008; Huang et al., 2004; Lester et al., 2014; Li et al., 2007; Lin et al., 2003; Tang and Zheng, 2010; Yang et al., 2006). Since the study area in south-central Taiwan is located roughly at the

onshore projection of the Tainan Basin, its structure and sediments deposited within it are of particular importance for better understanding the rocks that are currently being involved in the deformation within south-central Taiwan. The Tainan Basin comprises two Miocene depocentres called the Northern and Southern depressions, separated by a structural high called the Central Uplift (Fig. 1.2). The Miocene clastics in the Tainan Basin reach up to 6 km in thickness, and are overlain by up to 7 km (in the Southern Depression) of Pliocene to Holocene sediments (Lin et al., 2003). On the basis of seismic reflection and boreholes data, a number of different interpretations have been proposed for the current internal structure of the basin: for example, Lin et al. (2003) proposes that the Central Uplift is bound to the north by a NW-dipping extensional fault; Huang et al. (2004) suggests that the Central Uplift is bound to the south by a SE-dipping extensional fault; Chen and Yang (1996) suggest that the Central Uplift is bound by extensional faults on both sides. Most authors, however, suggest that the Tainan Basin is bound to the north by a system of SSE-dipping extensional faults that have been grouped together and called "B" (Lin et al., 2003) or Meishan (Yang et al., 2007) and Yichu faults (Lin et al., 2003).

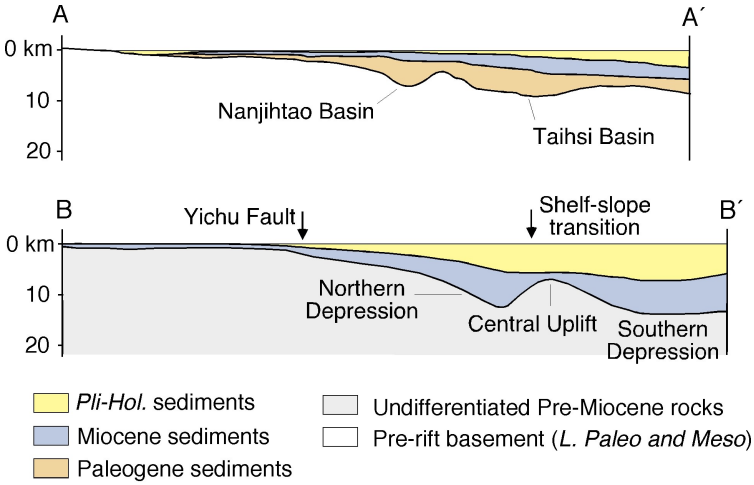

Fig. 1.2. Sections A-A´ and B-B´ from within the Nanjihtao, Taihsi, and Tainan basins to the west of the Taiwan mountain belt. The sections were drawn using the sedimentary thicknesses offshore Taiwan proposed by Lin et al. (2003). The location of the sections is given in Fig. 1.1.

1.2.2. The Taiwan mountain belt

The Taiwan mountain belt can be divided in five roughly N-S oriented tectonostratigraphic zones separated by major faults (Fig. 1.3). From west to east, these zones are: the Coastal Plain, the Western Foothills, the Hsuehshan Range, the Central Range, and the Coastal Range. The Coastal Plain, Western Foothills, Hsuehshan Range, and Central Range are forming as the result of deformation and uplift of syn- to post-rift Paleogene to Miocene clastics and older pre-rift continental margin rocks of the Eurasian margin, and the Pliocene and younger syn-orogenic sediments of the foreland basin (e.g., Byrne et al., 2011; Ho, 1988; Suppe, 1981). The Western Foothills are juxtaposed against the Hsuehshan Range along the Shuilikeng Fault in the north, and against the Central Range along the Chaochou Fault in the south (Fig. 1.3). To the east, the Hsuehshan Range is juxtaposed against the Central Range along the Lishan Fault. The Coastal Range is composed of volcanic rocks and arc-derived sediments of the Luzon Arc that are being thrust obliquely towards the northwest over the Central Range along the Longitudinal Valley Fault, which forms the suture between the Eurasian and the Philippine Sea plates (Fig. 1.3) (e.g., Chen et al., 2007; Shyu et al., 2008; Yu and Kuo, 2001).

The Coastal Plain and the Western Foothills form the frontal part of the mountain belt, and their structure is thought to be that of an imbricate thrust system linked to a sub-horizontal basal thrust developed at shallow depths within the crust (e.g., Alvarez-Marron et al., 2014; Brown et al., 2012; Carena et al., 2002; Suppe, 1976, 1981; Suppe and Namson, 1979; Yue et al., 2005). This imbricate thrust system is bound in the west by the Changhua Thrust, which is generally interpreted to coincide with the

deformation front of the mountain belt (e.g., Hsu et al., 2009; Yu et al., 1997; Fig. 1.3). There are uncertainties, however, on the structure of the more internal Hsuehshan and Central Ranges. According to some authors (e.g., Carena et al., 2002; Ding et al., 2001; Malavieille and Trullenque, 2009; Suppe, 1976, 1980b, 1981; Suppe and Namson, 1979; Yue et al., 2005), the sub-horizontal basal thrust beneath the Coastal Plain and the Western Foothills would extend eastward beneath the Hsuehshan and Central Range, and would steepen and deepen beneath the Coastal Range when it is thought to reach c. 60 km depth (e.g., Carena et al., 2002). In contrast, others suggested that the Hsuehshan and Central ranges would form a zone with steeply dipping faults rooted into the middle and even the lower crust (e.g., Bertrand et al., 2009, 2012; Brown et al., 2012; Gourley et al., 2007; Wu et al., 2004; Wu et al., 2014; Wu et al., 1997).

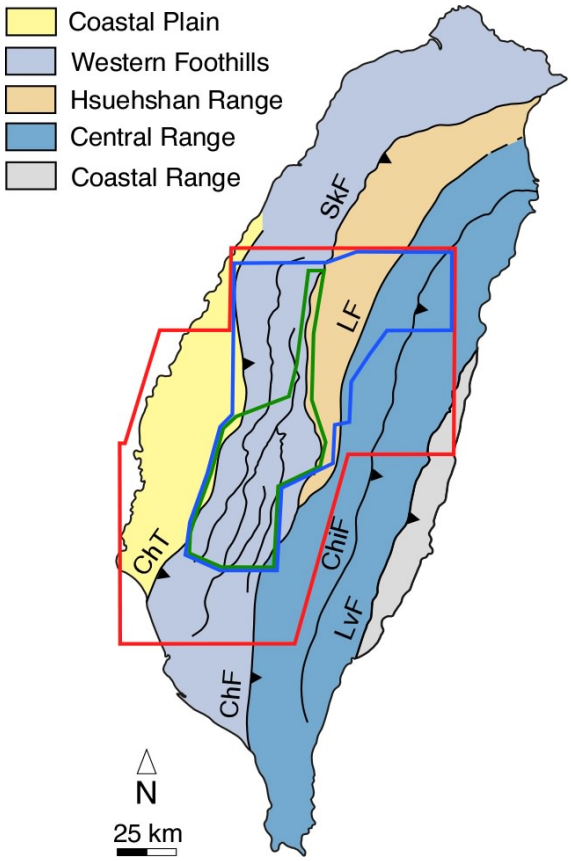

Fig. 1.3. Major tectonostratigraphic zones and bounding faults of the Taiwan mountain belt. The red box indicates the location of the area analysed using available geophysical datasets; the green box indicates the area mapped at the surface in collaboration with colleagues from ICTJA; the blue box indicates the location of the map shown in Geological map 1. ChF = Chaochou Fault, ChiF = Chinma Fault, ChT = Changhua Thrust, LF = Lishan Fault, LvF = Longitudinal Valley Fault, SkF = Shuilikeng Fault.

1.3. Objectives

The main aim of this thesis was to refine the structure of the south-central part of the Taiwan orogen taking into account the influence of pre-existing structures inherited from the Eurasian margin on its structural development. Since the south-central part of the Taiwan mountain belt is developing over the platform to slope areas of the Eurasian continental margin that have been shown to be in part controlled by Paleogene- and Miocene-aged fault-bound basins, the study area is an ideal laboratory to study the effects that inherited structures have on the development of the mountain belt. To achieve this aim, detailed objectives of the thesis included:

- Defining the structure and kinematics of the Shuilikeng Fault. The Shuilikeng Fault marks a significant change in the level of crustal involvement that takes place in south-central Taiwan across it, and along its entire length it forms the western bounding faults of rocks derived from the Hsuehshan Basin. This change in the level of crustal involvement is suggested by differences in metamorphic grade and stratigraphic levels involved in the deformation in the Western Foothills and the Hsuehshan Range. This significant change is accompanied by changes in the distribution of earthquake hypocentres, and P-wave velocities (Gourley et al., 2007; Huang et al., 2014; Kim et al., 2010; Kim et al., 2005; Kuo-Chen et al., 2012; Lin, 2007; Wu et al., 2004; Wu et al., 2014; Wu et al., 1997; Wu et al., 2007; Yamato et al., 2009). All these evidences point toward the Shuilikeng Fault as a key feature in the structural development of south-central Taiwan;

- Defining the deep structure beneath south-central Taiwan. The study area includes significant deep-seated seismicity, which suggests that deformation that is taking place within deep levels of the crust is actively contributing to the structural development of the mountain belt (e.g., Gourley et al., 2007; Wu et al., 2004; Wu et al., 2014; Wu et al., 1997). However, how this seismicity is integrated in the regional geological context is still not completely understood. To define the deep structure beneath the study area, the trend of the basement-cover interface was defined along with deep-seated fault systems.

1.4. Methodology

A multidisciplinary methodological approach was adopted in this study, which consisted in the integration of new surface geology data and structural analysis, with several available geophysical datasets. In particular, data derived from field mapping and structural geology techniques were combined with two tomography P-wave (Primary wave) velocity models (Kuo-Chen et al., 2012; Wu et al., 2007), and with a catalogue of earthquake hypocentres (Wu et al., 2008a; Wu et al., 2009) and focal mechanisms (Wu et al., 2010; Wu et al., 2008b). While surface geology data provided information on the shallow structure and kinematics, earthquake seismicity data provided information on the location, geometry and kinematics of fault systems at depth, and the P-wave velocity data helped define the velocity structure of the mountain belt from which insights on its structure at depth can be derived.

Data collection and processing was carried out both in the field and in the Seismological Laboratory of the Department of Geosciences of NTU in Taipei (Taiwan), in different periods during the realization of this thesis. Extensive geological mapping to collect new surface geology data was done in collaboration with Dr. Alvarez-Marron and Dr. Brown from ICTJA during three field campaigns of one month each carried out during the first, second, and fourth year of this thesis. Collaborators from CGS of Taiwan assisted for a period of two weeks during the first field campaign. The map area covered during this thesis is shown in green in Fig. 1.3 A. Laboratory work was carried out during a three- and one-month stays undertaken during the second and third year of this thesis, respectively, at the Department of Geosciences of NTU under the supervision of Prof. Wu and his collaborators. During these stays, the work carried out involved the managing of earthquake seismicity, focal mechanisms and P-wave velocity data, and the further processing of these data from within the study area. The area analysed using these geophysical datasets is shown in red in Fig. 1.3 A.

In the following paragraphs each technique used in the multidisciplinary methodological approach is described separately. In the presentation of the geophysical datasets, a description of the data themselves is provided first, followed by specific information on the work carried out at NTU, and by a description of the use made of these datasets to achieve the objectives of the thesis.

1.4.1. Field mapping

Field mapping was a fundamental technique used in this thesis and it was carried out at both 1:25.000 and 1:50.000 scales (see geological maps 1 and 2 in Appendix 1). In particular, during the first two field campaigns, geological mapping was carried out at 1:25.000 scale along the surface trace of the Shuilikeng Fault for over 100 km along its strike in central Taiwan (Fig. 1.3). These field campaigns were aimed at better defining this significant boundary between the Western Foothills and the Hsuehshan Range. During the final field campaign, geological mapping was carried out at 1:50.000 scale within the Western Foothills in the southern part of the study area. This field campaign was aimed at understanding the structure of this part of the mountain belt as it could provide key insights on the influence of inherited structures from the margin on the structural development of the mountain belt.

Because of the often high, rugged topography and dense forest cover in Taiwan, the mapping was carried out mainly following riverbeds and roads. The tracing of structural and stratigraphic boundaries from one river to another was aided by satellite imagery data and previous geological maps. Where available, the 1:50.000 scale geological maps of CGS as well as the Chinese Petroleum Corporation 1:100.000 scale maps were used as reference maps. The field mapping involved the measurement of the

orientation of surfaces such as bedding and cleavage, and that of fault planes and fold axes. For the determination of the kinematics of faults the orientation of lineations on fault surfaces, such as slickenlines and grooves, were also measured. In the kinematic analysis of these fault-slip data, and in particular in the analysis of those collected from the Shuilikeng Fault, the methodology of Marrett and Allmendinger (1990) was adopted. This methodology uses the linked Bingham distribution of the shortening and extension directions of a population of faults to calculate the average incremental principal strain axes (i.e., average P and T axes). In order to better visualise these results, the average incremental principal strain axes were input into the FaultKin software of Marrett and Allmendinger (1990) (http://www.geo.cornell.edu/geology/faculty/RWA/programs/faultkin.html) to calculate an average fault plane solution.

All the structural measurements collected in the field were used together to construct regional and detailed geological maps and cross-sections. Cross-sections were constructed using standard geometrical techniques in which the location of contacts in the shallow subsurface (c. 5 km) are determined using the geometric controls provided by the observed outcropping and borehole stratigraphic contacts, and the bedding dips.

1.4.2. P-wave velocity models

1.4.2.1. Data description

The P-wave velocity models of Wu et al. (2007) and, secondarily, that of Kuo-Chen et al. (2012) were used in this study. The P-wave velocity model of Wu et al. (2007) was built using earthquakes recorded by 751 stations deployed on the island of Taiwan by the Central Weather Bureau Seismic Network (CWBSN) and the Taiwan Strong Motion Instrumentation Program (TSMIP) (Fig. 1.4 A). Stations of TSMIP are mainly located in the western part of the study area, whereas those of CWBSN are widespread throughout the study area providing a good coverage of most parts of it. For the construction of the P-wave velocity model, earthquakes recorded by these stations over the years 1992 to 2005 were used. Within the study area, this P-wave velocity model is distributed over a grid of points horizontally spaced 7.5 km and 12.5 km in the WNW-ESE and NNE-SSW directions, respectively (Fig. 1.4). The vertical grid spacing increases with depth and the grid points are distributed at 0, 2, 4, 6, 9, 13 17, 21, 25, 30, 35, 50, 70, 90, 110, 140, and 200 km depth. The checkerboard test developed for this P-wave velocity model indicates an excellent resolution within south-central Taiwan in the first 40 km of the crust that are of importance for this thesis (Wu et al., 2007). For further details on the methods adopted in running the tomography inversion and the checkerboard test of the data the reader is referred to Wu et al. (2007).

The P-wave velocity model of Kuo-Chen et al. (2012) was built in the frame of the Taiwan Integrated Geodynamic Research (TAIGER) Project (http://taiger.binghamton.edu/), and comprises a regional and a local tomography. While the regional tomography was built using teleseismic events, the local one was constructed using both land explosions carried out during TAIGER Project and earthquakes from in and around Taiwan. During this thesis, only the local tomography was used. The local P-wave velocity model was constructed using a total of 2803 stations from both onshore and offshore Taiwan (Fig. 1.4 B). Within south-central Taiwan, the horizontal grid spacing of this model is 4 km in the east-west and north-south directions. The vertical grid spacing increases with depth and the grid points are at every 2 km in the upper 24 km of the crust, at every 4 km from 24 to 64 km depth, at every 8 km from 64 to 96 km depth, and at every 10 km from 96 to 116 km depth. The checkerboard test indicates a good resolution for the upper 54 km from within the study area in south-central Taiwan (Kuo-Chen et al.,

2012). For an overview of the model setup and the data handling the reader is referred to Kuo-Chen et al. (2012).

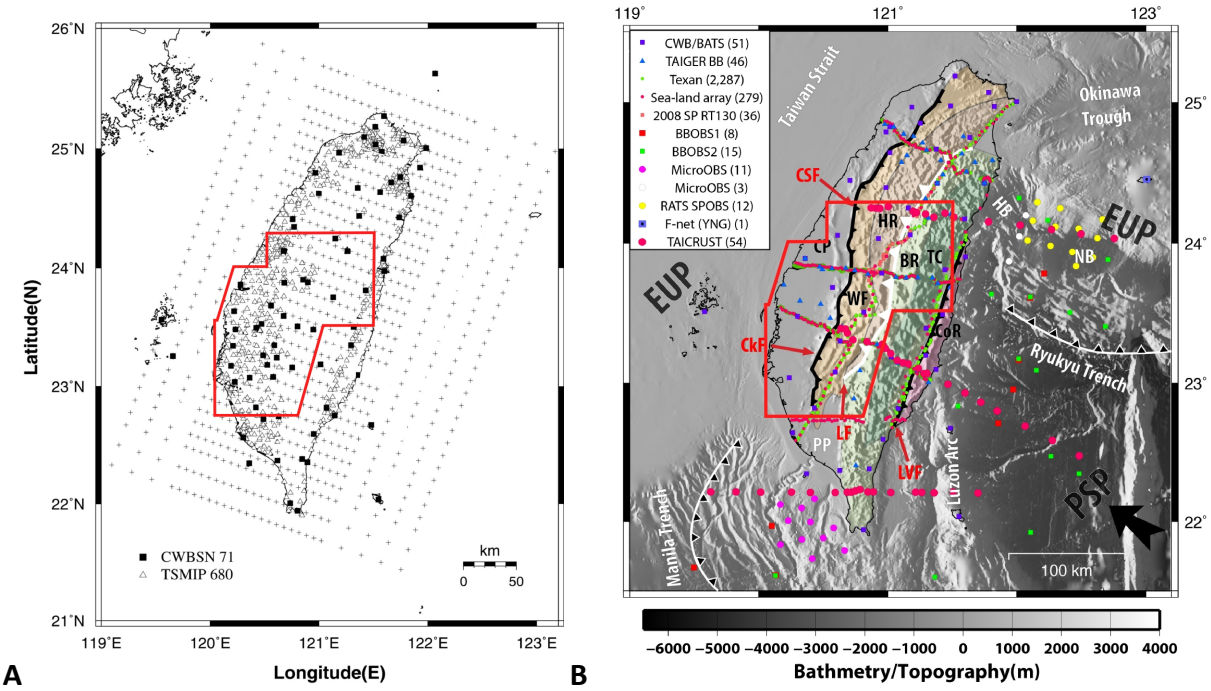

*Fig. 1.4. **A**, Distribution of CWBSN (black squares) and TSMIP (white triangles) stations used to construct the P-wave velocity model of Wu et al. (2007) (modified after Wu et al., 2007). The horizontal grid spacing of the velocity model is also shown (grid points are shown as crosses); **B**, distribution of the stations used to construct the P-wave velocity model of Kuo-Chen et al. (2012) (modified after Kuo-Chen et al., 2012). EUP = Eurasian Plate, PSP = Philippine Sea Plate. In both **A** and **B**, the red box indicates the area analysed in this thesis.*

1.4.2.2. Data processing and usage

Selected P-wave velocity data from the upper 40 km of the crust of the tomography model of Wu et al. (2007) were used to construct a three-dimensional P-wave velocity model for the study area. The checkerboard test data of Wu et al. (2007) were used to calculate the resolution of the P-wave velocity model built for south-central Taiwan along specific sections of importance for this thesis. A similar approach was used to construct a P-wave velocity model for south-central Taiwan from the seismic tomography of Kuo-Chen et al. (2012).

P-wave velocity data from both of these models were used to define the velocity structure beneath the study area. Given the differences in P-wave velocities between the platform and slope sediments of the sedimentary cover and the underlying basement rocks, tomography data can be used to differentiate between these two very different lithologies as well as to define a proxy for the interface between them (i.e., the basement-cover interface). In particular, P-wave velocities between 5.2 and 5.5 km/s have been used as a proxy for this interface. To test this interpretation for the basement-cover interface, the Ph.D. student worked in collaboration with Dr. Ayala from ICTJA who performed a three-dimensional stochastic gravity inversion of Bouguer anomaly data from within the study area (Yen and Hsieh, 2010; Yen et al., 1995). A four-layer input density model was built using densities obtained from the conversion of P-wave velocities derived from the tomography data using the method of Barton (1986), and the modelling program (Geomodeller software, Gibson et al. (2013)) was allowed to modify the densities and the surfaces between the layers until a close match between the observed and the calculated anomaly was obtained. Results of this test corroborated the interpretation of the basement-

cover interface to coincide with P-wave velocities comprised between 5.2 and 5.5 km/s. Once defined like this, the trend of the basement-cover interface beneath the study area in south-central Taiwan was of primary importance for determining the degree of basement rocks involved in the deformation beneath the study area.

1.4.3. Earthquake hypocentres and focal mechanisms

1.4.3.1. Data description

A catalogue of earthquake hypocentres recorded by stations of CWBSN, TSMIP, and the Japan Meteorological Agency (JMA) (Wu et al., 2008a; Wu et al., 2009) was used in this study. This catalogue includes seismic events from 1991 to 2011 within the map area of this thesis. The recorded seismic events range up to >7 M_L, and have been located using the 3D P-wave velocity model of Wu et al. (2007) described above. Details on the methodology adopted for the relocation can be found in Wu et al. (2008a); Wu et al. (2009).

The catalogue of earthquake focal mechanisms of Wu et al. (2010); Wu et al. (2008b) was also used. This catalogue includes focal mechanisms for the events from 1991 to 2011 within the study area. For the determination of the focal mechanisms, the first motion polarities of P-waves of events of $M_L \geq 4$ recorded by stations of CWBSN, TSMIP, and JMA were used (Wu et al., 2010; Wu et al., 2008b).

1.4.3.2. Data processing and usage

The catalogues of earthquake hypocentres of Wu et al. (2008a); Wu et al. (2009) and focal mechanisms of Wu et al. (2010); Wu et al. (2008b) were further processed using the collapsing methodology of Jones and Stewart (1997). This methodology is commonly used in the study of active fault systems to illuminate fault surfaces within clouds of earthquakes defined by scattered events. In particular, this methodology involves the determination of statistical measurements for standard errors in the depth, latitude and longitude for each event and the clustering of events with overlapping error spheroids. Data were collapsed using 3D spatial uncertainty of 4 standard deviations to truncate confidence ellipsoid and estimated variance in data. Hypocentre movements were compared with χ^2 distribution and repeated until minimum misfit was reached. To show the differences between the relocated catalogue of earthquake hypocentres before and after the collapsing, earthquake hypocentres from both these datasets were plotted on the same vertical section from the central part of the map area (Fig. 1.5). The reader can appreciate that uncollapsed earthquake hypocentres largely define open clouds of earthquakes from which it is difficult to distinguish active fault surfaces, whereas after the collapsing several linear clusters can be interpreted to image active faults.

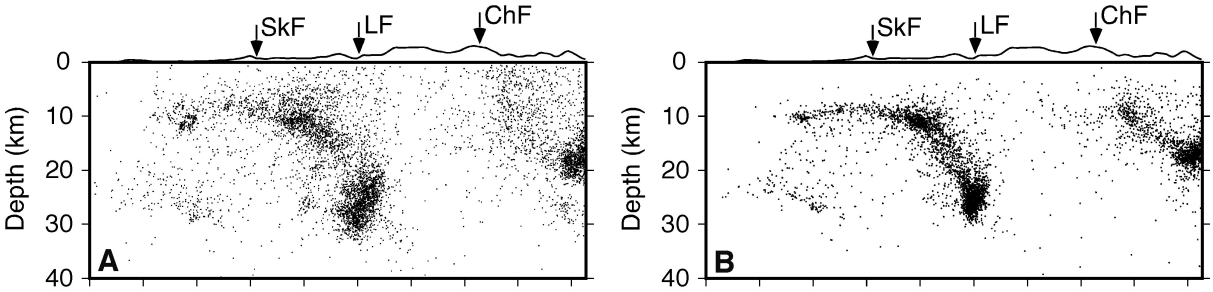

Fig. 1.5. ***A****, relocated earthquake hypocentres before and,* ***B****, after the collapsing carried out following the methodology of Jones and Stewart (1997). This section corresponds to the section B-B´ in Fig. 3.2., whose location is given in Geological map 1. Seismicity data are projected from 4.99 km on either side of the section.*

Further processing of the catalogue of earthquake focal mechanisms of Wu et al. (2010); Wu et al. (2008b) was also performed. In particular, the fault types (i.e. strike-slip, thrust, and normal) derived from the focal mechanisms were determined for the entire study area in south-central Taiwan using the technique of Zoback (1992), which takes into account the plunge of the P, B and T axes of each fault plane solution. Furthermore, to provide further information for the interpretation of the kinematics of the Shuilikeng Fault, focal mechanisms from along this fault have been grouped together in 5 km thick bins, and the average principal strain axes of each group were calculated using the methodology of Marrett and Allmendinger (1990).

The catalogue of relocated and collapsed earthquake hypocentres was used to gain insights into the location and geometry of fault systems at depth beneath the study area. Earthquake focal mechanisms were used to obtain insights on the kinematics of these fault systems.

1.4.4. 3D data analysis and visualization

To analyse the P-wave velocity models of the study area in south-central Taiwan, together with the collapsed catalogue of earthquake hypocentres and the determined fault types derived from the focal mechanisms, these data were first plotted in three-dimensions using the software Voxler (*v*. 3) by Golden Software (http://www.goldensoftware.com/products/voxler) (Fig. 1.6). This permitted to analyse these data together in the same 3D environment and to compare them. It also provided a means to realize preliminary vertical and horizontal sections in any orientations, and to extract several isovelocity surfaces from the P-wave velocity models that were of importance for this thesis (such as, for example, those between 5.2 and 5.5 km/s) (Fig. 1.6). Then, the Generic Mapping Tools (GMT, http://gmt.soest.hawaii.edu/) was used to produce final figures of the sections to be used in the publications.

A

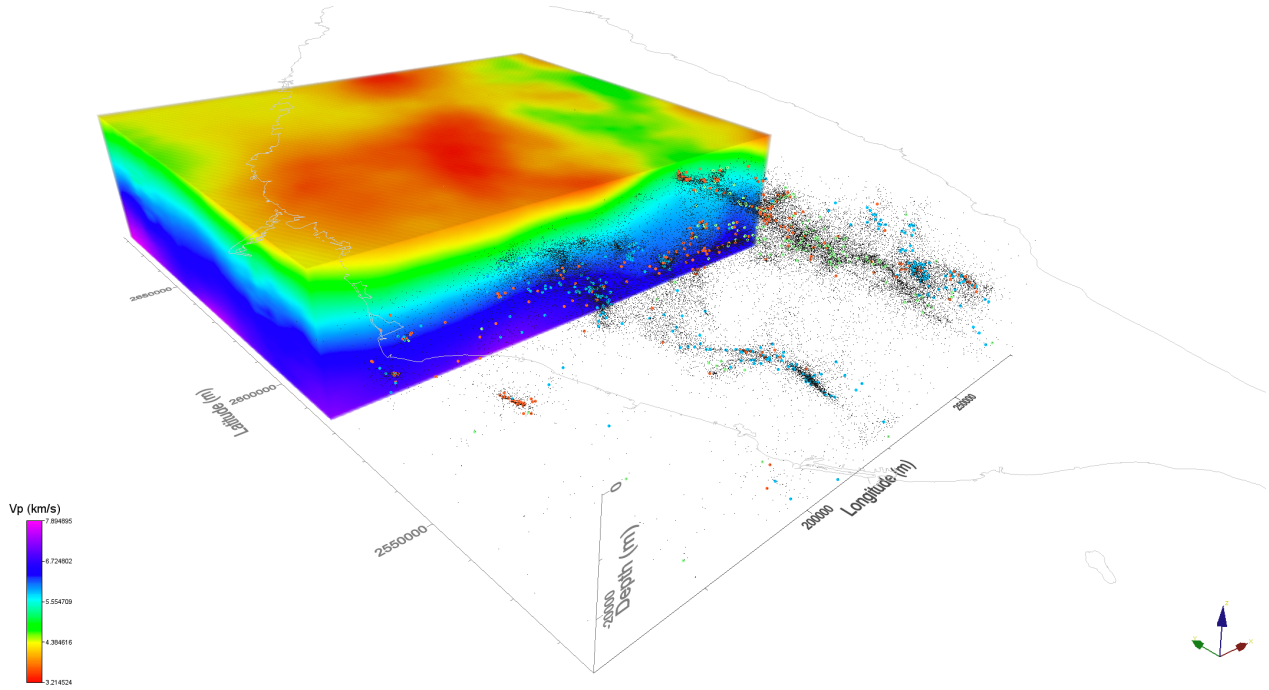

B

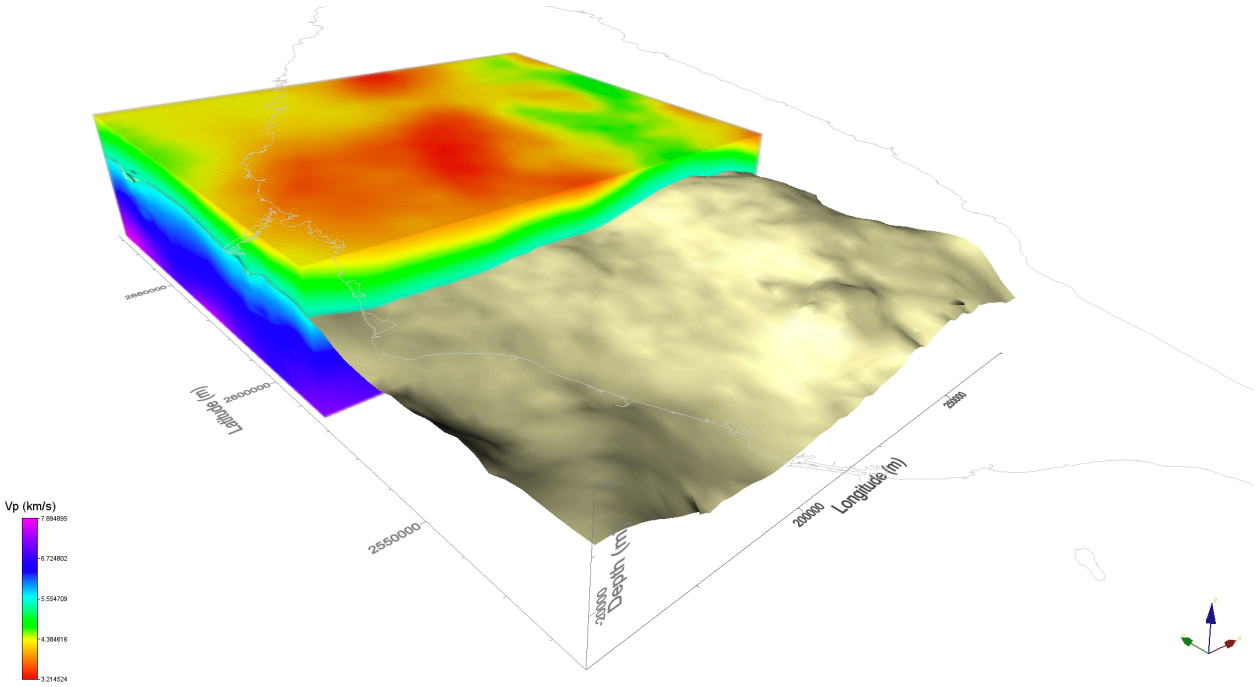

Fig. 1.6. ***A****, 3D P-wave velocity volume of Wu et al. (2007) and relocated and collapsed earthquake hypocentres and focal mechanisms from the study area in south-central Taiwan plotted using the software Voxler (v. 3). Small black dots correspond to earthquake hypocentres whereas blue, red, and green dots represent, respectively, thrust, strike-slip, and extensional fault types determined for the study area using the methodology of Zoback (1992);* ***B****, 3D P-wave velocity volume of Wu et al. (2007) and 5.5 km/s isovelocity surface through it. In both* ***A*** *and* ***B****, the grey line represents the coastline of the Taiwan island.*

1.5. Geology of south-central Taiwan

The study area in south-central Taiwan includes rocks of the Western Foothills, the Hsuehshan Range, and secondarily, the Central Range (Geological map 1). Therefore, in this section a brief overview of the stratigraphy and structure of these tectonostratigraphic zones is given.

1.5.1. The Western Foothills

The Western Foothills includes Pliocene to Holocene syn-orogenic sediments of the foreland basin underlayered by Oligocene to Miocene post-rift clastics of the Eurasian platform and slope, and Eocene-aged syn-rift clastics of the Paileng Formation and volcanics of the Tsukeng Formation (Figs. 1.7, 1.8, and Geological map 1) (e.g., Castelltort et al., 2011; Ho, 1988; Huang et al., 2013; Suppe, 1987; Yue et al., 2005). Since Oligocene and Eocene rocks do not crop out in the Western Foothills (except for a single outcrop of Tsukeng Formation in northern half of the map area) and largely define the outcropping geology of the Hsuehshan Range of the mountain belt within the map area, they are described in the next paragraph. In this thesis, a simplified chronostratigraphic scheme of the Miocene rocks of the Western Foothills is adopted following Brown et al. (2012) and Alvarez-Marron et al. (2014). According to this scheme, the Miocene rocks can be broadly divided in four formations that, in general, comprise a thick-bedded sandstone unit at the base and thin-bedded sandstone and shales at the top. From the oldest to the youngest, these formations are: the Takeng Formation, the Shimen (also called Nankang) Formation, the Nanchuang Formation, and the Kueichulin Formation (Fig. 1.7). According to some authors, the Kueichulin Formation corresponds to and forms the base of the syn-orogenic sediments of the foreland basin (Lin and Watts, 2002; Lin et al., 2003; Yu and Chou, 2001). In the central part of the study area (Fig. 1.8 and Geological map 1), sediments of these Miocene formations were mainly deposited on the platform part of the Eurasian margin. In this part of the mountain belt, the Takeng Formation is approximately 800 to 1000 m thick, the Shimen Formation is up to 500 m thick, the Nanchuang Formation is roughly 250 m thick, and the Kueichulin Formation can vary from 400 to 1500 m in thickness. However, southward, sediments of these Miocene formations were deposited within the depocentres of the Tainan Basin on the outer platform to slope part of the margin, and their thicknesses increase significantly. For example, in the southern half of the study area (Fig. 1.8 and Geological map 1), the thickness of the Shimen Formation (in this area called Nankang) can reach up to 1200 m, and that of the Nanchuang Formation up to 1500 m.

The Pliocene to Holocene syn-orogenic clastics of the foreland basin can be divided in two Plio-Pleistocene formations overlain by up to several hundred metres of Holocene alluvium and terrace deposits. The Plio-Pleistocene formations are: the Pliocene Cholan Formation, and the Pleistocene Toukoshan Formation (Fig. 1.7). The Cholan Formation is made up of nearly 2.5 km of interbedded mudstone, shale and sandstone and, at the base, comprises a several hundred metres thick member of shale, called the Chinshui shale. According to some authors, the Chinshui shale records the first appearance of clasts with a slaty cleavage thought to be eroded off the growing mountain belt, making the base of the Cholan Formation to coincide with the onset of the syn-orogenic sedimentation in the foreland basin (Covey, 2009; Hong, 1997; Teng, 1987). The Toukoshan Formation comprises a coarsening upward sequence of thick-bedded sandstone with shale interbeds, which is upward overlain by a conglomerate member, called the Toukoshan conglomerate, resulting in a total thickness for the Toukoshan Formation that can reach up to 5 km.

The Chinshui shale of the Cholan Formation has also a significant importance for the structure of the Western Foothills, since the basal thrust of the Western Foothills imbricate thrust system is thought to be located within it in central Taiwan (Fig. 1.8) (e.g., Alvarez-Marron et al., 2014; Brown et al., 2012; Suppe, 1976, 1981; Suppe and Namson, 1979; Yue et al., 2005). However, southward the increasing amount of Miocene sediments involved in the deformation suggests that the basal detachment ramps down section at least into Miocene sediments, and is likely rooted within the underlying Paleogene sediments or even into the older pre-rift basement (Fig. 1.8) (e.g., Alvarez-Marron et al., 2014; Hickman et al., 2002; Hung et al., 1999; Suppe, 1980a).

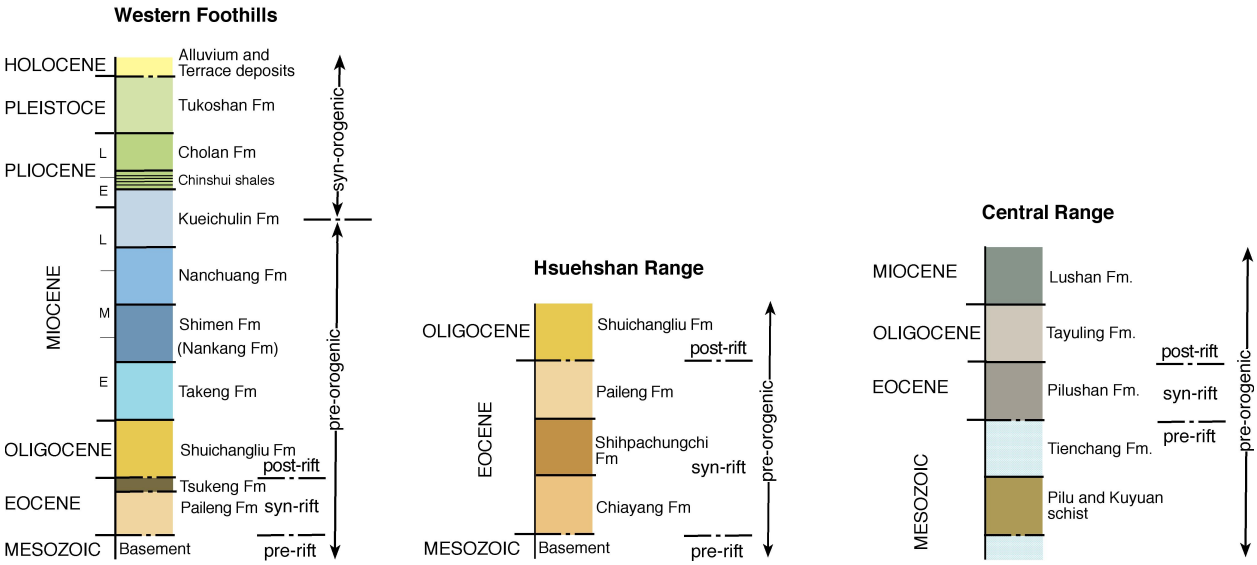

Fig. 1.7. Schematic tectonostratigraphic columns for geology of the study area in south-central Taiwan. Figure modified after articles 1 and 4 included in this thesis.

1.5.2. The Hsuehshan Range

In the hanging wall of the Shuilikeng Fault (Geological map 1), the Hsuehshan Range is largely made up of variably metamorphosed Eocene-aged syn-rift clastic sediments that were deposited in the so-called Hsuehshan Basin that was located on the platform during rifting of the Eurasian margin (Ho, 1988; Huang et al., 1997; Teng, 1990; Teng and Lin, 2004; Teng et al., 1991). These rocks are unconformably overlain by Oligocene-aged post-rift clastics. The stratigraphy of the Hsuehshan Range can be divided in four formations that, from the oldest to the youngest, are: the Chiayang Formation, the Shihpachungchi Formation, the Paileng Formation, and the Shuichangliu Formation (Fig. 1.7). The Chiayang Formation is composed of a thick-bedded sandstone unit overlain by an unknown thickness of slates with a well-developed penetrative slaty cleavage. The Shihpachungchi Formation comprises several hundreds metres of thin-bedded sandstone and mudstone. The age of these two formations is not known, but is inferred to be Early Eocene (Lee, 1979). The Chiayang and the Shihpachungchi formations are strongly folded and show a well-developed axial planar cleavage (Fig. 1.8). Their original thickness is, therefore, difficult to be determined, as their observed thickness is structural. The overlying Paileng Formation begins with a member of thick-bedded, coarse grained to pebble conglomerate quartzite and argillite (the Tachien Member, which has been dated as Early to Middle Eocene in age; Chen et al. (2009)), overlain by interbedded sandstone and argillite, which, locally, are overlain by several hundred metres thick coarse grained to pebble conglomerate quartzite. The Paileng Formation is disconformably overlain by the post-rift Shuichangliu Formation which comprises several hundred metres of Middle

Oligocene-aged interbedded sandstone and shale. Along much of the western part of the Hsuehshan Range, and in particular in the footwall of the Tili Thrust (Fig. 1.8 and Geological map 1), the rocks of these formations are weakly to moderately metamorphosed (Beyssac et al., 2007; Simoes et al., 2012) and have been exhumed from between 9.2 and 9.8 km depth (Sakaguchi et al., 2007). Eastward and southward, however, in the hanging wall of the Tili Thrust, they may reach up to lower greenschist facies (Clark et al., 1993) and have a penetrative pressure solution cleavage (Clark et al., 1993; Fisher et al., 2002; Fisher et al., 2007; Tillman and Byrne, 1995).

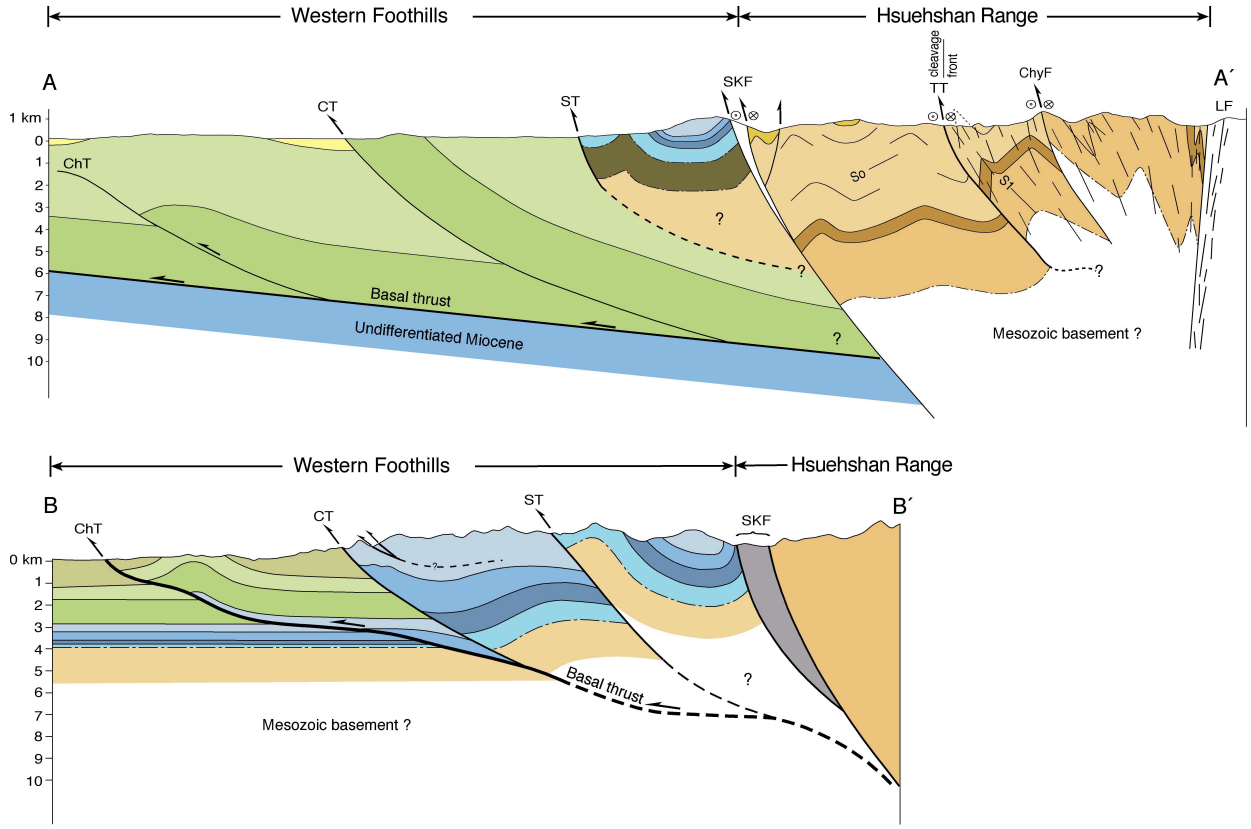

Fig. 1.8. Geological cross-sections through the study area. Their location is given in Geological map 1. Colours are as in Geological map 1. Figure modified after articles 1 and 4 included in this thesis.

1.5.3. The Central Range

In the hanging wall of the Lishan Fault in the north, and of the Chaochou Fault in the south (Geological map 1), the Central Range within the study area comprises three formations that, from the oldest to the youngest are: the Pilushan Formation, the Tayuling Formation, and the Lushan Formation (e.g., Ho, 1988) (Fig. 1.7). The Pilushan Formation consists of Eocene-aged slate and phyllite with local interbeds of sandstone. Throughout south-central Taiwan, this formation is in fault contact with the overlying Tayuling Formation that is Late Oligocene in age and is made up of slate, phyllite, and metasandstone. The overlying Lushan Formation is Middle Miocene in age and defines a large part of the outcropping geology of the western part of the Central Range within the map area (Geological map 1) (Beyssac et al., 2007; Lee et al., 2006; Simoes et al., 2007; Tillman and Byrne, 1995; Wiltschko et al., 2010). This formation comprises variably metamorphosed slates with a well-developed cleavage, and thin- to thick-bedded sandstone units (Fisher et al., 2002; Stanley et al., 1981; Wiltschko et al., 2010).

While the Pilushan Formation is thought to have been deposited in a shallow marine environment (Huang et al., 1997), foraminifera found in both the Tayuling and Lushan formations suggest that these two formations were deposited in an open marine environment at water depths of between 500 and 1500 m (Huang et al., 1997). In the eastern part of the Central Range within the study area in south-central Taiwan, rocks of the Pilushan Formation are overthrust by Mesozoic pre-rift basement rocks along the Chinma Fault (Geological map 1). These rocks are mainly comprised of marbles of the Tienchang Formation folded with minor lenses of schist of the Pilu and Kuyuan formations.

Chapter 2 - Articles

Presentation of the articles

In Article 1 a new structural model for the central part of the Taiwan mountain belt is proposed. Data presented in this article highlight that significant changes in the structure and the kinematics of the central Taiwan mountain belt take place from the Coastal Plain and the Western Foothills in the west, to the Hsuehshan and Central ranges in the east. In particular, new surface geology data, together with earthquake focal mechanisms and seismic energy release data, suggest that the Coastal Plain and the Western Foothills of the central Taiwan mountain belt are defined by an imbricate thrust system that is developing in a forward breaking sequence of deformation. This imbricate thrust system appears to be structurally and kinematically linked to a basal detachment at between 7 and 10 km depth, and spans from the Changhua Thrust in the west to the Shuilikeng Fault in the east. Like in previous interpretations, this basal detachment appears to be located at the base of the syn-orogenic sediments. However, the structure of the Hsuehshan and Central ranges of the mountain belt differs significantly from this structural model and is largely defined by a system of steeply dipping active faults that penetrate to a depth of 25 to 30 km or more. Data presented in in this article also indicates that these changes in structural style from the Coastal Plain and the Western Foothills to the Hsuehshan and Central ranges take place roughly across the Shuilikeng Fault. They also suggest that the Shuilikeng Fault, rather than being a single discrete feature, comprises a system of faults and folds that splay off the main fault, resulting in a regional map pattern that is suggestive of a transpressive fault zone.

Surface geology, earthquake hypocentre and focal mechanism data presented in Article 2 help place further constraints on the structure and kinematics of the Shuilikeng Fault, which has been shown from results of the previous article to be a key structure in central Taiwan. They also provide insights on how the imbricate thrust system that defines the structure of the Coastal Plain and Western Foothills links with the Hsuehshan Range to the east. In particular, new surface geology data indicate that along 100 km of its strike length in Central Taiwan, where observed in the field, the Shuilikeng Fault and the faults that splay off it are everywhere brittle features composed of breccia and fault gouge. Fault-slip data from a number of locations along the Shuilikeng fault indicate senses of slip that range from thrusting, to strike-slip, to extension. These fault-slip data indicate a nearly NW-SE average shortening direction along the strike length of the Shuilikeng Fault. The combination of these new surface geology data with earthquake hypocentre data indicate that the Shuilikeng Fault is steeply east-dipping and can be traced to greater than 20 km depth. Furthermore, earthquake focal mechanism data suggest that its kinematics is overall transpressive with the Hsuehshan Range in its hangingwall moving up towards the northwest, in consistence with the average NW-SE shortening direction as derived from fault-slip data at the surface.

The combination of geological, P-wave velocity, and earthquake hypocentre data presented in Article 3, helps interpret the Shuilikeng Fault from a regional perspective suggesting that it can be interpreted to invert a pre-existing rift-related fault that bound the Eocene-aged Hsuehshan Basin. They also show that the eastern bounding fault of the Hsuehshan Basin (i.e., the Lishan Fault) can be interpreted to coincide at depth with a cluster of hypocentres between 20 km and 30 km depth. The P-wave velocity model shows a shallowing of higher velocities beneath the Hsuehshan Range in central Taiwan that suggests that what was the basement of the Hsuehshan Basin may be currently being involved in the deformation. Furthermore, the defined deep extension of the bounding faults of the Hsuehshan Range appear to be corroborated by significant earthquakes that struck this part of Taiwan, such as, for example, the 6.2 M_L earthquake occurred in eastern Nantou on March 27th, 2013. In particular, most events associated with the Nantou earthquake occurred along the deep trace of the Shuilikeng and

Lishan faults. The consistence of the Nantou earthquake hypocentres with the interpreted deep locations of the bounding faults of the Hsuehshan Basin further indicates that these faults are significant structures contributing to mountain building in central Taiwan.

Surface geology data presented in Article 4 (in which the study area in expanded southward) indicate that the orogen in the Alishan area of Taiwan is evolving as an imbricate thrust system above a basal detachment that in the north, consistently with results from Article 1 of this thesis, is located at the base of the syn-orogenic sediments. However, the increasing amount of Miocene sediments involved in the deformation southward, indicates that in the south it ramps down section to locate within Miocene rocks. Geological cross-sections, as well as fault contour, stratigraphic cut-off, and branch line maps realized from the surface geology data, all indicate that there is also a change in elevation of this basal detachment as it shallows southward along the strike of the mountain belt. In the east, this basal detachment appears to merge with the Shuilikeng Fault, and to involve pre-Miocene rocks in the deformation. Furthermore, P-wave velocity data suggest that pre-Miocene rocks are involved in the deformation beneath the Alishan area. In this area a pre-existing NE-striking extensional fault system that formed the northern boundary of the Tainan Basin is being inverted together with a deep-seated north-south fault. These reactivating basement faults are folding the thrust system above it causing the along-strike changes in elevation of the basal detachment, and the uplift of Pre-Miocene sediments and basement rocks.

Finally, Article 5 provides an overall view of the deep structure of the entire study area in south-central Taiwan. The combination of seismic tomography, earthquake hypocentre, and gravity inversion data presented in this article indicate that beneath the Coastal Plain and the Western Foothills intense seismicity is taking place near the basement-cover interface. This suggests that the basement-cover interface is acting as an extensive level of detachment. This level of detachment is located at ≥10 km depth and is deeper towards the south, below the basal detachment proposed from surface geology for this part of the mountain belt (e.g., articles 1 and 4 of this thesis), and extends westward of the deformation front, as defined by the Changhua Thrust at the surface. However, across the Shuilikeng and the Chaochou faults, in consistency with what shown in Article 3 of this thesis, there appears to be a change in the style of deformation. Across these faults, earthquake hypocentres define steeply dipping clusters that extend to greater than 20 km depth, and rocks with high P-wave velocities are uplifted along them to form a culmination beneath the Hsuehshan and Central ranges of the mountain belt.

Article 1 - The structure and kinematics of the central Taiwan mountain belt derived from geological and seismicity data

Dennis Brown[1], Joaquina Alvarez-Marron[1], Martin Schimmel[1], Yih-Min Wu[2], and Giovanni Camanni[1]

[1]Institute of Earth Sciences Jaume Almera, ICTJA-CSIC, Lluis Sole i Sabaris s/n, 08028 Barcelona, Spain
[2]Department of Geosciences, National Taiwan University, Taipei, 106, Taiwan

Status of publication: published in "**Tectonics**", (2012), v. 31, no. 5, doi: 10.1029/2012TC003156

Contributions of the Ph.D. student to the article:

- Geological mapping at 1:25.000 and 1:50.000 scale along the surface trace of the Shuilikeng Fault, as well as in the southern part of the map area, within the Western Foothills in the footwall of the Shuilikeng Fault

The structure and kinematics of the central Taiwan mountain belt derived from geological and seismicity data

D. Brown,[1] J. Alvarez-Marron,[1] M. Schimmel,[1] Y.-M. Wu,[2] and G. Camanni[1]

Received 17 May 2012; revised 17 September 2012; accepted 20 September 2012; published 27 October 2012.

[1] The structure of the Taiwan mountain belt is thought to be that of an imbricate thrust and fold belt developed in a forward breaking sequence above a shallowly dipping basal detachment. In recent years, however, a growing amount of seismicity data from the internal part of the mountain belt indicates the existence of widespread fault activity in the middle and lower crust, suggesting that deeper levels of the crust must be involved in the deformation than predicted by the shallow detachment, imbricate thrust belt model. To address this issue, we present new geological mapping, together with earthquake focal mechanism and seismic energy release data from the central part of Taiwan. We concur with the interpretation that the foreland basin part of the Western Foothills comprises an imbricate thrust system that is developing as a forward breaking sequence that is structurally and kinematically linked to a basal detachment at between 7 and 10 km depth. To the east of the foreland basin, however, in the Hsuehshan and Central Ranges, our data show the presence of two fault systems. An earlier, inactive thrust system with a well-developed cleavage is cut by a system of steeply dipping active faults that penetrate to a depth of 25 to 30 km or more. In the Hsuehshan Range, the second fault system is best represented by a structural and kinematic model in which this part of the mountain belt forms a zone of transpression with a structural architecture similar to that of a crustal-scale positive flower structure. Eastward, in the Central Range, Mesozoic basement rocks are over thrusting strongly folded and cleaved deep water sediments of the first, now inactive, thrust system. The involvement of deep crustal levels and Mesozoic basement in the second fault system is suggestive of the reactivation of preexisting basin-bounding faults that were located on the Eurasian continental margin.

Citation: Brown, D., J. Alvarez-Marron, M. Schimmel, Y.-M. Wu, and G. Camanni (2012), The structure and kinematics of the central Taiwan mountain belt derived from geological and seismicity data, *Tectonics*, *31*, TC5013, doi:10.1029/2012TC003156.

1. Introduction

[2] The structure of the faulted and folded rocks involved in the Taiwan mountain belt (Figure 1) is often presented as an imbricate thrust and fold belt developed in a forward breaking sequence above a shallow, east dipping basal detachment [*Suppe*, 1980, 1981; *Ding et al.*, 2001; *Carena et al.*, 2002; *Yue et al.*, 2005; *Malavieille and Trullenque*, 2009]. The bulk of the data for this interpretation of the structure come from surface geological observations, shallow reflection seismics, and borehole data along the western flank of the mountain belt, in what is known as the Western Foothills [*Suppe*, 1981; *Namson*, 1981; *Mouthereau et al.*, 2001, 2002; *Hickman et al.*, 2002; *Yue et al.*, 2005] (Figure 1). The more internal part of the mountain belt is less well understood because of difficult access in this area of high, rugged topography and heavy forest cover. Nevertheless, collapsing [*Jones and Stewart*, 1997] and selective picking of relocated small-magnitude (between M_L 1 and 4) earthquake hypocenter data appear to validate the interpretation of extending a detachment from beneath the Western Foothills across the entire mountain belt in central Taiwan [*Carena et al.*, 2002]. Combining the seismicity data with surface geological data from published geological maps from the Western Foothills and the western part of the Hsuehshan Range (see section 2.1), *Yue et al.* [2005] have also interpreted the Taiwan mountain belt to have developed in a forward breaking sequence above a basal detachment that extends eastward, with ramps and flats, beneath the entire mountain belt. In this latter interpretation, the more internal units are structurally linked to the basal detachment, forming three imbricate thrust sheets with the largest of these, the Tili thrust sheet, transporting nearly the entire Taiwan mountain belt several tens of kilometers westward [see *Yue et al.*, 2005, Figure 16]. Other orogen-scale structural interpretations [e.g., *Malavieille and Trullenque*, 2009] have added faults and complexities, but maintain the forward

[1]Instituto de Ciencias de la Tierra "Jaume Almera," CSIC, Barcelona, Spain.
[2]Department of Geosciences, National Taiwan University, Taipei, Taiwan.

Corresponding author: D. Brown, Instituto de Ciencias de la Tierra "Jaume Almera", CSIC, Lluis sole i Sabaris s/n, ES-08028 Barcelona, Spain. (dbrown@ictja.csic.es)

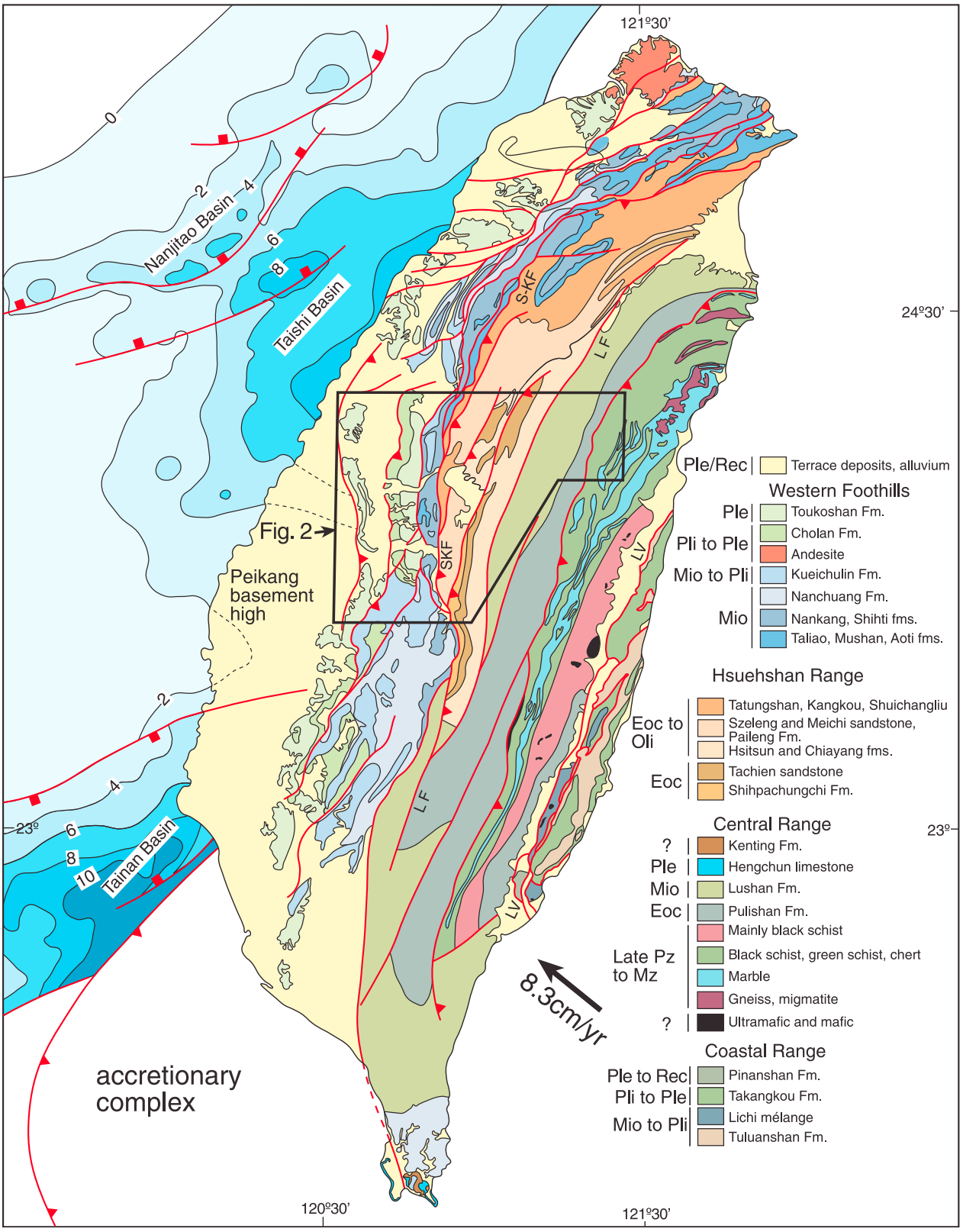

Figure 1. Geological map of Taiwan [after *C.-H. Chen et al.*, 2000]. The basin morphology and structure in the Taiwan Strait is from *Teng and Lin* [2004]. Contours denote the thickness of the Cenozoic sediments in the basins. Note the orientation of the basin-bounding faults relative to the convergence vector (8.3 cm/yr toward N49°W [*Yu et al.*, 1997]). The location of the Peikang basement high is shown, as is that of Figure 2. SKF = Shuilikeng fault, LF = Lishan fault, LV = Longitudinal Valley. Ple/Rec = Pleistocene/Recent, Pli = Pliocene, Mio = Miocene, Eoc = Eocene, Pz = Paleozoic, Mz = Mesozoic.

breaking imbricate thrust system with a shallowly dipping, throughgoing basal detachment.

[3] There is, however, a growing amount of geophysical data from the internal part of the mountain belt that indicates widespread fault activity in the middle and lower crust, well below the level of the proposed detachment [*Wu et al.*, 1997, 2004; *Gourley et al.*, 2007; *Mouthereau and Lacombe*, 2006; *Kaus et al.*, 2008; *Mouthereau et al.*, 2009; *Yamato et al.*, 2009; *Bertrand et al.*, 2009, 2012; *Wang et al.*, 2010; *Kuo-Chen et al.*, 2012]. For example, recent magnetotelluric experiments show a prominent electrical conductor that extends into the middle crust, crossing the proposed detachment [*Bertrand et al.*, 2009, 2012]. Similarly, analyses of seismicity data also indicate that there are several steeply dipping faults that penetrate into the middle and perhaps even the lower crust [e.g., *Wu et al.*, 1997, 2004; *Gourley et al.*, 2007]. On the basis of these data, it has been suggested that any model for the structural architecture of the Taiwan mountain belt needs to incorporate a number of steeply dipping active faults that involve nearly the entire crust [*Wu et al.*, 1997, 2004; *Gourley et al.*, 2007; *Mouthereau and Lacombe*, 2006; *Kaus et al.*, 2008; *Yamato et al.*, 2009; *Bertrand et al.*, 2009, 2012]. A corollary to this is that these faults would have to disrupt any forward breaking sequence and cut the basal detachment proposed in the imbricate fold and thrust belt model. This proposal therefore has significant implications for the geometric, mechanical and kinematic evolution of the Taiwan mountain belt that are very different from what has so far been presented on the basis of the imbricate thrust belt model.

[4] While seismicity, GPS, and thermochronological data can provide significant insights into the kinematics and mechanics of the Taiwan mountain belt, in order to further advance our understanding of the structures and the kinematics that provide the first-order constraints on these types of data, much more surface geology data are needed from its interior. In this paper we present new geological mapping in the central part of Taiwan which spans nearly the entire width of the mountain belt (Figure 1). These geological data are used to propose a revised stratigraphic scheme for the Hsuehshan Range and to determine the regional structural geology from which geometically constrained cross sections are constructed. These data are then integrated with earthquake focal mechanism and seismic energy release data to place constraints on a model for the structural architecture and kinematics of this part of the mountain belt that takes the relative deformation sequence and the deep seismicity into account. Details of the methodologies used in each of these steps are below. These data and the model interpreted from them are then discussed in relation to other local- and regional-scale structural and kinematic interpretations.

2. Geological Background

2.1. Tectonostratigraphic Zones

[5] The Taiwan mountain belt is divided into four roughly N-S oriented tectonostratigraphic zones that are separated by major faults (Figures 1 and 2). From west to east these zones are; the Western Foothills, the Hsuehshan Range, the Central Range, and the Coastal Range. The Western Foothills, Hsuehshan Range, and Central Range are forming as the result of deformation and uplift of Eocene to Miocene sediments and older continental margin rocks of Eurasia and the latest Miocene and younger synorogenic sediments in the foreland basin [e.g., *Suppe*, 1980; *Yue et al.*, 2005; *Mouthereau et al.*, 2001]. The Western Foothills form the frontal part of the mountain belt and is juxtaposed against the Hsuehshan Range along the Shuilikeng fault. To the east, the Hsuehshan Range is juxtaposed against the Central Range along the Lishan fault. The Coastal Range is composed of volcanic rocks and sedimentary basins of the Luzon arc, which is being thrust obliquely over the Eurasian margin along the Longitudinal Valley fault [e.g., *Yu and Kuo*, 2001; *Chen et al.*, 2007; *Shyu et al.*, 2008]. Below we give an overview of the outcropping stratigraphy of the Western Foothills, Hsuehshan Range, and the western part of the Central Range.

2.2. Stratigraphy

[6] The stratigraphy of the outcropping Eurasian continental margin in central Taiwan can be broadly divided into Permian to Cretaceous prerift clastic sediments, marble, and metaigneous rocks (which we here call basement), Eocene synrift clastic sediments that are unconformably overlain by early Oligocene clastics [e.g., *Chiu*, 1975; *Ho*, 1988; *Teng*, 1992; *Jahn et al.*, 1992; *Shaw*, 1996; *Huang et al.*, 1997, 2001; *Lin et al.*, 2003; *Teng and Lin*, 2004]. The Oligocene unconformity is interpreted to represent the rift-to-drift transition, or breakup unconformity [e.g., *Teng*, 1992; *Huang et al.*, 1997, 2001; *Lin et al.*, 2003; *Teng and Lin*, 2004]. The Oligocene is overlain by Miocene platform margin to slope clastic sediments which are in turn overlain by latest Miocene to Holocene synorogenic clastics of the foreland basin to the Taiwan mountain belt [e.g., *Chiu*, 1975; *Ho*, 1988; *Teng*, 1992; *Shaw*, 1996; *Huang et al.*, 1997, 2001; *Lin et al.*, 2003; *Teng and Lin*, 2004]. Below, the outcropping stratigraphy of each tectonostratigrapic zone is presented.

[7] The outcropping stratigraphy of the Western Foothills consists of Eocene through Miocene clastic sediments of the Eurasian platform margin and latest Miocene to Pliocene through Holocene synorogenic sediments [e.g., *Teng*, 1992] (Figures 2 and 3). The oldest unit that outcrops comprises volcanic rocks of the Tsukeng Formation. This formation was previously assigned either an Eocene or Oligocene age, but recent studies of large foraminifera and U-Pb dating of zircons from an ash layer at the top of the sequence indicates that it is late middle Eocene in age (C-Y. Huang, personal communication, 2012). A borehole through the Tsukeng Formation encountered Eocene age rocks of the Paileng Formation (see below) [*Chiu*, 1975]. The Tsukeng Formation is unconformably overlain by Miocene age, mostly shallow water clastic deposits, although some authors claim that the Oligocene Shuichangliu Formation is found above the Tsukeng Formation [e.g., *Chiu*, 1975; *Ho*, 1988]. In the study area, the Miocene can be broadly divided into four sedimentary sequences, each of which begins with a thick-bedded sandstone unit at the base and is overlain by thin-bedded sandstone (locally thick beds) and shale. Because of differences in the naming and discrimination of individual formations between the 1:50,000 geological maps in the study area, in this paper we define the following four sequences (Figure 3). The early Miocene Takeng Formation is approximately 800 to 1000 m thick and is overlain by the

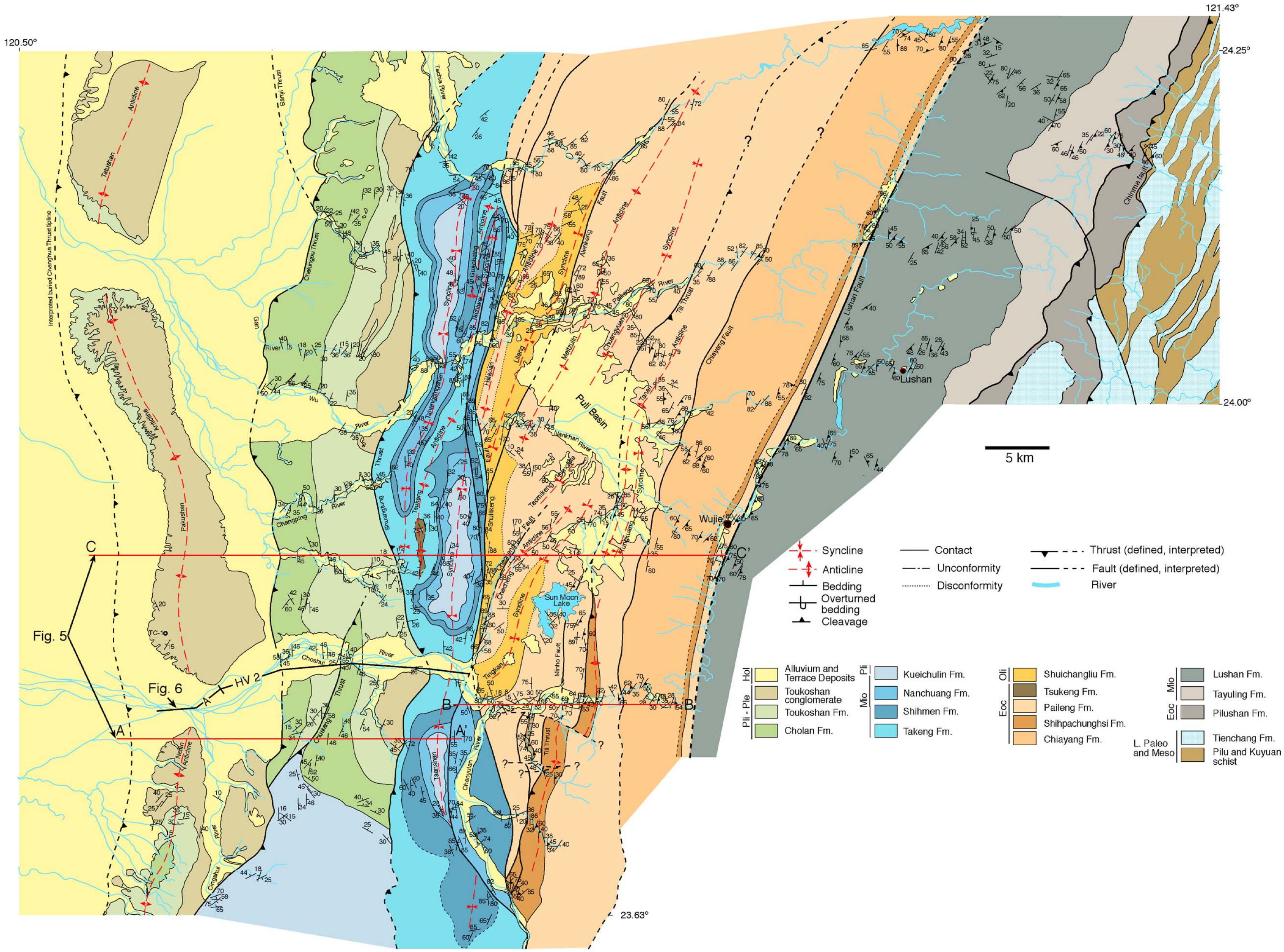
120.50°
121.43°
24.25°
24.00°
23.63°
5 km
Puli Basin
Sun Moon Lake
Lushan
Wujie
Fig. 5
Fig. 6
HV 2
A
A'
B
B'
C
C'
Syncline
Anticline
Bedding
Overturned bedding
Cleavage
Contact
Unconformity
Disconformity
Thrust (defined, interpreted)
Fault (defined, interpreted)
River
Hol
Alluvium and Terrace Deposits
Pli - Ple
Toukoshan conglomerate
Toukoshan Fm.
Cholan Fm.
Pli
Kueichulin Fm.
Mio
Nanchuang Fm.
Shihmen Fm.
Takeng Fm.
Oli
Shuichangliu Fm.
Eoc
Tsukeng Fm.
Paileng Fm.
Shihpachunghsi Fm.
Chiayang Fm.
Mio
Lushan Fm.
Tayuling Fm.
Eoc
Pilushan Fm.
L. Paleo and Meso
Tienchang Fm.
Pilu and Kuyuan schist

Figure 2

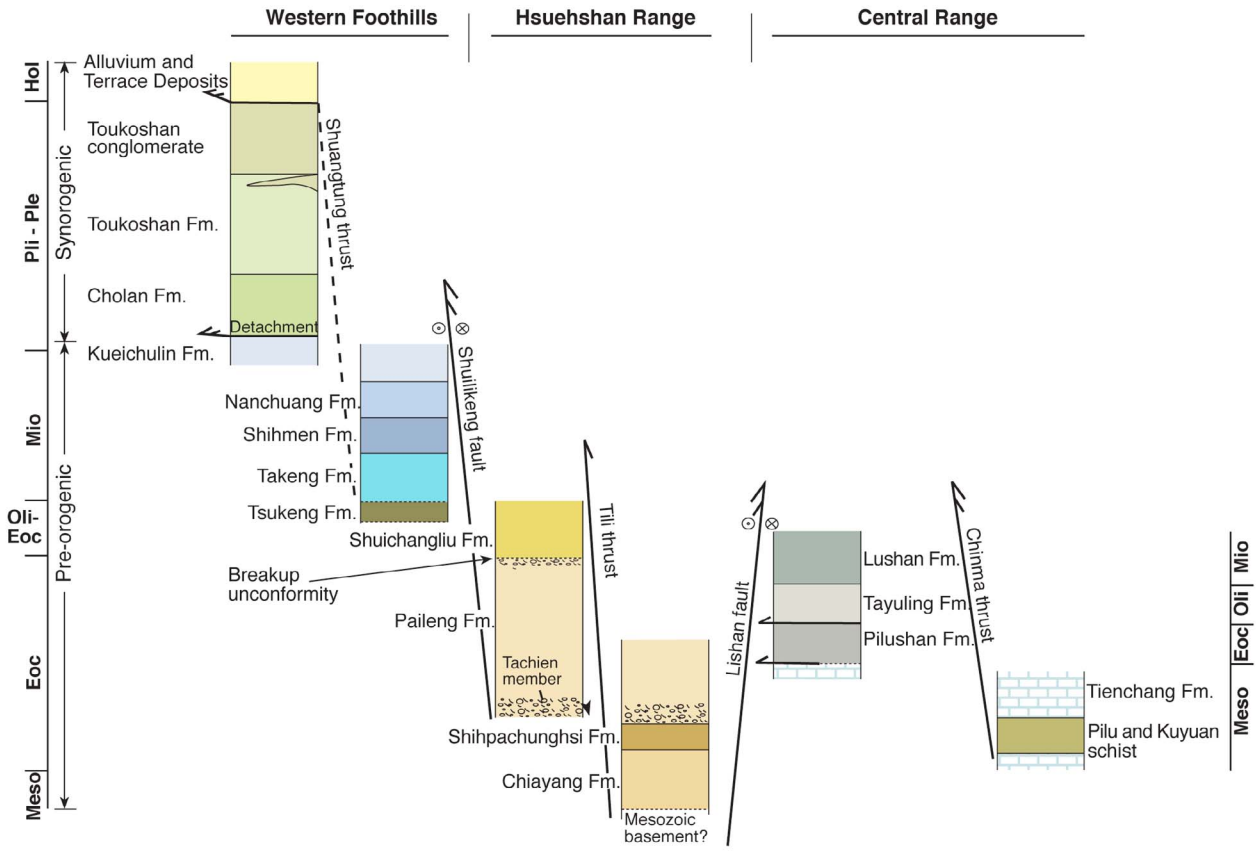

Figure 3. Schematic tectonostratigraphic columns for the outcropping geology of the different zones in central Taiwan. The preorogenic and synorogenic units are indicated for the Western Foothills and the Hsuehshan Range, as is the breakup unconformity. Note that the ages of the formations in the Central Range are a different scale. Faults with a single arrow head are D1, and those with a double arrow head are D2 (see section 5.2 for discussion of these two sequences of deformation).

up to 500 m thick Shihmen Formation, which is in turn overlain by the ~250 m thick Nanchuang Formation. The Nanchuang Formation is conformably overlain by the latest Miocene to early Pliocene Kueichulin Formation. There is some discussion as to whether the Pliocene age upper part of the Kueichulin Formation or the overlying Pliocene Chinshui shale is the first synorogenic sedimentary unit to appear in the foreland basin [e.g., *Teng*, 1987; *Covey*, 1986]. The Chinshui shale comprises a several hundred meter thick member at the base of the Pliocene to Pleistocene Cholan Formation. The Cholan Formation comprises approximately 2.5 km of interbedded mudstone, shale, and sandstone. The Cholan Formation is conformably overlain by the Pleistocene Toukoshan Formation, a coarsening upward sequence made up of thick-bedded sandstone with shale interbeds that, upward, becomes interfingered with, and eventually completely replaced by, conglomerate. In parts of the map area, the Toukoshan Formation may reach up to 5 km in thickness. The Toukoshan Formation is overlain by Holocene age gravels that, in places, are several hundred meters thick.

[8] The stratigraphy of the Hsuehshan Range in the study area is complicated by a complex structure and the almost complete lack of fossils. While the rocks in the Hsuehshan Range are assigned an Eocene and Oligocene age [e.g., *Ho*, 1988], in light of new structural and fossil data (see below) [*Chen et al.*, 2009], the stratigraphic sequence accepted up to now [e.g., *Ho*, 1988; *Lo and Yang*, 2002, *C.-Y. Huang et al.*, 2000] appears to have a number of problems. In this paper, we propose a new stratigraphic scheme that has arisen from our mapping in which the oldest stratigraphic unit is the Chiayang Formation (Figure 3). The Chiayang Formation begins with a sequence of thick-bedded sandstone at its base (the Yushan member), followed by an unknown thickness of strongly folded shale with a penetrative cleavage. It is not clear what lies below the Chiayang Formation since it is everywhere in fault contact with the rocks to the west. The Shipachungchi Formation is interpreted to overlie the Chiayang Formation, although the contact is not exposed. It is composed of several hundred meters of thin-bedded sandstone and mudstone. It is in turn overlain by the Paileng

Figure 2. Geological map of the study area in central Taiwan. The locations of the cross sections in Figure 5 and the seismic lines in Figure 6 are shown. A larger-scale version of this map is provided in Figure S1. Ple/Rec = Pleistocene/Recent, Pli = Pliocene, Mio = Miocene, Eoc = Eocene, Pz = Paleozoic, Mz = Mesozoic.

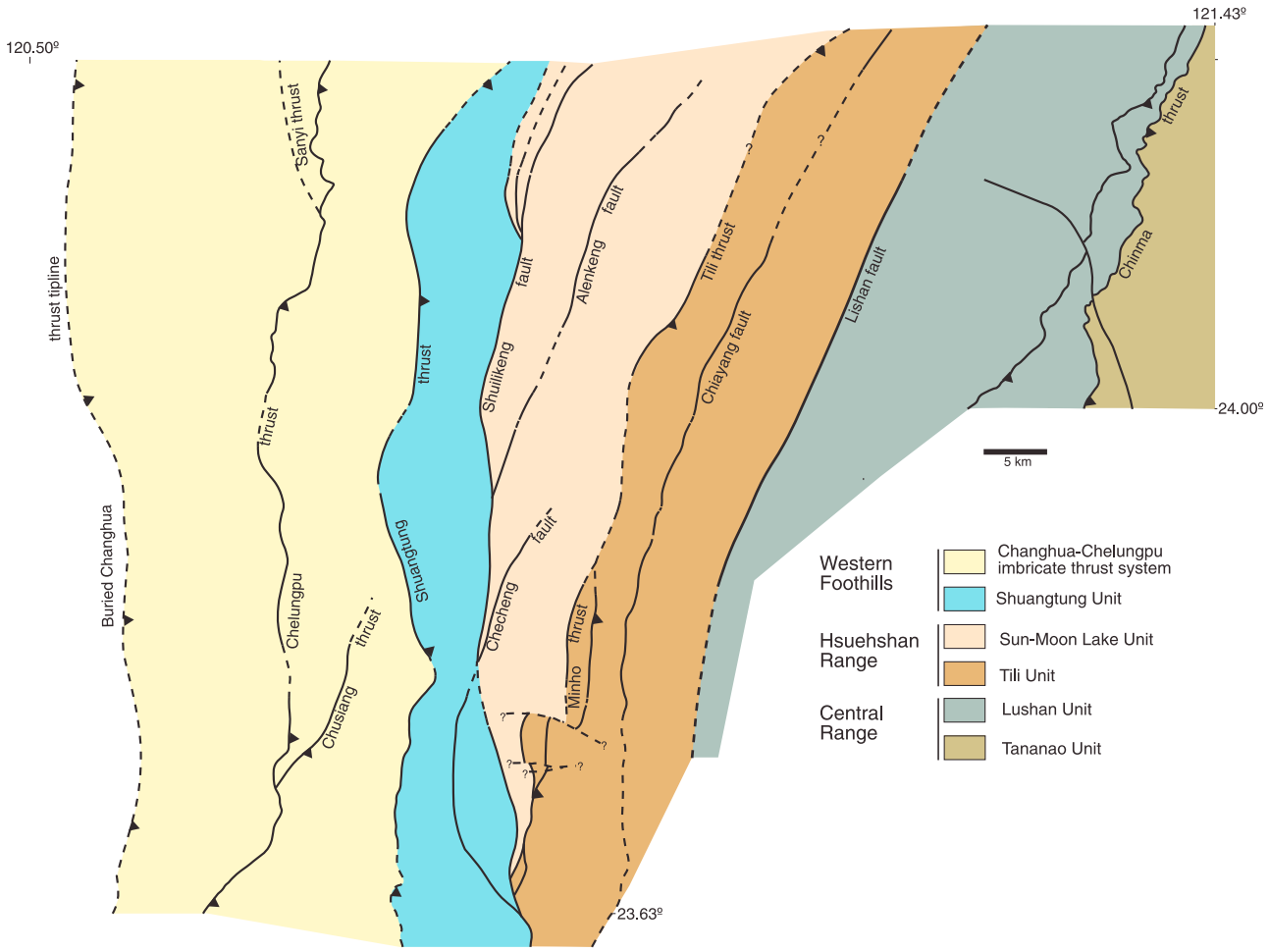

Figure 4. Map of the structural units discussed in the text.

Formation. This contact relationship is clear along, and to the south of, the Choshui River (Figure 2). The lowest part of the Paileng Formation, the Tachien member, has recently been dated by large foraminifera from outcrops along the Choshui River to the south of Wujie (Figure 2) as being late early to early middle Eocene in age [*Chen et al.*, 2009]. The Paileng Formation consists of thick-bedded, coarse-grained to pebble conglomerate quartzite and argillite at its base (the Tachien member), overlain by interbedded sandstone and bioturbated argillite, and topped by a several hundred meter thick, coarse-grained to pebble conglomerate quartzite with minor amounts of lithofragments and feldspar. The total thickness of the Paileng Formation is not known for sure, but it may be as much as 4 to 5 km, and it makes up a large part of the Hsuehshan Range (Figure 2). The Paileng Formation is unconformably overlain by several hundred meters of late early Oligocene interbedded sandstone and shale of the Shuichangliu Formation. Within our map area of the Hsuehshan Range there are no Miocene rocks above the Oligocene, although they do appear farther to the north. There is no evidence, other than in the Puli Basin, that the Pliocene and younger synorogenic sediments were ever deposited on top of the Hsuehshan Range.

[9] The eastern part of the Central Range in the study area is composed of Mesozoic marbles, with lesser lenses of schist (Figures 2 and 3). These Mesozoic rocks are both unconformably overlain by, and in fault contact with, the Pilushan Formation (Figure 2), which is made up of slate and phyllite with, locally, interbeds of sandstone, all of undifferentiated Eocene age. The Pilushan Formation is thought to have been deposited in a shallow marine environment [e.g., *Huang et al.*, 1997]. Strong folding and penetrative cleavage development, together with difficult access in the high mountains, make it impossible to determine the thickness of the Pilushan Formation. Along its western margin, the Pilushan Formation is in fault contact with the late Oligocene slate, phyllite and metasandstone of the Tayuling Formation (Figure 2), which in turn is overlain by the slate and thin to thick-bedded sandstone of the early to middle Miocene Lushan Formation (Figure 3). Intense folding and cleavage development make it impossible to determine the thickness of these two units. Foraminifera in both the Tayuling and the Lushan Formations suggest that they were deposited in an open marine environment at water depths of between 500 and 1500 m [*Chang*, 1976; *Huang et al.*, 1997]. The Lushan Formation is in contact with the rocks of the Hsuehshan Range to the west along the Lishan fault (Figure 2).

3. Structure

3.1. Methodology

[10] The study area in Central Taiwan (Figure 2: a larger-scale version of this map is available in Figure S1 in the

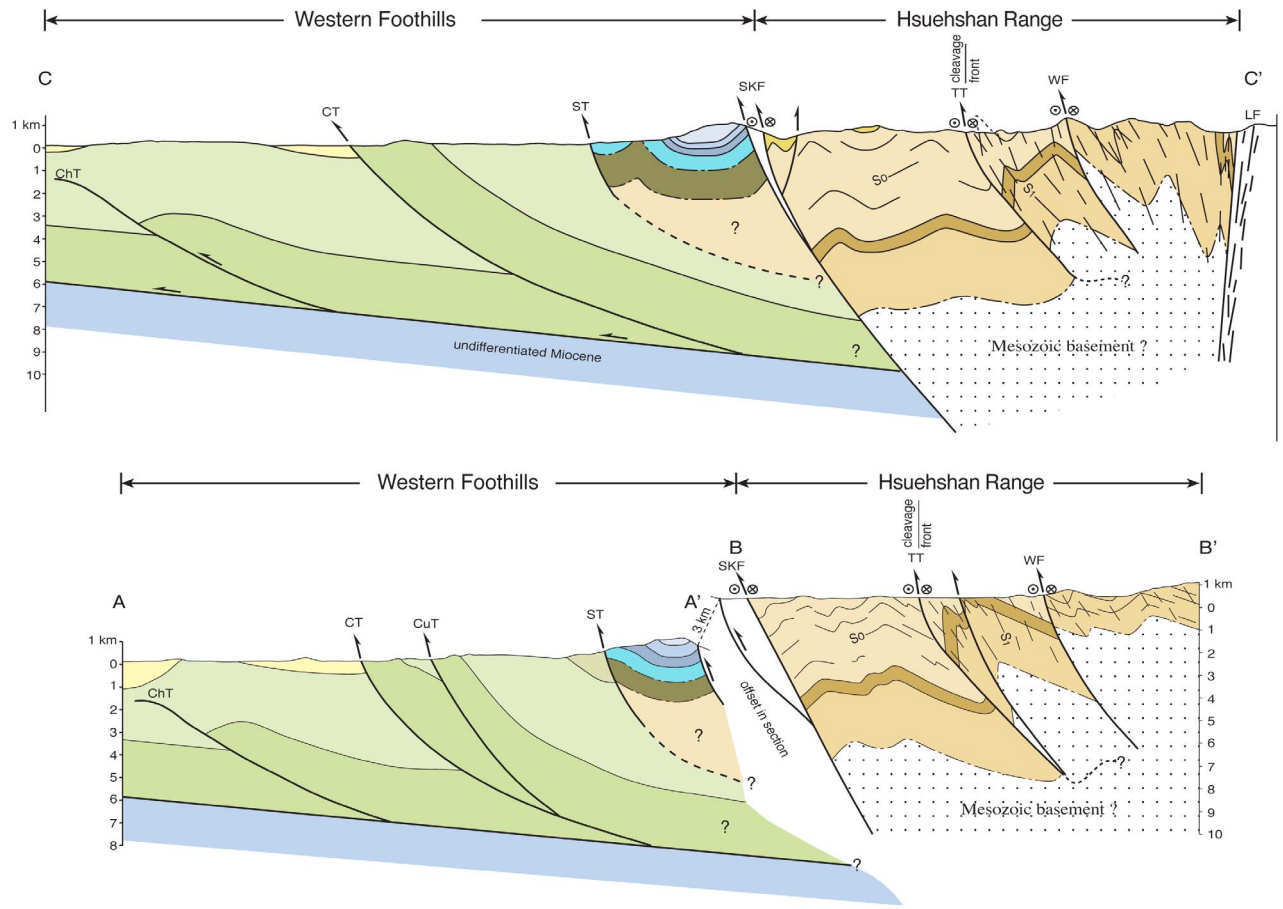

Figure 5. Upper crustal geological cross sections through the central and southern part of the map area. See Figure 2 for the location. ChT = Chuanghua thrust, CT = Chelungpu thrust, CuT = Chusiang thrust, ST = Shuangtung thrust, SKF = Shuilikeng fault, TT = Tili thrust, CF = Chiayang fault, LF = Lishan fault.

auxiliary material) covers slightly more than eight 1:50,000 scale topography maps.[1] Where available, the 1:50,000 scale geological maps of the Central Geological Survey were used as base maps, although all of the structural data and the map interpretation presented in Figure 2 are from our own data. There are no data in the north central and southeast parts of the map presented in Figure 2 because of lack of access. In the description of the structure that follows, the map area is divided into a number of individual units that are based on similarities in structure, stratigraphy, and kinematics. From west to east these are; the Changhua-Chelungpu imbricate thrust system, and the Shuangtung, Sun-Moon Lake, Tili, Lushan, and Tananao Units (Figure 4).

[11] Cross sections that are geometrically constrained from the surface geological data are presented for the southern and middle part of the map area in Figure 5. Cross sections for the northern part of the map area are not included for reasons related to the structural complexity found there (see below). The southernmost section is divided into two parts that are offset by 3 km. The cross sections were constructed using standard construction techniques [e.g., *Dahlstrom*, 1969; *Hossack*, 1979] in which the thicknesses of the formations are taken directly from the surface geological map, and bedding is projected into the subsurface using dip data measured along the section. The location of the basal detachment beneath the Western Foothills is determined using the geometric controls provided by the stratigraphy and the bedding dips, as well as reflection seismic profiles. In other areas, where difficulty in determining the location of a basal detachment where found, we use seismic energy release data to place constraints on the regional interpretation of the deep structure (section 4.2). Because of the often high, rugged topography and dense forest cover, the major faults in the map area are typically poorly exposed along their strike length so satellite images and air photos are used to interpolate their continuity between mapped locations. Below, earthquake focal mechanism data are used to help place further constraints on the kinematics derived from field data. Field geology and seismicity data all indicate that the dominant faults have an overall oblique thrusting through to strike-slip sense of displacement and therefore plane strain cannot be assumed. For this reason we have not provided restored sections, since they would misrepresent the total amount of displacement along most faults.

[1]Auxiliary material data sets are available at ftp://ftp.agu.org/apend/tec/2012tc003156. Other auxiliary material files are in the HTML. doi:10.1029/2012TC003156.

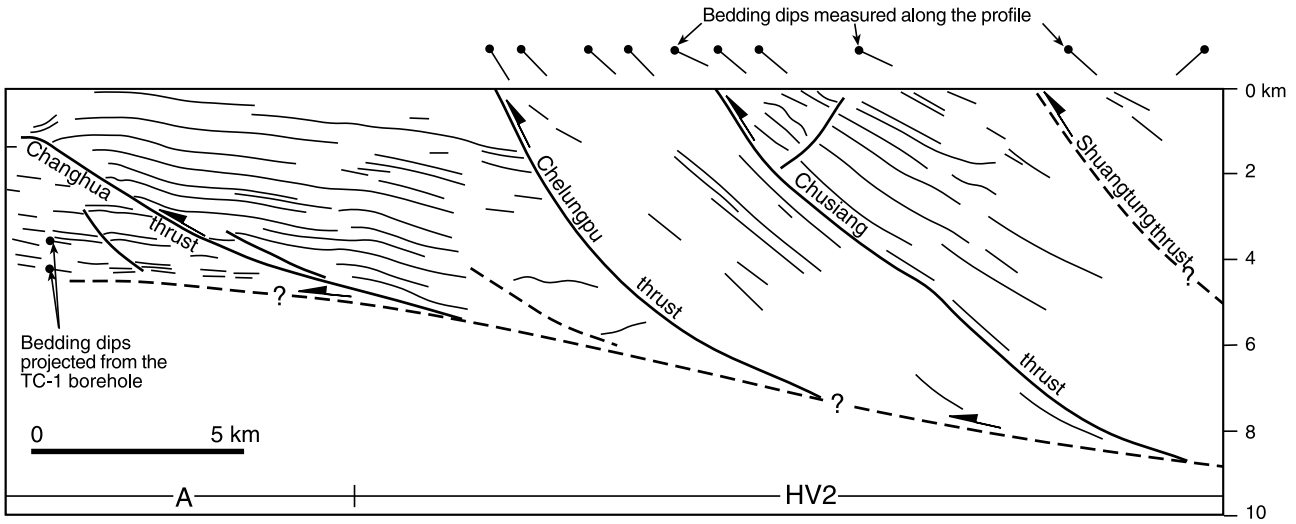

Figure 6. Line drawing of the seismic profiles A (taken from *Yue et al.* [2005]) and HV2 [*Wang et al.*, 2002]. The locations of these profiles are shown in Figure 2. The seismic profiles are available in Figure S2.

3.2. The Changhua-Chelungpu Imbricate Thrust System

[12] The buried Changhua thrust and its associated hanging wall ramp anticlines are developed entirely in the synorogenic Pliocene to Holocene sediments, forming the frontal structure of the mountain belt in central Taiwan (Figures 2 and 5). The structure of this poorly exposed thrust sheet is largely derived from published reflection seismic and borehole data (Figure 6; the uninterpreted data are available in Figure S2) and scarce surface geological data. The reflection seismic data show that the Pakushan anticline has shallow forelimb and back-limb dips that is well imaged in seismic HV2 along the Choshui River [see also *Mouthereau et al.*, 1999; *Wang et al.*, 2003; *Yue et al.*, 2005; *Simoes et al.*, 2007a]. However, farther south, the Neilin anticline plunges moderately (25° to 30°) northward and locally has a steep to slightly overturned forelimb and moderate back-limb dips (Figure 2).

[13] In the northern part of the map area, the Sanyi thrust (Figure 2), although not exposed here, has been intersected by several boreholes. It is interpreted to splay off the footwall of the Chelungpu thrust, placing Pliocene Kueichulin Formation on top of Holocene gravels [*Hung et al.*, 2009]. The Sanyi thrust outcrops in several places out of our map area. For example, along the Tachia River it affects the Holocene gravels and displays an oblique thrusting, top-to-the-northwest sense of movement [*Chen et al.*, 2003]. The Sanyi thrust sheet widens considerably northward, but this is out of the current study area and therefore will not be considered further here.

[14] To the north of the Choshui River, the Chelungpu thrust sheet is developed in the Pliocene and younger synorogenic sediments. In map view (Figure 2), it juxtaposes the Pliocene Cholan Formation against the Holocene alluvium in the Changhua thrust sheet along the Chelungpu thrust. South of the Choshui River, the Chelungpu thrust ramps down into the Kuechulin and Nanchuang Formations, placing them on top of the Holocene sediments and the Pleistocene Toukoshan Formation in the back limb of the Neilin anticline (Figure 2). The Chelungpu thrust sheet forms an overall monoclinal structure with bedding (S_0) that dips shallowly to moderately northeast to southeast (Figures 7 and S3.1), with some scatter caused by local structures. The Chelungpu fault zone outcrops only locally in the map area, so direct observations of its geometry and kinematics are rare. Where it does outcrop, it is a several tens of meters wide zone that ranges in deformation style from highly disrupted and discretely faulted shale to a gouge (see Figure S3.2). While kinematic indicators are largely absent in the Chelungpu fault zone, GPS data [*Yu et al.*, 1997, 2003; *Bos et al.*, 2003; *Lin et al.*, 2010; *Ching et al.*, 2011a], earthquake focal mechanism determinations derived from the 1999 Chi-Chi and other earthquakes [*Kao and Chen*, 2000; *Chang et al.*, 2000; *K. C. Chen et al.*, 2002; *Wu et al.*, 2008a, 2008b] and, locally, striations on the hanging wall of the 1999 Chi-Chi surface rupture [e.g., *Lee and Chan*, 2007] indicate that it is an oblique thrust with a top-to-the-northwest sense of movement. In the southern part of the Chelungpu thrust sheet, the Chusiang thrust (Figure S3.3) splays off of the Chelungpu thrust and puts Cholan Formation on top of Toukhshan Formation (Figures 2, 5, and 6). Along the Choshui River there is minor folding in the hanging wall of the Chusiang thrust, but overall bedding dips indicate that it is a monoclinal structure (Figure 2).

[15] Along nearly its entire length in the map area, the Chelungpu thrust is developed in the Chinshui shale, the basal member of the Cholan Formation, suggesting that it is a layer parallel thrust that detaches at this level in the stratigraphy (Figures 2 and 5). However, along the Gan River (Figures 2 and 8), the Chinshui shale is folded into an approximately kilometer wide hanging wall anticline that consists of roughly north and south plunging, box shaped to nearly isoclinal folds (Figure S3.4). In the back limb, bedding has a moderate, consistently eastward dip that projects over the anticline formed by the Chinshui shale. Farther south, along the Cingshuei River, the Nanchuang and

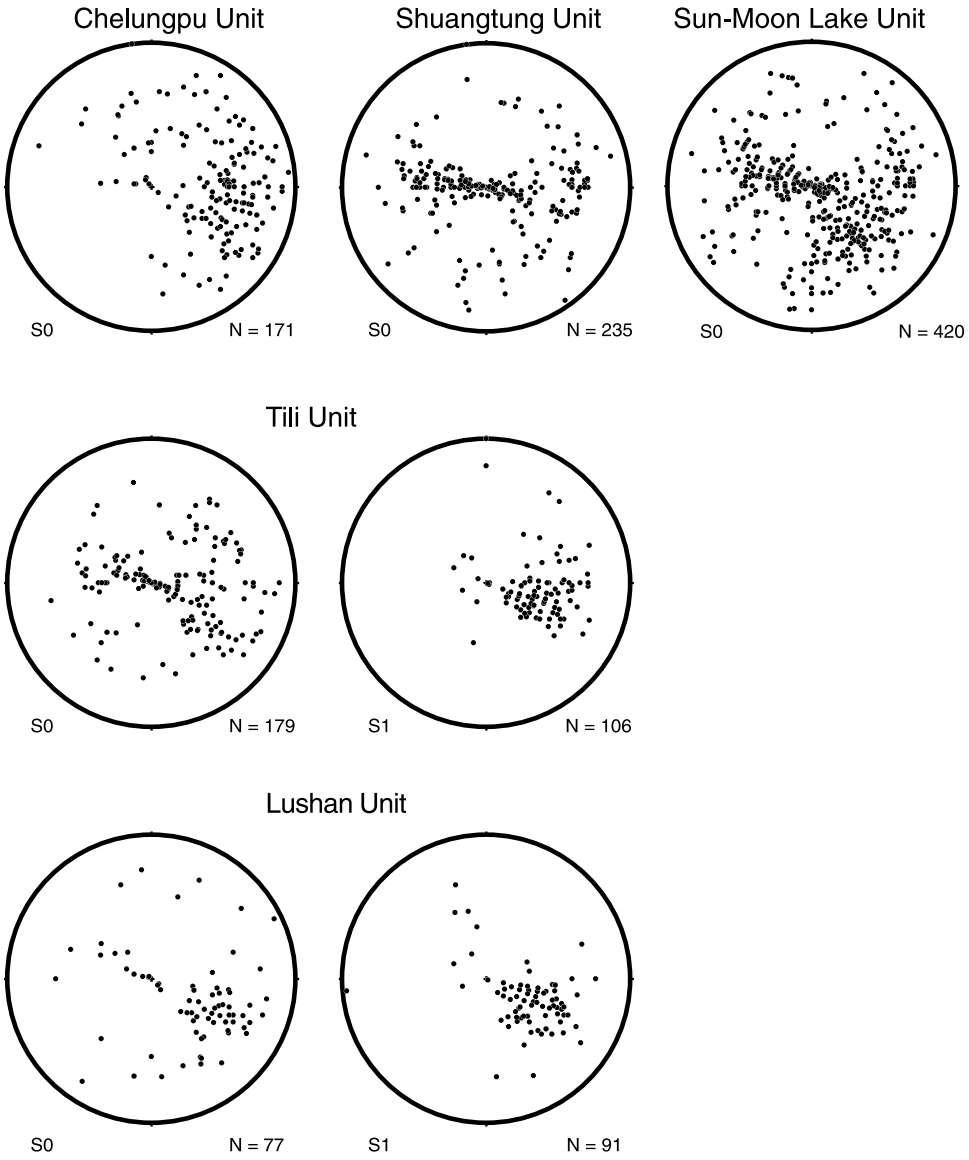

Figure 7. Lower hemisphere, equal-area stereographic projections of bedding and cleavage dip azimuths from the various structural units. These data were plotted using the Stereonet program by R. W. Allmendinger.

Kuechulin Formations are also folded into a series of hanging wall anticlines and synclines immediately above the Chelungpu thrust (Figure 8) (Figure S3.5). While these two areas may provide an opportunity to determine hanging wall cutoffs from which displacement along the Chelungpu thrust can be determined, we hesitate to do so on the basis of these two outcrops alone.

[16] Based on bedding dips and the reflection seismic data, the Changhua and Chelungpu thrusts can be interpreted to be listric faults that merge with a basal detachment that dips ∼6° eastward, forming an imbricate thrust system (Figures 5 and 6). The dip of the detachment is consistent with the footwall bedding dips below the Changhua thrust obtained from the borehole TC-1 (Figure 6), with the interpretation of reflection seismic data, and is in keeping with the dip interpreted by other studies [e.g., *Johnson and Segall*, 2004; *Mouthereau and Lacombe*, 2006; *Simoes et al.*, 2007a; *Lee and Chan*, 2007]. Hanging wall bedding dips are moderate along the area of the cross sections, and by maintaining formation thicknesses we interpret the Changhua and Chelungpu thrusts to merge with the basal detachment at ∼6 and between 8 and 9 km depth, respectively (Figures 5 and 6). This interpretation places the location of the 1999 Chi-Chi earthquake [*Wu et al.*, 2008a, 2008b] on the Chelungpu thrust, near where it merges with the basal detachment. It also fits well with the hypocenter locations of seismic events within the first 15 min of the Chi-Chi aftershock sequence [*Chang et al.*, 2007]. Other interpretations have the Chelungpu thrust splaying off the basal detachment at ∼4 to 10 km depth, or even more [*Kao and Chen*, 2000; *Chen et al.*, 2001b; *Johnson and Segall*, 2004; *Yue et al.*, 2005; *Mouthereau and Lacombe*, 2006; *Mouthereau et al.*, 2001; *Lin*, 2007; *Lee and Chan*, 2007; *Huang et al.*, 2008; *Yanites et al.*, 2010]. Based on the

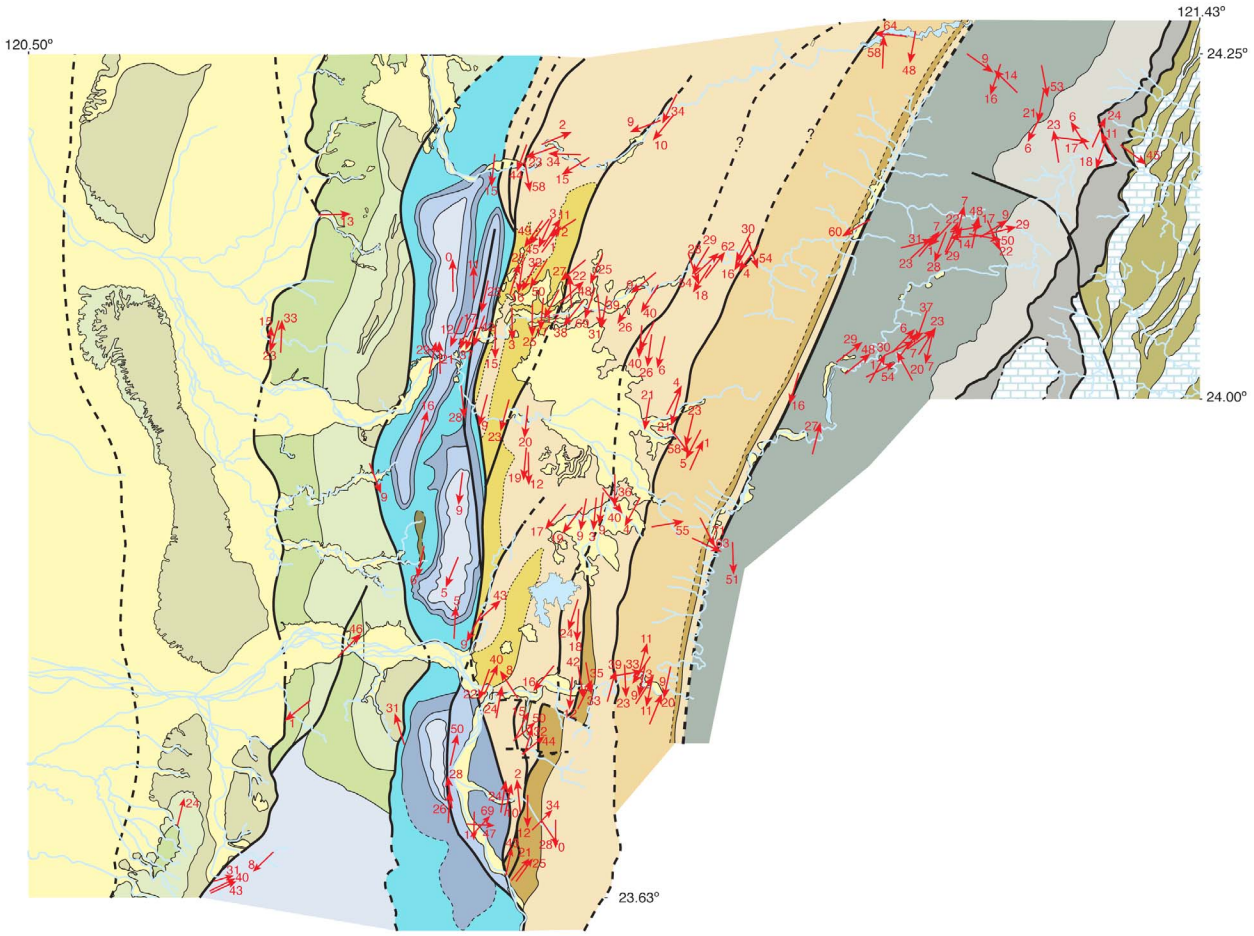

Figure 8. Map of fold axes orientations and plunge values throughout the study area. To the north of the Choshui River, fold axes plunge overall toward the south, whereas south of the river they take on a northward plunge.

disruption of seismic reflections, horizontal displacement on the Changhua thrust in the plane of the seismic profile appears to be on the order of 500 m [see also *Yue et al.*, 2005; *Mouthereau and Lacombe*, 2006; *Simoes et al.*, 2007a]. In our cross sections, the apparent displacement along the Chelungpu thrust is a minimum of ~15 km if the intersection of the Cholan Formation with the surface is restored to its footwall cutoff. We stress, however, that movement of material out of the plane of section by oblique thrusting, together with the scarcity of stratigraphic cutoffs, make it difficult to accurately determine the amount of displacement for the Chelungpu thrust sheet. Finally, the fact that to the south of the Choshui River the Chelungpu thrust cuts down section in the stratigraphy (Figure 2) indicates the presence of a lateral, or oblique, ramp that appears to strike roughly NE-SW.

3.3. The Shuangtung Unit

[17] In map view, the Shuangtung Unit comprises middle to late Eocene through to early Pliocene rocks which are juxtaposed against the late Miocene to Pleistocene rocks of the Chelungpu Unit along the Shuangtung thrust in the west, and in the east against the Eocene and Oligocene rocks of the Sun-Moon Lake and Tili Units along the Shuilikeng fault (see section 3.4) (Figure 2). The involvement of the older platform margin strata in the deformation indicates that the Shuangtung thrust ramps down into a deeper stratigraphic level than the basal detachment of the Changhua-Chelungpu imbricate thrust system.

[18] The Shuangtung thrust outcrops very poorly in the field and kinematic indicators are largely lacking. Coseismic and postseismic horizontal GPS velocities associated with the 1999 Chi-Chi earthquake indicate that it is an oblique thrust with a top-to-the-northwest sense of movement [*Yu et al.*, 2003; *Lin et al.*, 2010]. Along the Changping River (Figure 2), the fault is expressed as a narrow zone of gouge with a decameter-scale west verging hanging wall anticline–footwall syncline pair (Figure S3.6). Along the Wu River, a number of small faults indicate a top-to-the-northwest sense of movement. In the northern part of the map area, the Shuangtung thrust takes on a northeast strike, as do bedding traces in its hanging wall. The Shuangtung thrust has been poorly imaged in reflection seismic profiling (Figure 6), where it appears to be a moderately to steeply eastward dipping fault [see also *Wang et al.*, 2003; *Yue et al.*, 2005; *Simoes et al.*, 2007a, 2007b].

[19] The surface geology of the Shuangtung Unit comprises two wide "en echelon" synclines, the Tahenpingshan

and Taanshan synclines in the north and south, respectively (Figure 2). Note that here we interpret the Taanshan and Chichitashan synclines [*C.-S. Huang et al.*, 2000] to be the same structure. These synclines are separated by the narrow Tsukeng anticline that is cored in its southern part by the Eocene age Tsukeng Formation. These folds are non-cylindrical (Figure 8), as is shown by the weak great circle girdle formed by bedding dips within the unit (Figure 7), and are cut by both the Shuangtung thrust and the Shulilikeng fault.

[20] In the northern part of the map area, the eastern flank of the Shuangtung Unit is tightly folded (Figures S3.7 and S3.8 show vertical bedding along this limb) into the moderately southward plunging Guaosing anticline (Figure S3.9) and Tachiwei syncline (Figure 2). The eastern limb of the Tachiwei syncline and the eastern flank of the Taanshan syncline are cut by the high-angle, brittle Guaosing fault (Figures S3.10 and S3.11), which merges southward with the Shuilikeng fault. No kinematic indicators have been found along the Guaosing fault. Southward, the eastern limb of the Taanshan syncline becomes steeply west dipping and is cut by high-angle brittle faults. Several of these faults are well exposed along the western side of the Chenyulan River where they can be up to several hundred meters wide breccia zones that strike into and become lost in the alluvium of the river valley. In several locations we have found psuedotachylite within the breccia. Kinematic indicators such as stratigraphic cutoffs and slickenfibers developed on slip surfaces show that the faults have a complex kinematic history, but with a dominant sinistral strike-slip sense of movement.

[21] In both cross sections, the Shuangtung thrust juxtaposes a hanging wall ramp against a footwall ramp (Figure 5). We have little control on the dip or location of the Shuangtung thrust at depth, except that it carries Eocene age rocks in its hanging wall [*Chiu*, 1975; C-Y. Huang, personal communication, 2012]. There are, then, two possibilities for the interpretation of the structural provenance of the Shuangtung Unit. In the first, the Shaungtung thrust forms a ramp up from a deeper stratigraphic level than the Changhua-Chelungpu imbricate thrust system to form the bedding-parallel flat beneath it (the detachment). In this case, the Shuangtung Unit forms part of the imbricate system and must, therefore, restore back to a position farther east than that of the synorogenic sediments in the Chelungpu thrust sheet, indicating that it has accumulated a horizontal displacement of more than 15 km and has been uplifted more than 12 km (if a 6° basal detachment dip is assumed) [see, e.g., *Yue et al.*, 2005]. A second possibility is that the Shuangtung thrust is linked to the development of the Shuilikeng fault (see below) and represents a footwall shortcut breaching through the Changhua-Chelungpu imbricate thrust system and may involve both basement and cover rocks [see also *Mouthereau and Lacombe*, 2006; *Simoes et al.*, 2007b]. In this scenario (which we prefer), the Shuangtung Unit has accumulated ∼10 km of horizontal displacement and has been uplifted ∼9 km. Continued movement along the Shuilikeng fault has resulted in the eastern margin of the Shuangtung Unit being tightly folded and faulted. In this latter case, any synorogenic sediments that may have been deposited above the Miocene in the Shuangtung Unit in the map area have now been eroded away, although they do appear above the Miocene in the Changhua-Chelungpu imbricate thrust system farther to the south (Figure 2).

3.4. The Sun-Moon Lake Unit

[22] The Sun-Moon Lake Unit is composed of Eocene and Oligocene sediments of the Paileng and the Shuichangliu Formations (Figure 2) and represents a yet deeper level of involvement of the Eurasian margin sediments in the deformation. A deeper level of burial for these rocks has been suggested by *Sakaguchi et al.* [2007], who, on the basis of vitrinite reflection data, determined an increase in temperature of 90°C from the Shuangtung Unit to Sun-Moon Lake Unit, across the Shuilikeng fault. They estimate a maximum temperature of 284°C for the Paileng Formation, and suggest that the Sun-Moon Lake Unit rocks have been exhumed from between 9.2 and 9.8 km depth. The Sun-Moon Lake Unit is bound to the west by the Shuilikeng fault and to the east by the Tili thrust.

[23] The Shuilikeng fault is a high-angle (Figures S3.12 to S3.14), roughly linear, locally bifurcating brittle fault zone that coincides with a pronounced system of valleys that clearly demarcate the contact between the Shuangtung and the Sun-Moon Lake and Tili Units along nearly its entire length in Central Taiwan (Figure 2). Using river incision, channel morphology, and stream gradients along the Wu and Peikang rivers, *Yanites et al.* [2010] and *Sung et al.* [2000] suggest that the Shuilikeng fault is currently active, and has been throughout the Holocene. Furthermore, by comparing today's stream gradients with historical gradients from earlier mapping, *Sung et al.* [2000] suggest that the Shuilikeng fault has been active during the last 80 years. The Shuilikeng fault is poorly imaged in reflection seismic data, where it has been interpreted to dip steeply eastward and extend to deep in the middle crust (i.e., the Shuichangliu fault of *Wang et al.* [2002]). *Yue et al.* [2005] interpret the Shuilikeng fault to be the westward dipping displaced upper part of a preexisting extensional fault whose lower part, they suggest, coincides with an area of high seismic activity below their interpreted detachment.

[24] The surface geology of the Sun-Moon Lake Unit is defined by a number of roughly NE striking regional-scale folds and faults that splay off the Shuilikeng fault zone. Faults are often difficult to trace along strike, but where they crop out they are all brittle with mostly a top-to-the-northwest sense of movement. Here, unlike previous map interpretations, we recognize a fault along the eastern flank of the Lileng syncline, which we name the Alenkeng fault (Figure 2). While this fault has not been seen in outcrop, its presence is inferred from complex, nearly vertically plunging folds along the eastern margin of the syncline to the north of the Paikang River, and by the truncation of gently east dipping Shuichangliu Formation against vertical, west facing Paileng Formation on the north side of the Nankhan River (Figure 2). The regional anticlines associated with the major faults in the Sun-Moon Lake Unit have moderately to steeply west to northwest dipping forelimbs (Figures S3.15 and 3.16) that, northward, become steep to slightly overturned as folds tighten (Figure 2). These steep forelimbs can often be traced for tens of kilometers along strike, making them excellent structural markers in the rugged topography and monotonous stratigraphy of the Paileng Formation.

Folds have a broad back limb with bedding that dips shallowly to moderately toward the northeast to southwest, giving the synclines an open to slightly flat-bottomed geometry (Figure S3.17 and Figures S3.18 to S3.20 show further details of the stratigraphy and structure in the Sun-Moon Lake Unit). The folds are everywhere fault propagation folds, generally with a component of bedding parallel slip. Throughout most of the Sun-Moon Lake Unit, minor folds associated with the regional fold system have axes that (with some exceptions) plunge shallowly to moderately southward, but take on a more southwesterly plunge north of the Peikang River, and turn sharply to a nearly east-west plunge along the Tachia River, giving a scatter in the bedding dip azimuths (Figures 7 and 8). South of the Choshui River, fold axes have an overall northward plunge (Figure 8).

[25] In cross section, we have assumed a stratigraphic thickness template for the Sun-Moon Lake Unit as outlined in section 2. We interpret the Mesozoic basement to be in the shallow subsurface on the basis of the velocity structure determined from seismic tomography [*Wu et al.*, 2007; *Lin*, 2007]. The regional-scale structure of the Sun-Moon Lake Unit in the southern part of the map area is that of a hanging wall ramp composed of a wide antiformal structure with a number of associated minor folds. On the basis of the surface geology, in the cross sections we interpret the Shuilikeng fault to be a steeply east dipping feature that extends to ~10 km depth where it ramps down to a deeper level than the Western Foothills basal detachment (Figure 5). Below, we will use seismicity data to interpret how the Shuilikeng fault extends deeper into the crust and to place constraints on its kinematics. Further north, between the Peikang and the Tachia rivers, faults, regional bedding strikes, and fold axes undergo a pronounced change in orientation toward a more northeast to easterly strike and plunge (Figures 2, 7, and 8). This change in the structural orientation is suggestive of a roughly NE-SW striking lateral, or oblique, footwall ramp.

3.5. The Tili Unit

[26] The surface geology of the Tili Unit is composed of the Chiayang and Shipachungchi Formations, and the lower (Tachien) and middle members of the Paileng Formation. Much of the northeastern part of the Tili Unit is difficult to access, so we have only a relatively small data set from there. The Tili Unit is bound to the west by the Tili thrust and to the east by the Lishan fault. The Tili thrust marks an abrupt change in the deformation style and metamorphic conditions in the Taiwan mountain belt. It is the western limit of cleavage development. South of the Choshui River, the Tili Unit appears to be offset to the west before it bends into, and terminates against, the Shuilikeng fault (Figure 2). On the basis of Raman spectroscopy of carbonaceous material, *Beyssac et al.* [2007] estimate metamorphic temperatures in the Tili Unit to range from ~350°C to greater than 450°C, significantly higher than the 284°C determined for the Sun-Moon Lake Unit [*Sakaguchi et al.*, 2007] [see also *Simoes et al.*, 2012].

[27] Where it outcrops, the Tili thrust is a wide zone of deformation in which numerous small faults interact with each other (see Figure 3.21 for an example of the complex deformation around the Tili thrust). The largest of these splays occurs in the southern part of the map area, where the Minho thrust splays off the Tili thrust to form a several tens of kilometers long horse. South of the Choshui River, the Minho and Tili thrusts are offset some 5 to 10 km to the west. A number of east-west striking, both northward and southward dipping thrust and strike-slip faults outcrop in this area. Although it is not possible to trace any one of these faults in outcrop through the forest and high topography, using satellite imagery we interpret the offset in the Tili Unit to be related to them. The Tili Unit contains a moderate to steeply east to east-southeast dipping (Figure 7) pressure solution cleavage that is axial planar to minor asymmetric, west vergent folds found in outcrop (Figure S3.22), and to the regional fold structure [see also *Clark et al.*, 1993; *Tillman and Byrne*, 1995; *Fisher et al.*, 2002]. There is some local scatter in the dip directions of the cleavage, especially in the northern and southern parts of the map area where they are affected by the Lishan and Shuilikeng faults, respectively.

[28] The regional structure of the Tili Unit is that of the west verging, moderately southward plunging Tanan anticline (Figures 2 and 5), which has a several kilometer wide, steep to slightly overturned forelimb and a wide (Figure S3.23), moderately eastward dipping back limb (Figures 2 and 5). The geometry of the Tanan anticline is that of a fault propagation fold (see Figure S3.24 for an example of the fold style). As in the Sun-Moon Lake Unit, bedding dip directions (and here cleavage) take on a complex pattern in the northern part of the map area (Figure 2) (see also *Tillman and Byrne* [1995] for details of cleavage orientations in the northern part of the Tili Unit). The back limb of the Tanan anticline is cut by the Chiayang fault (Figure S3.25), which juxtaposes Chiayang Formation against the Tachien member of the Paileng Formation (Figure 2). The Chiayang fault can be traced throughout the map area as a several hundred meter wide zone of brittle deformation. Sparse kinematic indicators found in outcrops along the Choshui, Paikang and Tachia rivers suggest that this is a highly oblique thrust to strike-slip fault. North of the Choshui River, minor folds in the Tili Unit have an overall shallow southward plunge, although this can be highly complex where, locally, folds become reclined (i.e., the fold axis plunges downdip in the axial plane) (Figure 7). South of the Choshui River, minor folds in the Tili Unit generally plunge toward the north. Along its eastern flank, the lower part of the Paileng Formation in the back limb of the Tanan anticline has been rotated into a vertical position against the Lishan fault (Figures 2, 5, and S3.26).

[29] In the cross sections, the Tili thrust is interpreted to be a relatively steeply dipping fault that penetrates into the Mesozoic basement, juxtaposing a hanging wall ramp against a footwall ramp (Figure 5). This interpretation is based on the fact that along its strike length in the map area the Tili thrust cuts across the topography from the northeast to the southwest, suggesting that it is a steeply dipping feature. An alternative interpretation is that it shallows into a detachment within the complexly and strongly folded Chiayang Formation, and/or at the interface with the basement. We stress, though, that there is no geological evidence to support either of these interpretations. Finally, with the current data set it is not possible to determine if back rotation and steepening of the Tili thrust has taken place with the progressive development of the fault units to the west.

[30] Eastward, the Tili Unit is bound by the Lishan fault, a north to northeast striking high-angle fault that has a marked topographic expression throughout much of central and northern Taiwan. In several interpretations of the geology of Taiwan the Lishan fault has been largely ignored [e.g., *C.-H. Chen et al.*, 2000; *Yue et al.*, 2005]. Others have suggested, however, that the Lishan fault is a geologically complex, steeply west dipping structure whose geophysical signature indicates that it can be traced into the middle and perhaps even the lower crust and that it has an overall top-to-the-east oblique thrusting to strike-slip faulting sense of movement [*Clark et al.*, 1993; *Lee et al.*, 1997; *Bos et al.*, 2003; *Wu et al.*, 2004; *Bertrand et al.*, 2009, 2012]. Neither of these interpretations has been supported by a clearly defined fault surface in the field. In our map area, however, the Lishan fault outcrops in a number of places, where it is an up to 1 km wide ductile shear zone (Figures S3.27–S3.29) that juxtaposes the early to middle Eocene [*Chen et al.*, 2009] lower members of the Paileng Formation to the west against the middle Miocene Lushan Formation to the east. In the upper reaches of the Choshui River, near the town of Wujie, the fault is very well exposed. Here, it is a several hundred meter wide shear zone that displays a strong strain gradient from lower strain at the margins to very high strain at its center. Kinematic indicators, such as sheared boundins, sheared lithoclasts, and rare subhorizontal lineations indicate a sinistral sense of strike-slip movement. Furthermore, the Lishan fault has medium metamorphic grade rocks being exhumed in its hanging wall (up to ∼450°C [*Beyssac et al.*, 2007; *Simoes et al.*, 2012]). All of these features combine to suggest that the Lishan fault penetrates to below the brittle ductile transition (since ductilely deformed rocks now appear at the surface), and into rocks that were at middle to lower crustal metamorphic conditions.

3.6. The Lushan Unit

[31] The Lushan Unit is composed of the deep water shales and sandstones of the middle Miocene Tayuling and Lushan Formations, and here we also include the Eocene Pilushan Formation. The difference in age and depth of deposition between the Pilushan Formation and the Tayuling Formation (see section 2.2) is suggestive of either an unconformity or a structural break. The complexity of the structure across the contact supports the interpretation of a fault, although no clearly defined fault was seen in our map area. The Lushan Unit is bound to the west by the Lishan fault and to the east by the Chinma fault. Despite its poor exposure, we have mapped several sections along its western flank and one complete section in the north (Figure 2). However, the poor exposure combined with the monotonous lithology does not provide any marker horizon that allows correlation of structures to be made from north to south. This is further complicated by the gradual southward disappearance of bedding in the Lushan Formation. Metamorphic temperatures in the Lushan Unit are estimated to be <300°C, significantly less than that determined from the Tili Unit to the west [*Beyssac et al.*, 2007; *Simoes et al.*, 2012].

[32] Folds in the Lushan Unit have a wavelength of several hundred meters to a kilometer, are roughly west verging (Figure 2), and generally northeast to southwest plunging (Figure 7). They have steep to overturned forelimbs and moderately dipping back limbs. Locally, however, minor folds are very tight, with interlimb angles on the order of 10° to 30°. These folds often plunge downdip in their axial plane. A spaced axial planar cleavage is developed throughout the unit (but not always in the thick-bedded sandstones) (Figure S3.30) and has an overall moderate southeast dip (Figure 6), although dip directions become more variable northward (Figure 2). We have observed a crenulation cleavage in only one outcrop, indicating that a second phase of folding is not widespread in the Lushan Unit. Zones of very high strain are found locally along its western flank. For example, near the western side of the town of Lushan (Figure 2), one shear zone is several hundred meters wide, contains abundant lithoclasts with symmetrical strain shadows (Figure S3.31), rootless folds, and widely spaced kink bands (Figure S3.32). Unfortunately, these high-strain zones cannot be traced away from the outcrop in which they occur, and their kinematics are typically ambiguous. The western margin of the Lushan Unit is strongly deformed by the Lishan fault.

3.7. The Tananao Unit

[33] The Mesozoic rocks of the Tananao Unit have been interpreted to be either unconformably overlain by the Pulishan Formation [*Suppe*, 1976; *Yue et al.*, 2005] or to be in fault contact with it [*Clark et al.*, 1993; *Fisher et al.*, 2002; *Gourley et al.*, 2007; *Beyssac et al.*, 2007]. The contact between these two units is exposed along the Central Cross Island Highway, at the Chinma tunnel (Figure S3.33). Here, the banded marbles that are typical of the Tananao Unit in the Taroko Gorge (Figure S3.34) are overprinted by a penetratively developed mylonititic foliation that dips ∼60° toward the east (Figure S3.35). Our current mapping only extends 2 km east of this contact, so in this paper we will not address the geology of the Mesozoic rocks of the Tananao Unit.

4. Earthquake Data

[34] In sections 4.1 and 4.2, focal mechanism type maps and seismic energy release depth slices and cross sections are presented for earthquake data within the map area. Key to the interpretation of these data is the accuracy of the hypocenter location and of the focal mechanism solution [*Wu et al.*, 2008a, 2008b]. Precise earthquake locations rely on several factors such as record quality, station coverage, the adopted methodology of relocation, and the velocity model. The Central Weather Bureau Seismic Network (CWBSN) and Taiwan Strong Motion Instrumentation Program (TSMIP) stations consist of about 900 free-field stations spread over the entire Taiwan mountain belt, with a dense array of these within the study region. Events recorded in both the CWBSN and TSMIP data sets were relocated using the 3-D velocity model of *Wu et al.* [2007, 2009]. By using the 3-D velocity model and dense station coverage, the root-mean-squares of the traveltime residuals are shortened to less than 0.15 s [*Wu et al.*, 2003, 2008a]. This, together with results from recent test explosions, gives an uncertainty of ±2 km in hypocenter locations. First motion polarities from 834 of the relocated events within the study area were suitable for focal mechanism determinations, which are calculated using the genetic algorithm [*Wu et al.*, 2008b] to explore the entire model space and to assess the robustness

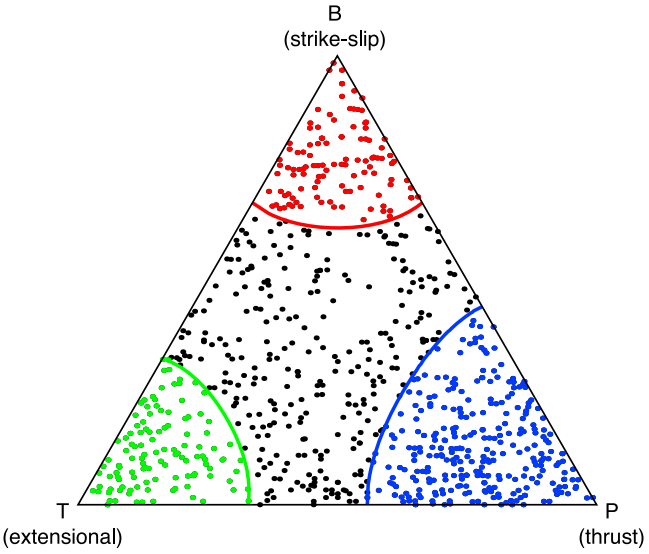

Figure 9. Triangular plot showing the fault mechanism distribution for the study area [after *Frohlich*, 2001]. These data are available in Data Set S1.

of solutions. A complete description of the methodology and the uncertainties involved in the calculation of the focal mechanisms is given by *Wu et al.* [2008b].

[35] While small, we stress that the scale of these uncertainties in the location of individual seismic events and focal mechanisms, together with uncertainties in determining the exact subsurface location of faults from surface geology, make it difficult to assign any particular seismic event to the smaller faults in the map area. It is, however, possible to distinguish a number of the major bounding faults. Because of the scale of the analyses and the uncertainties involved, this data set provides further constraints on the regional interpretation of the structure and kinematics derived from the surface geology. Therefore, in this section, we return to the regional tectonostratigraphic terminology of Western Foothills, Hsuehshan Range, and Central Range.

4.1. Focal Mechanism Data

4.1.1. Methodology

[36] Focal mechanism data are updated from the database of *Wu et al.* [2010] to cover the period from 1991 to 2009 (Data Set S1). Focal mechanism solutions from this data set were used to determine the P, T, and B axes of each event, which were then plotted according to the method of *Frohlich* [1992, 2001] (Figure 9). Although information such as the incremental slip direction and fault plane strike are lost in this analysis, the focal mechanism types provide important information on fault kinematics, dividing the seismic events loosely into fields that define thrusts (P axis), extensional faults (T axis), strike-slip faults (B axis), and "other" faults. Once the focal mechanism types were characterized in this way they were plotted in situ in the same volume used for the energy release analysis (see section 4.2) and depth slices were cut at 5 km intervals (Figure 10). For the depth slices, events were projected vertically for a maximum of 2.49 km either side of the slice, assuring that no single event appears on two different slices.

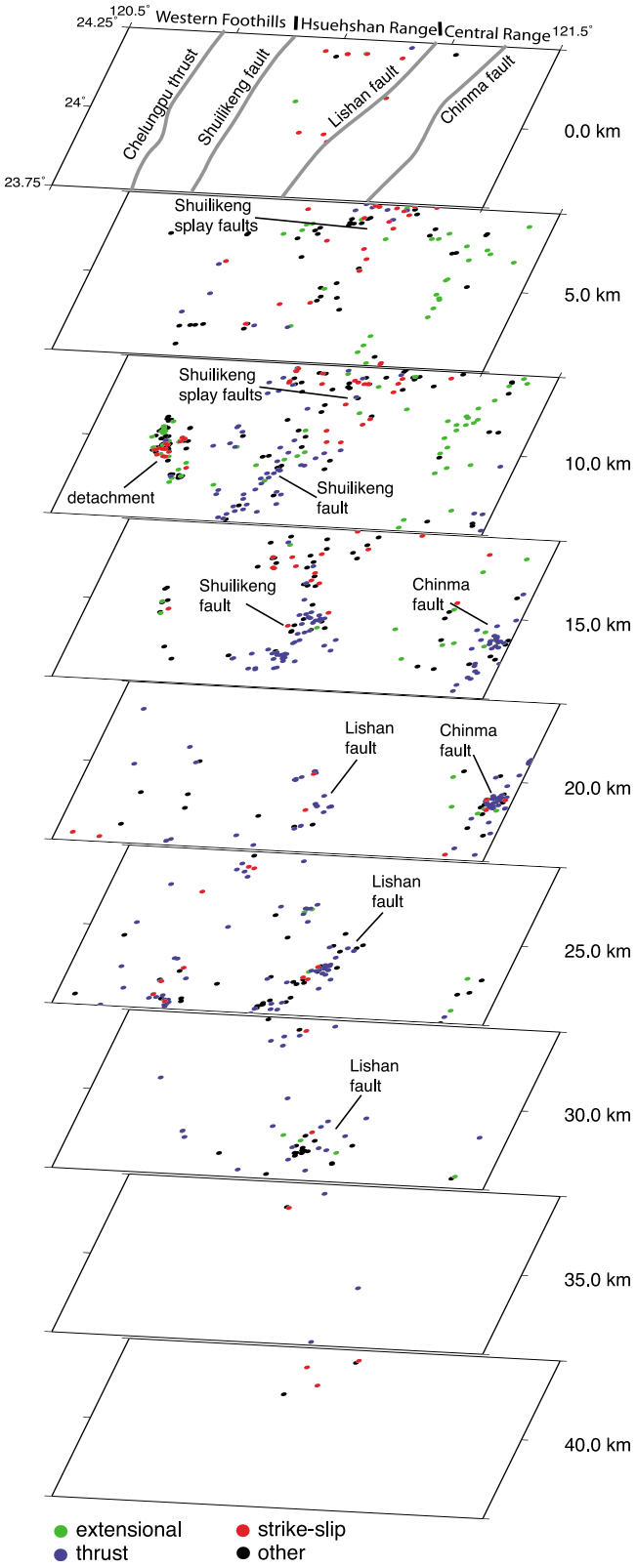

Figure 10. Fault mechanism depth slices through the map area. See text for discussion.

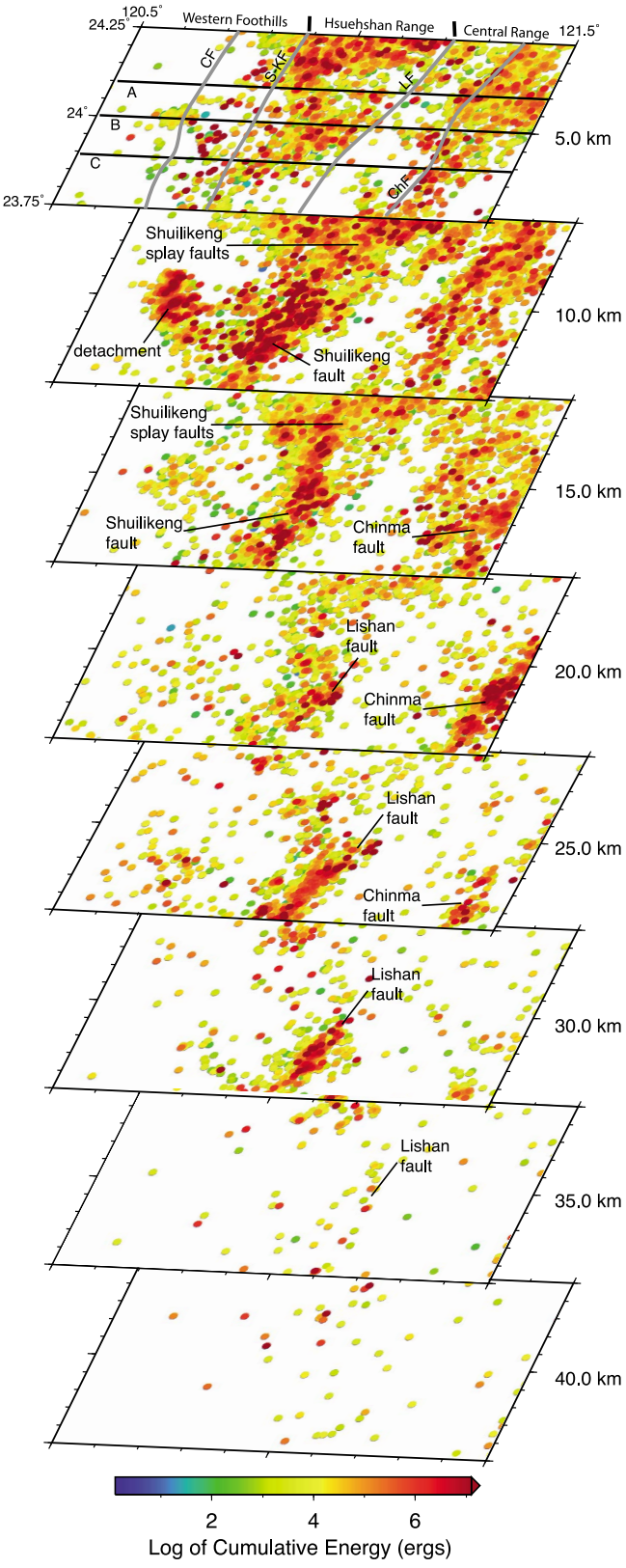

Figure 11. Seismic energy release depth slices for the study area. Note the coincidence of the linear highs which are interpreted to be related to the basal detachment, the Shuilikeng and Lishan faults. The data set from which these energy releases were calculated is available in Data Set S2.

4.1.2. Fault Mechanisms in Central Taiwan

[37] Figure 9 displays an overall random scatter, with a weak clustering in the thrust field. The depth slices (Figure 10), however, show a complex distribution of fault mechanisms, both within a single depth slice and with depth. In the Western Foothills, the upper 15 km of crust is dominated by strike-slip, extensional, and "other" faults, with a cluster of these centered at ~10 km depth that we interpret to be related to the basal detachment beneath the Changhua-Chelungpu imbricate thrust system. Thrust mechanisms are rare in the upper 15 km of the Western Foothills, but become more important, along with "other" types, from ~15 to 30 km depth. Eastward, the Hsuehshan Range displays a very complex pattern of fault types. In the northern part of the map area, the upper 15 km is dominated by strike-slip and "other" fault mechanisms, with a minor number of thrust and extensional events that are interpreted to belong to the faults that splay off the Shuilikeng fault. In the south, beginning at ~10 km depth, the Hsuehshan Range is dominated by a near linear cluster of thrusts that extend to between 15 and 20 km depth that we interpret to be related to the Shuilikeng fault. Between ~20 to 30 km depth, the southeastern flank of the Hsuehshan Range is dominated by thrust and "other" mechanisms, with lesser strike-slip and rare extensional mechanisms that are interpreted to be related to the Lishan fault. The upper 10 km of the part of the Central Range covered in this study is dominated by extensional fault mechanisms, with thrust fault mechanisms becoming increasingly important in the southeastern part of the map, from ~15 to 25 km depth. We interpret these to be related to the Chinma fault. Similar results to those outlined above were obtained in central Taiwan by *Wu et al.* [2010] and *Mouthereau et al.* [2009].

4.2. Seismic Energy Release Data

4.2.1. Methodology

[38] Earthquake hypocenter maps and sections with a large number of seismic events can provide important information about the regional geometry of fault systems. Nevertheless, there are several disadvantages to this methodology. For example, clustering of events may be misleading in the visual inspection of maps and sections, since small-magnitude events cannot be distinguished from large ones. With an energy increase of about a factor of 30 for each unit increase in magnitude, the cumulative energy released by many small events may not reach the energy of a single large event, and this can mask the important structures where major earthquakes occur. Also, in hypocenter cross sections, events are generally projected over distances of 10 km or more onto the plane of section. Many of these events may be related to structures that are not present in the plane of the section, or which intersect it in a completely different place from where the events are projected. The advantages of using the cumulative energy release method are that zones of high-magnitude earthquakes are readily distinguished and imaged in situ. Following this, we assume that the highs in cumulative energy release are related to earthquakes taking place along major faults. A limitation of the cumulative energy release modeling is the recurrence time of earthquakes, which can significantly bias the results locally and may account for areas of low-energy release.

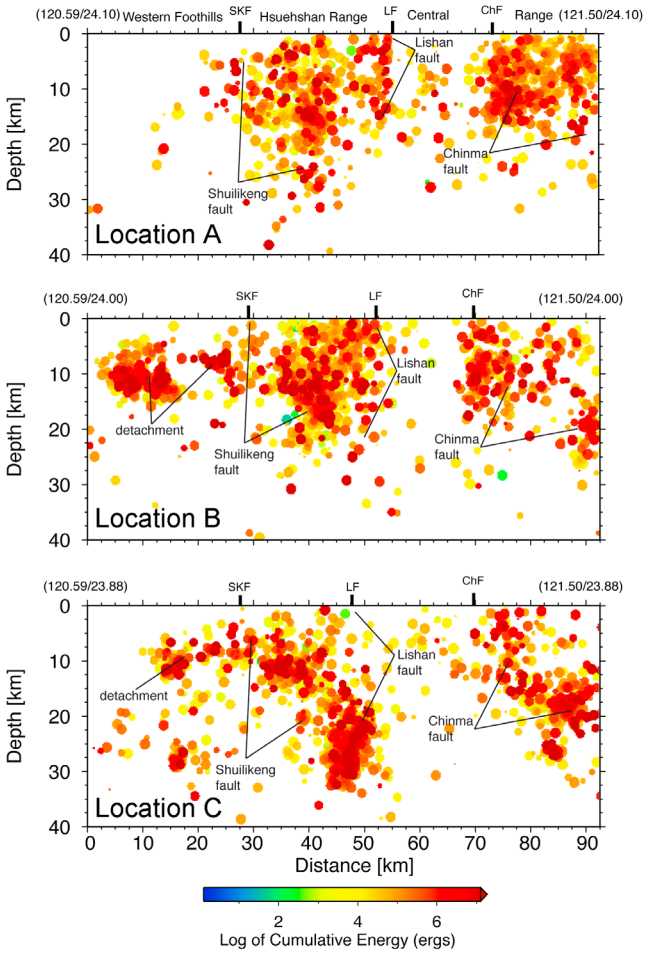

Figure 12. Seismic energy release sections. The sections labeled A, B, and C and their locations are shown in Figure 11. SKF = Shuilikeng fault, LF = Lishan fault, ChF = Chinma fault.

[39] For our seismic energy release modeling in central Taiwan, 34,819 events of $>M_L = 2$ were extracted from the 1991 to 2008 database of relocated earthquakes [e.g., *Wu et al.*, 2008a] (Data Set S2). In accordance with the Taiwan Central Weather Bureau Seismic Network Earthquake Catalogue [*Shin*, 1993], the local magnitude M_L is used to compute the seismic energy release (E, units are in ergs) for each event using the empirical relation

$$\log\ E = 9.4 + 2.14\ M_L - 0.054\ M_L{**}2$$

of *Gutenberg and Richter* [1956]. The relation used by *Jeng et al.* [2002] to study the energy release in the Taiwan subduction zones has also been tested, but without any significant change in the results. In this study, cumulative seismic energy release was determined in a 3-D volume using a discretized 100 m grid in which the energy is summed for all events that are located within a sphere of 2 km diameter centered at each grid point. Horizontal and vertical slices were then cut through the volume.

4.2.2. Seismic Energy Release in Central Taiwan

[40] The seismic energy released in the Western Foothills is scattered throughout the upper 30 km of crust, with minor amounts being released to a depth of at least 40 km (Figures 11 and 12). There is a marked high that is centered at about 10 km depth (±5 km) in the central and southern part of the map area, and a lesser high along its eastern flank (Figures 11 and 12). The high centered at ~10 km depth approximately coincides with the beginning of the low P wave velocity perturbation that marks the top of the Peikang basement high [*Wu et al.*, 2007]. This high in energy release can be interpreted to image the basal detachment of the Changhua-Chelungpu imbricate thrust system (Figures 11, 12b, and 12c). The relative increase in cumulative energy release in the upper 10 km of crust along the eastern flank of the Western Foothills seems to be related to earthquakes occurring along Chelungpu and Shuangtung thrusts. There is a scattering of energy release to ~40 km beneath the Western Foothills. While this is obviously related to elastic strain release within the Peikang basement high, we cannot associate it with any particular faults.

[41] There is an abrupt increase in cumulative energy release from the Western Foothills to the Hsuehshan Range that reaches a depth of ~30 km (Figures 11 and 12). Along the western flank of the Hsuehshan Range, the increase in cumulative energy release dips steeply eastward and projects to the surface at the location of the Shuilikeng fault (Figures 11 and 12). Along its eastern flank, there is a steeply westward dipping to vertical truncation of energy release that projects to the surface at the location of the Lishan fault (Figure 11). In the southeastern part of the map area (Figures 11 and 12c), from ~20 to 35 km depth, there is a steeply west dipping high in the cumulative energy release that also projects to the Lishan fault at the surface. The high-energy release in the central part of the Hsuehshan Range is likely due to activity along the mapped faults that splay off the Shuilikeng fault (Figure 11).

[42] In the western part of the Central Range, the seismic energy release is relatively low and is scattered throughout the crust to a depth of at least 40 km. With the present data set we are unable to determine any relationship between cumulative seismic energy release and geological structures in the western part of the Central Range. Eastward, there is an abrupt increase in the amount of energy being released in the upper 20 to 30 km of crust. This area corresponds to the Western Metamorphic Shear Zone of *Gourley et al.* [2007], who suggest that it is a steeply west dipping oblique extensional fault. At the surface, however, the western margin of this high coincides with the location of the Chinma fault (Figures 11 and 12), the ~60° eastward dipping shear zone that is transporting the Mesozoic and older crystalline basement rocks westward over the Paleogene and younger rocks to the west.

5. Discussion

5.1. Structure and Fault Kinematics

[43] The surface geological mapping presented here indicates that in Central Taiwan, from the buried Changhua thrust in the west to the Tananao Unit in the east, the mountain belt can be divided into six distinct, roughly northeast-southwest trending fault-bounded units (Figure 4). In this section we bring together the geological and geophysical data to discuss the crustal structure of these units and the kinematics of their bounding faults.

[44] The surface geological data and the cumulative seismic energy release data presented here both corroborate the previous interpretations of a gently eastward dipping detachment at about 7 to 10 km depth below the Western Foothills (Figure 5) [e.g., *Suppe*, 1980, 1981; *Ding et al.*, 2001; *Carena et al.*, 2002; *Yue et al.*, 2005]. For an alternative interpretation in which there is extensive basement involvement see, for example, *Mouthereau and Petit* [2003], *Mouthereau and Lacombe* [2006], and *Simoes et al.* [2007b] (and section 5.3). The differences in the depth to the detachment between the various data sets is a result of the uncertainties in the methodology of cross section construction, the choice of migration velocities and lack of a clear reflection in the seismic profile (Figure 6), and in the location of seismic events in the energy release data (Figure 12). Like the previous interpretations mentioned above, to the north of the Choshui River we place the detachment to the Changhua-Chelungpu imbricate thrust system within the Chinshui shale member of the Cholan Formation synorogenic sediments. South of the Choshui River, however, there is a significant change in the location of this basal thrust as it ramps down section into the older Miocene rocks, placing them on top of Pleistocene rocks in the Neilin anticline (Figure 2) [see also *Mouthereau and Lacombe*, 2006]. The seismicity data show that all types of fault mechanisms are active within this imbricate thrust system and along the detachment (Figure 10), indicating that it has complex kinematics and therefore a pure thrusting mechanism cannot be assumed [see also *Wu et al.*, 2010]. These data, together with rare kinematic indicators found in the field and the horizontal component of the surface displacements determined from the GPS data [e.g., *Yu et al.*, 2003; *Bos et al.*, 2003; *Lin et al.*, 2010], all indicate that a top-to-the-northwest (oblique) sense of movement is taking place.

[45] We recognize that there are problems in interpreting the geometry of the Shuangtung thrust at depth (see section 3.3). On the basis of this study, we suggest that since it cuts down section through the Miocene and into Eocene age Paileng Formation rocks it is more likely to be structurally and kinematically linked to the Sun-Moon Lake Unit, although its eastern flank has been cut by the Shuilikeng fault. With the current data, however, it is not possible to determine the nature of this linkage. A possible example of how a frontal imbricate thrust system links with a regional transpressive fault system comes from the South Island of New Zealand [e.g., *Walcott*, 1998]. In the surface geology, the Shuangtung thrust places Miocene rocks on top of the upper part of the Toukoshan Formation, indicating that it was active during the late Pleistocene to Holocene. The seismic energy release in the shallow subsurface beneath the Shuangtung Unit, together with aftershocks of the Chi-Chi earthquake [*R.-Y. Chen et al.*, 2002] suggest that the Shuangtung thrust is currently active [see also *Sung et al.*, 2000].

[46] Unlike the previous interpretations in which the Western Foothills detachment extends eastward beneath the Hsuehshan and Central Ranges [e.g., *Carena et al.*, 2002; *Yue et al.*, 2005], we suggest that it appears to be truncated by, or is perhaps somehow linked with, the Shuilikeng fault zone. (Figures 5 and 12). See, for example, the aftershocks that occurred within the first 24 h of the Chi-Chi earthquake [*Chang et al.*, 2007]. The data presented here indicate that the Shuilikeng fault, rather than being a single discrete feature, comprises a system of faults and folds that splay off the main fault, resulting in a regional map pattern that is strongly suggestive of a transpressive or strike-slip system fault zone (for examples of these types of map patterns, see *Sylvester* [1988], *Butler et al.* [1998], *Walcott* [1998], *Kirkpatrick et al.* [2008], *Murphy et al.* [2011], and *Leever et al.* [2011]). This Shuilikeng fault "system" dominates the structure of the Sun-Moon Lake Unit in the map area. The bending of folds (e.g., the Tingkan syncline or the Tsukeng anticline), together with the bending and truncation of the Tili Unit, against the Shuilikeng fault indicates that it has a sinistral component of displacement (Figure 2). However, earthquake focal mechanisms determined for the Sun-Moon Lake Unit show that the Shuilikeng fault "system" displays complex kinematics, with a clear range from strike-slip and "other" mechanisms in the upper ∼15 km of crust in the north, to predominantly thrusting at deeper levels in the southern part. Beginning at the southern margin of our map area and continuing farther south, *Chang et al.* [2007] and *Wu et al.* [2010] show that the dominant focal mechanism along the Shuilikeng fault is strike slip. The seismic energy release data show that Shuilikeng fault coincides with a significant, eastward deepening of the seismicity beneath the Hsuehshan Range (Figure 12), so we therefore interpret the fault zone to dip steeply eastward and to extend to at least 25 to 30 km depth. Geomorphological data indicate that the Shuilikeng fault has been active throughout the Holocene and continues to be so [*Sung et al.*, 2000; *Yanites et al.*, 2010]. Aftershocks that took place within the first 24 h after the Chi-Chi earthquake also indicate that the Shuilikeng fault is active [cf. *Chang et al.*, 2007].

[47] The Tili thrust marks a clear structural and metamorphic boundary in the Hsuehshan Range. It juxtaposes lower metamorphic grade rocks of the Sun-Moon Lake Unit against higher-grade rocks with a well-developed cleavage in the Tili Unit. It also represents an abrupt change in structural style from the Sun-Moon Lake Unit, with tighter, west vergent fault propagation folding becoming dominant and a well-developed axial planar cleavaged being developed. From the data presented here we cannot discriminate the geometry or the kinematics of the Tili thrust.

[48] In this paper we identify a clearly defined zone of intense ductile strain that coincides with the location of the Lishan fault. This high-strain zone, together with the recent finding of large foraminifera that are assigned to the NP14 biozone [*Chen et al.*, 2009] in rocks along the western side of the Lishan fault confirm that it juxtaposes early to middle Eocene higher metamorphic grade rocks of the Tili Unit against middle Miocene lower metamorphic grade rocks of the Lushan Unit [see also *Clark et al.*, 1993; *Lee et al.*, 1997; *Wu et al.*, 2004; *Beyssac et al.*, 2007; *Bertrand et al.*, 2009, 2012; *Simoes et al.*, 2012]. Surface structural data and the seismic energy release data indicate that it is a vertical to steeply west dipping structure that extends to ∼35 km depth (Figure 12) [see also *Clark et al.*, 1993; *Tillman and Byrne*, 1995; *Wu et al.*, 2004; *Chang et al.*, 2007; *Bertrand et al.*, 2009, 2012]. This interpretation of the dip and depth of penetration of the Lishan fault is also justified by the pronounced gradient across it in the Bouguer gravity anomaly, from a low beneath the Hsuehshan Range to a high beneath the Central Range [*Wu et al.*, 1997; *Yen et al.*, 1998; *Hwang*

et al., 2007]. Locally, rare kinematic indicators point to a sinistral sense of movement, whereas focal mechanism data indicate that the overall kinematics are quite complex [*Wu et al.*, 2004; *Chang et al.*, 2007; *Wu et al.*, 2010]. Modeling of GPS data suggests that it has a sinistral sense of slip [*Bos et al.*, 2003]. These data, together with the seismic activity along parts of the Lishan fault in our map area (Figures 11 and 12) indicate that it is currently active.

[49] To the east of the Lishan fault, the Lushan Unit displays highly nonclyndrical folding. In general, the structure displays an overall northwest vergence, which we can determine from the well developed, moderately southeast dipping cleavage. This is in agreement with the kinematics determined by *Tillman and Byrne* [1995] and *Fisher et al.* [2002]. The low P wave velocity modeled in the shallow subsurface beneath the Lushan Unit [*Rau and Wu*, 1995; *Wu et al.*, 2007; *Kuo-Chen et al.*, 2012] suggests that the unit is on the order of 3 to 5 km thick. However, because of the lack of seismicity in this part of the Central Range, it is not possible to determine the deep subsurface structure.

[50] We have very few geological data from the Tananao Unit, which is being thrust westward over the Lushan Unit along the Chinma fault (Figure 2). To the east of this fault there is extensive seismic energy release to a depth of at least 30 km. The change in seismicity from the Lushan to the Tananao Unit is near vertical, which led *Gourley et al.* [2007] to suggest that the Chinma fault dips steeply westward. However, this fault outcrops very well along the Central Cross Island Highway, where it clearly dips ~60° to the southeast [see also *Tillman and Byrne*, 1995]. The focal mechanism data show that the upper 10 km of crust in the Tananao Unit is dominated by extension [see also *Crespi et al.*, 1996], whereas thrusting is dominant below this.

[51] Finally, in our map area we identify two areas in which there are important changes in the structural trend. For example, to the north of the Paikang River there is a systematic change in the orientation of structures from a roughly northerly trend to a more easterly trend along the Tachia River (Figure 2). This can be seen to affect individual structures, such as the Hsiaoan anticline (Figure 2) which becomes turned up on its end along the Tachia River. There is also a marked change in the earthquake focal mechanisms, with strike-slip faults becoming more important northward (Figure 10). A second such structure appears to affect the area immediately south of the Choshui River. North of the river, the regional trend of fold axes has an overall southerly plunge, whereas south of the river it takes on a northerly plunge (Figure 8). Also, the Tili Unit is offset dextrally to the south of the river (Figure 2). Southward, the Chelungpu thrust clearly ramps down into deeper and older stratigraphy, moving it westward over the top of the Neilin anticline.

5.2. Sequence of Deformation

[52] Based on overprinting relationships within our map area, we suggest a deformation sequence for mountain building in this part of Taiwan that consists of two phases (D1 and D2) (Figure 13). The onset of D1 takes place with the arrival of the Eurasia continental margin at the subduction zone (Figure 13a). The Eurasia margin in the Taiwan area is well known to contain several large rift basins [e.g., *Teng*, 1990, 1992; *Huang et al.*, 2001; *Teng and Lin*, 2004; *Lin and Watts*, 2002; *Lin et al.*, 2003] that have been variably affected by the deformation related to the Taiwan orogeny. In Figure 13 we give a schematic representation of what the Taiwan part of the margin could have looked like and what the distribution of the preorogenic sediments involved in the deformation may have been at time T0. Note that we represent the Hsuehshan Basin as a graben structure rather than a half graben as suggested by *Teng et al.* [1991] and *Teng and Lin* [2004]. This allows for easier reconstruction of the original position of the Tili Unit by letting us place the D1 detachment near the top of the prerift basement (Figure 13b). It also provides an explanation for the nature and presence of the Peikang basement high (see also Figure 1).

[53] We interpret the earliest deformation (D1) associated with the Taiwan orogeny in our map area to be the development and emplacement of the Tili and Lushan Units at time T1, when the extended continental margin had entered into the subduction zone (Figure 13b). It is difficult to accurately constrain the age and timing of emplacement of these units, but the first appearance of lithic clasts containing a cleavage in the fore-arc region of the Coastal Range and in the Western Foothills foreland basin sediments occurred during the early Pliocene, or some 3.5 to 4 Myr ago [*Lee*, 1963; *Chi et al.*, 1981; *Covey*, 1986; *Dorsey*, 1987; *Teng*, 1987, 1990; *Huang et al.*, 2006]. This indicates that rocks with a cleavage (i.e., the Tili and Lushan Units) were exhumed and being eroded by this time. Consequently, the leading edge of the continental margin must have entered into the subduction zone at some time prior to the early Pliocene if these units where to be deformed and emplaced by this time. A further indication that the deformation and emplacement of the Tili and Lushan Units is one of the earliest events recorded in the map area is given by the geometric relationships between the rocks in these units and faults. For example, the Tili Unit is cut by the Shuilikeng fault system in the southwest (Figure 2) and appears to be cut by the Lishan fault in the northeast (just out of the current map area). Similarly, along its western flank the Lushan Unit is cut by the Lishan fault and, in the east, by the Chinma fault. These geometric relationships indicate that activity along the Shuilikeng, Lishan, and Chinma faults must postdate the early emplacement of the Tili and Lushan Units. We therefore suggest that, despite the different metamorphic conditions undergone by the Tili and Lushan Units, that there is a close enough similarity in the structural style and in the orientations of bedding and cleavage between the two to interpret that they developed as a roughly NW vergent thrust stack at the same time, early on in the history of the Taiwan mountain belt, and that they were both being emplaced by at least the early Pliocene. This is in contrast to the model presented by *Tillman and Byrne* [1995], for example, who suggest that these units were emplaced in two distinct phases of deformation. The Tili and Lushan Units were subsequently breached by, and juxtaposed along, the Lishan fault at some unknown time. From our data we interpret the Tili and Lushan Units to now be inactive.

[54] The next phase of the deformation sequence in the study area (D2) is interpreted to be related to reactivation of preexisting extensional faults as the full thickness of the continental margin arrived at the subduction zone (T2 in Figure 13). This resulted in the formation of the Chinma fault, the Lishan fault, the Shuilikeng fault system, and the

emplacement of the Shuangtung Unit and the Changhua-Chelungpu imbricate thrust system. D2 structures are currently active and, to the east of the Shuilikeng fault, form a regional-scale basement culmination (Figure 13c). In this scenario, the Hsuehshan Range forms a zone of transpression with a structural architecture similar to that of a crustal-scale positive flower (or pop-up) structure that is bound by the Shuilikeng and Lishan faults (Figure 5), and in which there is a large amount of seismic activity and seismic energy release (Figures 12 and 13). This structural architecture was first proposed by *Clark et al.* [1993] based on observations in the Tili and Lushan Units in the NE part of

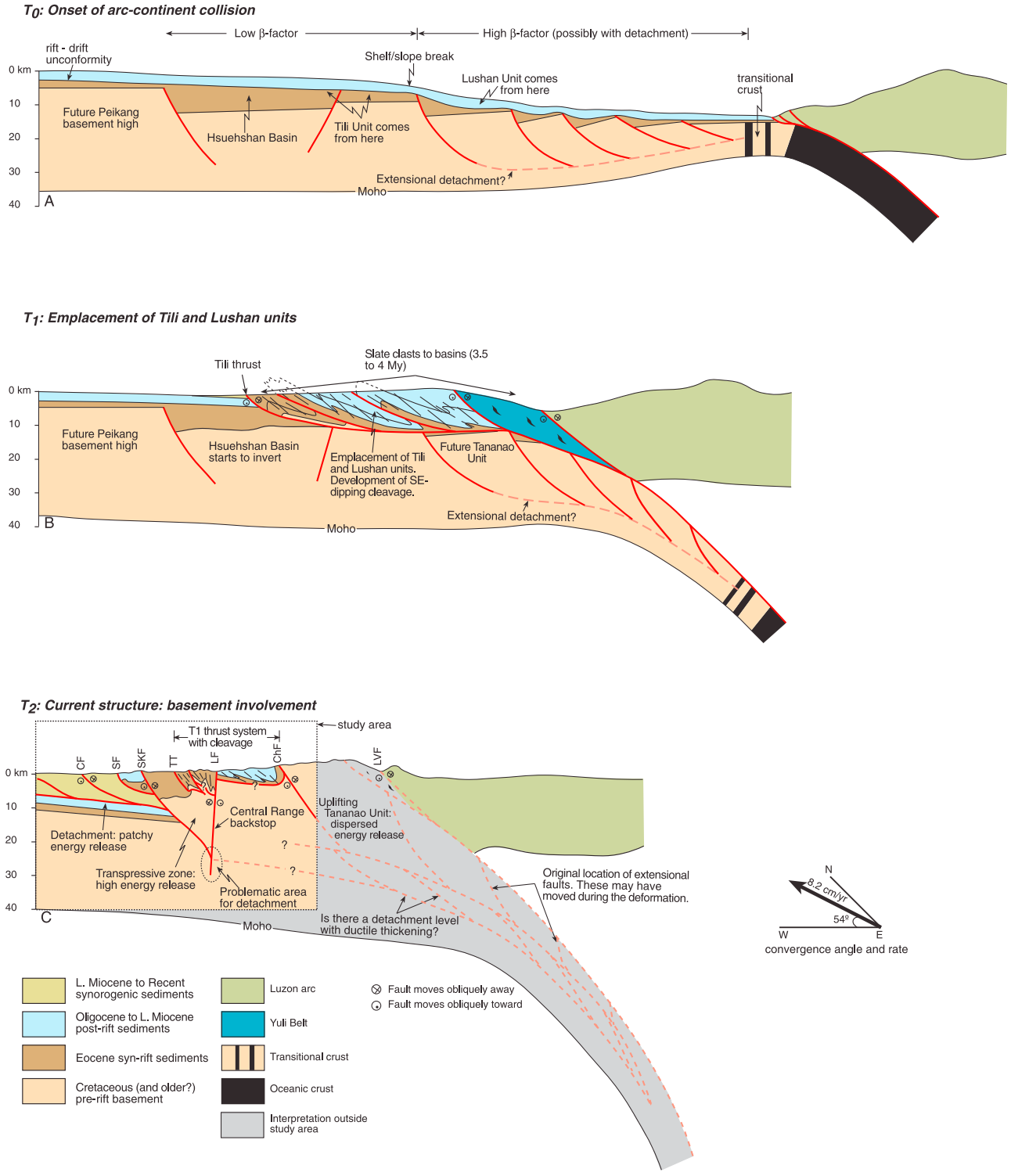

Figure 13

our map area (Figure 2). Our data suggest that a transpressional structural architecture is developed throughout the Hsuehshan Range between at least the Tachia River in the North and the Choshui River in the South. Farther to the south of our map area, the Shuilikeng fault and the Lishan fault merge, although little is known about how these faults interact at the surface. Nevertheless, the geological and focal mechanism data indicate that they are both steeply dipping features with complex kinematics that extend well into the middle and perhaps even the lower crust (Figure 13). Furthermore, the seismic energy release data suggest that they interact at depth (Figure 11), possibly with the Lishan fault extending deeper into the crust than does the Shuilikeng fault (Figure 13c). It is not possible to constrain when this fault system became active.

[55] As indicated in section 5.1., we are uncertain how the Shuangtung thrust links with the Changhua-Chelungpu imbricate system and with this transpressive structure. The presence of Eocene rocks in the Shuangtung Unit suggests that the Shuangtung thrust may have developed as a footwall shortcut fault that was linked to, and eventually cut by the Shuilikeng fault. See *Narr and Suppe* [1994] for theoretical and real examples of how these structures develop. On the basis of foreland basin sedimentation, geomorphic structures, and magnetostratigraphy, *W.-S. Chen et al.* [2000, 2001a], *Simoes and Avouac* [2006], and *Simoes et al.* [2007a, 2007b] suggest a forward breaking fault sequence, in which the Shuangtung thrust became active at circa 1.1 Ma, the Chelungpu thrust at 0.7 to 0.9 Ma., and the Changhua at 0.62 to 0.65 Ma.

[56] Uplift and erosion of the Tananao Unit along the Chinma fault appears to have been taking place by at least the latest Pleistocene (1.4 Ma), depositing metamorphic clasts into the fore-arc basin in the Coastal Range [*Dorsey*, 1987]. Zircon and apatite fission track ages [e.g., *Liu et al.*, 2001; *Lee et al.*, 2006; *Fuller et al.*, 2006] also indicate that the Tananao Unit was being exhumed by the early part of the Pleistocene. At the Chinma Tunnel, along the Central Cross Island Highway, the Tananao Unit clearly overthrusts the Lushan Unit providing unequivocal evidence that it postdates the emplacement of this later unit. Extensive seismicity indicates that the Chinma fault is still active.

5.3. Tectonic Implications for the Orogen Architecture

[57] On the basis of the data presented here, we agree with previous authors [e.g., *Suppe*, 1980, 1981; *Namson*, 1981; *Ding et al.*, 2001; *Carena et al.*, 2002; *Yue et al.*, 2005] that in our map area the Changhua-Chelungpu imbricate thrust system is structurally linked to a basal detachment at the base of the synorogenic sediments in the foreland basin. Southward, involvement of the Miocene in the thrusting indicates that this basal thrust ramps downward in the stratigraphy (Figure 2) [e.g., *Hickman et al.*, 2002; *Mouthereau et al.*, 2002; *Mouthereau and Lacombe*, 2006]. These data also suggest, however, that a structural and kinematic model in which the Hsuehshan Range forms a deep-rooted zone of transpression between the Shuilikeng and Lishan faults better fits the available data than that of an imbricate thrust system with a shallow, throughgoing detachment. Depending on the estimation of the Moho depth [e.g., *Rau and Wu*, 1995; *McIntosh et al.*, 2005; *Wu et al.*, 2007], the Lishan fault may be interpreted to cut nearly the entire crust (Figure 13c). In this scenario, the Hsuehshan Range and its bounding faults take up a significant amount of the oblique arc-continent convergence within the Eurasian margin [see also *Mouthereau et al.*, 2009; *Hsu et al.*, 2009; *Wu et al.*, 2010], with the western part of the Central Range acting as a vertical to steeply west dipping backstop to the transpressional belt [see also *Clark et al.*, 1993; *Yamato et al.*, 2009; *Mouthereau et al.*, 2009]. A corollary to this is that there is no structural linkage in the form of a detachment between the Hsuehshan and Central Ranges, and therefore no (or very limited) material transfer across the Lishan fault into the Central Range as has been suggested by others [e.g., *Fuller et al.*, 2006; *Simoes et al.*, 2007b; *Fisher et al.*, 2007; *Bertrand et al.*, 2012]. East of the Lishan fault, the Central Range can be interpreted to be deforming by inversion of preexisting extensional faults that affect the prerift basement (Tananao Unit) (Figure 13c). A key question that arises is whether or not these reactivated faults are linked to a deep detachment level beneath the Central Range.

[58] Using geological data and modeling approaches various authors [e.g., *Tillman and Byrne*, 1995; *Simoes et al.*, 2007a; *Yamato et al.*, 2009; *Mouthereau et al.*, 2009; *Ching et al.*, 2011b] have suggested that there is a basal detachment in the middle to lower crust beneath the Hsuehshan and Central Ranges. This detachment is thought to either cut steeply (17°) upsection toward the west with (or without) significant underplating taking place [e.g., *Simoes et al.*, 2007a; *Ching et al.*, 2011b], to remain as a subhorizontal feature in the lower crust before ramping steeply upsection toward the mountain front [e.g., *Yamato et al.*, 2009;

Figure 13. Schematic evolutionary model for the development of the Taiwan mountain belt. (a) The onset of arc-continent collision. The interpreted precollisional locations of the units described in the text are shown. The extensional detachment is interpreted for the outermost margin where there was likely to have been a high β factor [*McKenzie*, 1978]. The Yuli Belt, which is not mentioned in the text, is the eastern part of the Tananao Unit and is interpreted to be part of the Late Cretaceous basement [e.g., *Yui et al.*, 2012]. (b) The late Miocene to early Pliocene emplacement, uplift and erosion of the Tili and Lushan Units. The amount of displacement and thrust sheet stacking represented are purely interpretative. (c) The current structure in a W-E oriented section along section C–C′ in Figure 5 and eastward across the Central and Coastal Ranges, into the arc. The location of our study area is indicated by the dashed box and in color. To the east of the study area, shown in gray, the structure is purely interpretive. The location of a possible deep detachment beneath the Central Range is indicated. Also indicated is the problematic area for the extrapolation of a detachment across the Lishan fault. The convergence vector is from *Yu et al.* [1997] and is only for T2. The Moho is an interpretation based on the velocity models of *Rau and Wu* [1995], *McIntosh et al.* [2005], *Wu et al.* [2007], and *Ustaszewski et al.* [2012]. CT = Chelungpu thrust, ST = Shuangtung thrust, SKF = Shuilikeng fault, LF = Lishan fault, ChF = Chinma fault, LvF = Longitudinal Valley fault.

Mouthereau et al., 2009], or to be the result of a second phase of deep level thrusting that ramps stepwise upsection toward the deformation front [*Tillman and Byrne*, 1995]. While all of these models present viable possibilities for a deep basal detachment, most do not take into account the significance of a deeply penetrating Lishan fault (except *Tillman and Byrne* [1995]) (see Figure 13), and do not fully take into account the preexisitng three-dimensional structure of the continental margin.

[59] How a continental margin deforms during convergence depends to a large degree on its preexisting structural architecture, and how this is oriented relative to the convergence vector [e.g., *Dewey et al.*, 1986; *Brown et al.*, 1999, 2011; *Manatschal*, 2004; *Mohn et al.*, 2010; *Byrne et al.*, 2011; *Reston and Manatschal*, 2011; *Harris*, 2011]. Geological and geophysical data from a number of continental margins and mountain belts worldwide have shown that the rift architecture can be very complex and can include an extensional detachment below the outer margin where there is a high β factor [e.g., *Reston et al.*, 1996; *Manatschal*, 2004; *Mohn et al.*, 2010; *Reston and Manatschal*, 2011]. Reactivation of preexisting basement faults and the inversion of sedimentary basins along a margin can control the location, geometry, and kinematics of structures in the developing mountain belt including the basal detachment, and will often result in the development of lateral structures, basement involvement in thrust sheets, and the formation of basement culminations [e.g., *Laubscher*, 1987; *Glen*, 1985; *Hatcher and Williams*, 1986; *Rodgers*, 1987; *Woodward*, 1988; *Schmidt et al.*, 1988; *Bryant and Nichols*, 1988; *Cooper and Williams*, 1989; *Narr and Suppe*, 1994; *Wibberley*, 1997; *Perez-Estaun et al.*, 1997; *Butler et al.*, 1997; *Brown et al.*, 1997, 1999, 2006; *Oncken et al.*, 1999; *Manatschal*, 2004; *Mohn et al.*, 2010; *Reston and Manatschal*, 2011]. The Eurasian margin involved in the deformation of the Taiwan mountain belt has been shown to have contained a number of deep extensional basins that were active throughout the Eocene, Oligocene, and Miocene [*Lin et al.*, 2003; *Teng and Lin*, 2004; *Teng*, 1987; *Huang et al.*, 1997, 2001; *Byrne et al.*, 2011] (Figure 1). The importance of these features on the development of the three-dimensional structure of the Taiwan mountain belt is well known [e.g., *Wu et al.*, 1997; *Mouthereau et al.*, 2002; *Mouthereau and Lacombe*, 2006; *Wu et al.*, 2007; *Hwang et al.*, 2007; *Byrne et al.*, 2011] although still not completely understood. It is possible, therefore, that an hypothetical extensional detachment beneath what was the outer margin is now being reactivated to form a level of deep detachment beneath the Central Range (Figure 13). This detachment may be a zone of ductile thickening (underplating in the models of *Simoes et al.* [2007a] and *Ching et al.* [2011b]) in the form of duplexing and/or thrust stacking of extensional fault blocks. We stress, however, that with the current data sets it is not possible to unequivocally define such a detachment level beneath the Central Range, and very difficult to extend it westward across the Lishan fault and below the Hsuehshan Range to link it with the Changhua-Chelungpu imbricate thrust system (Figure 13).

[60] An alternative model for the development of the Taiwan Orogen is the "lithosphere plate collision" model of *Wu et al.* [1997] in which there is no subduction of the Eurasian margin beneath the Luzon arc, the Central Range appears as a completely different lithology from the zones to the west, and there is no detachment beneath the Taiwan mountain belt. In this model, the Eurasian margin is indenting the Luzon arc and is deforming along steep faults that locally involve the whole crust and upper mantle. While it is commonly accepted that the whole lithosphere is involved in plate tectonics, including subduction and collision systems [e.g., *Gerya*, 2011; *Afonso and Zlotnik*, 2011], the overall rheological and structural model put forward by *Wu et al.* [1997, Figure 16] for the deforming continental crust in Taiwan does not appear to fit well with the currently available geological, thermochonological, and geophysical data. Nor does it fit well with the tectonic processes determined from other well known examples from either fossil or active arc-continent collisions [see, e.g., *Brown and Ryan*, 2011, and references therein]. Nevertheless, it does bring to the forefront the problems associated with the interpretations of, for example, the Lishan fault (or even its existence), and the need to provide a geological model for the evolution of the Taiwan mountain belt that accounts for the deep crustal seismicity.

6. Conclusions

[61] This paper presents new geological mapping in the Western Foothills, the Hsuehshan Range, and the western part of the Central Range in central Taiwan that, together with earthquake focal mechanism and seismic energy release data, place constraints on the structural architecture, fault kinematics, and relative timing of the development of the Taiwan mountain belt. On the basis of similarities in structure, stratigraphy, and kinematics the Western Foothills, Hsuehshan Range, and Central Range can be further subdivided into six fault-bound units. Structural overprinting relationships between these units shows that the Taiwan mountain belt has evolved during at least two distinct, but progressive phases in the deformation sequence. The recognition of these two phases is essential for determining the crustal-scale structural evolution of the mountain belt.

[62] The first stage of deformation (D1) took place during the late Miocene to early Pliocene and emplaced slope sediments northwestward to form a thrust stack with the Tili and Lushan Units (Figure 13). Both these units underwent a distinct metamorphic grade and deformation style that includes a penetrative pressure solution cleavage [e.g., *Clark et al.*, 1993; *Tillman and Byrne*, 1995; *Fisher et al.*, 2002; *Beyssac et al.*, 2007; *Simoes et al.*, 2012]. The Tili and Lushan Units began to provide clasts to the foreland and fore-arc basins by the early Pliocene [e.g., *Covey*, 1986; *Dorsey*, 1987], thereby placing an upper limit on the age of the earlier deformation of the Taiwan mountain belt. Our data suggest that D1 structures are no longer active.

[63] The second phase of deformation (D2) is interpreted, in part, to involve the reactivation of preexisting extensional faults on the continental margin and slope to form a basement culmination. These faults clearly cut the D1 structures [see also *Clark et al.*, 1993; *Tillman and Byrne*, 1995; *Lee et al.*, 1997]. Our data show that D2 structures are currently active and are responsible for the development of a transpressional zone within the Hsuehshan Range that is bound by the Lishan fault in the east and the Shuilikeng fault system in the west. The imbricate thrust system of the Western

Foothills is linked to this transpressional zone and is active. Uplift of the Tananao unit in the east [see *Dorsey*, 1987] is coeval with the transpressive deformation in the Hsuehshan Range and the Western Foothills.

[64] A consequence of the recognition of the two phase deformation sequence in the Taiwan mountain belt is that it did not everywhere develop as a forward breaking imbricate thrust system with a shallowly eastward dipping basal detachment in the upper crust [e.g., *Suppe*, 1980, 1981; *Ding et al.*, 2001; *Carena et al.*, 2002; *Yue et al.*, 2005; *Malavieille and Trullenque*, 2009]. Nevertheless, the data presented here do support the interpretations by these authors of an imbricate thrust system (the Changhua-Chelungpu imbricate thrust system) within the foreland basin sediments of the Western Foothills, but it also shows that this thrust system is related to the D2 deformation sequence. The data do not support the extrapolation of an imbricate thrust system structural architecture eastward into the Hsuehshan and Central Ranges. Instead, the data suggest that the D2 transpressive fault system active in the Hsuehshan Range is deeply rooted, affecting nearly the entire crust. A corollary to this is that the orogen does not have a wedge-shaped structural architecture with throughgoing basal detachment that links the entire mountain belt from the Changhua thrust in the west to below the Central Range in the east. It is possible, however, with our data to interpret a deep detachment level beneath much of the Central Range (Figure 13c), as some authors have already indicated [e.g., *Tillman and Byrne*, 1995; *Simoes et al.*, 2007a; *Yamato et al.*, 2009; *Mouthereau et al.*, 2009; *Ching et al.*, 2011b]. This hypothetical detachment may have formed by the reactivation of an earlier extensional detachment that had developed on the outer slope of the margin, in the area with a high β factor (Figure 13).

[65] Finally, in our map area we identify two areas in which there are important changes in the structural trend: (1) to the north of the Paikang River there is a systematic change in the orientation of structures from a roughly northerly trend to a more easterly trend along the Tachia River and (2) immediately south of the Choshui River there is a change in the regional trend of fold axes, and the Chelungpu thrust ramps down into deeper and older stratigraphy. We interpret these changes in structure to be caused by the reactivation of preexisitng basement faults that are related to the Tainan and Taishi basins [see also, e.g., *Mouthereau et al.*, 2002; *Mouthereau and Lacombe*, 2006; *Byrne et al.*, 2011].

[66] **Acknowledgments.** This research was carried out with the aid of grants by CSIC–Proyectos Intramurales 2006 3 01 010, and MICINN: CGL2009-11843-BTE. We would like to thank the Department of Earth Sciences, NCKU, Tainan, for its support of students during field work. We are especially indebted to Her Dai-Jie, Chien Chih-Wei, E Justin, and of course Huang Chi-Yue. We also want to thank the Central Geological Survey, in particular, Chu Hao-Tsu and Chen Mien-Ming for all of their help and advice. M. Simoes kindly provided the reflection seismic profile. Reviews of this manuscript by F. Mouthereau, T. Byrne, E. Casciello, and an anonymous reviewer helped to clarify a number of ideas.

References

Afonso, J. C., and S. Zlotnik (2011), The subductability of the continental lithosphere: The before and after story, in *Arc-Continent Collision*, edited by D. Brown and P. D. Ryan, pp. 53–86, Springer, New York.

Bertrand, E., M. Unsworth, C.-W. Chiang, C.-S. Chen, C.-C. Chen, F. Wu, E. Türkoglu, H.-L. Hsu, and G. Hill (2009), Magnetotelluric evidence for thick-skinned tectonics in central Taiwan, *Geology*, *37*, 711–714, doi:10.1130/G25755A.1.

Bertrand, E., M. Unsworth, C.-W. Chiang, C.-S. Chen, C.-C. Chen, F. Wu, E. Türkoglu, H.-L. Hsu, and G. Hill (2012), Magnetotelluric imaging beneath the Taiwan orogen: An arc-continent collision, *J. Geophys. Res.*, *117*, B01402, doi:10.1029/2011JB008688.

Beyssac, O., M. Simoes, J. P. Avouac, K. A. Farley, Y.-G. Chen, Y.-C. Chan, and B. Goffé (2007), Late Cenozoic metamorphic evolution and exhumation of Taiwan, *Tectonics*, *26*, TC6001, doi:10.1029/2006TC002064.

Bos, A. G., W. Spakman, and M. C. J. Nyst (2003), Surface deformation and tectonic setting of Taiwan inferred from a GPS velocity field, *J. Geophys. Res.*, *108*(B10), 2458, doi:10.1029/2002JB002336.

Brown, D., and P. D. Ryan (Eds.) (2011), *Arc-Continent Collision*, 493 pp., Springer, New York.

Brown, D., J. Alvarez-Marron, A. Perez-Estaun, Y. Gorozhanina, V. Baryshev, and V. Puchkov (1997), Geometric and kinematic evolution of the foreland thrust and fold belt in the southern Urals, *Tectonics*, *16*, 551–562, doi:10.1029/97TC00815.

Brown, D., J. Alvarez-Marron, A. Perez-Estaun, V. Puchkov, and C. Ayala (1999), Basement influence on foreland thrust and fold belt development: An example from the southern Urals, *Tectonophysics*, *308*, 459–472, doi:10.1016/S0040-1951(99)00147-X.

Brown, D., P. Spadea, V. Puchkov, J. Alvarez-Marron, R. Herrington, A. P. Willner, R. Hetzel, and Y. Gorozhanina (2006), Arc-continent collision in the southern Urals, *Earth Sci. Rev.*, *79*, 261–287, doi:10.1016/j.earscirev.2006.08.003.

Brown, D., et al. (2011), Arc-continent collision: The making of an orogen, in *Arc-Continent Collision*, edited by D. Brown and P. D. Ryan, pp. 477–493, Springer, New York.

Bryant, B., and D. J. Nichols (1988), Late Mesozoic and early Tertiary reactivation of an ancient crustal boundary along the Uinta trend and its interaction with the Sevier orogenic belt, in *Interaction of the Rocky Mountain Foreland and Cordilleran Thrust Belt*, edited by C. J. Schmidt and W. J. Perry, *Mem. Geol. Soc. Am.*, *171*, 411–430.

Butler, R. W. H., R. E. Holdsworth, and G. E. Lloyd (1997), The role of basement reactivation in continental deformation, *J. Geol. Soc.*, *154*, 69–71, doi:10.1144/gsjgs.154.1.0069.

Butler, R. W. H., S. Spencer, and H. M. Griffiths (1998), The structural response to evolving plate kinematics during transpression: Evolution of the Lebanese restraining bend of the Dead Sea transform, in *Continental Transpressional and Transtensional Tectonics*, edited by R. E. Holdsworth, R. A. Strachan, and J. F. Dewey, *Geol. Soc. Spec. Publ.*, *135*, 81–106.

Byrne, T., Y.-C. Chan, R.-J. Rau, C.-Y. Lu, Y.-H. Lee, and Y.-J. Wang (2011), The arc-continent collision in Taiwan, in *Arc-Continent Collision*, edited by D. Brown and P. D. Ryan, pp. 213–245, Springer, New York.

Carena, S., J. Suppe, and H. Kao (2002), Active detachment of Taiwan illuminated by small earthquakes and its control of first-order topography, *Geology*, *30*, 935–938, doi:10.1130/0091-7613(2002)030<0935:ADOTIB>2.0.CO;2.

Chang, C.-H., Y.-M. Wu, T.-C. Shin, and C.-Y. Wang (2000), Relocating the 1999 Chi-Chi earthquake, Taiwan, *Terr. Atmos. Oceanic Sci.*, *11*, 581–590.

Chang, C.-H., Y.-M. Wu, L. Zhao, and F. Wu (2007), Aftershocks of the 1999 Chi-Chi, Taiwan, earthquake: The first hour, *Bull. Seismol. Soc. Am.*, *97*, 1245–1258, doi:10.1785/0120060184.

Chang, L.-S. (1976), The Lushanian stage in the Central Range of Taiwan and its fauna, in *Progress in Micropaleontology, Selected Papers in Honor of Prof. Kiyoshi Asano*, edited by Y. Takayanagi and T. Saito, pp. 27–55, Micropaleontol. Press, New York.

Chen, C.-H., et al. (2000), Geological map of Taiwan, scale 1:500,000, Cent. Geol. Sur., Taipei.

Chen, K.-C., B.-S. Huang, J.-H. Wang, and H.-Y. Yen (2002), Conjugate thrust faulting associated with the 1999 Chi-Chi, Taiwan, earthquake sequence, *Geophys. Res. Lett.*, *29*(8), 1277, doi:10.1029/2001GL014250.

Chen, M.-M., N.-T. Yu, H.-T. Chu, K.-S. Shea, and Y.-C. Hsieh (2009), Larger foraminifera in the so-called "Meichi Sandstone" of Wujie area, southern Hsuehshan Range, *Spec. Publ. 22*, pp. 227–242, Cent. Geol. Surv., Taipei.

Chen, R.-Y., H. Kao, C.-S. Chang, and K.-W. Kuo (2002), Determination of earthquake fault plane from strong-motion waveform inversion, paper presented at 9th Symposium on the Geophysics of Taiwan, Chin. Geophys. Union, Taipei.

Chen, W.-S., et al. (2000), The evolution of foreland basins in the western Taiwan: Evidence from the Plio-Pleistocene sequences, *Bull. Cent. Geol. Surv.*, *13*, 136–156.

Chen, W.-S., K. D. Ridgway, C.-S. Horng, Y.-G. Chen, K.-S. Shea, and M.-G. Yeh (2001a), Stratigraphic architecture, magnetostratigraphy, and incised valley systems of the Pliocene-Pleistocene collisional marine

foreland basin of Taiwan, *Geol. Soc. Am. Bull.*, *113*, 1249–1271, doi:10.1130/0016-7606(2001)113<1249:SAMAIV>2.0.CO;2.
Chen, W.-S., et al. (2001b), 1999 Chi-Chi earthquake: A case study on the role of thrust-ramp structures for generating earthquakes, *Bull. Seismol. Soc. Am.*, *91*, 986–994, doi:10.1785/0120000731.
Chen, W.-S., Y.-G. Chen, R.-C. Shih, T.-K. Liu, N.-W. Huang, C.-C. Lin, S.-H. Sung, and K.-J. Lee (2003), Thrust-related river terrace development in relation to the 1999 Chi-Chi earthquake rupture, Western Foothills, central Taiwan, *J. Asian Earth Sci.*, *21*, 473–480, doi:10.1016/S1367-9120(02)00072-X.
Chen, W.-S., et al. (2007), Late Holocene paleoearthquake activity in the middle part of the Longitudinal Valley Fault, eastern Taiwan, *Earth Planet. Sci. Lett.*, *264*, 420–437, doi:10.1016/j.epsl.2007.09.043.
Chi, W.-R., J. Namson, and J. Suppe (1981), Stratigraphic record of plate interactions in the Coastal Range of eastern Taiwan, *Mem. Geol. Soc. China*, *4*, 491–530.
Ching, K.-E., R.-J. Rau, K. M. Johnson, J.-C. Lee, and J.-C. Hu (2011a), Present-day kinematics of active mountain building in Taiwan from GPS observations during 1995–2005, *J. Geophys. Res.*, *116*, B09405, doi:10.1029/2010JB008058.
Ching, K.-E., M.-L. Hsieh, K. M. Johnson, K.-H. Chen, R.-J. Rau, and M. Ying (2011b), Modern vertical deformation rates and mountain building in Taiwan from precise leveling and continuous GPS observations, 2000–2008, *J. Geophys. Res.*, *116*, B08406, doi:10.1029/2011JB008242.
Chiu, H.-T. (1975), Miocene stratigraphy and its relation to the Palaeogene rocks in west-central Taiwan, *Pet. Geol. Taiwan*, *12*, 51–80.
Clark, M. B., D. M. Fisher, C.-Y. Lu, and C.-H. Chen (1993), Kinematic analyses of the Hsuehshan Range, Taiwan: A large-scale pop-up structure, *Tectonics*, *12*, 205–217, doi:10.1029/92TC01711.
Cooper, M. A., and G. D. Williams (1989), *Inversion Tectonics*, *Geol. Soc. Spec. Publ.*, *44*, 375 pp.
Covey, M. (1986), The evolution of foreland basins to steady state: Evidence from the western Taiwan foreland basin, in *Foreland Basins*, edited by P. A. Allen and P. Homewood, *Spec. Publ. Int. Assoc. Sedimentol.*, *8*, 77–90, Oxford, U. K.
Crespi, J. M., Y.-C. Chan, and M. S. Swaim (1996), Synorogenic extension and exhumation of the Taiwan hinterland, *Geology*, *24*, 247–250, doi:10.1130/0091-7613(1996)024<0247:SEAEOT>2.3.CO;2.
Dahlstrom, C. D. A. (1969), Balanced cross sections, *Can. J. Earth Sci.*, *6*, 743–757, doi:10.1139/e69-069.
Dewey, J. F., M. R. Hempton, W. S. F. Kidd, F. Saroglu, and A. M. C. Sengör (1986), Shortening of continental lithosphere: The neotectonics of eastern Anatolia—A young collision zone, in *Collision Tectonics*, edited by M. P. Coward and A. C. Ries, *Geol. Soc. Spec. Publ.*, *19*, 3–36.
Ding, Z.-Y., Y.-Q. Yang, Z.-X. Yao, and G.-H. Zhang (2001), A thin-skinned collisional model for the Taiwan orogeny, *Tectonophysics*, *332*, 321–331, doi:10.1016/S0040-1951(00)00289-4.
Dorsey, R. J. (1987), Provenance evolution and unroofing history of a modern arc-continent collision: Evidence from petrology of Plio-Pleistocene sandstones, eastern Taiwan, *J. Sediment. Petrol.*, *58*, 208–218.
Fisher, D. M., C.-Y. Lu, and H.-T. Chu (2002), Taiwan slate belt: Insights in the ductile interior of an arc-continent collision, in *Geology and Geophysics of an Arc-Continent Collision, Taiwan*, edited by T. B. Byrne and C.-S. Liu, *Spec. Pap. Geol. Soc. Am.*, *358*, 93–106.
Fisher, D. M., S. Willet, E.-C. Yeh, and M. B. Clark (2007), Cleavage fronts and fans as reflections of orogen stress and kinematics in Taiwan, *Geology*, *35*, 65–68, doi:10.1130/G22850A.1.
Frohlich, C. (1992), Triangle diagrams: Ternary graphs to display similarity and diversity of earthquake focal mechanisms, *Phys. Earth Planet. Inter.*, *75*, 193–198, doi:10.1016/0031-9201(92)90130-N.
Frohlich, C. (2001), Display and quantitative assessment of distributions of earthquake focal mechanisms, *Geophys. J. Int.*, *144*, 300–308, doi:10.1046/j.1365-246x.2001.00341.x.
Fuller, C. W., S. D. Willet, D. Fisher, and C.-Y. Lu (2006), A thermomechanical wedge model of Taiwan constrained by fission-track thermochronometry, *Tectonophysics*, *425*, 1–24, doi:10.1016/j.tecto.2006.05.018.
Gerya, T. (2011), Intra-oceanic subduction zones, in *Arc-Continent Collision*, edited by D. Brown and P. D. Ryan, pp. 23–52, Springer, New York.
Glen, R. A. (1985), Basement control on the deformation of cover basins: An example from the Cobar district in the Lachlan Fold Belt, Australia, *J. Struct. Geol.*, *7*, 301–315, doi:10.1016/0191-8141(85)90037-9.
Gourley, J. R., T. Byrne, Y.-C. Chan, F. Wu, and R. J. Rau (2007), Fault geometries illuminated from seismicity in central Taiwan: Implications for crustal scale structural boundaries in the northern Central Range, *Tectonophysics*, *445*, 168–185, doi:10.1016/j.tecto.2007.08.013.
Gutenberg, B., and C. A. F. Richter (1956), Earthquake magnitude, intensity, energy, and acceleration, *Bull. Seismol. Soc. Am.*, *46*, 105–145.
Harris, R. (2011), The nature of the Banda arc-continent collision in the Timor region, in *Arc-Continent Collision*, edited by D. Brown and P. D. Ryan, pp. 163–211, Springer, New York.
Hatcher, R. D., and R. T. Williams (1986), Mechanical model for single thrust sheets Part I: Taxonomy of crystalline thrust sheets and their relationships to the mechanical behavior of orogenic belts, *Geol. Soc. Am. Bull.*, *97*, 975–985, doi:10.1130/0016-7606(1986)97<975:MMFSTS>2.0.CO;2.
Hickman, J. B., D. V. Wiltschko, J.-H. Hung, P. Fang, and Y. Bock (2002), Structure and evolution of the active fold-and-thrust belt of southwestern Taiwan from Global Positioning System analysis, in *Geology and Geophysics of an Arc-Continent Collision, Taiwan*, edited by T. B. Byrne and C.-S. Liu, *Spec. Pap. Geol. Soc. Am.*, *358*, 75–92.
Ho, C.-S. (1988), *An introduction to the geology of Taiwan: Explanatory text of the geological map of Taiwan*, Cent. Geol. Sur, Taipei.
Hossack, J. R. (1979), The use of balanced cross-sections in the calculation of orogenic contraction: A review, *J. Geol. Soc.*, *136*, 705–711, doi:10.1144/gsjgs.136.6.0705.
Hsu, Y.-J., S.-B. Yu, M. Simmons, L.-C. Kuo, and H.-Y. Chen (2009), Interseismic crustal deformations in the Taiwan plate boundary zone revealed by GPS observations, seismicity, and earthquake focal mechanisms, *Tectonophysics*, *479*, 4–18, doi:10.1016/j.tecto.2008.11.016.
Huang, C., Y.-C. Chan, J.-C. Hu, J. Angelier, and J.-C. Lee (2008), Detailed surface co-seismic displacement of the 1999 Chi-Chi earthquake in western Taiwan and implication of fault geometry in the shallow subsurface, *J. Struct. Geol.*, *30*, 1167–1176, doi:10.1016/j.jsg.2008.06.001.
Huang, C.-S., K.-S. Shea, and M.-M. Chen (2000), *Geological map of Taiwan: Sheet 32*, Puli, Cent. Geol. Sur, Taipei.
Huang, C.-Y., W.-Y. Wu, C.-P. Chang, S. Tsao, P.-B. Yuan, C.-W. Lin, and K.-Y. Xia (1997), Tectonic evolution of accretionary prism in the arc-continent collision terrane of Taiwan, *Tectonophysics*, *281*, 31–51, doi:10.1016/S0040-1951(97)00157-1.
Huang, C.-Y., P.-B. Yuan, C.-W. Lin, T.-K. Wang, and C.-P. Chang (2000), Geodynamic processes of Taiwan arc-continent collision and comparison with analogs in Timor, Papua New Guinea, Urals, and Corsica, *Tectonophysics*, *325*, 1–21, doi:10.1016/S0040-1951(00)00128-1.
Huang, C.-Y., K. Xia, P. B. Yuan, and P.-G. Chen (2001), Structural evolution from Paleogene extension to latest Miocene-Recent arc-continent collision offshore Taiwan: Comparison with on land geology, *J. Asian Earth Sci.*, *19*, 619–639, doi:10.1016/^367-9120(00)00065-1.
Huang, C.-Y., P.-B. Yuan, and S.-J. Tsao (2006), Temporal and spatial records of active arc-continent collision in Taiwan: A synthesis, *Geol. Soc. Am. Bull.*, *118*, 274–288, doi:10.1130/B25527.1.
Hung, J.-H., K.-F. Ma, C.-Y. Wang, H. Ito, W. Lin, and E.-C. Yeh (2009), Subsurface structure, physical properties, fault-zone characteristics and stress state in scientific drill holes of Taiwan Chelungpu Fault drilling project, *Tectonophysics*, *466*, 307–321, doi:10.1016/j.tecto.2007.11.014.
Hwang, C., Y.-S. Hsiao, H.-C. Shih, M. Yang, K.-H. Chen, R. Forsberg, and A. V. Olesen (2007), Geodetic and geophysical results from a Taiwan airborne gravity survey: Data reduction and accuracy assessment, *J. Geophys. Res.*, *112*, B04407, doi:10.1029/2005JB004220.
Jahn, B.-M., W.-R. Chi, and T.-F. Yui (1992), A Late Permian formation of Taiwan (marbles from Chia-Li well No. 1): Pb-Pb isochron and Sr isotope evidence, and its regional geological significance, *J. Geol. Soc. China*, *35*, 193–218.
Jeng, F.-S., M.-L. Lin, C.-Y. Lu, and K.-P. Huang (2002), Characteristics of seismic energy release of subduction zones—Examples from Taiwan, *Eng. Geol.*, *67*, 17–38, doi:10.1016/S0013-7952(02)00107-2.
Johnson, K. M., and P. Segall (2004), Imaging the ramp-décollement geometry of the Chelungpu fault using coseismic GPS displacements from the 1999 Chi-Chi, Taiwan earthquake, *Tectonophysics*, *378*, 123–139, doi:10.1016/j.tecto.2003.10.020.
Jones, R. H., and R. C. Stewart (1997), A method for determining significant structures in a cloud of earthquakes, *J. Geophys. Res.*, *102*, 8245–8254, doi:10.1029/96JB03739.
Kao, H., and W.-P. Chen (2000), The Chi-Chi earthquake sequence: Active, out-of-sequence thrust faulting in Taiwan, *Science*, *288*, 2346–2349, doi:10.1126/science.288.5475.2346.
Kaus, B. J. P., C. Steedman, and T. W. Becker (2008), From passive continental margin to mountain belt: Insights from analytical and numerical modeling and application to Taiwan, *Phys. Earth Planet. Inter.*, *171*, 235–251, doi:10.1016/j.pepi.2008.06.015.
Kirkpatrick, J. D., Z. K. Shipton, J. P. Evans, S. Micklethwaite, S. J. Lim, and P. McKillop (2008), Strike-slip fault terminations at seismogenic depths: The structure and kinematics of the Glacier Lakes fault, Sierra Nevada United States, *J. Geophys. Res.*, *113*, B04304, doi:10.1029/2007JB005311.
Kuo-Chen, H., F. T. Wu, and S. W. Roecker (2012), Three-dimensional P velocity structures of the lithosphere beneath Taiwan from the analysis

of TAIGER and related seismic data sets, *J. Geophys. Res.*, *117*, B06306, doi:10.1029/2011JB009108.

Laubscher, H. P. (1987), Die tektonische Entwicklung der Nordschweitz, *Eclogae Geol. Helv.*, *80*, 287–303.

Lee, J.-C., and Y.-C. Chan (2007), Structure of the 1999 Chi-Chi earthquake rupture and interaction of thrust faults in the active fold belt of western Taiwan, *J. Asian Earth Sci.*, *31*, 226–239, doi:10.1016/j.jseaes.2006.07.024.

Lee, J. C., J. Angelier, and H.-T. Chu (1997), Polyphase history and kinematics of a complex major fault zone in the northern Taiwan mountain belt: The Lishan fault, *Tectonophysics*, *274*, 97–115, doi:10.1016/S0040-1951(96)00300-9.

Lee, P.-J. (1963), Lithofacies of the Toukoshan-Cholan Formation of western Taiwan, *Proc. Geol. Soc. China*, *6*, 41–50.

Lee, Y.-H., C.-C. Chen, T.-K. Liu, H.-C. Ho, H.-Y. Lu, and W. Lo (2006), Mountain building mechanisms in the southern Central Range of the Taiwan orogenic belt—From accretionary wedge deformation to arc-continent collision, *Earth Planet. Sci. Lett.*, *252*, 413–422, doi:10.1016/j.epsl.2006.09.047.

Leever, K. A., R. H. Gabrielsen, J. I. Faleide, and A. Braathen (2011), A transpressional origin for the West Spitsbergen fold-and-thrust belt: Insight from analog modeling, *Tectonics*, *30*, TC2014, doi:10.1029/2010TC002753.

Lin, A. T., and A. Watts (2002), Origin of the west Taiwan basin by orogenic loading and flexure of a rifted continental margin, *J. Geophys. Res.*, *107*(B9), 2185, doi:10.1029/2001JB000669.

Lin, A. T., A. Watts, and P. Hesselbo (2003), Cenozoic stratigraphy and subsidence history of the South China Sea margin in the Taiwan region, *Basin Res.*, *15*, 453–478, doi:10.1046/j.1365-2117.2003.00215.x.

Lin, C.-H. (2007), Tomographic image of crustal structures across the Chelungpu fault: Is the seismogenic layer structure- or depth-dependent?, *Tectonophysics*, *443*, 271–279, doi:10.1016/j.tecto.2007.01.022.

Lin, K.-C., J.-C. Hu, K.-E. Ching, J. Angelier, R.-J. Rau, S.-B. Yu, C.-H. Tsai, T.-C. Shin, and M.-H. Huang (2010), GPS crustal deformation, strain rate, and seismic activity after the 1999 Chi-Chi earthquake in Taiwan, *J. Geophys. Res.*, *115*, B07404, doi:10.1029/2009JB006417.

Liu, T.-K., S. Hsieh, Y.-G. Chen, and W.-S. Chen (2001), Thermokinematic evolution of the Taiwan oblique-collision mountain belt as revealed by zircon fission track dating, *Earth Planet. Sci. Lett.*, *186*, 45–56, doi:10.1016/S0012-821X(01)00232-1.

Lo, W., and C.-N. Yang (2002), *Geological map of Taiwan, sheet 26, Wushe*, scale *1:50,000*, Cent. Geol. Surv., Taipei.

Malavieille, J., and G. Trullenque (2009), Consequences of continental subduction on forearc basin and accretionary wedge deformation in SE Taiwan: Insights from analogue modeling, *Tectonophysics*, *466*, 377–394, doi:10.1016/j.tecto.2007.11.016.

Manatschal, G. (2004), New models for evolution of magma-poor rifted margins based on a review of data and concepts from West Iberia and the Alps, *Int. J. Earth Sci.*, *93*, 432–466, doi:10.1007/s00531-004-0394-7.

McIntosh, K., Y. Nakamura, T.-K. Wang, R.-C. Shih, A. Chen, and C.-S. Liu (2005), Crustal-scale seismic profiles across Taiwan and the western Philippine Sea, *Tectonophysics*, *401*, 23–54, doi:10.1016/j.tecto.2005.02.015.

McKenzie, D. (1978), Some remarks on the development of sedimentary basins, *Earth Planet. Sci. Lett.*, *40*, 25–32, doi:10.1016/0012-821X(78)90071-7.

Mohn, G., G. Manatschal, O. Müntener, M. Beltrando, and E. Masini (2010), Unravelling the interaction between tectonic and sedimentary processes during lithospheric thinning in the Alpine Tethys margins, *Int. J. Earth Sci.*, Suppl 1, *99*, 75–101, doi:10.1007/s00531-010-0566-6.

Mouthereau, F., and O. Lacombe (2006), Inversion of the Paleogene Chinese continental margin and thick-skinned deformation in the Western Foreland of Taiwan, *J. Struct. Geol.*, *28*, 1977–1993, doi:10.1016/j.jsg.2006.08.007.

Mouthereau, F., and C. Petit (2003), Rheology and strength of the Eurasian continental lithosphere in the foreland of the Taiwan collision belt: Constraints from seismicity, flexure, and structural styles, *J. Geophys. Res.*, *108*(B11), 2512, doi:10.1029/2002JB002098.

Mouthereau, F., O. Lacombe, B. Deffontaines, J. Angelier, H.-T. Chu, and C.-T. Lee (1999), Quaternary transfer faulting and belt front deformation at Pakuashan (western Taiwan), *Tectonics*, *18*, 215–230, doi:10.1029/1998TC900025.

Mouthereau, F., O. Lacombe, B. Deffontaines, J. Angelier, and S. Brusset (2001), Deformation history of the southwestern Taiwan foreland thrust belt: Insights from tectono-sedimentary analyses and balanced cross-sections, *Tectonophysics*, *333*, 293–318, doi:10.1016/S0040-1951(00)00280-8.

Mouthereau, F., B. Deffontaines, O. Lacombe, and J. Angelier (2002), Variations along the strike of the Taiwan thrust belt: Basement control on structural style, wedge geometry, and kinematics, in *Geology and Geophysics of an Arc-Continent Collision, Taiwan*, edited by T. B. Byrne and C.-S. Liu, *Spec. Pap. Geol. Soc. Am.*, *358*, 31–54.

Mouthereau, F., C. Fillon, and K.-F. Ma (2009), Distribution of strain rates in the Taiwan orogenic wedge, *Earth Planet. Sci. Lett.*, *284*, 361–385, doi:10.1016/j.epsl.2009.05.005.

Murphy, J. B., J. W. F. Waldron, D. J. Kontak, G. Pe-Piper, and D. J. W. Piper (2011), Minas Fault Zone: Late Paleozoic history of an intra-continental orogenic transform fault in the Canadian Appalachians, *J. Struct. Geol.*, *33*, 312–328, doi:10.1016/j.jsg.2010.11.012.

Namson, J. (1981), Structure of the western foothills belt, Miaoli-Hsinchu area, Taiwan. 1. Southern part, *Pet. Geol. Taiwan*, *18*, 31–51.

Narr, W., and J. Suppe (1994), Kinematics of basement-involved compressive structures, *Am. J. Sci.*, *294*, 802–860, doi:10.2475/ajs.294.7.802.

Oncken, O., C. von Winterfeld, and U. Dittmar (1999), Accretion of a rifted passive margin: The Late Paleozoic Rhenohercynian fold and thrust belt (Middle European Variscides), *Tectonics*, *18*, 75–91, doi:10.1029/98TC02763.

Perez-Estaun, A., J. Alvarez-Marron, D. Brown, V. Puchkov, Y. Gorozhanina, and V. Baryshev (1997), Along-strike structural variations in the foreland thrust and fold belt of the southern Urals, *Tectonophysics*, *276*, 265–280, doi:10.1016/S0040-1951(97)00060-7.

Rau, R.-J., and F. T. Wu (1995), Tomographic imaging of lithospheric structures under Taiwan, *Earth Planet. Sci. Lett.*, *133*, 517–532, doi:10.1016/0012-821X(95)00076-O.

Reston, T., and G. Manatschal (2011), Rifted margins: Building blocks of later collision, in *Arc-Continent Collision*, edited by D. Brown and P. D. Ryan, pp. 3–21, Springer, New York.

Reston, T., C. M. Krawczyk, and D. Klaeschen (1996), The S reflector west of Galica (Spain): Evidence from prestack depth migration for detachment faulting during continental breakup, *J. Geophys. Res.*, *101*, 8075–8091, doi:10.1029/95JB03466.

Rodgers, J. (1987), Chains of basement uplifts within cratons marginal to orogenic belts, *Am. J. Sci.*, *287*, 661–692, doi:10.2475/ajs.287.7.661.

Sakaguchi, A., A. Yanagihara, K. Ujiie, H. Tanaka, and M. Kameyama (2007), Thermal maturity of a fold–thrust belt based on vitrinite reflectance analysis in the Western Foothills complex, western Taiwan, *Tectonophysics*, *443*, 220–232, doi:10.1016/j.tecto.2007.01.017.

Schmidt, C. J., J. M. O'Neill, and W. C. Brandon (1988), Influence of Rocky Mountain foreland uplifts on the development of the frontal fold and thrust belt, southwestern Montana, in *Interaction of the Rocky Mountain Foreland and Cordilleran Thrust Belt*, edited by C. J. Schmidt and W. J. Perry, *Mem. Geol. Soc. Am.*, *171*, 171–201.

Shaw, C.-L. (1996), Stratigraphic correlation and isopach maps of the Western Taiwan Basin, *Terr. Atmos. Oceanic Sci.*, *7*, 333–360.

Shin, T.-C. (1993), The calculation of local magnitude from the simulated Wood–Anderson seismograms of the short-period seismograms in Taiwan area, *Terr. Atmos. Oceanic Sci.*, *4*, 155–170.

Shyu, J. B. H., K. Sieh, Y.-G. Chen, R.-Y. Chuang, Y. Wang, and L.-H. Chung (2008), Geomorphology of the southernmost Longitudinal Valley Fault: Implications for evolution of the active suture of eastern Taiwan, *Tectonics*, *27*, TC1019, doi:10.1029/2006TC002060.

Simoes, M., and J. P. Avouac (2006), Investigating the kinematics of mountain building in Taiwan from the spatiotemporal evolution of the foreland basin and western foothills, *J. Geophys. Res.*, *111*, B10401, doi:10.1029/2005JB004209.

Simoes, M., J. P. Avouac, Y.-G. Chen, A. K. Singkvi, C.-Y. Wang, M. Jaiswal, Y.-C. Chan, and S. Bernard (2007a), Kinematic analysis of the Pakuashan fault tip fold, west central Taiwan: Shortening rate and age of folding inception, *J. Geophys. Res.*, *112*, B03S14, doi:10.1029/2005JB004198.

Simoes, M., J. P. Avouac, O. Beyssac, B. Goffé, K. A. Farley, and Y.-G. Chen (2007b), Mountain building in Taiwan: A thermokinematic model, *J. Geophys. Res.*, *112*, B11405, doi:10.1029/2006JB004824.

Simoes, M., O. Beyssac, and Y.-G. Chen (2012), Late Cenozoic metamorphism and mountain building in Taiwan: A review, *J. Asian Earth Sci.*, *46*, 92–119, doi:10.1016/j.jseaes.2011.11.009.

Sung, Q.-C., Y.-C. Chen, H. Tsai, Y.-G. Chen, and W.-S. Chen (2000), Comparison study on the coseismic deformation of the 1999 Chi-Chi earthquake and long-term stream gradient changes along the Chelungpu fault in central Taiwan, *Terr. Atmos. Oceanic Sci.*, *11*, 735–750.

Suppe, J. (1976), Décollement folding in southwestern Taiwan, *Pet. Geol. Taiwan*, *13*, 25–35.

Suppe, J. (1980), A retrodeformable cross section of northern Taiwan, *Proc. Geol. Soc. China*, *23*, 46–55.

Suppe, J. (1981), Mechanics of mountain building and metamorphism in Taiwan, *Geol. Soc. China Mem*, *4*, 67–89.

Sylvester, A. G. (1988), Strike-slip faults, *Geol. Soc. Am. Bull.*, *100*, 1666–1703, doi:10.1130/0016-7606(1988)100<1666:SSF>2.3.CO;2.

Teng, L.-S. (1987), Stratigraphic records of the late Cenozoic Penglai Orogeny of Taiwan, *Acta Geol. Taiwanica*, *25*, 205–224.

Teng, L.-S. (1990), Geotectonic evolution of the late Cenozoic arc-continent collision in Taiwan, *Tectonophysics*, *183*, 57–76, doi:10.1016/0040-1951(90)90188-E.

Teng, L.-S. (1992), Geotectonic evolution of Tertiary continental margin basins of Taiwan, *Pet. Geol. Taiwan*, *27*, 1–19.

Teng, L.-S., and A.-T. Lin (2004), Cenozoic tectonics of the China continental margin; Insights from Taiwan, in *Aspects of the Tectonic Evolution of China*, edited by J. Malpas et al., *Geol. Soc. Spec. Publ.*, *226*, 313–332.

Teng, L.-S., Y. Wang, C.-H. Tang, C.-Y. Huang, T.-C. Huang, M.-S. Yu, and A. Ke (1991), Tectonic aspects of the Paleogene depositional basin of northern Taiwan, *Proc. Geol. Soc. China*, *34*, 313–336.

Tillman, K. S., and T. B. Byrne (1995), Kinematic analysis of the Taiwan slate belt, *Tectonics*, *14*, 322–341, doi:10.1029/94TC02451.

Ustaszewski, K., Y.-M. Wu, J. Suppe, H.-H. Huang, C.-H. Chang, and S. Carena (2012), Crust-mantle boundaries in the Taiwan-Luzon arc-continent collision system determined from local earthquake tomography and 1D models: Implications for the mode of subduction polarity reversal, *Tectonophysics*, doi:10.1016/j.tecto.2011.12.029, in press.

Walcott, R. I. (1998), Modes of oblique compression: Late Cenozoic tectonics of the South Island of New Zealand, *Rev. Geophys.*, *36*, 1–26, doi:10.1029/97RG03084.

Wang, C.-Y., C.-L. Li, F.-C. Su, M.-T. Leu, M.-S. Wu, S.-H. Lai, and C.-C. Chern (2002), Structural mapping of the 1999 Chi-Chi earthquake fault, Taiwan, by seismic reflection methods, *Terr. Atmos. Oceanic Sci.*, *13*, 211–226.

Wang, C.-Y., S.-Y. Kuo, W.-L. Shyu, and J.-W. Hsiao (2003), Investigating near surface structures under the Changhua fault, west-central Taiwan by the reflection seismic method, *Terr. Atmos. Oceanic Sci.*, *14*, 343–367.

Wang, H.-L., H.-W. Chen, and L. Zhu (2010), Constraints on average Taiwan reference Moho discontinuity model—Receiver function analysis using BATS data, *Geophys. J. Int.*, *183*, 1–19.

Wibberley, C. A. J. (1997), A mechanical model for the reactivation of compartmental faults in basement thrust sheets, Muzelle region, western Alps, *J. Geol. Soc.*, *154*, 123–128, doi:10.1144/gsjgs.154.1.0123.

Woodward, N. B. (1988), Primary and secondary basement controls on thrust sheet geometries, in *Interaction of the Rocky Mountain Foreland and Cordilleran Thrust Belt*, edited by C. J. Schmidt and W. J. Perry, *Mem. Geol. Soc. Am.*, *171*, 353–366.

Wu, F., R.-J. Rau, and D. Salzberg (1997), Taiwan Orogeny; thin-skinned or lithospheric collision? An introduction to active tectonics in Taiwan, *Tectonophysics*, *274*, 191–220, doi:10.1016/S0040-1951(96)00304-6.

Wu, F., C.-S. Chang, and Y. M. Wu (2004), Precisely relocated hypocentres, focal mechanisms and active orogeny in central Taiwan, in *Aspects of the Tectonic Evolution of China*, edited by J. Malpas et al., *Geol. Soc. Spec. Publ.*, *226*, 333–354.

Wu, Y.-M., C.-H. Chang, N.-C. Hsiao, and F.-T. Wu (2003), Relocation of the 1998 Rueyli, Taiwan, earthquake sequence using three-dimensions velocity structure with stations corrections, *Terr. Atmos. Oceanic Sci.*, *14*, 421–430.

Wu, Y.-M., C.-H. Chang, L. Zhao, J. B. H. Shyu, Y.-G. Chen, K. Sieh, and J. P. Avouac (2007), Seismic tomography of Taiwan: Improved constraints from a dense network of strong motion stations, *J. Geophys. Res.*, *112*, B08312, doi:10.1029/2007JB004983.

Wu, Y.-M., C.-H. Chang, L. Zhao, T.-L. Teng, and M. Nakamura (2008a), A comprehensive relocation of earthquakes in Taiwan from 1991 to 2005, *Bull. Seismol. Soc. Am.*, *98*, 1471–1481, doi:10.1785/0120070166.

Wu, Y.-M., L. Zhao, C. H. Chang, and Y. J. Hsu (2008b), Focal mechanism determination in Taiwan by genetic algorithm, *Bull. Seismol. Soc. Am.*, *98*, 651–661, doi:10.1785/0120070115.

Wu, Y.-M., J. B. H. Shyu, C.-H. Chang, L. Zhao, M. Nakamura, and S.-K. Hsu (2009), Improved seismic tomography offshore northeastern Taiwan: Implications for subduction and collision processes between Taiwan and the southernmost Ryukyu, *Geophys. J. Int.*, *178*(2), 1042–1054, doi:10.1111/j.1365-246X.2009.04180.x.

Wu, Y.-M., Y.-J. Hsu, C.-H. Chang, L.-S. Teng, and M. Nakamura (2010), Temporal and spatial variation of stress field in Taiwan from 1991 to 2007: Insights from comprehensive first motion focal mechanism catalog, *Earth Planet. Sci. Lett.*, *298*, 306–316, doi:10.1016/j.epsl.2010.07.047.

Yamato, P., F. Mouthereau, and E. Burov (2009), Taiwan mountain building: Insights from 2-D thermomechanical modelling of a rheologically stratified lithosphere, *Geophys. J. Int.*, *176*, 307–326, doi:10.1111/j.1365-246X.2008.03977.x.

Yanites, B. J., G. E. Tucker, K. J. Mueller, Y.-G. Chen, T. Wilcox, S.-Y. Huang, and K.-W. Shi (2010), Incision and channel morphology across active structures along the Peikang River, central Taiwan: Implications for the importance of channel width, *Geol. Soc. Am. Bull.*, *122*, 1192–1208, doi:10.1130/B30035.1.

Yen, H.-Y., Y.-H. Yeh, and F. T. Wu (1998), Two-dimensional crustal structures of Taiwan from gravity data, *Tectonics*, *17*, 104–111, doi:10.1029/97TC02697.

Yu, S.-B., and L. C. Kuo (2001), Present day crustal motion along the Longitudinal Valley Fault, eastern Taiwan, *Tectonophysics*, *333*, 199–217, doi:10.1016/S0040-1951(00)00275-4.

Yu, S.-B., H. Y. Chen, and L. C. Kuo (1997), Velocity field of GPS stations in the Taiwan area, *Tectonophysics*, *274*, 41–59, doi:10.1016/S0040-1951(96)00297-1.

Yu, S.-B., Y.-J. Hsu, L. C. Kuo, H.-C. Chen, H.-Y. Chen, and C.-C. Liu (2003), GPS measurement of postseismic deformation following the 1999 Chi-Chi, Taiwan, earthquake, *J. Geophys. Res.*, *108*(B11), 2520, doi:10.1029/2003JB002396.

Yue, L.-F., J. Suppe, and J.-H. Hung (2005), Structural geology of a classic thrust belt earthquake: The 1999 Chi-Chi earthquake Taiwan (Mw = 7.6), *J. Struct. Geol.*, *27*, 2058–2083, doi:10.1016/j.jsg.2005.05.020.

Yui, T.-F., K. Maki, C.-Y. Lan, T. Hirata, H.-T. Chu, Y. Kon, T.-D. Yokoyama, B.-M. Jahn, and W. G. Ernst (2012), Detrital zircons from the Tananao Metamorphic Complex of Taiwan: Implications for sediment provenance and Mesozoic tectonics, *Tectonophysics*, *541–543*, 31–42, doi:10.1016/j.tecto.2012.03.013.

Article 2 - The Shuilikeng fault in the central Taiwan mountain belt

Giovanni Camanni[1], Dennis Brown[1], Joaquina Alvarez-Marron[1], Yih-Min Wu[2], and Hsi-An Chen[2]

[1]Institute of Earth Sciences Jaume Almera, ICTJA-CSIC, Lluis Sole i Sabaris s/n, 08028 Barcelona, Spain
[2]Department of Geosciences, National Taiwan University, Taipei, 106, Taiwan

Status of publication: published in "**Journal of the Geological Society, London**", (2014), v. 171, p. 117-130, doi: 10.1144/jgs2013-014

Contributions of the Ph.D. student to the article:

- Manuscript conception and writing;
- Geological mapping at 1:25.000 scale throughout the map area;
- Construction of geometrically constrained cross-sections;
- Structural analysis of field data;
- Kinematic analysis of fault-slip data;
- Analysis of earthquake hypocentre data;
- Kinematic analysis of earthquake focal mechanisms data and determination of average principal strain axes

Journal of the Geological Society, London, Vol. **171**, 2014, pp. 117–130. doi: 10.1144/jgs2013-014
Published *Online First* on September 12, 2013

The Shuilikeng fault in the central Taiwan mountain belt

GIOVANNI CAMANNI[1*], DENNIS BROWN[1], JOAQUINA ALVAREZ-MARRON[1], YIH-MIN WU[2] & HSI-AN CHEN[2]

[1]*Institute of Earth Sciences Jaume Almera, ICTJA-CSIC, Lluis Sole i Sabaris s/n, 08028 Barcelona, Spain*

[2]*Department of Geosciences, National Taiwan University, Taipei, 106, Taiwan*

**Corresponding author (e-mail: gcamanni@ictja.csic.es)*

Abstract: For over 200 km along strike the Shuilikeng fault of Taiwan separates Miocene rocks of the Western Foothills from the largely Eocene and Oligocene rocks of the Hsuehshan Range to the east. Despite its importance in the Taiwan mountain belt, the structure and kinematics of the Shuilikeng fault are not well known. Here, we present results from new geological mapping along 100 km of its strike length. At the surface, the Shuilikeng fault is a steeply east-dipping brittle fault with a series of splays and bifurcations. Along its southern part, it cuts an earlier fold and fault system. Outcrop kinematic data vary widely, from thrusting to strike-slip. The surface data are integrated with a relocated and collapsed seismicity database to interpret the fault location at depth. These data indicate that the Shuilikeng fault can be traced to greater than 20 km depth. Some 260 focal mechanisms from this dataset indicate that its kinematics is overall transpressive. From a regional perspective, we interpret the Shuilikeng fault to reactivate a pre-existing rift-related basin-bounding fault to the east of which rocks in the Hsuehshan Range are being exhumed.

The Taiwan mountain belt is often cited as an example *par excellence* of a thin-skinned fold-and-thrust belt (i.e. the sedimentary carapace of the margin is detached above the pre-rift basement) underlain by a shallow detachment that ramps down into the basement only in the easternmost part of the thrust belt (Suppe 1980, 1981, 1987; Tillman & Byrne 1995; Wang *et al.* 2000; Ding *et al.* 2001; Carena *et al.* 2002; Yue *et al.* 2005; Malavieille & Trullenque 2009). Although there is general agreement that this thin-skinned structural model is correct along much of the western part of the orogen, recent studies have suggested that the structure and level of crustal involvement in its internal part may differ significantly from that model (e.g. Wu *et al.* 1997, 2004; Gourley *et al.* 2007; Brown *et al.* 2012). This change takes place across the Shuilikeng fault. Even before it was shown to be a fault, Ichikawa *et al.* (1927) recognized that an important contact existed between what today are known to be Miocene rocks to the west and Eocene–Oligocene rocks to the east. In more recent compilations of Taiwan geology (e.g. Chinese Petroleum Company 1982, 1994; Ho 1988; Chen *et al.* 2000) this contact has been clearly defined as a fault (albeit with different names; see below) that extends from south of Yushan Mountain in central Taiwan to the north coast (Fig. 1). In our study area in central Taiwan (Figs 1 and 2), surface geology (e.g. rock ages, structural style, amount of deformation, level of exhumation), a significant increase in the number and the deeper crustal level of seismic events to the east of the fault and, eastward, higher P-wave velocities at shallower depths, all coincide to indicate a significant change across the Shuilikeng fault (Fig. 1) (Wang *et al.* 2000; Kim *et al.* 2005, 2010; Beyssac *et al.* 2007; Lin 2007; Sakaguchi *et al.* 2007; Simoes *et al.* 2007, 2012; Wu *et al.* 2007; Yamato *et al.* 2009; Brown *et al.* 2012; Kuo-Chen *et al.* 2012). Despite the large amount of data that points toward its importance as a major boundary in the Taiwan orogen, the detailed structure and kinematics of the Shuilikeng fault are not well known. Consequently, it has been interpreted in different ways; for example, as a layer-parallel thrust (the Chukou thrust of Suppe 1981), as a steeply eastward-dipping thrust that extends to deep in the middle crust (the Shuichangliu fault of Wang *et al.* 2002, or the Tulungwan thrust of Rodriguez-Roa & Wiltschko 2010), as a westward-dipping displaced upper part of a pre-existing west-dipping extensional fault (Yue *et al.* 2005), or as a steeply east-dipping transpressional fault that penetrates well into the middle crust (Brown *et al.* 2012). Also, Wiltschko *et al.* (2010) linked it with the Chaochou fault in the south. Neither there is any consensus on whether the Shuilikeng fault is currently active, although recently Sung *et al.* (2000) and Yanites *et al.* (2010) have used river incision, channel morphology and stream gradients along several rivers in central Taiwan to suggest that the Shuilikeng fault has been active throughout the Holocene. By comparing today's stream gradients with those from earlier mapping, Sung *et al.* (2000) furthermore suggested that it has been active during the last 80 years. Nevertheless, even with the large number of earthquakes around it (e.g. Wu *et al.* 2008*a*), seismicity or changes in global positioning system (GPS) velocities are generally not attributed to the Shuilikeng fault (there are exceptions: Yue *et al.* (2005) and Bos *et al.* (2003), respectively), and no surface ruptures have been described from it.

Despite the uncertainties in whether or not the Shuilikeng fault is currently active, there are clear indications from the geological and geophysical data that it is a major structural boundary within the Taiwan mountain belt. Given the wide range of structural interpretations noted above, it is also clear that more detailed studies of the fault are needed to advance our understanding of the structure and kinematics of this orogen. In this paper we present the results of new 1:25000 scale geological mapping and structural analysis along *c.* 100 km (a little less than one-half of its length) of the Shuilikeng fault in central Taiwan (Figs 1 and 2) that further define its map pattern, outcropping structure and kinematics. To help correlate these outcrop data with the location and geometry of the Shuilikeng fault at depth we integrate them with a collapsed seismicity dataset derived from the relocated seismicity database of Wu *et al.* (2008*a*) updated to 2011. Our field kinematic data are augmented by 264 focal mechanism solutions derived from events along the Shuilikeng fault that help place further constraints on its kinematics and recent activity. Finally, we interpret the regional structure and kinematics of the Shuilikeng fault within the context of the Taiwan orogen.

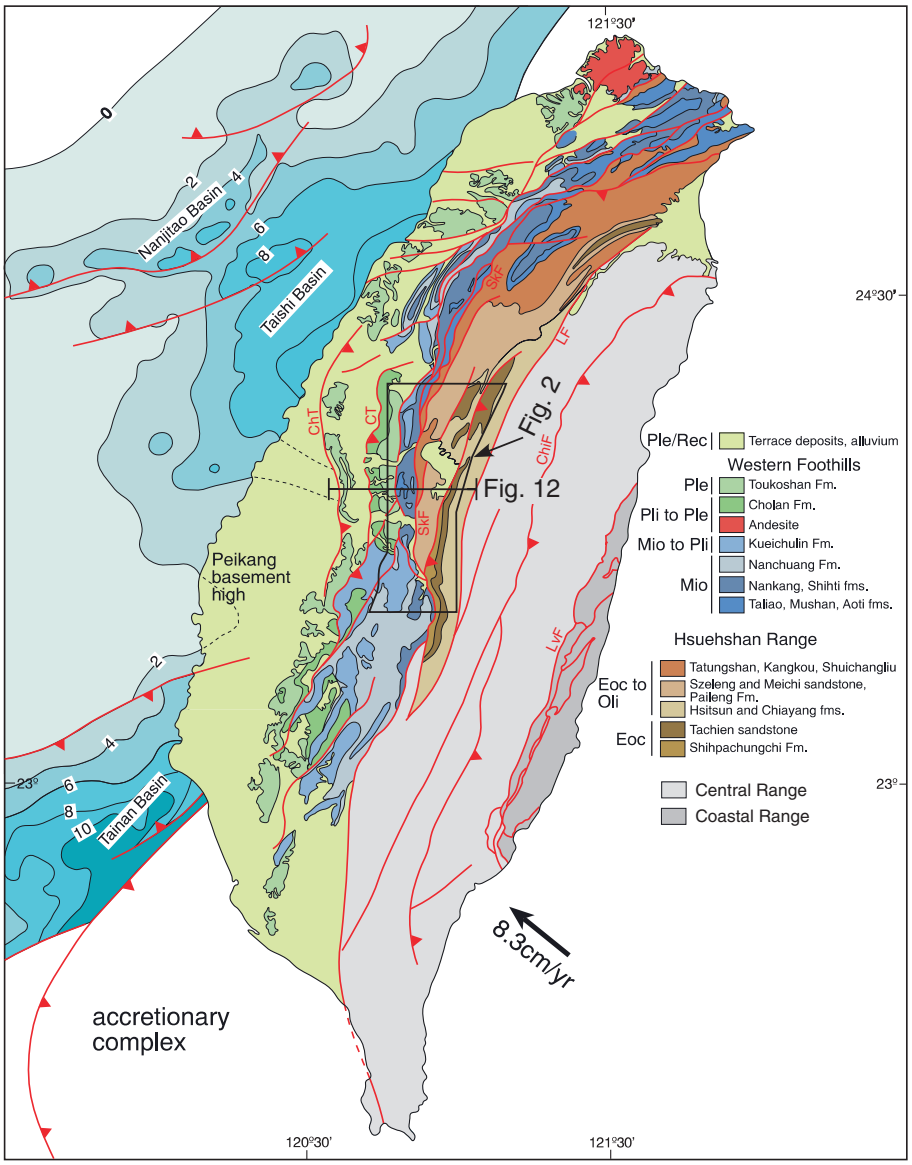

Fig. 1. Simplified geological map of the Taiwan mountain belt (modified after Chen *et al.* 2000). The locations of the study area in Figure 2 and of the crustal cross-section in Figure 12 are shown. Contours offshore indicate the thickness (in km) of the Palaeocene to Miocene sediments in the basins (from Teng & Lin 2004). ChiF, Chinma fault; ChT, Chuanghua thrust; CT, Chelungpu thrust; LF, Lishan fault; LvF, Longitudinal Valley fault; SkF, Shuilikeng fault.

Geological setting

The Taiwan orogen is forming as the result of the latest Miocene to present oblique collision that is taking place between the Luzon arc and the rifted margin of the SE part of Eurasia (Suppe 1984; Huang *et al.* 1997, 2000, 2006; Sibuet & Hsu 2004; Byrne *et al.* 2011). The resultant Taiwan mountain belt is divided into four roughly north–south-oriented tectonostratigraphic zones that are separated by major faults (Fig. 1). From west to east, these zones are the Western Foothills, the Hsuehshan Range, the Central Range and the Coastal Range. The Western Foothills, Hsuehshan Range and Central Range are forming as the result of deformation and uplift of Eocene to Miocene sediments and older pre-rift continental margin rocks of Eurasia and the latest Miocene and younger synorogenic sediments of the foreland basin (e.g. Suppe 1980; Byrne *et al.* 2011; Brown *et al.* 2012). In this paper, we discuss the Western Foothills, which structurally form the frontal part of the mountain belt, and the adjacent Hsuehshan Range. The latter is a more strongly deformed and variably metamorphosed zone to the east (Fig. 1). The focus of this paper is the boundary between these two tectonostratigraphic zones, the Shuilikeng fault. Below we give a brief overview of the outcropping stratigraphy and structure of the Western Foothills and the Hsuehshan Range. Throughout the paper we follow the stratigraphic scheme and nomenclature of Brown *et al.* (2012).

In our study area in central Taiwan (Figs 1 and 2), the Western Foothills are formed by an imbricate thrust system involving latest Miocene to present synorogenic clastic sediments of the foreland basin that, in their easternmost part, are overthrust by Eocene to Miocene unmetamorphosed shallow-water clastic deposits of the Eurasian platform along the Shuangtung thrust (e.g. Suppe 1987; Ho 1988; Yue *et al.* 2005; Castelltort *et al.* 2011; Brown *et al.* 2012; Huang *et al.* 2013). The imbricate thrust system that forms the Western Foothills appears to be linked to a shallow, gently east-dipping detachment developed near the top of the Miocene or at the base of the Pliocene synorogenic sediments (e.g. Suppe 1980, 1981; Ding *et al.* 2001; Carena *et al.* 2002; Yue *et al.* 2005; Brown *et al.* 2012). For an alternative interpretation in which there is extensive basement involvement the reader should see, for example, Mouthereau & Petit (2003), Mouthereau & Lacombe (2006), Simoes *et al.* (2007) and Rodriguez-Roa & Wiltschko (2010). Eastward of the Shuilikeng fault, the Hsuehshan Range is made up

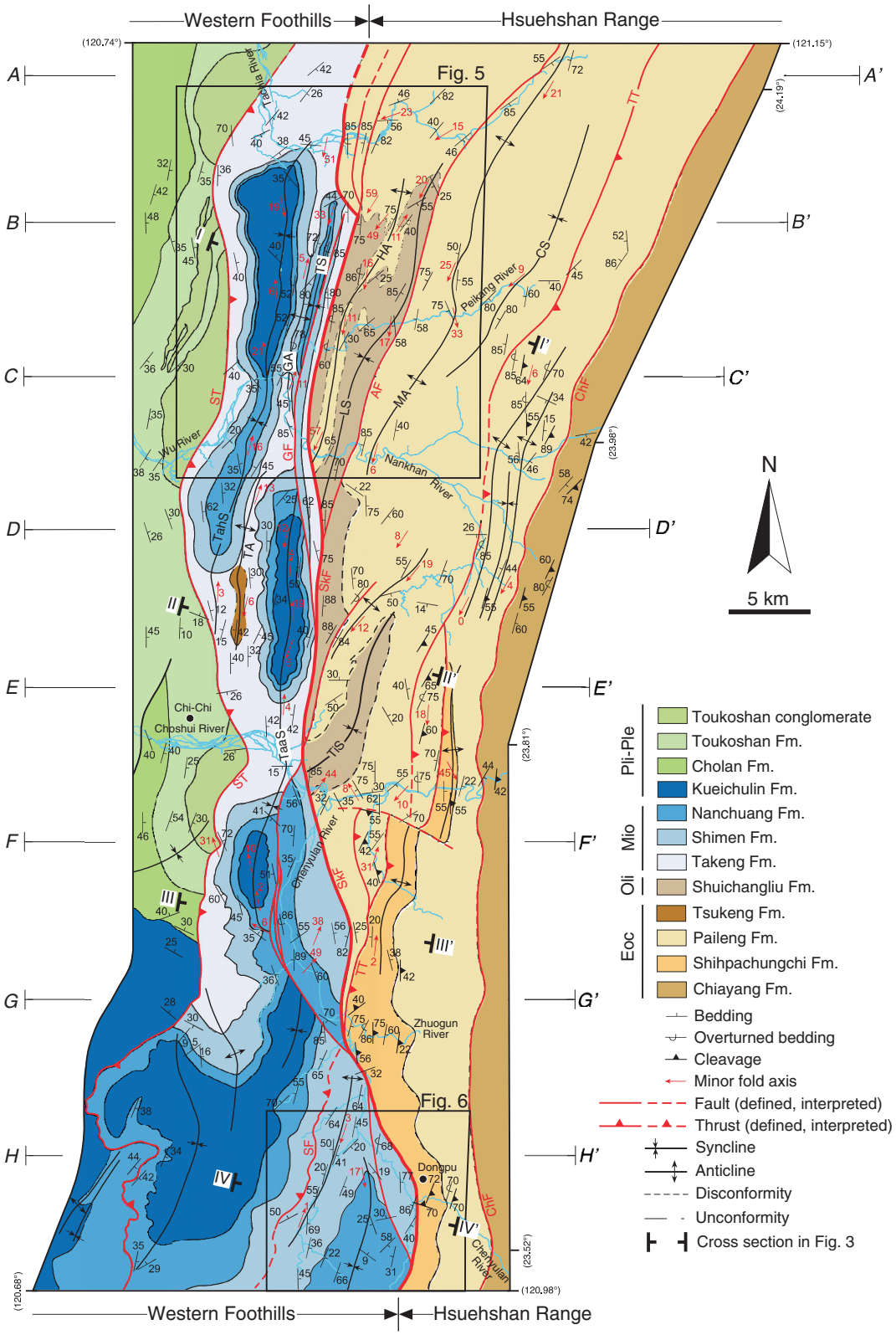

Fig. 2. Geological map of the study area across the Shuilikeng fault in central Taiwan. The location of the map is indicated in Figure 1. The locations of the seismicity sections in Figure 10 (from A–A' to H–H') are shown in black. Fault abbreviations: AF, Alenkeng fault; ChF, Chiayang fault; GF, Guaosing fault; SkF, Shuilikeng fault; SF, Shenmu fault; ST, Shuangtung thrust; TT, Tili thrust. Fold abbreviations: CS, Chuangyuan syncline; GA, Guaosing anticline; HA, Hsiaoan anticline; LS, Lileng syncline; MA, Meitzulin anticline; TA, Tsukeng anticline; TiS, Tingkan syncline; TS, Tachiwei syncline; TaaS, Taanshan syncline; TahS, Tahenpingshan syncline.

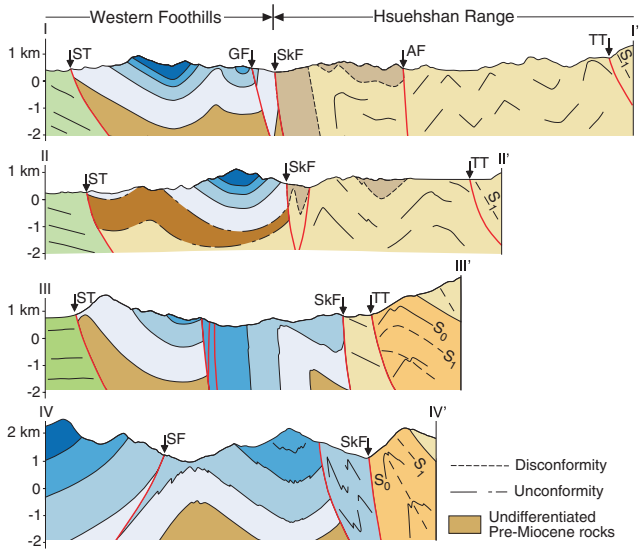

Fig. 3. Geological cross-sections throughout the map area. Their location is indicated in Figure 2. Fault and fold abbreviations, and colours, are as in Figure 2.

of variably metamorphosed Eocene clastic sediments that were deposited in the so-called Hsuehshan Basin during rifting of the Eurasian margin that are disconformably overlain by post-rift Oligocene shale and sandstone (Ho 1988; Huang *et al.* 1997; Lin *et al.* 2003; Teng & Lin 2004). Along much of the western part of the Hsuehshan Range, these rocks are weakly to moderately metamorphosed (Beyssac *et al.* 2007; Simoes *et al.* 2012) and, at least in the central part of the study area, they have been exhumed from between 9.2 and 9.8 km depth (Sakaguchi *et al.* 2007). Eastward and southward, however, in the hanging wall of the Tili thrust (Fig. 2), these rocks reach lower greenschist facies (Clark *et al.* 1993) and have a penetrative pressure solution cleavage (Clark *et al.* 1993; Tillman & Byrne 1995; Fisher *et al.* 2002, 2007; Brown *et al.* 2012).

The Shuilikeng fault at the surface

The Shuilikeng fault crops out poorly along most of its length, limiting direct acquisition of data on its deformation mechanisms, geometry and kinematics. Therefore, the approach taken in this study was to collect field data along and across it to construct the regional map pattern (Fig. 2) and cross-sections (Fig. 3), as well as analyse bedding dips and fold axes (Fig. 4). Where possible, fault orientation and kinematic indicator data were taken (see below). We present local, detailed maps and serial cross-sections from two areas to compare and contrast the differences in structural style along the strike of the fault (Figs 5 and 6).

Regional map pattern

In central Taiwan, a pronounced system of nearly north–south-oriented valleys clearly demarcates the contact between the Miocene rocks of the Western Foothills and the Eocene to Oligocene rocks of the Hsuehshan Range. This contact marks the surface trace of the Shuilikeng fault. The rectilinear map pattern of the fault, in which its trace cuts roughly straight across the

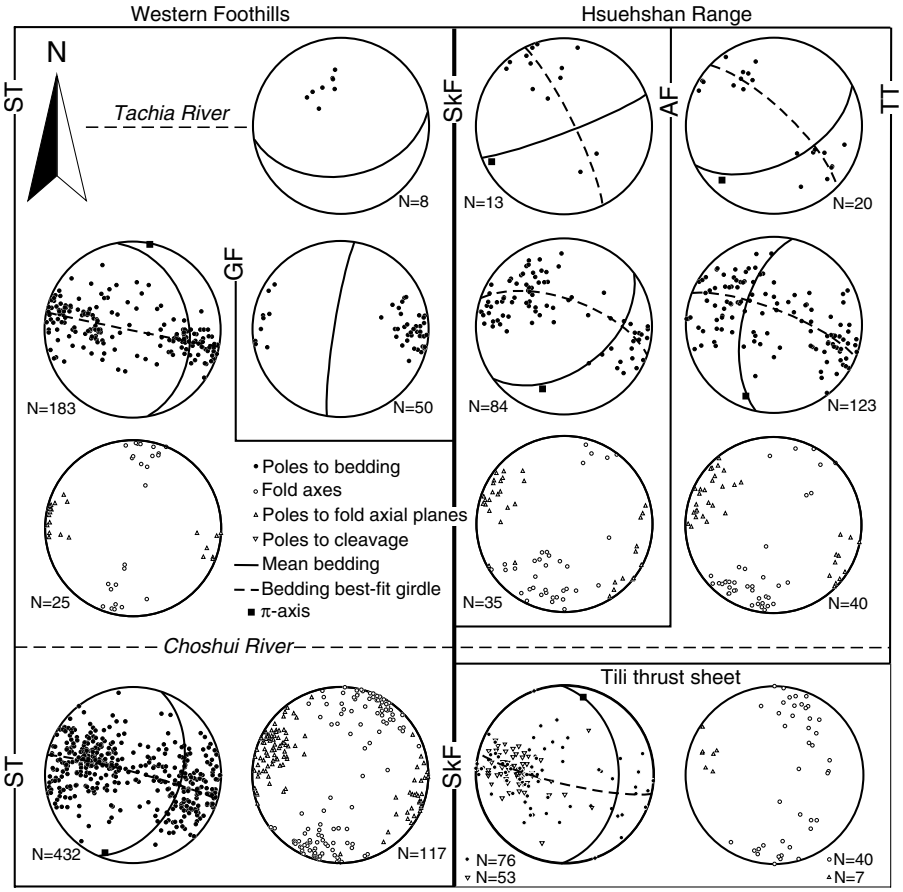

Fig. 4. Stereoplots (lower hemisphere, equal-area projection) of the main structural features within the study area. The grid indicates the subdivision of the map area into sub-areas bounded by the main faults that crop out within the map area. Fault abbreviations are as in Figure 2. The clockwise rotation of all the structural features towards an ENE–WSW orientation along the Tachia River should be noted. Also, the poles to bedding in the area between the Shuilikeng and the Alenkeng faults define two maxima consistent with asymmetric folds (e.g. the Hsiaoan anticline) made up of a steeply NW- to WNW-dipping to overturned forelimb and a moderately SE- to ESE-dipping backlimb.

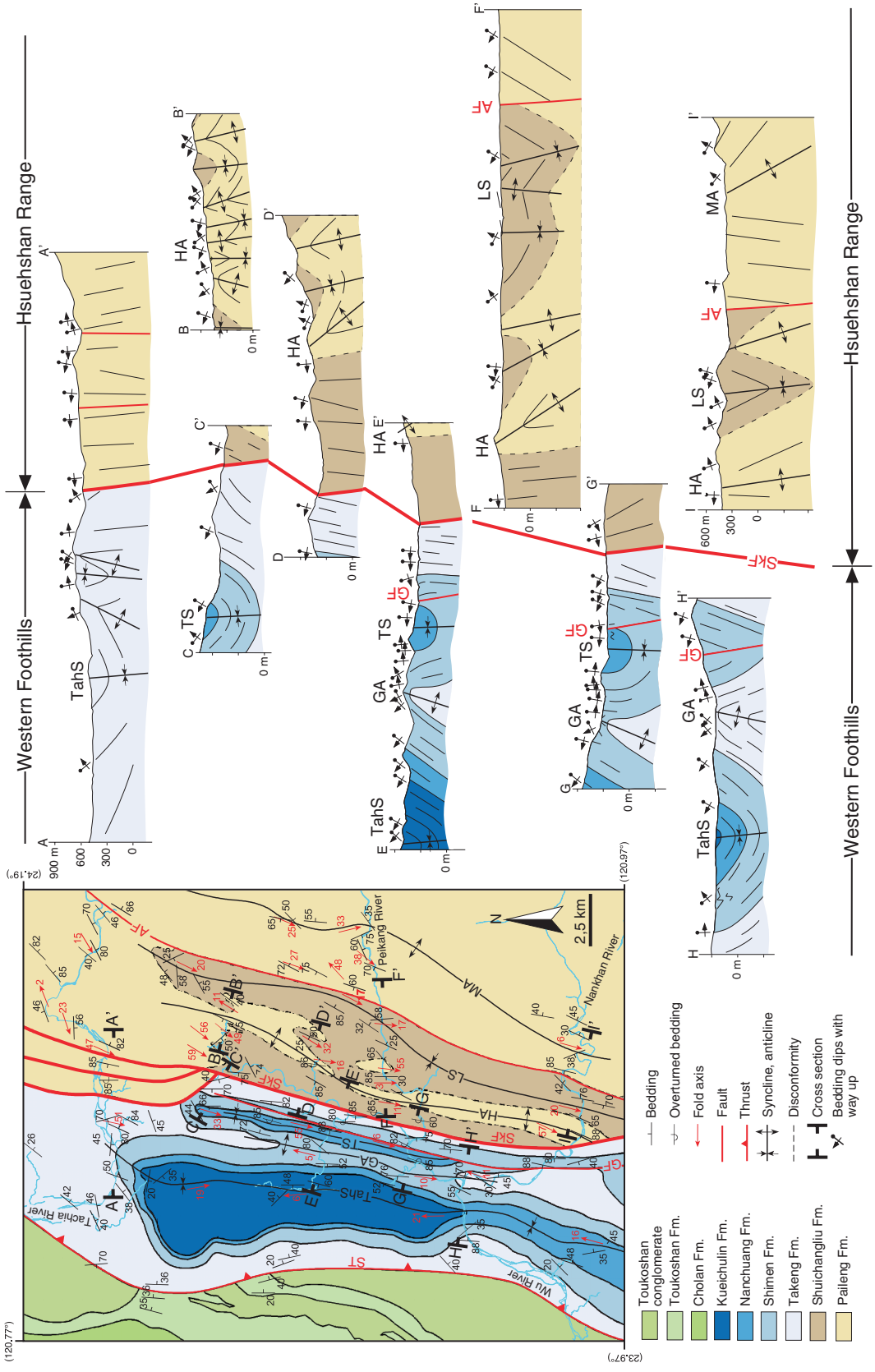

Fig. 5. Detailed geological map and serial cross-sections in the northern part of the map area. The location of the map is indicated in Figure 2. Fault and fold abbreviations are as in Figure 2.

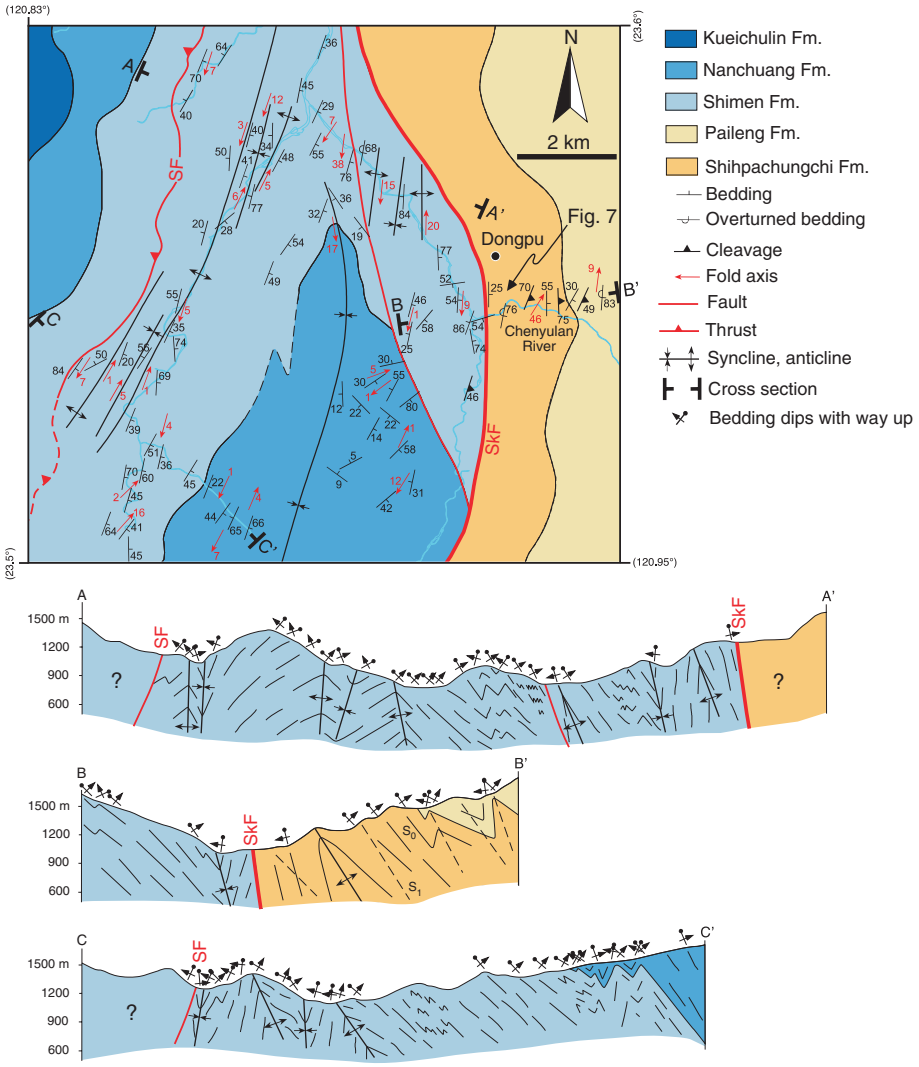

Fig. 6. Detailed geological map and serial cross-sections in the southern part of the map area. The location of the map is indicated in Figure 2. Fault and fold abbreviations are as in Figure 2.

topography, suggests that at the surface it has a steep dip. Within the study area, there are also notable changes from north to south in the map pattern of the fault (Fig. 2). These changes take place across the Choshui River (Figs 2, 3 and 4).

To the north of the Choshui River, the regional structure is that of open, symmetric synclines and anticlines developed west of the Shuilikeng fault and asymmetric slightly west-verging folds to the east (Figs 2 and 3). At a larger scale (Fig. 5), in its hanging wall the Shuilikeng fault juxtaposes weakly metamorphosed Eocene and Oligocene rocks in the west-verging Hsiaoan anticline (HA in Fig. 2) against lower Miocene rocks in open to locally very tight synclines and anticlines in its footwall (see section I–I' in Fig. 3). The Hsiaoan anticline is non-cylindrical, with a vertical to slightly overturned forelimb and with a roughly WSW plunge along the Tachia River and a moderate SW plunge farther south (Fig. 4) where its hinge appears to merge with the Shuilikeng fault (Fig. 5). Folds in the hanging wall of the Shuilikeng fault are cut by several NE–SW-striking faults. For example, the Alenkeng fault cuts the backlimb of the Hsiaoan anticline and places Eocene rocks on top of Oligocene (AF in Figs 2, 3 and 5). In this area, to the west of the Shuilikeng fault, the Tachiwei syncline and Guaosing anticline (TS and GA in Figs 2 and 5) form a gently north- and south-plunging (Fig. 4), tight fold pair that, locally, have a slight east vergence (Fig. 5). The Guaosing fault (GF in Figs 2, 3 and 5) cuts across the eastern limb of the Tachiwei syncline (Fig. 5), suggesting that it either post-dates, or is a late feature in the development of the fold pair. Southward, the southern limb of the Tingkan syncline (TiS in Fig 2) is overturned against the Shuilikeng fault and both limbs are cut by it, suggesting that it predates or records progressive deformation along the fault.

South of the Choshui River, the Shuilikeng fault takes on an anastomosing map pattern in which we can identify two fault-bound lenses of steeply west-dipping to locally overturned Miocene rocks (Figs 2 and 3). In this area, the Tili thrust (TT in Fig. 2) approaches and is cut by the Shuilikeng fault. This is especially apparent along the Zhuogun River (Fig. 2) where the cleavage in the hanging wall of the Tili thrust is folded into an anticline whose forelimb directly abuts the Shuilikeng fault (Fig. 3, section III–III'). Where it abuts the Shuilikeng fault, the rocks in the Tili thrust sheet form a kilometre-scale, tight, west-verging, overall NNE-plunging, anticline with a steep to slightly overturned forelimb and a ESE-dipping axial planar pressure solution cleavage (Fig. 4) (see sections III–III' and IV–IV' in Fig. 3, and section B–B' in Fig. 6). In thin section, we have observed rare, fine-grained biotite replacing chlorite along the cleavage planes, suggesting that these rocks are in greenschist facies, as indicated by Clark *et al.* (1993), Beyssac *et al.* (2007) and Sakaguchi *et al.* (2007). To the west, the Miocene rocks are unmetamorphosed and, adjacent to the fault, the structure is dominated by intense faulting and folding developed on a tens of metres scale

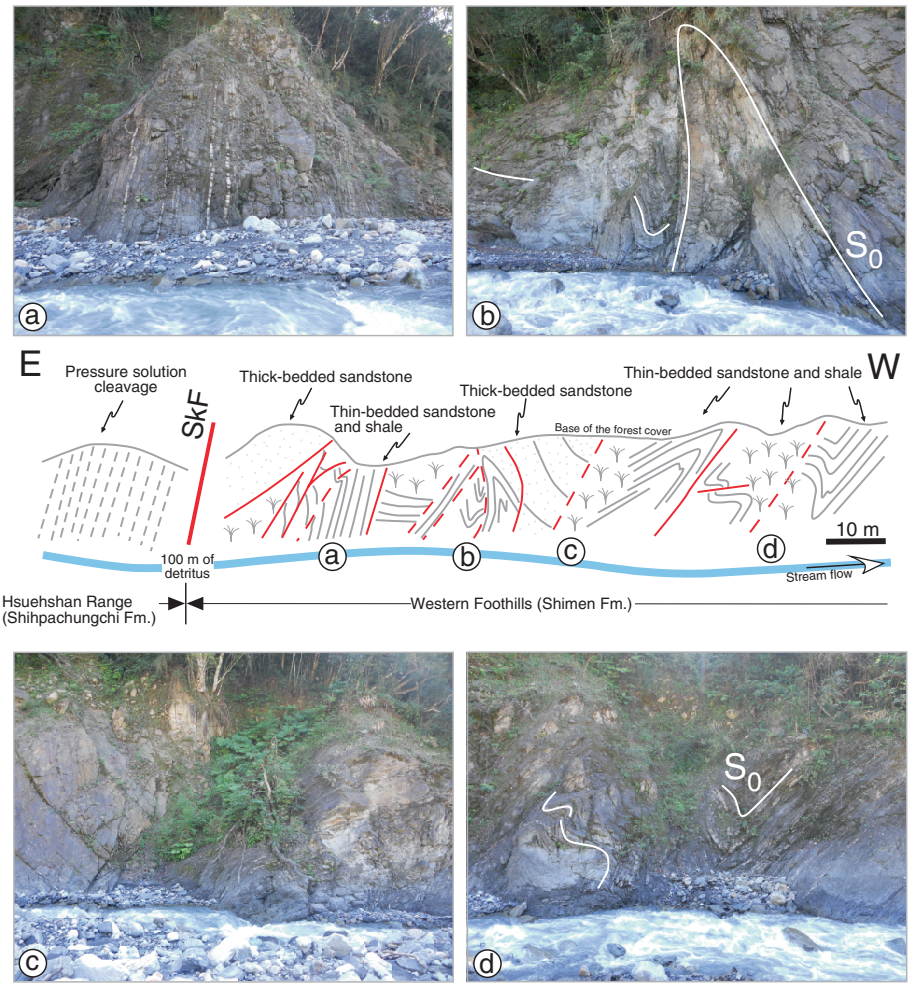

Fig. 7. Sketch and photographs of the high-strain zone developed within the Miocene that defines the Shuilikeng fault in the southernmost part of the map area along the Chenyulan River. The disharmonic folding of the thin-bedded sandstone and shale units and the brecciation of the thick-bedded sandstone units should be noted. The approximate location of the sketch is indicated in Figure 6.

(Fig. 6) that, farther west, becomes a complex interaction of kilometre-scale synclines and anticlines (Fig. 2) that are beyond the scope of this paper. In the area adjacent to the fault, folds are mildly non-cylindrical but with a general shallow NNE–SSW plunge, and are mainly WNW-verging (Figs 4 and 6). A good example of this can be found in the Chenyulan River immediately south of the village of Dongpu (Fig. 6). Here, the Eocene Shihpachungchi Formation can be observed to directly overlie the Middle Miocene Shimen Formation. The Eocene rocks are strongly sheared and tightly folded into a west-verging anticline (Fig. 6, section B–B'). The Miocene rocks in the footwall form a zone of intense brittle faulting and folding of several hundred metres in width (Fig. 7). The majority of the faults are east-dipping and kinematic indicators such as slickenfibres on slip surfaces and small bedding displacements indicate an overall top-to-the-west sense of movement, although we stress that the kinematics is highly variable (see the section on kinematics below). Fold geometries in this area are often very complex, as thick-bedded sandstone units display various degrees of brecciation and boundinage whereas more thin-bedded sandstone and shale units show disharmonic folding (Fig. 7).

Deformation mechanism and kinematics

In the kinematic analysis of fault-slip data, we adopted the approach of Marrett & Allmendinger (1990), which uses the linked Bingham distribution of the shortening and extension directions of a population of faults to calculate the average incremental principal strain axes (i.e. average P and T axes), giving an average fault plane solution.

Where observed in the field, the Shuilikeng fault is everywhere a brittle feature composed of breccia and fault gouge (Fig. 8). Fault and slickenfibre orientation data from a number of locations along the Shuilikeng fault indicate senses of slip that range from thrusting, to strike-slip, to extension. In several localities, slickenfibres developed on slip surfaces, small bedding displacements across discrete faults, and minor fold vergence indicate that all three senses of movement have taken place at different times in the same outcrop. Despite these local complexities, the averaged fault plane solutions indicate a nearly NW–SE to east–west average shortening direction (P axis in Fig. 9) along the length of the Shuilikeng fault. The T axes, however, range from steeply plunging to subhorizontal, resulting in average fault plane solutions for single outcrops that range from thrusting to strike-slip (Fig. 9).

The Shuilikeng fault at depth

Fault location and geometry

On the basis of formation thicknesses, bedding dips, reflection seismic data and standard cross-section construction techniques, Brown *et al.* (2012) have interpreted the location of the Shuilikeng fault at depth in the upper 10 km. For other interpretations in which the Shuilikeng fault (under different names) is interpreted to extend to 10 km and beyond, the reader should see, for example, Wang *et al.*

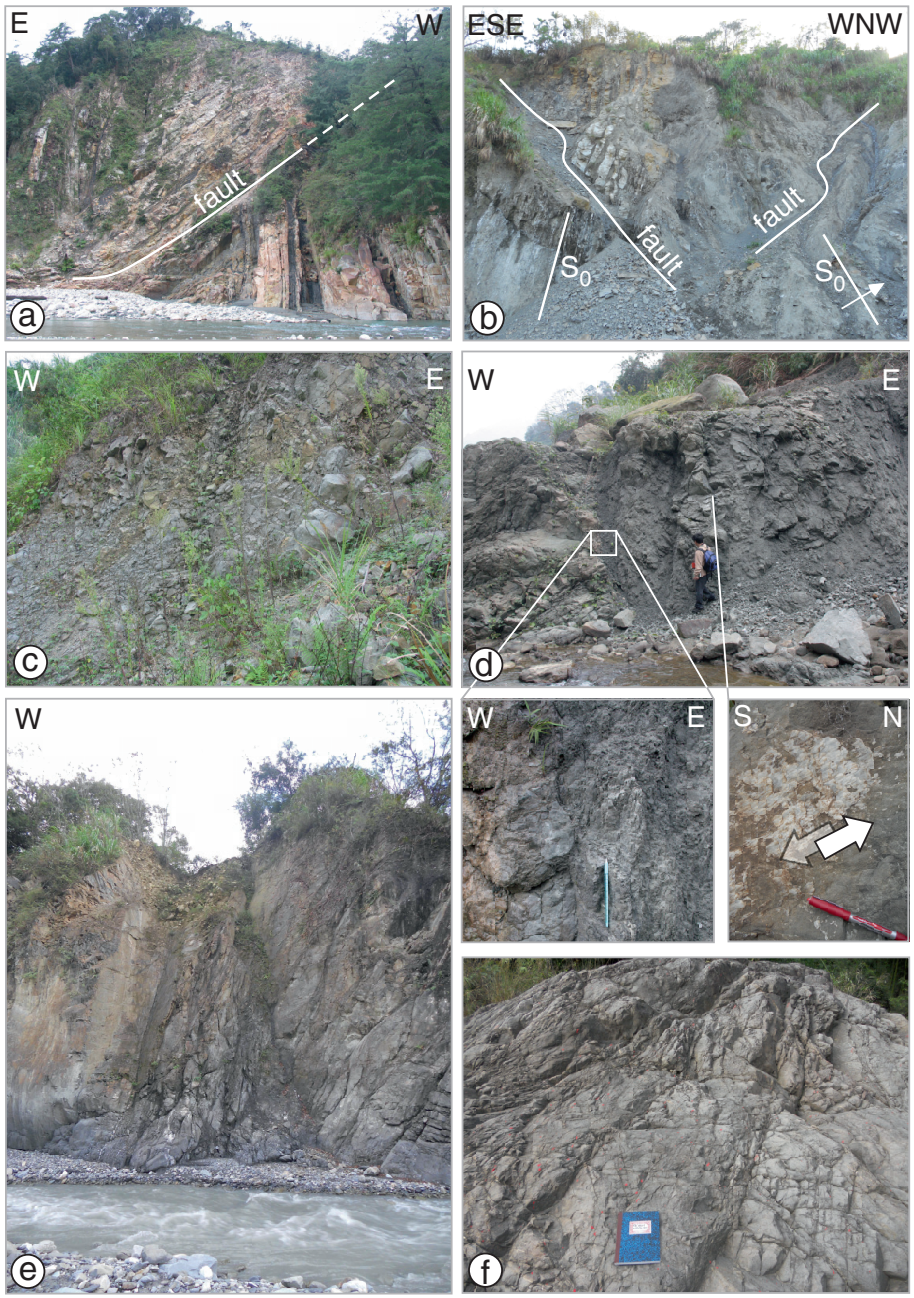

Fig. 8. Field photographs (their location is indicated in Fig. 9). (**a**) Splay of the Shuilikeng fault across the Tachia River in the northernmost part of the map area. (**b, c**) Complex fault zone (**b**) and fault breccia (**c**) that define the Guaosing fault. (**d**) Fault breccia and fault gouge of the Shuilikeng fault immediately south of the Choshui River. (Note slickenfibres on a minor fault surface within this breccia zone indicating a left-lateral strike-slip sense of movement.) (**e, f**) Fault breccia developed within the Shimen Formation that defines the Shuilikeng fault in the southernmost part of the map area, around Dongpu.

(2000) and Rodriguez-Roa & Wiltschko (2010). Here, to interpret the location and geometry of the Shuilikeng fault below 10 km depth, we use the relocated seismicity database of Wu *et al.* (2008*a*; updated to 2011 in our study area) which contains events that range up to >7 M_L. In this paper, these data have been further processed using the collapsing technique of Jones & Stewart (1997), which involves the determination of statistical measurements for standard errors in the depth, latitude and longitude for each event and the clustering of events with overlapping error spheroids. These collapsed data were then plotted in a 3D volume and parallel vertical sections were cut 10 km apart (Figs 2 and 10). Events were projected onto the sections from 4.99 km on either side to avoid having the same event on any two sections. The sections are confined to the upper 20 km of crust to avoid any interference with earthquakes that could be related to the Lishan fault (the structural boundary between the Hsuehshan Range and the Central Range; see, e.g. Lee *et al.* 1997).

The pattern of seismicity in the cross-sections varies significantly from north to south across the study area (Fig. 10). In the northernmost part (sections A–A' and B–B'), the seismic events form a cloud from which we are unable to discriminate any fault zone. In the central part of the map area (sections C–C', D–D', E–E' and F–F'), however, there is a roughly horizontal open cluster of events at 10 km depth (detachment in Fig. 10) that nearly coincides with the location of the basal detachment beneath the Western Foothills (Carena *et al.* 2002; Yue *et al.* 2005; Brown *et al.* 2012). At *c*. km 20, between *c*. 10 and 20 km depth, there is a large, tight cluster of hypocentres that dips *c*. 45–50° eastward (SkF in Fig. 10). This east-dipping cluster of seismicity extends downward from the deep trace of the Shuilikeng fault defined in cross-section by Rodriguez-Roa & Wiltschko (2010) and Brown *et al.* (2012), or along its deep trace as defined by Wang *et al.* (2000). We therefore interpret

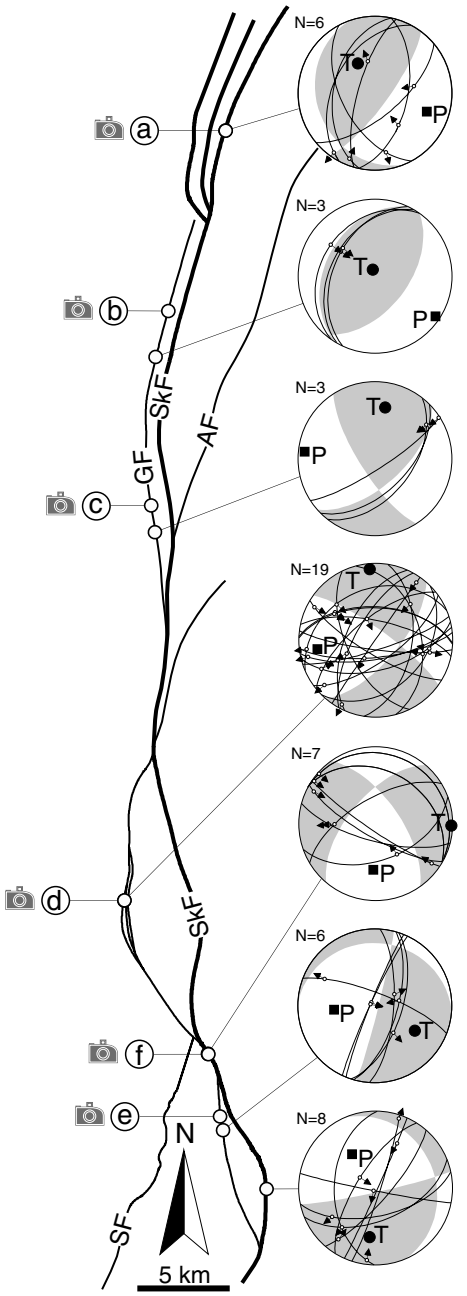

Fig. 9. Fault-slip data (lower hemisphere, equal-area projection) from the Shuilikeng and Guaosing faults. The average P and T axes determined using these data are shown, as are the average fault plane solutions. Fault planes are represented as great circles and the arrows indicate the sense of movement of the hanging-wall block of the faults. The lowercase letters indicate the location of the photographs in Figure 8.

the Shuilikeng fault to link with this cluster of events and to extend to at least 20 km depth. The extensive cloud of seismicity to the east of the surface location of the Shuilikeng fault and above its interpreted subsurface location, especially in sections C–C' and D–D', could possibly be related to the faults in the hanging wall of the Shuilikeng fault discussed above. Southward, in sections G–G' and H–H', the trace of the Shuilikeng fault is less clearly defined from the seismicity pattern, although it can still be interpreted to dip moderately eastward (Fig. 10).

Fault kinematics: earthquake focal mechanisms

To gain insight into the kinematics of the Shuilikeng fault at depth we have used the database of earthquake focal mechanisms of Wu *et al.* (2008*b*, 2010), updated to 2011 in our map area (Fig. 11). The 264 events presented in Figure 11 have been relocated using the 3D velocity model of Wu *et al.* (2007, 2009) and then have been collapsed using the method described in the previous section. In our analysis, the map area has been divided into three zones whose north–south extent were determined to coincide with the beginning of a clear east-dipping band of seismicity in the vertical sections (i.e. between sections B–B' and C–C', and F–F' and G–G'), and east–west to include what we interpret to be the extent of the Shuilikeng fault and the faults in its hanging wall at the surface (Fig. 11). These zones were then divided into four 5 km thick bins, to a depth of 20 km. The fault types (i.e. strike-slip, thrust, normal and other) derived from the focal mechanisms were calculated using the technique of Zoback (1992), which takes into account the plunge of the P, B and T axes of each fault plane solution. To provide further information for the interpretation of the kinematics, all events within each 5 km thick bin were grouped together and the average principal strain axes were calculated using the method of Marrett & Allmendinger (1990) (Fig. 11). For the sake of brevity, below we describe only the average fault plane solutions.

In the northern part of the study area (area 'a' in Fig. 11), there are no data in the upper 5 km. In the bin from 5 to 10 km depth, the average P and T axes are roughly subhorizontal and trend NNW–SSE and ENE–WSW, respectively, resulting in a strike-slip average fault plane solution. From 10 to 20 km depth, however, their trend changes, with the P axis remaining horizontal and trending NW–SE and the T axis becoming nearly vertical, giving a thrust average fault plane solution. In the central part of the map area (area 'b' in Fig. 11), again, there are no data in the first 5 km. In all three bins from 5 to 20 km depth, the average P axis is nearly horizontal and trend NW–SE, whereas the average T axis is vertical, giving a thrust average fault plane solution at all depths. Finally, in the southern part of the map area (area 'c' in Fig. 11), in the bin from 0 to 5 km depth, the average P and T axes are roughly subhorizontal and trend WNW–ESE and NNE–SSW, respectively, giving a strike-slip average fault plane solution. However, from 5 to 15 km depth the T axis becomes vertical, resulting in a thrust average fault plane solution. There are not enough events in the 15–20 km bin to determine statistically meaningful principal strain axes.

Discussion

By combining surface geology and seismicity data, the Shuilikeng fault in central Taiwan can be interpreted to be a brittle fault that dips eastward and reaches more than 20 km depth (Fig. 12). For about 100 km along its strike-length the map pattern defined by the Shuilikeng fault (Fig. 2) is similar to that of other well-known transpressive to strike-slip fault systems (Wilcox *et al.* 1973; Sylvester 1988; Butler *et al.* 1998; Walcott 1998; Nicol & Van Dissen 2002; Kirkpatrick *et al.* 2008; Leever *et al.* 2011; Murphy *et al.* 2011; Dooley & Schreurs 2012). Along its southern end, it cuts an earlier fault and fold system, juxtaposing greenschist-facies rocks in its hanging wall (with a pressure solution cleavage) against unmetamorphosed rocks in its footwall. In the northern part, however, the relationships between the Shuilikeng fault and structures that splay off it are often ambiguous, although from the data given in the previous sections we interpret them to be coeval and linked. The constraints placed on the Shuilikeng fault dip and location in the subsurface by the surface geology (formation thickness and dip,

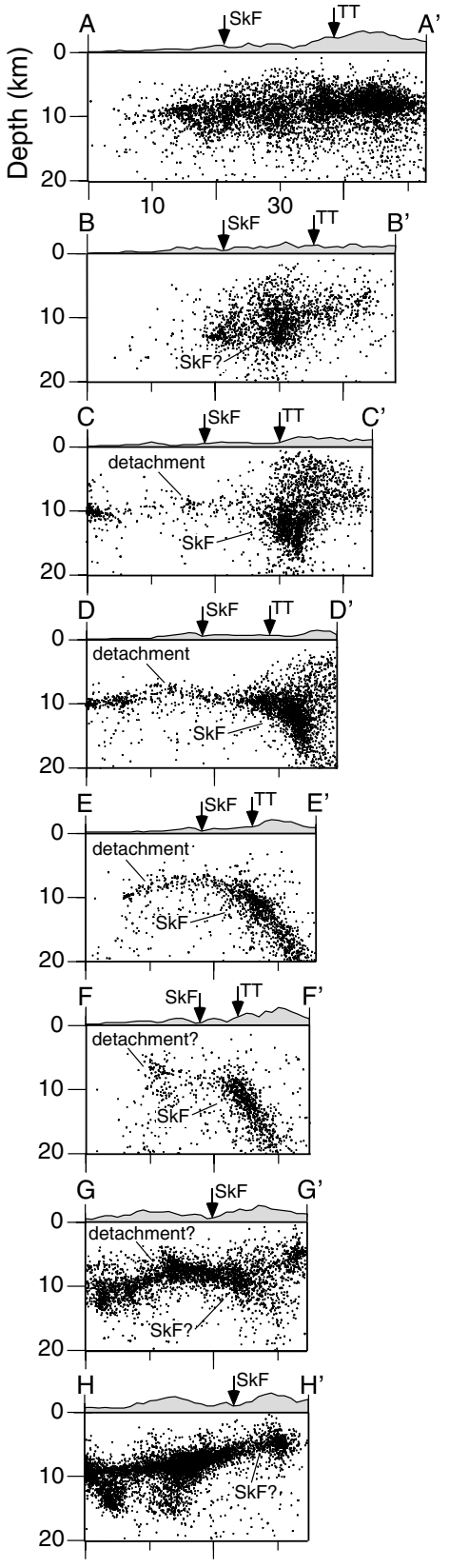

Fig. 10. Seismicity sections through the map area. Seismicity data are projected from 4.99 km on either side of the section. It should be noted how, from section C–C' to section F–F', an east-dipping cluster of seismicity that projects nearly to the location of the Shuilikeng fault at the surface is recognizable. The location of the sections is indicated in Figure 2. SkF, Shuilikeng fault; TT, Tili thrust.

faults, folds etc.) allow it to be extrapolated to a depth of around 10 km (Fig. 12). Although there are uncertainties in this extrapolation, at 10 km depth it coincides with a cluster of east-dipping seismicity that extends to over 20 km depth (Fig. 12). We interpret this seismicity to be related to a steeply dipping fault whose upward trace projects to the Shuilikeng fault at the surface and, we think, is linked to it. Consequently, we interpret the Shuilikeng fault to be an active deep-seated main structure of the Taiwan orogen. Westward, a subhorizontal cluster of seismicity can be interpreted as the detachment to the imbricate stack mapped there, linking it to the thick-skinned deformation east of the Shuilikeng fault (Fig. 12). More work needs to be carried out to determine how this linkage works. Throughout our study area, the kinematics of the Shuilikeng fault is somewhat variable in the surface geological data, whereas the focal mechanism data more consistently indicate NW-directed shortening with strike-slip being active locally in the upper 10 km (Figs 9 and 11). Variability in the surface dataset is possibly the result of successive, overlapping ruptures, whereas variability in the focal mechanism data can, in part, be associated with minor faults. It might also be the result of mechanical decoupling between the kinematics of the fault core and that of the regional fault that has generated it, as suggested for other seismogenic faults (e.g. the San Andreas Fault; Chester *et al.* 1993). Both datasets are consistent, however, with the overall kinematics of the roughly north–south-striking Shuilikeng fault as being transpressive, with the hanging wall moving up toward the NW.

The Eocene rocks of the Hsuehshan Range have been interpreted by Teng *et al.* (1991), Huang *et al.* (1997) and Teng & Lin (2004) to be synrift sediments deposited in a graben or half-graben (the Hsuehshan Basin) on the continental margin of Eurasia. Those researchers further interpreted the Oligocene and Miocene rocks to be post-rift sediments deposited on the margin platform. Although there is a general consensus that the eastern bounding fault of the Hsuehshan Basin probably coincided with the current Lishan fault (Lee *et al.* 1997; Huang *et al.* 1997; Lin *et al.* 2003; Teng & Lin 2004; Wiltschko *et al.* 2010), there is little consensus about the location or even the presence of a western bounding fault (for exceptions see Huang *et al.* 1997; Lee *et al.* 1997). However, for just over 200 km the Shuilikeng fault forms a structural boundary between predominantly Miocene rocks to the west and Eocene rocks of the Hsuehshan Basin to the east (in the north, Oligocene to Miocene rocks also appear; Fig. 1). We suggest, therefore, that the Shuilikeng fault, which at least in central Taiwan penetrates to 20 km or more depth (and must, therefore, affect the basement), can be interpreted to be a major structure that formed along the western margin of the Hsuehshan Basin in the Eocene.

It has been shown that such pre-existing structures on a continental margin can play an important role in many aspects of the evolution of an orogen during mountain building (e.g. Wiltschko & Eastman 1983; Hatcher & Williams 1986; Laubscher 1987; Rodgers 1987; Woodward 1988; Schmidt *et al.* 1988; Narr & Suppe 1994; Butler *et al.* 1997; Pérez-Estaún *et al.* 1997; Brown *et al.* 1999). For example, their reactivation may lead to the inversion of pre-existing rift basins and to the uplift of the synrift rocks and their basement (Bonini *et al.* 2012, and references therein). How the shortening in central Taiwan is resolved to form single faults and fault systems is in general complex (e.g. Bos *et al.* 2003; Gourley *et al.* 2007; Mouthereau *et al.* 2009; Wu *et al.* 2010; Ching *et al.* 2011) and, in many cases, conditioned by the presence of pre-collisional rift basins that were present on the Eurasian margin (e.g. Wu *et al.* 1997; Mouthereau *et al.* 2002; Mouthereau & Lacombe 2006; Hwang *et al.* 2007; Byrne *et al.* 2011; Brown *et al.* 2012). Faults bounding the basins around the Peikang Basement High (see Teng *et al.* (1991), Teng & Lin (2004) and Byrne *et al.* (2011) for an overview of this feature) (Fig. 1), with their significant amount of

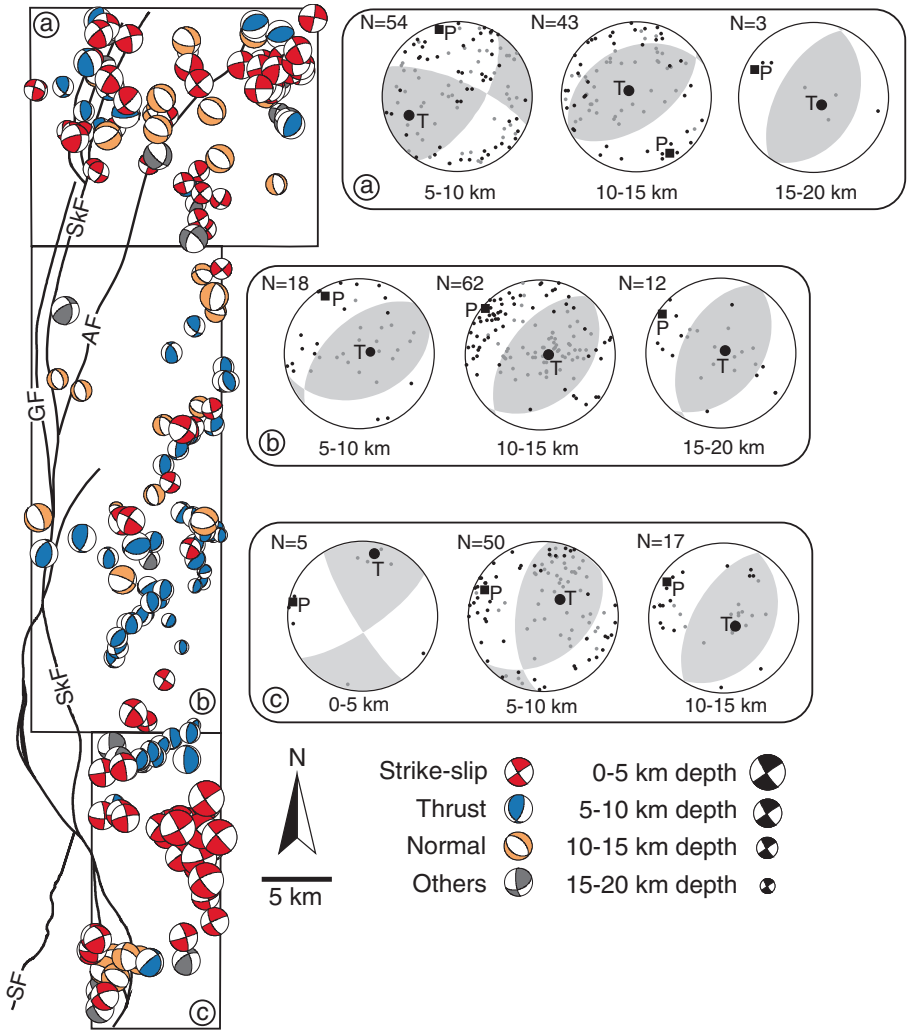

Fig. 11. Earthquake focal mechanisms and variations of the average strain field throughout the map area. The average principal strain axes are calculated from 0 to 20 km depth, at 5 km depth intervals.

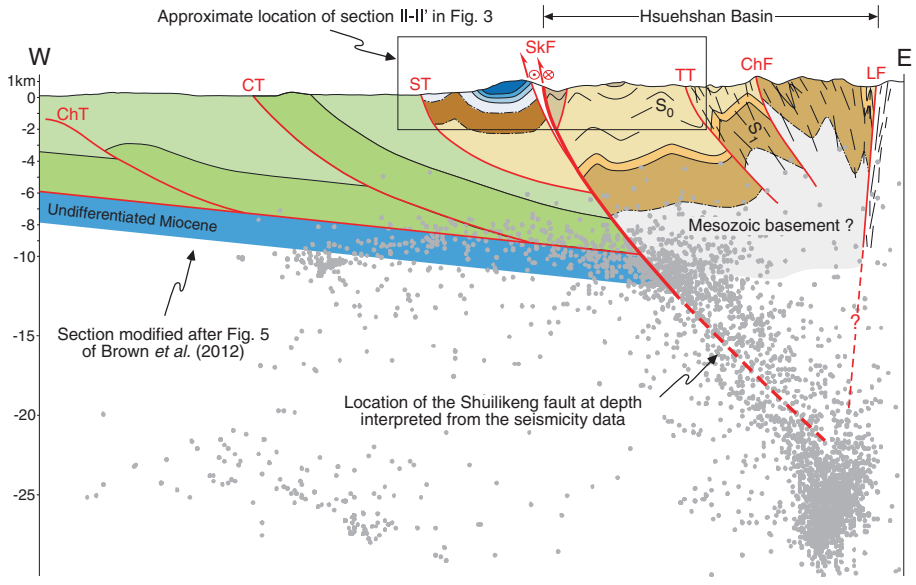

Fig. 12. Crustal cross-section through the central part of the study area (modified after Brown *et al.* 2012). The location is indicated in Figure 1. Seismicity data are projected from 4.99 km on either side of the section. Fault abbreviations are as in Figures 1 and 2, and colours are as in Figure 2.

seismic activity, are an important example of how this mechanism of reactivation of pre-existing basin faults can affect the structural development of the mountain belt (Rau & Wu 1995; Mouthereau *et al.* 2002; Mouthereau & Lacombe 2006; Wu *et al.* 2007; Byrne *et al.* 2011; Chi 2012; Mirakian *et al.* 2012). In central Taiwan, the Shuilikeng fault forms part of this fault system, although how it interacts with many of the other faults around the Peikang Basement High is still not completely understood. Nevertheless, our data suggest that this part of the Shuilkeng fault is currently active and that the western margin of the Hsuehshan Basin is being inverted and exhumed along it. Several researchers have shown that P-wave velocities also increase eastward across the Shuilikeng fault (Kim *et al.* 2005, 2010; Lin 2007; Wu *et al.* 2007; Kuo-Chen *et al.* 2012). If we assume that the Eocene rocks in the Hsuehshan Range are synrift, then the pre-rift Mesozoic basement beneath them should be being exhumed to be within a few kilometres of the surface and these rocks should have higher P-wave velocities. This interpretation is partly corroborated by the thermal data of Sakaguchi *et al.* (2007), who suggested that the Eocene rocks to the east of the Shuilikeng fault have been exhumed from *c*. 10 km depth, which would be in agreement with basement rocks reaching the shallow subsurface in this part of the Hsuehshan Range. This interpretation is also supported by the surface geology (e.g. rock ages, structural style, amount of deformation, level of exhumation), the significant increase in the number and the deeper crustal level of seismic events to the east of the fault and, eastward, higher P-wave velocities at shallower depths (Wang *et al.* 2000; Kim *et al.* 2005, 2010; Beyssac *et al.* 2007; Lin 2007; Sakaguchi *et al.* 2007; Simoes *et al.* 2007, 2012; Wu *et al.* 2007; Yamato *et al.* 2009; Brown *et al.* 2012; Kuo-Chen *et al.* 2012). Based on these data, the regional-scale structure of the Hsuehshan Range in the study area can be interpreted to be a basement-cored anticlinorium (Brown *et al.* 2012; see also Clark *et al.* 1993, for discussion of it as a 'pop-up' structure) (Fig. 12). The highest structural and topographic level that the basement reaches in central Taiwan is over 3000 m above sea level, to the east in the Central Range (see fig. 13 of Brown *et al.* (2012) for a regional interpretation of this structure).

Conclusions

We show that in central Taiwan the Shuilikeng fault is a brittle fault along the western limit of the outcropping Oligocene and Eocene rocks of the Hsuehshan Range. Although kinematic data collected from outcrops along the fault show a degree of variability, when combined with an extensive focal mechanism dataset from within the hypocentre cluster, the overall fault mechanism is clearly transpressive. In its southern part it clearly cuts the Tili thrust and the Tingkan syncline. Northward, however, the relationships between faults and folds splaying off the Shuilikeng fault are not so clear, although they appear to be related to the transpressive deformation taking place in its hanging wall. On the basis of geometrical constraints used for regional cross-section construction (Fig. 12), the surface trace of the Shuilikeng fault can be extrapolated to *c*. 10 km depth where, in the central part of our study area, it coincides with an east-dipping cluster of seismicity. We interpret this cluster of earthquake hypocentres to project from greater than 20 km depth, upward along the Shuilikeng fault to its location at the surface. As a consequence we interpret the fault to be active. This hypocentre cluster may link with a subhorizontal cluster to the west, beneath the imbricate stack of the Western Foothills, but our data provide no clues as to how this entire system works kinematically or mechanically. More work needs to be carried out to clarify this. In a regional context, the Shuilikeng fault can be interpreted to be reactivating a pre-existing fault that was along the western boundary of the Hsuehshan Basin, inverting the basin and causing uplift and exhumation of the Eocene synrift rocks and most probably its underlying basement.

We would like to thank L.-Y. Chao for providing the code for calculating the collapsed seismicity dataset presented in this paper. T. Byrne and an anonymous reviewer are thanked for their constructive comments on the paper. This research was carried out with the aid of grants by CSIC—Proyectos Intramurales 2006 301010, and CGL2009-11843-BTE, and JAE-Predoc.

References

Beyssac, O., Simoes, M., Avouac, J.P., Farley, K.A., Chen, Y.-G., Chan, Y.-C. & Goffé, B. 2007. Late Cenozoic metamorphic evolution and exhumation of Taiwan. *Tectonics*, **26**, http://dx.doi.org/10.1029/2006TC002064.

Bonini, M., Sani, F. & Antonielli, B. 2012. Basin inversion and contractional reactivation of inherited normal faults: A review based on previous and new experimental models. *Tectonophysics*, **522–523**, 55–88, http://dx.doi.org/10.1016/j.tecto.2011.11.014.

Bos, A.G., Spakman, W. & Nyst, M.C.J. 2003. Surface deformation and tectonic setting of Taiwan inferred from a GPS velocity field. *Journal of Geophysical Research*, **108**, http://dx.doi.org/10.1029/2002JB002336.

Brown, D., Alvarez-Marron, J., Perez-Estaun, A., Puchkov, V. & Ayala, C. 1999. Basement influence on foreland thrust and fold belt development: An example from the southern Urals. *Tectonophysics*, **308**, 459–472, http://dx.doi.org/10.1016/S0040-1951(99)00147-X.

Brown, D., Alvarez-Marron, J., Schimmel, M., Wu, Y.M. & Camanni, G. 2012. The structure and kinematics of the central Taiwan mountain belt derived from geological and seismicity data. *Tectonics*, **31**, http://dx.doi.org/10.1029/2012TC003156.

Butler, R.W.H., Holdsworth, R.E. & Lloyd, G.E. 1997. The role of basement reactivation in continental deformation. *Journal of the Geological Society, London*, **154**, 69–71, http://dx.doi.org/10.1144/gsjgs.154.1.0069.

Butler, R.W.H., Spencer, S. & Griffiths, H.M. 1998. The structural response to evolving plate kinematics during transpression: evolution of the Lebanese restraining bend of the Dead Sea Transform. *In:* Holdsworth, R.E., Strachan, R.A. & Dewey, J.F. (eds) *Continental Transpressional and Transtensional Tectonics.* Geological Society, London, Special Publications, **135**, 81–106, http://dx.doi.org/10.1144/GSL.SP.1998.135.01.06.

Byrne, T., Chan, Y.C., Rau, R.J., Lu, C.Y., Lee, Y.H. & Wang, Y.J. 2011. The arc–continent collision in Taiwan. *In*: Brown, D. & Ryan, P.D. (eds) *Arc–Continent Collision*. Springer, Berlin, 213–245.

Carena, S., Suppe, J. & Kao, H. 2002. Active detachment of Taiwan illuminated by small earthquakes and its control of first-order topography. *Geology*, **30**, 935–938, http://dx.doi.org/10.1130/0091-7613(2002)0302.0.CO;2.

Castelltort, S., Nagel, S., *et al.* 2011. Sedimentology of early Pliocene sandstones in the south-western Taiwan foreland: Implications for basin physiography in the early stages of collision. *Journal of Asian Earth Sciences*, **40**, 52–71, http://dx.doi.org/10.1016/j.jseaes.2010.09.005.

Chen, C.-H., Ho, H.-C., *et al.* 2000. *Geological Map of Taiwan. 1:500,000 scale*. Central Geological Survey, Taipei.

Chester, F.M., Evans, J.P. & Biegel, R.L. 1993. Internal structure and weakening mechanisms of the San Andreas Fault. *Journal of Geophysical Research*, **98**, 771–786, http://dx.doi.org/10.1029/92JB01866.

Chi, W.-C. 2012. Coseismic indentor-related deformation during the termination of subduction and its associated geophysical characteristics: an example from Taiwan. *Lithosphere*, **4**, 594–602, http://dx.doi.org/10.1130/L193.1.

Chinese Petroleum Company 1982. *Geological map No. 4. Taichung, 1:100,000*. Taiwan Petroleum Exploration Division, Chinese Petroleum Company, Taipei.

Chinese Petroleum Company 1994. *Geological map No. 3. Miaoli, 1:100,000*. Taiwan Petroleum Exploration Division, Chinese Petroleum Company, Taipei.

Ching, K.-E., Rau, R.-J., Johnson, K.M., Lee, J.-C. & Hu, J.-C. 2011. Present-day kinematics of active mountain building in Taiwan from GPS observations during 1995–2005. *Journal of Geophysical Research*, **116**, http://dx.doi.org/10.1029/2010JB008058.

Clark, M.B., Fisher, D.M., Lu, C.-Y. & Chen, C.-H. 1993. Kinematic analyses of the Hsüehshan Range, Taiwan: a large-scale pop-up structure. *Tectonics*, **12**, 205–217, http://dx.doi.org/10.1029/92TC01711.

Ding, Z.Y., Yang, Y.Q., Yao, Z.X. & Zhang, G.H. 2001. A thin-skinned collisional model for the Taiwan orogeny. *Tectonophysics*, **332**, 321–331, http://dx.doi.org/10.1016/S0040-1951(00)00289-4.

Dooley, T.P. & Schreurs, G. 2012. Analogue modelling of intraplate strike-slip tectonics: A review and new experimental results. *Tectonophysics*, **574–575**, 1–71, http://dx.doi.org/10.1016/j.tecto.2012.05.030.

Fisher, D.M., Lu, C.-Y. & Chu, H.-T. 2002. Taiwan slate belt: Insights into the ductile interior of an arc–continent collision. *In*: Byrne, T. & Liu, C.S. (eds) *Geology and Geophysics of an Arc–Continent Collision, Taiwan*.

Geological Society of America, Special Papers, **358**, 93–106, http://dx.doi.org/10.1130/0-8137-2358-2.9.

Fisher, D.M., Willett, S., Yeh, E.-C. & Clark, M.B. 2007. Cleavage fronts and fans as reflections of orogen stress and kinematics in Taiwan. *Geology*, **35**, 65–68, http://dx.doi.org/10.1130/G22850A.1.

Gourley, J.R., Byrne, T., Chan, Y.-C., Wu, F. & Rau, R.-J. 2007. Fault geometries illuminated from seismicity in central Taiwan: implications for crustal scale structural boundaries in the northern Central Range. *Tectonophysics*, **445**, 168–185, http://dx.doi.org/10.1016/j.tecto.2007.08.013.

Hatcher, R.D. & Williams, R.T. 1986. Mechanical model for single thrust sheets Part I: Taxonomy of crystalline thrust sheets and their relationships to the mechanical behavior of orogenic belts. *Geological Society of America Bulletin*, **97**, 975–985, http://dx.doi.org/10.1130/0016-7606(1986)972.

Ho, C.-S. 1988. *An introduction to the geology of Taiwan: Explanatory text of the geological map of Taiwan*. Central Geological Survey, Taipei.

Huang, C.-Y., Wu, W.-Y., Chang, C.-P., Tsao, S., Yuan, P.B., Lin, C.-W. & Xia, K.-Y. 1997. Tectonic evolution of accretionary prism in the arc–continent collision terrane of Taiwan. *Tectonophysics*, **281**, 31–51, http://dx.doi.org/10.1016/S0040-1951(97)00157-1.

Huang, C.-Y., Yuan, P.B., Lin, C.-W., Wang, T.K. & Chang, C.-P. 2000. Geodynamic processes of Taiwan arc–continent collision and comparison with analogs in Timor, Papua New Guinea, Urals and Corsica. *Tectonophysics*, **325**, 1–21, http://dx.doi.org/10.1016/S0040-1951(00)00128-1.

Huang, C.-Y., Yuan, P.B. & Tsao, S.J. 2006. Temporal and spatial records of active arc–continent collision in Taiwan: A synthesis. *Geological Society of America Bulletin*, **118**, 274–288, http://dx.doi.org/10.1130/B25527.1.

Huang, C.-Y., Chi, W.-R., *et al.* 2013. The first record of Eocene tuff in a Paleogene rift basin near Nantou, Western Foothills, central Taiwan. *Journal of Asian Earth Sciences*, **69**, 3–16, http://dx.doi.org/10.1016/j.jseaes.2013.02.022.

Hwang, C., Hsiao, Y.-S., Shih, H.-C., Yang, M., Chen, K.-H., Forsberg, R. & Olesen, A.V. 2007. Geodetic and geophysical results from a Taiwan airborne gravity survey: Data reduction and accuracy assessment. *Journal of Geophysical Research*, **112**, http://dx.doi.org/10.1029/2005JB004220.

Ichikawa, Y., Honma, U., Haruta, M., Hamaoto, K., Ichihara, H. & Suzuki, T. 1927. *Geological Map of Taiwan*. Government-General of Taiwan, Taipei.

Jones, R.H. & Stewart, R.C. 1997. A method for determining significant structures in a cloud of earthquakes. *Journal of Geophysical Research*, **102**, 8245–8254, http://dx.doi.org/10.1029/96JB03739.

Kim, K.-H., Chiu, J.-M., Pujol, J., Chen, K.-C., Huang, B.-S., Yeh, Y.-H. & Shen, P. 2005. Three-dimensional VP and VS structural models associated with the active subduction and collision tectonics in the Taiwan region. *Geophysical Journal International*, **162**, 204–220, http://dx.doi.org/10.1111/j.1365-246X.2005.02657.x.

Kim, K.-H., Chen, K.-C., Wang, J.-H. & Chiu, J.-M. 2010. Seismogenic structures of the 1999 Mw 7.6 Chi-Chi, Taiwan, earthquake and its aftershocks. *Tectonophysics*, **489**, 119–127, http://dx.doi.org/10.1016/j.tecto.2010.04.011.

Kirkpatrick, J.D., Shipton, Z.K., Evans, J.P., Micklethwaite, S., Lim, S.J. & McKillop, P. 2008. Strike-slip fault terminations at seismogenic depths: The structure and kinematics of the Glacier Lakes fault, Sierra Nevada, United States. *Journal of Geophysical Research*, **113**, http://dx.doi.org/10.1029/2007JB005311.

Kuo-Chen, H., Wu, F.T. & Roecker, S.W. 2012. Three-dimensional P velocity structures of the lithosphere beneath Taiwan from the analysis of TAIGER and related seismic data sets. *Journal of Geophysical Research*, **117**, http://dx.doi.org/10.1029/2011JB009108.

Laubscher, H.P. 1987. Die tektonische Entwicklung der Nordschweiz. *Eclogae Geologicae Helvetiae*, **80**, 287–303.

Lee, J.-C., Angelier, J. & Chu, H.-T. 1997. Polyphase history of a complex major fault zone in the northern Taiwan mountain belt: The Lishan Fault. *Tectonophysics*, **274**, 97–115, http://dx.doi.org/10.1016/S0040-1951(96)00300-9.

Leever, K.A., Gabrielsen, R.H., Faleide, J.I. & Braathen, A. 2011. A transpressional origin for the West Spitsbergen fold-and-thrust belt: Insight from analog modeling. *Tectonics*, **30**, http://dx.doi.org/10.1029/2010TC002753.

Lin, C.-H. 2007. Tomographic image of crustal structures across the Chelungpu fault: Is the seismogenic layer structure- or depth-dependent? *Tectonophysics*, **443**, 271–279, http://dx.doi.org/10.1016/j.tecto.2007.01.022.

Lin, A.T., Watts, A.B. & Hesselbo, S.P. 2003. Cenozoic stratigraphy and subsidence history of the South China Sea margin in the Taiwan region. *Basin Research*, **15**, 453–478, http://dx.doi.org/10.1046/j.1365-2117.2003.00215.x.

Malavieille, J. & Trullenque, G. 2009. Consequences of continental subduction on forearc basin and accretionary wedge deformation in SE Taiwan: Insights from analogue modeling. *Tectonophysics*, **466**, 377–394, http://dx.doi.org/10.1016/j.tecto.2007.11.016.

Marrett, R. & Allmendinger, R.W. 1990. Kinematic analysis of fault-slip data. *Journal of Structural Geology*, **12**, 973–986, http://dx.doi.org/10.1016/0191-8141(90)90093-E.

Mirakian, D.C., Crespi, J.M., Byrne, T.B., Huang, C., Ouimet, W.B. & Lewis, J.C. 2012. Tectonic implications of nonparallel topographic and structural curvature in the higher elevations of an active collision zone, Taiwan. *Lithosphere*, http://dx.doi.org/10.1130/L232.1.

Mouthereau, F. & Lacombe, O. 2006. Inversion of the Paleogene Chinese continental margin and thick-skinned deformation in the Western Foreland of Taiwan. *Journal of Structural Geology*, **28**, 1977–1993, http://dx.doi.org/10.1016/j.jsg.2006.08.007.

Mouthereau, F. & Petit, C. 2003. Rheology and strength of the Eurasian continental lithosphere in the foreland of the Taiwan collision belt: Constraints from seismicity, flexure, and structural styles. *Journal of Geophysical Research*, **108**, http://dx.doi.org/10.1029/2002JB002098.

Mouthereau, F., Deffontaines, B., Lacombe, O. & Angelier, J. 2002. Variations along the strike of the Taiwan thrust belt: basement control on structural style, wedge geometry, and kinematics. *In*: Byrne, T. & Liu, C.S. (eds) *Geology and Geophysics of an Arc–Continent Collision, Taiwan*. Geological Society of America, Special Papers, **358**, 31–54.

Mouthereau, F., Fillon, C. & Ma, K.F. 2009. Distribution of strain rates in the Taiwan orogenic wedge. *Earth and Planetary Science Letters*, **284**, 361–385, http://dx.doi.org/10.1016/j.epsl.2009.05.005.

Murphy, J.B., Waldron, J.W.F., Kontak, D.J., Pe-Piper, G. & Piper, D.J.W. 2011. Minas Fault Zone: late Paleozoic history of an intra-continental orogenic transform fault in the Canadian Appalachians. *Journal of Structural Geology*, **33**, 312–328, http://dx.doi.org/10.1016/j.jsg.2010.11.012.

Narr, W. & Suppe, J. 1994. Kinematics of basement-involved compressive structures. *American Journal of Science*, **294**, 802–860, http://dx.doi.org/10.2475/ajs.294.7.802.

Nicol, A. & Van Dissen, R. 2002. Up-dip partitioning of displacement components on the oblique-slip Clarence Fault, New Zealand. *Journal of Structural Geology*, **24**, 1521–1535, http://dx.doi.org/10.1016/S0191-8141(01)00141-9.

Pérez-Estaún, A., Alvarez-Marrón, J., Brown, D., Puchkov, V., Gorozhanina, Y. & Baryshev, V. 1997. Along-strike structural variations in the foreland thrust and fold belt of the southern Urals. *Tectonophysics*, **276**, 265–280, http://dx.doi.org/10.1016/S0040-1951(97)00060-7.

Rau, R.-J. & Wu, F.T. 1995. Tomographic imaging of lithospheric structures under Taiwan. *Earth and Planetary Science Letters*, **133**, 517–532, http://dx.doi.org/10.1016/0012-821X(95)00076-O.

Rodgers, J. 1987. Chains of basement uplifts within cratons marginal to orogenic belts. *American Journal of Science*, **287**, 661–692, http://dx.doi.org/10.2475/ajs.287.7.661.

Rodriguez-Roa, F.A. & Wiltschko, D.V. 2010. Thrust belt architecture of the central and southern Western Foothills of Taiwan. *In*: Goffey, G.P., Craig, J., Needham, T. & Scott, R. (eds) *Hydrocarbons in Contractional Belts*. Geological Society, London, Special Publications, **348**, 137–168, http://dx.doi.org/10.1144/SP348.8.

Sakaguchi, A., Yanagihara, A., Ujiie, K., Tanaka, H. & Kameyama, M. 2007. Thermal maturity of a fold–thrust belt based on vitrinite reflectance analysis in the Western Foothills complex, western Taiwan. *Tectonophysics*, **443**, 220–232, http://dx.doi.org/10.1016/j.tecto.2007.01.017.

Schmidt, C.J., O'Neill, J.M. & Brandon, W.C. 1988. Influence of Rocky Mountain foreland uplifts on the development of the frontal fold and thrust belt, southwestern Montana. *In*: Schmidt, C.J. & Perry, W.J. (eds) *Interaction of the Rocky Mountain Foreland and the Cordilleran Thrust Belt*. Geological Society of America, Memoirs, **171**, 171–201.

Sibuet, J.-C. & Hsu, S.-K. 2004. How was Taiwan created?. *Tectonophysics*, **379**, 159–181, http://dx.doi.org/10.1016/j.tecto.2003.10.022.

Simoes, M., Avouac, J.P., Beyssac, O., Goffé, B., Farley, K.A. & Chen, Y.-G. 2007. Mountain building in Taiwan: a thermokinematic model. *Journal of Geophysical Research*, **112**, http://dx.doi.org/10.1029/2006JB004824.

Simoes, M., Beyssac, O. & Chen, Y.-G. 2012. Late Cenozoic metamorphism and mountain building in Taiwan: a review. *Journal of Asian Earth Sciences*, **46**, 92–119, http://dx.doi.org/10.1016/j.jseaes.2011.11.009.

Sung, Q., Chen, Y.-C., Tsai, H., Chen, Y.-G. & Chen, W.-S. 2000. Comparison study on the coseismic deformation of the 1999 Chi-Chi earthquake and long-term stream gradient changes along the Chelungpu Fault in central Taiwan. *Terrestrial, Atmospheric and Oceanic Sciences*, **11**, 735–750.

Suppe, J. 1980. A retrodeformable cross section of northern Taiwan. *Proceedings, Geological Society of China*, **23**, 46–55.

Suppe, J. 1981. Mechanics of mountain building and metamorphism in Taiwan. *Memoir of the Geological Society of China*, **4**, 67–89.

Suppe, J. 1984. Kinematics of arc–continent collision, flipping of subduction, and back-arc spreading near Taiwan. *Memoir of the Geological Society of China*, **6**, 21–33.

Suppe, J. 1987. The active Taiwan mountain belt. *In*: Schaer, J.P. & Rodgers, J. (eds) *The Anatomy of Mountain Ranges*. Princeton University Press, Princeton, NJ, 277–293.

Sylvester, A.G. 1988. Strike-slip faults. *Geological Society of America Bulletin*, **100**, 1666– 1703, http://dx.doi.org/10.1130/0016-7606(1988)1002.3.CO;2.

Teng, L.S. & Lin, A.T. 2004. Cenozoic tectonics of the China continental margin: insights from Taiwan. *In*: Malpas, J., Fletcher, C.J.N., Ali, J.R. & Aitchison, J.C. (eds) *Aspects of the Tectonic Evolution of China*. Geological Society, London, Special Publications, **226**, 313–332, http://dx.doi.org/10.1144/GSL.SP.2004.226.01.17.

Teng, L.S., Wang, Y., Tang, C.-H., Huang, C.-Y., Huang, T.-C., Yu, M.-S. & Ke, A. 1991. Tectonic aspects of the Paleogene depositional basin of northern Taiwan. *Proceedings, Geological Society of China*, **34**, 313–336.

Tillman, K.S. & Byrne, T.B. 1995. Kinematic analysis of the Taiwan Slate Belt. *Tectonics*, **14**, 322–341, http://dx.doi.org/10.1029/94TC02451.

Walcott, R.I. 1998. Modes of oblique compression: late Cenozoic tectonics of the South Island of New Zealand. *Reviews of Geophysics*, **36**, 1–26, http://dx.doi.org/10.1029/97RG03084.

Wang, C.-Y., Chang, C.-H. & Yen, H.-Y. 2000. An interpretation of the 1999 Chi-Chi earthquake in Taiwan based on the thin-skinned thrust model. *Terrestrial, Atmospheric and Oceanic Sciences*, **11**, 609–630.

Wang, C.-Y., Li, C.-L., Su, F.-C., Leu, M.-T., Wu, M.-S., Lai, S.-H. & Chern, C.-C. 2002. Structural mapping of the 1999 Chi-Chi earthquake fault, Taiwan by seismic reflection methods. *Terrestrial, Atmospheric and Oceanic Sciences*, **13**, 211–226.

Wilcox, R.E., Harding, T.P. & Seely, D.R. 1973. Basic wrench tectonics. *AAPG Bulletin*, **57**, 74–96.

Wiltschko, D. & Eastman, D. 1983. Role of basement warps and faults in localizing thrust fault ramps. *In*: Hatcher, R.D., Williams, H. & Zietz, I. (eds) *Contributions to the Tectonics and Geophysics of Mountain Chains*. Geological Society of America, Memoirs, **158**, 177–190.

Wiltschko, D., Hassler, L., Hung, J.-H. & Liao, H.-S. 2010. From accretion to collision: motion and evolution of the Chaochou Fault, southern Taiwan. *Tectonics*, **29**, http://dx.doi.org/10.1029/2008TC002398.

Woodward, N.B. 1988. Primary and secondary basement controls on thrust sheet geometries. *In*: Schmidt, C.J. & Perry, W.J. (eds) *Interaction of the Rocky Mountain Foreland and the Cordilleran Thrust Belt*. Geological Society of America, Memoirs, **171**, 353–366.

Wu, F.T., Rau, R.J. & Salzberg, D. 1997. Taiwan orogeny: thin-skinned or lithospheric collision? *Tectonophysics*, **274**, 191–220, http://dx.doi.org/10.1016/S0040-1951(96)00304-6.

Wu, F.T., Chang, C.-H. & Wu, Y.-M. 2004. Precisely relocated hypocentres, focal mechanisms and active orogeny in Central Taiwan. *In*: Malpas, J., Fletcher, C.J.N., Ali, J.R. & Aitchison, J.C. (eds) *Aspects of the Tectonic Evolution of China*. Geological Society, London, Special Publications, **226**, 333–354, http://dx.doi.org/10.1144/gsl.sp.2004.226.01.18.

Wu, Y.-M., Chang, C.-H., Zhao, L., Shyu, J.B.H., Chen, Y.-G., Sieh, K. & Avouac, J.-P. 2007. Seismic tomography of Taiwan: Improved constraints from a dense network of strong motion stations. *Journal of Geophysical Research*, **112**, B08312, http://dx.doi.org/10.1029/2007JB004983.

Wu, Y.-M., Chang, C.-H., Zhao, L., Teng, T.L. & Nakamura, M. 2008*a*. A comprehensive relocation of earthquakes in Taiwan from 1991 to 2005. *Bulletin of the Seismological Society of America*, **98**, 1471–1481, http://dx.doi.org/10.1785/0120070166.

Wu, Y.-M., Zhao, L., Chang, C.-H. & Hsu, Y.-J. 2008*b*. Focal-mechanism determination in Taiwan by genetic algorithm. *Bulletin of the Seismological Society of America*, **98**, 651–661, http://dx.doi.org/10.1785/0120070115.

Wu, Y.-M., Shyu, J.B.H., Chang, C.-H., Zhao, L., Nakamura, M. & Hsu, S.-K. 2009. Improved seismic tomography offshore northeastern Taiwan: Implications for subduction and collision processes between Taiwan and the southernmost Ryukyu. *Geophysical Journal International*, **178**, 1042–1054, http://dx.doi.org/10.1111/j.1365-246X.2009.04180.x.

Wu, Y.-M., Hsu, Y.-J., Chang, C.-H., Teng, L.S.-y & Nakamura, M. 2010. Temporal and spatial variation of stress field in Taiwan from 1991 to 2007: Insights from comprehensive first motion focal mechanism catalog. *Earth and Planetary Science Letters*, **298**, 306–316, http://dx.doi.org/10.1016/j.epsl.2010.07.047.

Yamato, P., Mouthereau, F. & Burov, E. 2009. Taiwan mountain building: Insights from 2-D thermomechanical modelling of a rheologically stratified lithosphere. *Geophysical Journal International*, **176**, 307–326, http://dx.doi.org/10.1111/j.1365-246X.2008.03977.x.

Yanites, B.J., Tucker, G.E., Mueller, K.J., Chen, Y.G., Wilcox, T., Huang, S.Y. & Shi, K.W. 2010. Incision and channel morphology across active structures along the Peikang River, central Taiwan: Implications for the importance of channel width. *Geological Society of America Bulletin*, **122**, 1192–1208, http://dx.doi.org/10.1130/B30035.1.

Yue, L.-F., Suppe, J. & Hung, J.-H. 2005. Structural geology of a classic thrust belt earthquake: the 1999 Chi-Chi earthquake, Taiwan (Mw = 7.6). *Journal of Structural Geology*, **27**, 2058–2083, http://dx.doi.org/10.1016/j.jsg.2005.05.020.

Zoback, M.L. 1992. First- and second-order patterns of stress in the lithosphere: the World Stress Map Project. *Journal of Geophysical Research*, **97**, 11703–11728, http://dx.doi.org/10.1029/92JB00132.

Received 27 February 2013; revised typescript accepted 15 July 2013.
Scientific editing by Quentin Crowley.

Article 3 - Basin inversion in central Taiwan and its importance for seismic hazard

Giovanni Camanni[1], Chi-Hsuan Chen[2, 3], Dennis Brown[1], Joaquina Alvarez-Marron[1], Yih-Min Wu[2], Hsi-An Chen[2], Hsin-Hua Huang[2], Hao-Tsu Chu[3], Mien-Ming Chen[3], and Chien-Hsin Chang[4]

[1]Institute of Earth Sciences Jaume Almera, ICTJA-CSIC, Lluis Sole i Sabaris s/n, 08028 Barcelona, Spain
[2]Department of Geosciences, National Taiwan University, Taipei, 106, Taiwan
[3]Central Geological Survey, P.O. Box 968, Taipei 235, Taiwan
[4]Central Weather Bureau, Taipei 10048, Taiwan

Status of publication: published in "**Geology**", (2014), v. 42, no. 2, p. 147-150, doi: 10.1130/G35102.1

Contributions of the Ph.D. student to the article:

- Manuscript conception and writing;
- Construction of geometrically constrained cross-section A-A´;
- Analysis of earthquake hypocentre data;
- Analysis of P-wave velocity data

Basin inversion in central Taiwan and its importance for seismic hazard

Giovanni Camanni[1], Chi-Hsuan Chen[2,3], Dennis Brown[1], Joaquina Alvarez-Marron[1], Yih-Min Wu[3], Hsi-An Chen[3], Hsin-Hua Huang[3], Hao-Tsu Chu[2], Mien-Ming Chen[2], and Chien-Hsin Chang[4]
[1]Institute of Earth Sciences Jaume Almera, ICTJA-CSIC, Lluis Sole i Sabaris s/n, 08028 Barcelona, Spain
[2]Central Geological Survey, P.O. Box 968, Taipei 235, Taiwan
[3]Department of Geosciences, National Taiwan University, Taipei 106, Taiwan
[4]Central Weather Bureau, Taipei 10048, Taiwan

ABSTRACT

On 27 March 2013, a 6.2 M_L earthquake occurred at 19 km depth in eastern Nantou, central Taiwan. Over a 2 week period it was followed by more than 680 aftershocks that ranged to 5 M_L. Most events occurred below the ~10-km-deep detachment fault predicted for this part of the mountain belt, coinciding with other precisely located hypocenters that indicate that much of the crust in this area is seismically active. We combine geological data with a three-dimensional (3-D) P-wave velocity model derived from local tomography and earthquake hypocenters to determine a model for the structure of central Taiwan. Much of the surface geology of the area comprises the uplifted Eocene rocks of the Hsuehshan Basin. The 3-D P-wave velocity model shows a shallowing of higher velocities across the Hsuehshan Basin and hypocenter data indicate that its western bounding fault is clearly defined by an eastward-dipping band of events that extends to >20 km depth. The eastern bounding fault is interpreted to coincide at depth with a cluster of events between 20 and 30 km depth. These data suggest that the preexisting, rift-related extensional faults of the Hsuehshan Basin are currently being reactivated and the basin is being inverted. We present hypocenter data from the Nantou sequence that corroborate this interpretation and show the importance of choosing the correct structural model when assessing seismic risk.

INTRODUCTION

In an arc-continent collision orogeny such as that of Taiwan, the development of a foreland fold-and-thrust belt depends, among other factors, on the thickness profile of the subducting margin crust, the presence and size of the rift basins within it, and the geometry of the platform and slope sedimentary sequences prior to collision (Brown et al., 2011; Harris, 2011). The response of these primary factors to the deformation is determined, to a large degree, by the rheology of the crust, the orientation of the rift basins and their bounding faults relative to the plate convergence vector, and the convergence rate (Sibson, 1995; Poblet and Lisle, 2011).

Many foreland fold-and-thrust belts worldwide (Rodgers, 1990; Poblet and Lisle, 2011) include a deformed sedimentary cover of a rifted continental margin (Fig. 1A) that is detached above the underlying basement (basement is defined here as any pre-rift rocks), often within or at the base of the lowermost postrift sediments, to form what is termed a thin-skinned thrust system (e.g., Poblet and Lisle, 2011) (Fig. 1B). In a thin-skinned thrust system the expected distribution of seismicity would be a narrow, subhorizontal cluster of events around the basal detachment (Ni and Barazangi, 1984; Carena et al., 2002), scattered events along individual faults above it, and rare events below it where rocks are thought to undergo little deformation (Davis et al., 1983; Dahlen et al., 1984). In this scenario, only in the interior part of the mountain belt, where rocks are exhumed along deeply penetrating faults, should any notable increase in the seismic velocities at shallow depths be expected. If, however, the inherited rift-related basin-bounding faults are reactivated, the deformation will penetrate deeper parts of the crust, causing the synrift sediments and the underlying basement to be uplifted and exhumed (Jackson, 1980) in what is termed basin inversion, or thick-skinned deformation (e.g., Poblet and Lisle, 2011) (Fig. 1C). In areas undergoing basin inversion, seismicity can be expected to take place along the reactivating rift-related faults and display steeply inclined hypocenter clusters that possibly extend into the middle and even lower crust (Jackson, 1980; Okada et al., 2007; Sibson, 2009). The uplift of deeply buried sediments and basement will result in increased seismic velocities closer to the surface.

Determining the deformation mode of a foreland fold-and-thrust belt is important for identifying fault source when assessing seismic hazard in an area, and therefore in developing risk models and management protocols for seismic risk within this part of the orogen (Loh et al., 1991; Campbell et al., 2002; Cheng et al., 2007). Furthermore, an accurate structural model also provides information on the expected geometry of faults, which is an important factor in hazard modeling because the dip of a fault can greatly influence the magnitude of an earthquake along it, with steeper dips resulting in higher magnitude events (Cheng et al., 2007).

In this paper we combine geological data with earthquake hypocenters and a three-dimensional (3-D) P-wave velocity model to determine the structure beneath the Hsuehshan Basin in central Taiwan. We find that a model in which preexisting, rift-related extensional faults that bound the basin are being reactivated and inverted better fits the available data than does a structural model in which there is a shallow, through-going basal detachment (e.g., Carena et al., 2002; Yue et al., 2005).

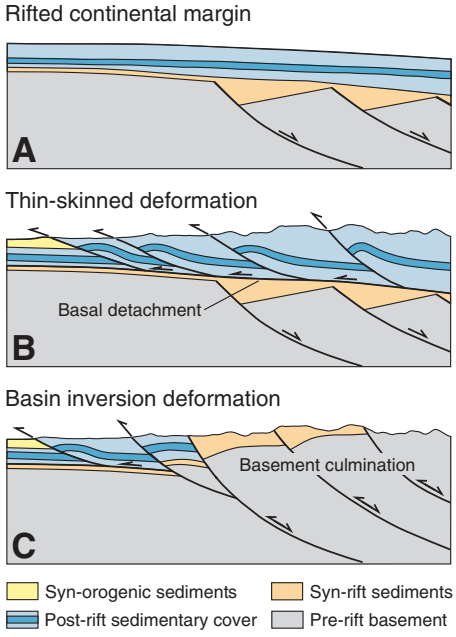

Figure 1. Evolution from rifted continental margin to foreland fold-and-thrust belt. In this figure, plane strain is assumed. A: Idealized rifted continental margin. B: Thin-skinned deformation style: rift-related faults are inactive and only sedimentary cover of A is involved in deformation. C: Basin inversion (or thick-skinned deformation) style: rift-related faults are reactivated and cause deepening in level of deformation.

GEOLOGICAL BACKGROUND

The rifted continental margin of southeast Eurasia has been colliding with the Luzon arc of the Philippine Sea plate since at least the Late Miocene, resulting in the Taiwan orogen (Sibuet and Hsu, 2004). This part of the Eurasian continental margin contains a number of Eocene rift basins (Lin et al., 2003; Teng and Lin, 2004; Yang et al., 2006); the sediments of the Eocene Hsuehshan Basin currently occupy a significant part of the Taiwan orogen (Lin et al., 2003) (Fig. 2A). The basin is bound to the west

GEOLOGY, February 2014; v. 42; no. 2; p. 147–150; Data Repository item 2014039 | doi:10.1130/G35102.1 | Published online 13 December 2013

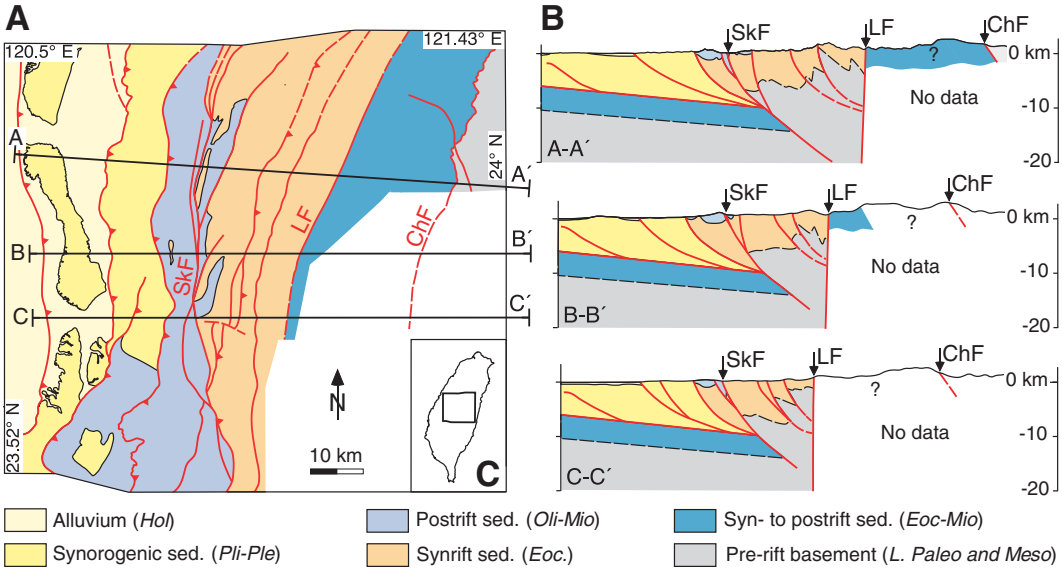

Figure 2. A: Simplified geological map of study area in central Taiwan. B: Geological cross sections through study area (modified after Brown et al., 2012). C: Location of study area. ChF—Chinma fault; LF—Lishan fault; SkF—Shuilikeng fault; Hol—Holocene; Pli—Pliocene; Ple—Pleistocene; Oli—Oligocene; Mio—Miocene; Eoc.—Eocene; L. Paleo—Late Paleocene; Meso—Mesozoic.

by the Shuilikeng fault and to the east by the Lishan fault. The synrift sediments of these basins are overlain by Oligocene to Late Miocene postrift platform and slope sediments that can be as much as several kilometers thick and are variably deformed within the orogen. The onset of synorogenic deposition might have begun as early as the latest Miocene, and continues today. The sedimentary package within the foreland basin can reach 6 km or more in thickness, and the deformation front is within it.

The Eocene synrift rocks of the Hsuehshan Basin now occupy topographically higher ground and structurally overlie Pleistocene rocks of the foreland basin along the Shuilikeng fault (Brown et al., 2012; Camanni et al., 2013) (Fig. 2B). This suggests that inversion of the Hsuehshan Basin is taking place and that the synrift sediments and their underlying basement rocks are being uplifted and exhumed (Clark et al., 1993; Brown et al., 2012).

BASIN INVERSION

To test the hypothesis that inversion of the Hsuehshan Basin is taking place, we use a 3-D P-wave velocity model revised from Wu et al. (2007), and earthquake hypocenters that have been relocated using this model (e.g., Wu et al., 2008), which we collapse using the methodology of Jones and Stewart (1997) (Fig. 3A). We then add the geologically determined fault interpretation (Fig. 3B) in order to evaluate whether ongoing seismic activity is consistent with a shallow detachment or requires inversion of deep-seated rift-related extensional faults that bound the Hsuehshan Basin.

From km 0 to roughly the Shuilikeng fault at km 30, the P-wave velocities in all 3 sections of Figure 3 display an ~8-km-thick low-velocity zone that correlates well with the Miocene and younger postrift and synorogenic sediments. Eastward, this low P-wave velocity zone shallows, and higher velocities appear closer to the surface (with minor complications in section C-C′). The shallowing of higher P-wave velocity material to the east of the Shuilikeng fault (SkF in Fig. 3) is clearly indicated by the 5.5 km s^{-1} isovelocity line, which we interpret to be the top of the low-grade metasedimentary basement clastics intersected in boreholes in western Taiwan (Chiu, 1975; Shaw, 1996). This shallow high-velocity zone is a robust feature that has been recognized in a number of other studies, regardless of the method of tomographic inversion (Rau and Wu, 1995; Kim et al., 2005, 2010; Lin, 2007; Kuo-Chen et al., 2012).

All 3 sections display east-dipping clusters of hypocenters between approximately km 30 and 50, and ~10–20 km depth. Particularly in sections B-B′ and C-C′, this cluster projects to the surface at the mapped location of the Shuilikeng fault (Fig. 3) and, in section B-B′, joins westward with a thin, subhorizontal cluster of hypocenters that marks the location of the basal detachment known to be in this area (Carena et al., 2002; Yue et al., 2005; Brown et al., 2012), forming a linked fault system. In sections B-B′ and C-C′, a cluster of hypocenters at approximately km 50 and between 20 and 30 km depth is interpreted to project to the surface at the location of the Lishan fault (LF in Fig. 3; for a similar interpretation, see Wu et al., 2004; Gourley et al., 2007). Farther east, at approximately km 80, an open to tight cluster of hypocenters appears to be associated with the Chinma fault (ChF in Fig. 3), which places Mesozoic basement on top of Eocene and younger slope-derived sediments.

NANTOU EARTHQUAKE SEQUENCE

Hypocenters from the Nantou earthquake sequence (Fig. 4) have been relocated using the same 3-D velocity model and collapsing methodology as those shown in Figure 3. The majority of the hypocenters plot along the deep trace of the Shuilikeng fault and a number of them, including the main shock, plot within the cluster interpreted to be associated with the Lishan fault. Focal mechanisms that we determined for the four events of $M_L > 4$ have reverse fault-plane solutions (Fig. 4). The coincidence of the Nantou earthquake hypocenters with the interpreted deep locations of the bounding faults of the Hsuehshan Basin determined from the data presented herein further indicates that these faults are important structures contributing to mountain building in central Taiwan.

DISCUSSION AND CONCLUSIONS

The combination of geological, P-wave velocity, and earthquake hypocenter data presented here suggests that the basin inversion model (Fig. 1C) for deformation in central Taiwan is a viable alternative to the previously accepted thin-skinned model (e.g., Davis et al., 1983; Dahlen et al., 1984; Suppe, 1987; Carena et al., 2002; Yue et al., 2005; Malavieille and Trullenque, 2009) (Fig. 1B). Significant seismic activity along the margins of the Hsuehshan Basin and shallowing of higher P-wave velocity material in the area occupied by the Hsuehshan Basin provide strong evidence that the reactivation of its bounding faults and the uplift and exhumation of its synrift sediments and basement rocks compose the dominant deformation style in this part of central Taiwan. The data show that the deformation reaches at least 30 km beneath the Hsuehshan Basin, further suggesting that basement rocks must be involved in the deformation in this region (see also Wu et al., 1997, 2004; Gourley et al., 2007; Brown et al., 2012; Chuang et al., 2013). However, we cannot determine if there is a deep level of detachment at

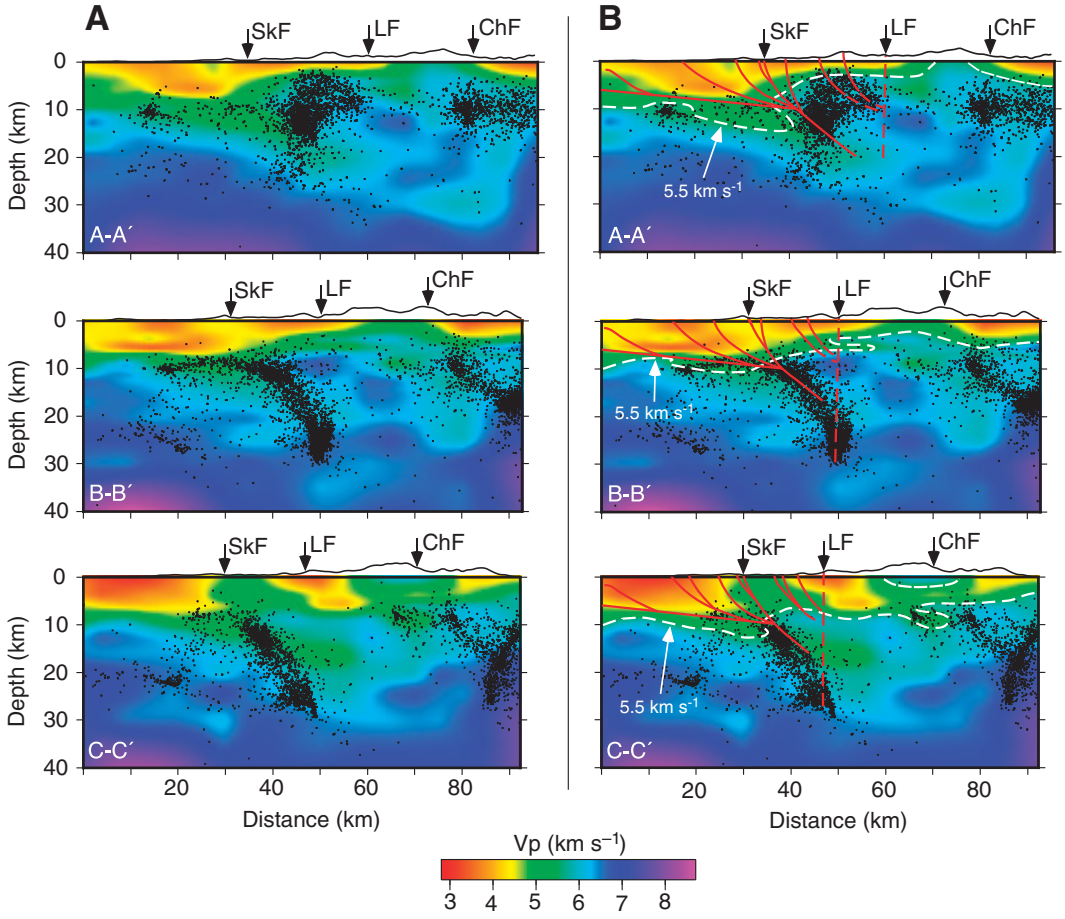

Figure 3. A: Uninterpreted vertical sections through three-dimensional (3-D) P-wave velocity model (Wu et al., 2007) and relocated (Wu et al., 2008) and collapsed seismicity used in this study. ChF—Chinma fault, LF—Lishan fault, SkF—Shuilikeng fault. B: Interpreted vertical sections. Hypocenters are projected from 4.99 km on either side of sections (section locations are in Fig. 2). Spatial uncertainty of hypocenters was determined as horizontal and vertical location errors following Wu et al. (2008), and can be found in hypocenter database (available from authors or at http://seismology.gl.ntu.edu.tw/download_04.htm). Data were collapsed using 3-D spatial uncertainty of 4 standard deviations (methodology of Jones and Stewart, 1997) to truncate confidence ellipsoid and estimated variance in data. Hypocenter movements were compared with χ^2 distribution and repeated until minimum misfit was reached. For comparison, uncollapsed seismicity data are provided in Figure DR1 in the GSA Data Repository[1]. Faults on interpreted sections are derived from surface geological and hypocenter data only. Dashed white line indicates 5.5 km s^{-1} isovelocity line that we use as reference for top of basement.

these depths beneath the Hsuehshan and Central ranges with the current data sets.

The Nantou earthquakes highlight the need for a revised structural model for central Taiwan that provides a more precise framework for seismic risk assessment than the currently used thin-skinned model. We suggest that a model in which preexisting basins that were located on the Eurasian margin are being inverted along deep penetrating faults provides a viable explanation for the Nantou earthquake sequence, and therefore gives a new perspective for identifying fault source when assessing seismic risk in the area. In the light of this new structural model, the Shuilikeng and the Lishan faults are both candidates for future damaging earthquakes such as the Nantou main shock.

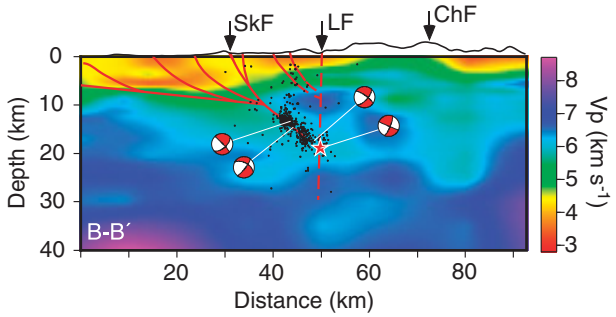

Figure 4. P-wave velocity model B-B′ with geologically determined faults and collapsed 27 March to 15 April 2013 Nantou, central Taiwan, sequence hypocenters. SkF—Shuilikeng fault, LF—Lishan fault, ChF—Chinma fault. Red star indicates location of 6.2 M_L main shock. Hypocenters have been projected from 4.99 km on either side of section, for total of 418 events.

ACKNOWLEDGMENTS

Discussions with Emilio Casciello, Andrea Festa, and Andrés Pérez-Estaún on the structural architecture of orogens helped to clarify our ideas. We thank Beatriz Gaite and Martin Schimmel for their help with processing the tomography data. This research was carried out with the aid of grants by Consejo Superior de Investigaciones Científicas (CSIC) Proyectos Intramurales 2006 301010, Ministerio de Ciencia e Innovación CGL2009-11843-BTE, and the CSIC predoctoral program Junta para la Ampliación de Estudios (JAE-Predoc). We also wish to thank the Editor, Bob Holdsworth, and three anonymous reviewers for their constructive comments on this manuscript.

REFERENCES CITED

Brown, D., and 15 others, 2011, Arc-continent collision: The making of an orogen, *in* Brown, D., and Ryan, P.D., eds., Arc-continent collision: Frontiers in Earth Sciences: New York, Springer, p. 477–493, doi:10.1007/978-3-540-88558-0_17.

Brown, D., Alvarez-Marron, J., Schimmel, M., Wu, Y.-M., and Camanni, G., 2012, The structure and kinematics of the central Taiwan mountain belt derived from geological and seismicity data: Tectonics, v. 31, TC5013, doi:10.1029/2012TC003156.

Camanni, G., Brown, D., Alvarez-Marron, J., Wu, Y.-M., and Chen, H.-A., 2013, The Shuilikeng fault in the central Taiwan mountain belt: Geological Society of London Journal, doi:10.1144/jgs2013-014.

Campbell, K.W., Thenhaus, P.C., Barnhard, T.P., and Hampson, D.B., 2002, Seismic hazard model for loss estimation and risk management in Taiwan: Soil Dynamics and Earthquake Engineering, v. 22, p. 743–754, doi:10.1016/S0267-7261(02)00095-7.

[1]GSA Data Repository item 2014039, supplementary geological and geophysical information, is available online at www.geosociety.org/pubs/ft2014.htm, or on request from editing@geosociety.org or Documents Secretary, GSA, P.O. Box 9140, Boulder, CO 80301, USA.

Carena, S., Suppe, J., and Kao, H., 2002, Active detachment of Taiwan illuminated by small earthquakes and its control of first-order topography: Geology, v. 30, p. 935–938, doi:10.1130/0091-7613(2002)030<0935:ADOTIB>2.0.CO;2.

Cheng, C.-T., Chiou, S.-J., Lee, C.-T., and Tsai, Y.-B., 2007, Study on probabilistic seismic hazard maps of Taiwan after Chi-Chi earthquake: Journal of GeoEngineering, v. 2, p. 19–28.

Chiu, H.-T., 1975, Miocene stratigraphy and its relation to the Palaeogene rocks in west-central Taiwan: Petroleum Geology of Taiwan, v. 12, p. 51–80.

Chuang, R.Y., Johnson, K.M., Wu, Y.-M., Ching, K.-E., and Kuo, L.-C., 2013, A midcrustal ramp-fault structure beneath the Taiwan tectonic wedge illuminated by the 2013 Nantou earthquake series: Geophysical Research Letters, v. 40, p. 1–5, doi:10.1002/grl.51005.

Clark, M.B., Fisher, D.M., Lu, C.-Y., and Chen, C.-H., 1993, Kinematic analyses of the Hsuehshan Range, Taiwan: A large-scale pop-up structure: Tectonics, v. 12, p. 205–217, doi:10.1029/92TC01711.

Dahlen, F.A., Suppe, J., and Davis, D., 1984, Mechanics of fold-and-thrust belts and accretionary wedges: Cohesive coulomb theory: Journal of Geophysical Research, v. 89, p. 10087–10101, doi:10.1029/JB089iB12p10087.

Davis, D., Suppe, J., and Dahlen, F.A., 1983, Mechanics of fold-and-thrust belts and accretionary wedges: Journal of Geophysical Research, v. 88, p. 1153–1172, doi:10.1029/JB088iB02p01153.

Gourley, J.R., Byrne, T., Chan, Y.-C., Wu, F., and Rau, R.-J., 2007, Fault geometries illuminated from seismicity in central Taiwan: Implications for crustal scale structural boundaries in the northern Central Range: Tectonophysics, v. 445, p. 168–185, doi:10.1016/j.tecto.2007.08.013.

Harris, R., 2011, The nature of the Banda arc-continent collision in the Timor region, *in* Brown, D., and Ryan, P.D., eds., Arc-continent collision: Frontiers in Earth Sciences: New York, Springer, p. 163–211, doi:10.1007/978-3-540-88558-0_7.

Jackson, J.A., 1980, Reactivation of basement faults and crustal shortening in orogenic belts: Nature, v. 283, p. 343–346, doi:10.1038/283343a0.

Jones, R.H., and Stewart, R.C., 1997, A method for determining significant structures in a cloud of earthquakes: Journal of Geophysical Research, v. 102, p. 8245–8254, doi:10.1029/96JB03739.

Kim, K.-H., Chiu, J.-M., Pujol, J., Chen, K.-C., Huang, B.-S., Yeh, Y.-H., and Shen, P., 2005, Three-dimensional VP and VS structural models associated with the active subduction and collision tectonics in the Taiwan region: Geophysical Journal International, v. 162, p. 204–220, doi:10.1111/j.1365-246X.2005.02657.x.

Kim, K.-H., Chen, K.-C., Wang, J.-H., and Chiu, J.-M., 2010, Seismogenic structures of the 1999 Mw 7.6 Chi-Chi, Taiwan, earthquake and its aftershocks: Tectonophysics, v. 489, p. 119–127, doi:10.1016/j.tecto.2010.04.011.

Kuo-Chen, H., Wu, F.T., and Roecker, S.W., 2012, Three-dimensional P velocity structures of the lithosphere beneath Taiwan from the analysis of TAIGER and related seismic data sets: Journal of Geophysical Research, v. 117, B06306, doi:10.1029/2011JB009108.

Lin, A.T., Watts, A.B., and Hesselbo, S.P., 2003, Cenozoic stratigraphy and subsidence history of the South China Sea margin in the Taiwan region: Basin Research, v. 15, p. 453–478, doi:10.1046/j.1365-2117.2003.00215.x.

Lin, C.-H., 2007, Tomographic image of crustal structures across the Chelungpu fault: Is the seismogenic layer structure- or depth-dependent?: Tectonophysics, v. 443, p. 271–279, doi:10.1016/j.tecto.2007.01.022.

Loh, C.H., Yeh, Y.T., Jean, W.Y., and Yeh, Y.H., 1991, Seismic hazard analysis in the Taiwan area using a bounded fault-rupture model: Seismological Society of America Bulletin, v. 81, p. 265–272.

Malavieille, J., and Trullenque, G., 2009, Consequences of continental subduction on forearc basin and accretionary wedge deformation in SE Taiwan: Insights from analogue modeling: Tectonophysics, v. 466, p. 377–394, doi:10.1016/j.tecto.2007.11.016.

Ni, J., and Barazangi, M., 1984, Seismotectonics of the Himalayan collision zone: Geometry of the underthrusting Indian Plate beneath the Himalaya: Journal of Geophysical Research, v. 89, p. 1147–1163, doi:10.1029/JB089iB02p01147.

Okada, T., Hasegawa, A., Suganomata, J.I., Umino, N., Zhang, H., and Thurber, C.H., 2007, Imaging the heterogeneous source area of the 2003 M6.4 northern Miyagi earthquake, NE Japan, by double-difference tomography: Tectonophysics, v. 430, p. 67–81, doi:10.1016/j.tecto.2006.11.001.

Poblet, J., and Lisle, R.J., 2011, Kinematic evolution and structural styles of fold-and-thrust belts, *in* Poblet, J., and Lisle, R.J., eds., Kinematic evolution and structural styles of fold-and-thrust belts: Geological Society of London Special Publication 349, p. 1–24, doi:10.1144/SP349.1.

Rau, R.-J., and Wu, F.T., 1995, Tomographic imaging of lithospheric structures under Taiwan: Earth and Planetary Science Letters, v. 133, p. 517–532, doi:10.1016/0012-821X(95)00076-O.

Rodgers, J., 1990, Fold-and-thrust belts in sedimentary rocks; Part 1, Typical examples: American Journal of Science, v. 290, p. 321–359, doi:10.2475/ajs.290.4.321.

Shaw, C.-L., 1996, Stratigraphic correlation and isopach maps of the Western Taiwan Basin: Terrestrial, Atmospheric and Oceanic Sciences, v. 7, p. 333–360.

Sibson, R.H., 1995, Selective fault reactivation during basin inversion: Potential for fluid redistribution through fault-valve action, *in* Buchanan, J.G., and Buchanan, P.G., eds., Basin inversion: Geological Society of London Special Publication 88, p. 3–19, doi:10.1144/GSL.SP.1995.088.01.02.

Sibson, R.H., 2009, Rupturing in overpressured crust during compressional inversion—The case from NE Honshu, Japan: Tectonophysics, v. 473, p. 404–416, doi:10.1016/j.tecto.2009.03.016.

Sibuet, J.-C., and Hsu, S.-K., 2004, How was Taiwan created?: Tectonophysics, v. 379, p. 159–181, doi:10.1016/j.tecto.2003.10.022.

Suppe, J., 1987, The active Taiwan mountain belt, *in* Schaer, J.P., and Rodgers, J., eds., The anatomy of mountain ranges: Princeton, New Jersey, Princeton University Press, p. 277–293.

Teng, L.S., and Lin, A.T., 2004, Cenozoic tectonics of the China continental margin: Insights from Taiwan, *in* Malpas, J., et al., eds., Aspects of the tectonic evolution of China: Geological Society of London Special Publication 226, p. 313–332, doi:10.1144/GSL.SP.2004.226.01.17.

Wu, F.T., Rau, R.-J., and Salzberg, D., 1997, Taiwan orogeny: Thin-skinned or lithospheric collision?: Tectonophysics, v. 274, p. 191–220, doi:10.1016/S0040-1951(96)00304-6.

Wu, F.T., Chang, C.-H., and Wu, Y.-M., 2004, Precisely relocated hypocentres, focal mechanisms and active orogeny in central Taiwan, *in* Malpas, J., et al., eds., Aspects of the tectonic evolution of China: Geological Society of London Special Publication 226, p. 333–354, doi:10.1144/GSL.SP.2004.226.01.18.

Wu, Y.-M., Chang, C.-H., Zhao, L., Shyu, J.B.H., Chen, Y.-G., Sieh, K., and Avouac, J.-P., 2007, Seismic tomography of Taiwan: Improved constraints from a dense network of strong motion stations: Journal of Geophysical Research, v. 112, B08312, doi:10.1029/2007JB004983.

Wu, Y.-M., Chang, C.-H., Zhao, L., Teng, T.L., and Nakamura, M., 2008, A comprehensive relocation of earthquakes in Taiwan from 1991 to 2005: Seismological Society of America Bulletin, v. 98, p. 1471–1481, doi:10.1785/0120070166.

Yang, K.-M., Huang, S.-T., Wu, J.-C., Ting, H.-H., and Mei, W.-W., 2006, Review and new insights on foreland tectonics in western Taiwan: International Geology Review, v. 48, p. 910–941, doi:10.2747/0020-6814.48.10.910.

Yue, L.-F., Suppe, J., and Hung, J.-H., 2005, Structural geology of a classic thrust belt earthquake: The 1999 Chi-Chi earthquake Taiwan (Mw=7.6): Journal of Structural Geology, v. 27, p. 2058–2083, doi:10.1016/j.jsg.2005.05.020.

Manuscript received 9 September 2013
Revised manuscript received 28 October 2013
Manuscript accepted 5 November 2013

Printed in USA

Article 4 - Structural complexities in a foreland thrust belt inherited from the shelf-slope transition: Insights from the Alishan area of Taiwan

Joaquina Alvarez-Marron[1], Dennis Brown[1], Giovanni Camanni[1], Yih-Min Wu[2], and Hao Kuo-Chen[3]

[1]Institute of Earth Sciences Jaume Almera, ICTJA-CSIC, Lluis Sole i Sabaris s/n, 08028 Barcelona, Spain
[2]Department of Geosciences, National Taiwan University, Taipei, 106, Taiwan
[3]Institute of Geophysics, National Central University, Jhongli, Taiwan

Status of publication: published in "**Tectonics**", (2014), v. 33, no. 7, p. 1322-1339, doi: 10.1002/2014TC003584

Contributions of the Ph.D. student to the article:

- Geological mapping at 1:25.000 and 1:50.000 scale throughout the northern half of the map area;
- Analysis of earthquake hypocentre data (not presented in the final version of the manuscript);
- Analysis of P-wave velocity data

AGU PUBLICATIONS

Tectonics

RESEARCH ARTICLE
10.1002/2014TC003584

Key Points:
- Mapping in Taiwan gives information on fault reactivation at shelf-slope break
- Identify an important, northeast striking lateral structure
- *P* wave model points to the presence of a basement culmination

Correspondence to:
J. Alvarez-Marron,
jalvarez@ictja.csic.es

Citation:
Alvarez-Marron, J., D. Brown, G. Camanni, Y.-M. Wu, and H. Kuo-Chen (2014), Structural complexities in a foreland thrust belt inherited from the shelf-slope transition: Insights from the Alishan area of Taiwan, *Tectonics*, *33*, 1322–1339, doi:10.1002/2014TC003584.

Received 11 MAR 2014
Accepted 23 MAY 2014
Accepted article online 5 JUN 2014
Published online 10 JUL 2014

Structural complexities in a foreland thrust belt inherited from the shelf-slope transition: Insights from the Alishan area of Taiwan

Joaquina Alvarez-Marron[1], Dennis Brown[1], Giovanni Camanni[1], Yih-Min Wu[2], and Hao Kuo-Chen[3]

[1]Institute of Earth Sciences Jaume Almera, ICTJA-CSIC, Barcelona, Spain, [2]Department of Geosciences, National Taiwan University, Taipei, Taiwan, [3]Institute of Geophysics, National Central University, Jhongli, Taiwan

Abstract The Alishan area of Taiwan spans the transition from the platform with full thickness of the Eurasian continental margin in the north to the thinning crust of its slope in the south. This part of the foreland thrust and fold belt includes important along-strike changes in structure, stratigraphy, and seismic velocities. In this paper we present the results of new geological mapping from which we build geological cross sections both across and along the regional structural trend. Fault contour, stratigraphic cutoff, and branch line maps provide 3-D consistency between the cross sections. Minimum shortening is estimated to be ~15 km with displacement overall to the northwest. A *P* wave velocity model helps constrain the structure at depth by providing insight into the possible rock units that are present there. *P* wave velocities of ≥ 5.2 km/s point toward the presence of basement rocks in the shallow subsurface throughout much of the southeastern part of the area, forming a basement culmination. The changes in strike of thrusts and fold axial traces, the changing elevation of thrusts and stratigraphic contacts, and the growing importance of Middle Miocene sediments that take place from north to south are interpreted to be associated with a roughly northeast striking lateral structure coincident with the northern flank of this basement culmination. These transverse structures appear to be associated with the inversion of Eocene- and Miocene-age extensional faults along what was the shelf-slope transition in the Early Oligocene, uplifting the margin sediments and their higher *P* wave velocity basement during Pliocene-Pleistocene thrusting.

1. Introduction

The oblique collision that is taking place in Taiwan between the southeastern part of the continental margin of Eurasia and the leading edge of the intraoceanic Philippine Sea Plate means that the entire profile of the margin, from the full thickness of the crust (platform) in the north to the thinning crust of the slope toward the ocean-continent transition just offshore southern Taiwan, is now involved in the deformation within the foreland thrust and fold belt [e.g., *Teng*, 1990; *Huang et al.*, 1997; *Teng and Lin*, 2004; *Hsu et al.*, 2004; *Lin et al.*, 2003, 2008; *Eakin et al.*, 2014] (Figure 1). This makes Taiwan an ideal laboratory in which to study the importance that the preexisting structural architecture and the different morphological parts of a continental margin have on the early evolution of a foreland thrust and fold belt. The extensional tectonic history of the southeastern margin of Eurasia began with rifting in the Early Eocene and culminated with the development of oceanic crust in the South China Sea by Late Eocene to Early Oligocene times [e.g., *Sibuet and Hsu*, 1997, 2004; *Lin et al.*, 2003; *Li et al.*, 2007]. At this time the shelf-slope break (or necking zone of *Mohn et al.* [2012]) was located just north of its current position [cf. *Teng*, 1987; *Lin et al.*, 2003] (see inset for Figure 1). Rifting resulted in a number of deep, roughly northeast trending basins that were filled with Eocene-age clastic sediments and then unconformably overlain by Oligocene-age sediments [*Teng*, 1992; *Lin et al.*, 2003, 2008; *Teng and Lin*, 2004]. Extension on the outer part of the margin (slope), although minor, was also widespread during the Middle to Late Miocene [*Lin et al.*, 2003; *Ding et al.*, 2008], resulting in the development of a number of extensional basins and changes in the associated Miocene stratigraphy. A number of models have been proposed for how the convergent history between the Eurasian and Philippine Sea plates progressed from intraoceanic subduction in the Miocene to todays arc-continent collision [e.g., *Suppe*, 1984; *Teng*, 1987; *Lee and Lawver*, 1994; *Hall*, 1996, 2001; *Sibuet and Hsu*, 1997, 2004; *Yu et al.*, 1997; *Malavielle et al.*, 2002; *Li et al.*, 2007]. All agree that the Philippine Sea Plate in the vicinity of Taiwan is moving northwestward relative to Eurasia (Figure 1) and that since about the Middle Miocene the subduction zone has advanced westward, causing the leading edge of the Philippine Sea Plate to obliquely override the slope of the continental margin in that direction (see, for example, the GPS data of

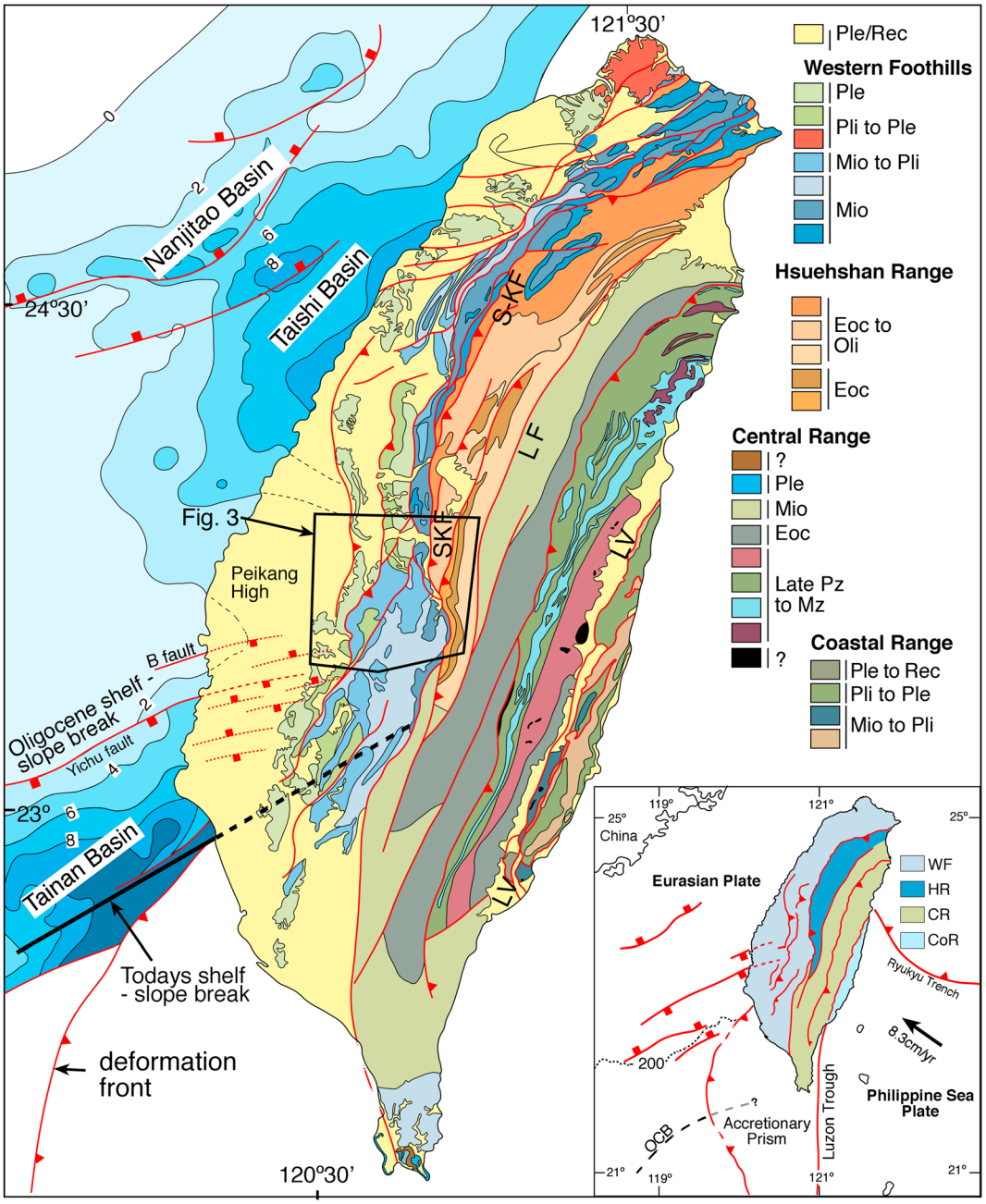

Figure 1. Geological map of Taiwan [after *Chen et al.*, 2000]. Basin locations and structure in the Taiwan Strait is from *Teng and Lin* [2004]. Contours in the offshore basins denote the depth to the top of the Mesozoic basement. The locations of the B and Yichu faults are shown, as are the current shelf-slope break and its estimated location along the southern flank of the Peikang high at the beginning of the Oligocene. The location of Figure 3 is also shown. SKF = Shuilikeng fault, LF = Lishan fault, LV = Longitudinal Valley. The inset shows the tectonostratigraphic units and the tectonic setting discussed in the text (WF = Western Foothills, HR = Hsuehshan Range, CR = Central Range, CoR = Coastal Range). The convergence vector of 8.3 cm/yr between the Philippine Sea Plate and the southeastern part of the Eurasian Plate is also given. OCB = ocean-continent boundary, and the −200 isobath marks the current shelf-slope break. East of the Luzon Trough is the Luzon arc.

Yu et al. [1997] and *Ching et al.* [2011]). In this scenario, the ocean-continent transition, the Early Oligocene and todays shelf-slope break, and the major extensional basins on the slope of the continental margin in the southwest of Taiwan (all oriented approximately N60°E) are nearly perpendicular to the convergence vector but highly oblique to the westward advance of the overriding upper plate [*Lin et al.*, 2003; *Hsu et al.*, 2004; *Yeh and Hsu*, 2004; *Yu et al.*, 1997; *Yu*, 2004; *Li et al.*, 2007; *Ching et al.*, 2011] (Figure 1).

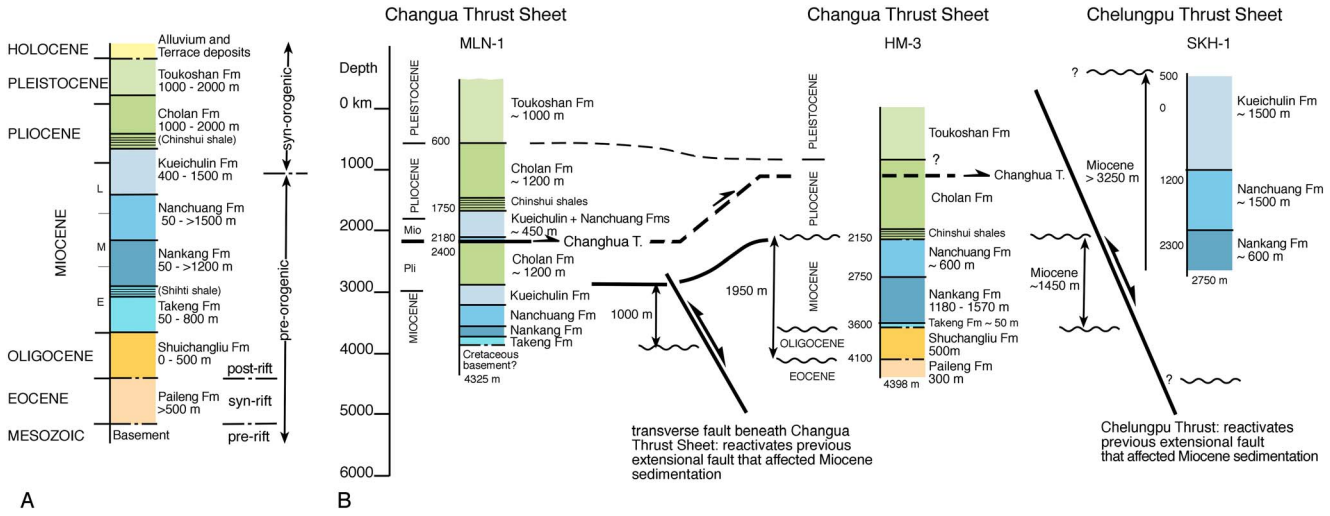

Figure 2. (a) Simplified stratigraphic column showing the formation names discussed in the text. (b) Stratigraphic columns of boreholes MLN-1, HM-3, and SKH-1 (taken from *Chiu* [1975] and *Yang et al.* [2007]) with an interpretation of the relationships between them. The interpreted location of the Changhua thrust in HM-3 is shown.

The Early Oligocene change from platform to slope in the southeast Eurasian margin took place across the Alishan area (Figure 1). This makes the Alishan area of particular interest for the study of how inherited structural and sedimentological features of the continental margin are influencing the development of this part of the foreland thrust and fold belt. With this aim, and also to further the understanding of this important area in the geology of Taiwan, we present the results of new geological mapping and geological cross sections that we integrate with available borehole data, and a *P* wave (*Vp*) velocity model. The 3-D interpretation obtained for the structure of the Alishan area provides insights on the role that inherited continental margin features play during the development of thrust systems. For the sake of clarity, throughout the paper, a distinction is made between the Alishan area (shown by the box in Figure 1) and the topographic feature of the Alishan Ranges.

2. Geological Background

2.1. Tectonostratigraphic Zones of Taiwan

The Taiwan orogen can be divided into four roughly N-S oriented tectonostratigraphic zones (Figure 1). These zones are separated by major faults and comprise parts of the continental margin and the colliding volcanic arc [*Teng*, 1992; *Huang et al.*, 1997; *Lin et al.*, 2003; *Sibuet and Hsu*, 1997, 2004]. From west to east these zones are the Western Foothills, the Hsuehshan Range, the Central Range, and the Coastal Range. The Western Foothills, Hsuehshan Range, and Central Range are formed as the result of shortening and uplift of the continental margin of Eurasia [*Suppe*, 1980; *Yue et al.*, 2005; *Mouthereau et al.*, 2001]. The Coastal Range is composed of volcanic rocks and sedimentary basins of the Luzon arc, which is accreting obliquely and end-on to the Eurasian margin along the Longitudinal Valley fault [*Yu and Kuo*, 2001; *Chen et al.*, 2007; *Shyu et al.*, 2008]. In this paper we focus on the Alishan area, part of the Western Foothills in what is geographically known as central Taiwan (Figure 1).

2.2. Stratigraphy

The stratigraphy of the Alishan area determined from outcrop and borehole data comprises Mesozoic to recent sediments (Figure 2a). The Mesozoic rocks are predominantly Cretaceous (with minor Jurassic) prerift clastic sediments of the Eurasian margin basement of southeast China [*Chiu*, 1975; *Ho*, 1988; *Jahn et al.*, 1992]. Above this basement there are Eocene synrift clastic sediments that are unconformably overlain by Early to Late Oligocene clastics [*Chiu*, 1975; *Ho*, 1988; *Teng*, 1992; *Shaw*, 1996; *Lin et al.*, 2003; *Teng and Lin*, 2004]. The Early Oligocene unconformity is interpreted to represent the rift-to-drift transition (or breakup unconformity) in the margin and its subsequent thermal subsidence during the opening of the South China Sea [*Teng*, 1992; *Huang et al.*, 1997, 2001; *Lin et al.*, 2003; *Teng and Lin*, 2004]. Oligocene rocks are not present everywhere [*Chiu*, 1975; *Shaw*, 1996; *Lin et al.*, 2003]. Where present they are conformably overlain by Neogene clastics, and where they are not present, the Neogene may unconformably overlie either the Eocene or the Mesozoic [*Lin et al.*, 2003, 2008]. The

Miocene largely comprises preorogenic shallow water sediments deposited along a delta front within several systems of Miocene-age rift basins [*Ho*, 1988; *Lin et al.*, 2003]. The Late Miocene through Holocene rocks make up the synorogenic sediments to the Taiwan orogen. Thickness changes on the order of several hundreds to greater than 1000 m are common in all of the preorogenic sequences [e.g., *Chiu*, 1975; *Ho*, 1988; *Shaw*, 1996], both across thrusts and within a single thrust sheet [*Yang et al.*, 2007; *Tensi et al.*, 2006; *Rodriguez-Roa and Wiltschko*, 2010]. For example, the Miocene sequences increase in thickness from ~1000 m in borehole MLN-1 to ~1500 m in borehole HM-3, and more than 2750 m in borehole SKH-1 (Figure 2b). Our mapping suggests that these changes are in part due to structural repetitions within individual formations (see below).

The nomenclature used for the various stratigraphic units throughout the Western Foothills is variable (for an overview of this problem, see *Yang et al.* [2007], *Tensi et al.* [2006], and *Rodriguez-Roa and Wiltschko* [2010]). Therefore, in this work we have adopted the nomenclature shown in Figure 2a. It maintains continuity with that used in our previous mapping to the north of Alishan [*Brown et al.*, 2012; *Camanni et al.*, 2014], which is based on the stratigraphic sequence presented in the Central Geological Survey 1:50,000 scale map 32 (Puli) [*Huang et al.*, 2000]. The only difference here is that we have changed the name Shihmen Formation to Nankang Formation, which is the more generally used name in this area. The ages are consistent with correlations done by *Shea et al.* [2003] and *Tensi et al.* [2006].

Cretaceous rocks do not outcrop in the study area, but have been reported from several boreholes in western Taiwan [*Chiu*, 1975; *Jahn et al.*, 1992]. Their thickness is unknown. About 300 m of Eocene rocks have been intersected in borehole HM-3 (Figure 2b), although their base was not reached [*Chiu*, 1975; *Shaw*, 1996]. In our cross-section interpretations, the thickness of the Eocene ranges from 500 to $>$ 1000 m and it is called the Paileng Formation. Oligocene rocks do not crop out in the study area, but they have also been intersected in borehole HM-3 (Figure 2b) where they are up to ~500 m thick [*Chiu*, 1975]. We therefore use this as the maximum thickness for the Oligocene, letting it thin and disappear eastward where the Miocene directly overlies the Eocene. We call the Oligocene rocks the Shuichangliu Formation.

The Miocene rocks are divided into four formations (Figure 2a) that, from bottom to top, are the Early Miocene Takeng Formation, the Early to Middle Miocene Nankang Formation (part of it corresponds with the Shihmen Formation), the Middle to Late Miocene Nanchuang Formation, and the Late Miocene to Early Pliocene Kueichulin Formation. The Takeng Formation only outcrops in the NE part of the map area, in the core of the Takeng anticline, where it is approximately 500 to 800 m thick, although the base is not seen. The Nankang Formation outcrops along much of the eastern part of our map area, where it comprises predominantly highly folded and faulted Shihti shale (the basal part on Nankang), hampering a determination of the stratigraphic thickness. Borehole SHK-1 intersected about 600 m of Nankang Formation without reaching its base (Figure 2b). The Nanchuang Formation outcrops throughout the map area, although several kilometers to the north it is absent within the Miocene sequence. In many areas it is intensely folded and faulted making it difficult to estimate its thickness. In the eastern part of our map area, along the southern part of the Chenyulan River (Figure 3), the Nanchuang Formation is approximately 800 m thick, whereas in the west, along the Cingshui River, we have mapped a little over 1000 m of it. Borehole SHK-1 (Figure 3) intersects ~1500 m of Nanchuang but does not mention folding. The latest Miocene to Early Pliocene Kueichulin Formation has very significant changes in thickness in the map area, ranging from about 2000 m thick in the hanging wall of the Chelungpu thrust to ~500 m thick in the Lukushan syncline (Figure 3). The SHK-1 borehole intersected ~1500 m of Kueichulin Formation (Figure 2b).

There is some uncertainty as to whether or not the Kueichulin Formation is the first synorogenic sedimentary unit to appear in the foreland basin of the Taiwan mountain belt. *Yu and Chou* [2001]; *Lin and Watts* [2002], and *Lin et al.* [2003] argue on the basis of geometric relationships observed between the Nanchuang and the Kueichulin Formations in reflection seismic data that there is an angular unconformity between the two that marks the onset of synorogenic sedimentary deposition in the foreland basin. *Teng* [1987]; *Covey* [1986], and *Hong* [1997] suggest, however, that the first appearance of slate clasts derived from the rising Taiwan mountain belt to the east is in the Pliocene Chinshui shale, and that these are the first synorogenic sediments. We place the onset of synorogenic sedimentation within the Kueichulin Formation (Figure 2a).

The Chinshui shale comprises a several hundred meter thick unit at the base of the Pliocene to Pleistocene Cholan Formation. The Cholan Formation comprises up to 2500 m of interbedded mudstone, shale, and sandstone. To the north of the Choshui River (and within the map area), the contact between the Cholan and the

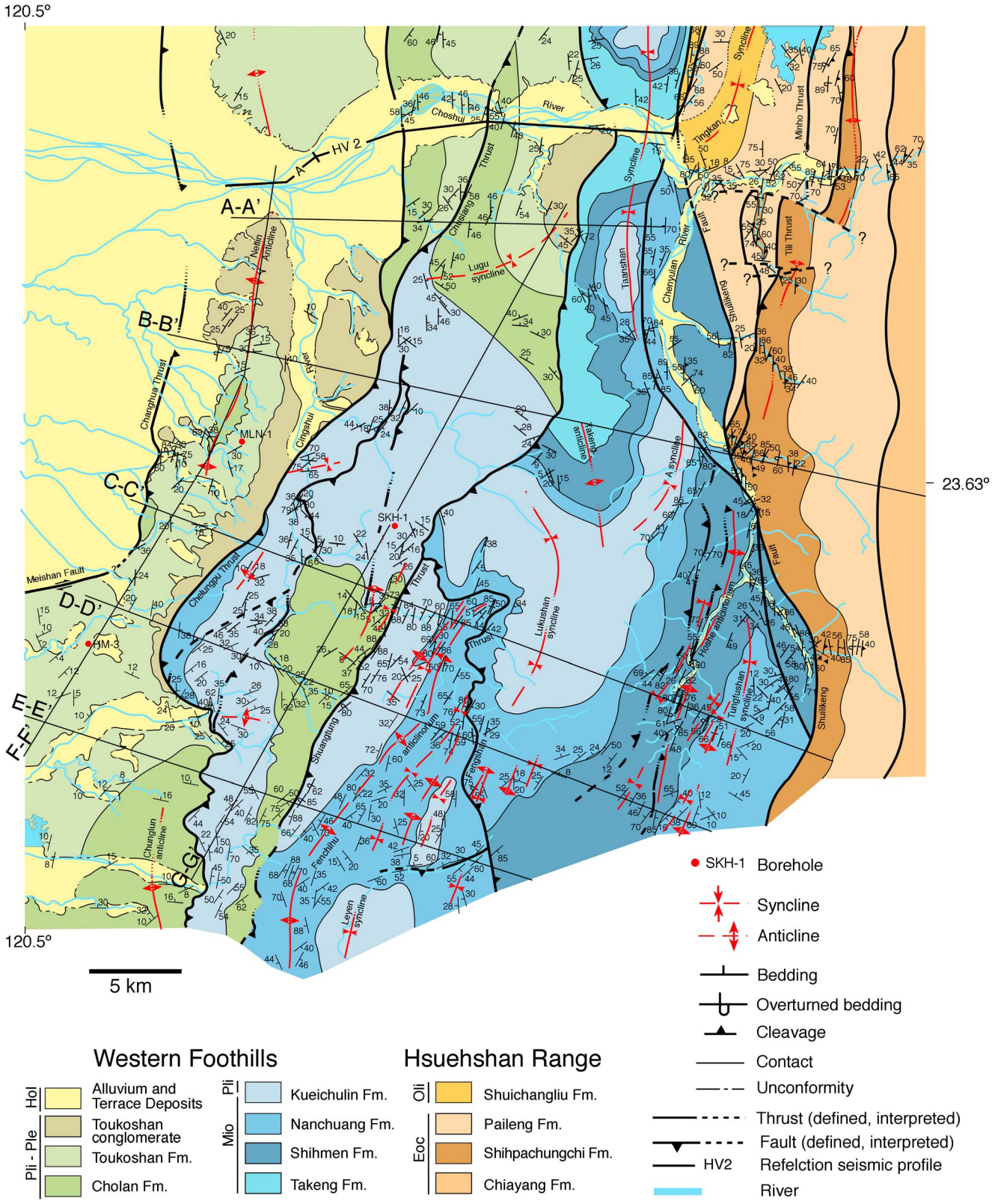

Figure 3. Geological map of the Alishan area. Section A is from *Brown et al.* [2012]. The locations of the geological sections shown in Figures 4 and 5 are shown. Sections A to E also correspond to the locations of the vertical *P* wave velocity sections shown in Figure 8. The names of individual structures discussed in the text are also provided. The locations of reflection seismic lines A and HV 2 from *Wang et al.* [2002] are given.

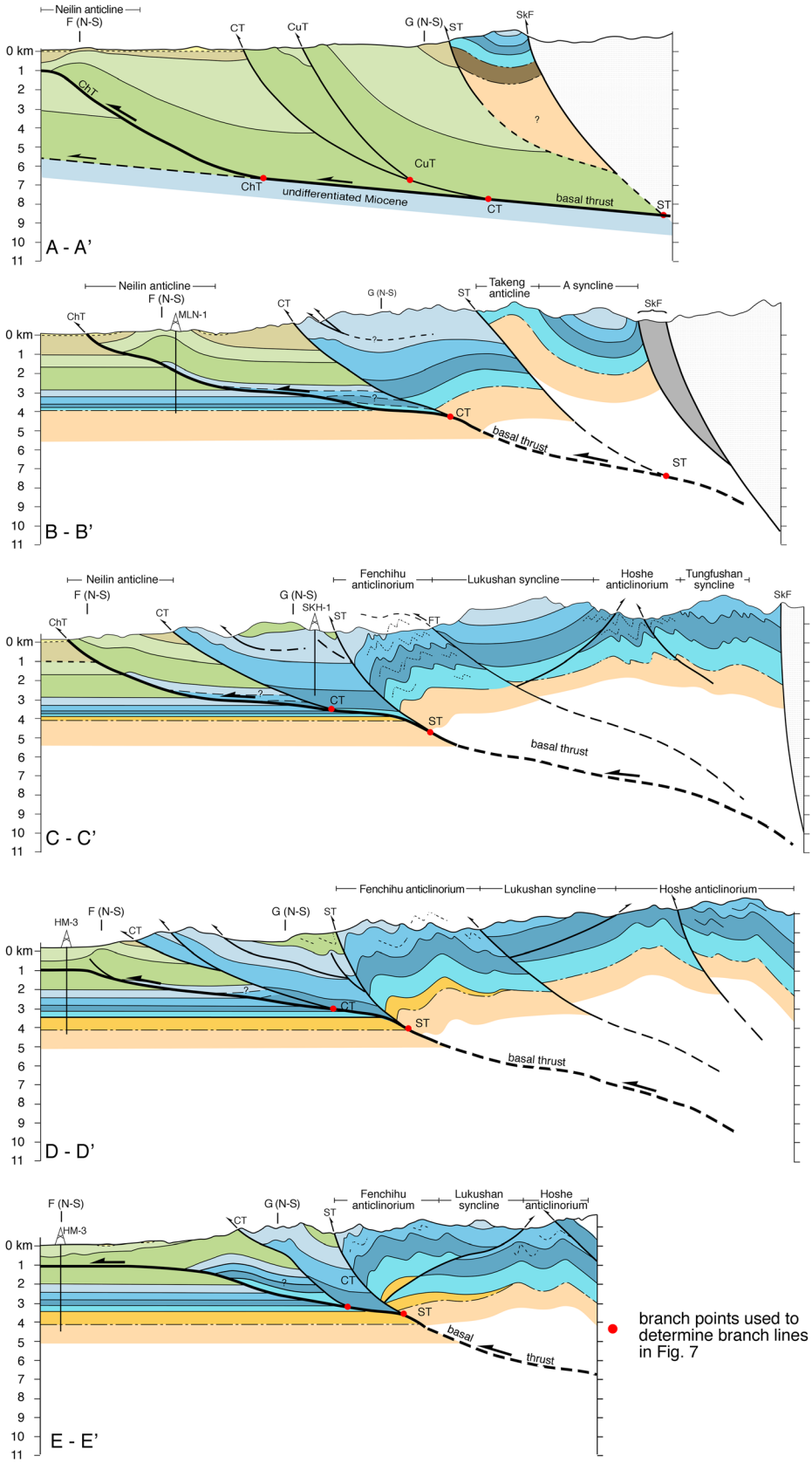

Figure 4

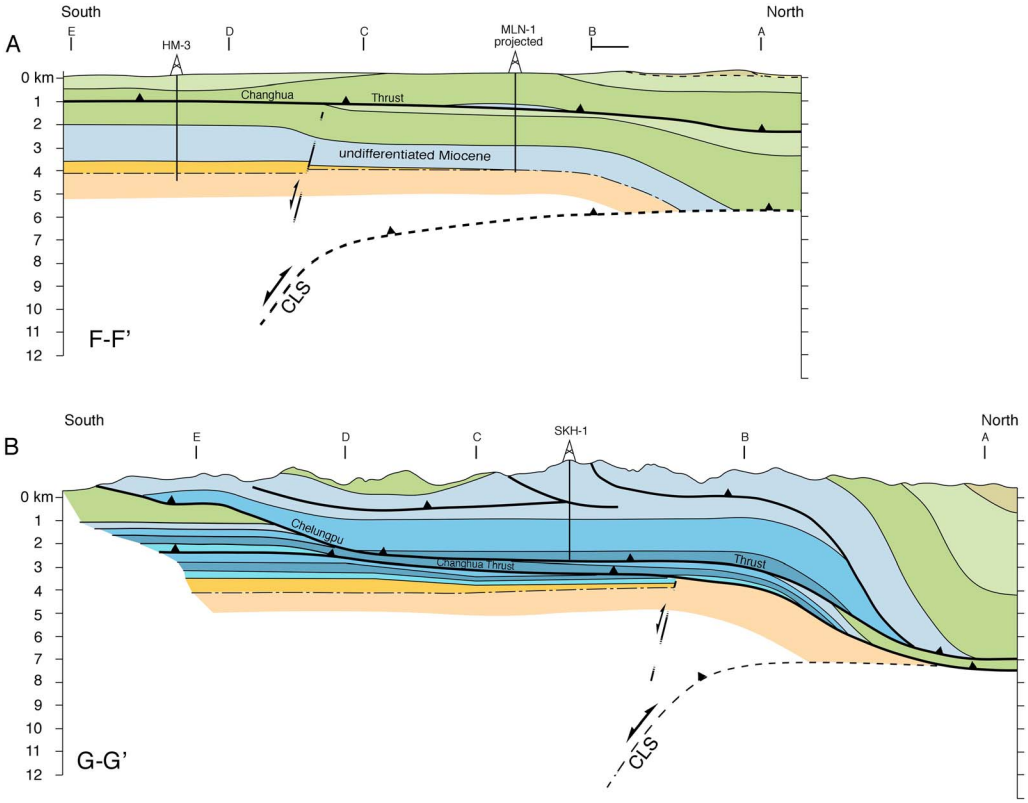

Figure 5. Roughly along strike geological sections F-F′ and G-G′ (see Figure 3 for location) through (a) the Changhua and (b) the Chelungpu thrust sheets. The projected location of the boreholes is shown. Note the shallowing in elevation of thrust surfaces and stratigraphic contacts toward the south, between sections A and B. A transverse fault beneath the Changhua thrust in F-F′ corresponds to that mentioned in Figure 2. CLS = Choshui lateral structure.

Kueichulin formations is not exposed but is thought to be tectonic [e.g., *Yue et al.*, 2005; *Yang et al.*, 2007; *Rodriguez-Roa and Wiltschko*, 2010], whereas to the south it is a conformable sedimentary contact [e.g., *Nagel et al.*, 2013] (see also section 3 below). The Cholan Formation is conformably overlain by the Pleistocene Toukoshan Formation, a coarsening upward sequence made up of thick-bedded sandstone with shale interbeds that, upward, becomes interfingered with, and eventually completely replaced by conglomerate. The Toukoshan Formation can reach up to 4000 m in thickness. To the south of the Alishan area (and out of our map area), the Toukoshan Formation conglomerate disappears as the Pleistocene in that area was deposited in a marine environment that was typically nearshore to foreshore [*Covey*, 1984; *Chen et al.*, 2001; *Nagel et al.*, 2013]. The Toukoshan Formation is overlain by Holocene-age gravels that, in places, are several hundred meters thick.

3. Structure of the Alishan Area

3.1. Methodology

A number of authors [e.g., *Yang et al.*, 2006, 2007; *Mouthereau and Lacombe*, 2006; *Rodriguez-Roa and Wiltschko*, 2010; *Tsai et al.*, 2012] have investigated the structure of parts of the Alishan area, generally presenting cross sections that are largely based on the 1:100,000 geological map [*Chinese Petroleum Company* (*CPC*), 1986], borehole, and reflection seismic data of the Chinese Petroleum Company (CPC). In this study, new geological field mapping was carried out at a 1:50,000 scale over most of the Alishan area; the easternmost part was mapped at 1:25,000 scale [*Camanni et al.*, 2014]. Where available, the 1:50,000 scale

Figure 4. Geological cross sections through the Alishan area. Their locations are shown in Figure 3. The projected locations of the boreholes are shown. The names of individual structures discussed in the text are also provided. The branch points used to construct the maps in Figure 6 are also given. ChT = Changhua thrust, CT = Chelungpu thrust, ST = Shuangtung thrust, FT = Fengshan thrust, and SkF = Shuilikeng fault.

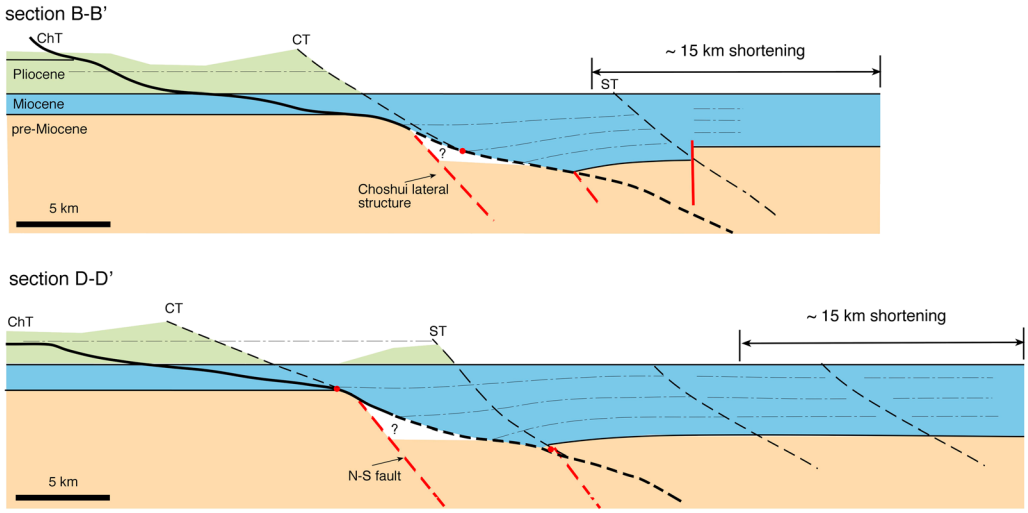

Figure 6. Restored sections B-B′ and D-D′. Both sections have been restored using only the Pliocene, Miocene, and pre-Miocene sedimentary packages while conserving the area and line length. In the restoration it is assumed that the top of the Kueichulin is horizontal. Vertical and horizontal scales are the same. The estimated minimum shortening is 15 km. Fault abbreviations are as in Figure 4. See.

geological maps of the Central Geological Survey and the CPC 1:100,000 scale map [*CPC*, 1986] were used as reference maps. The geological map (Figure 3), structural data, and cross sections presented below are, however, our own. The stratigraphic scheme used in the mapping (Figure 2a) is based on a number of sources [e.g., *CPC*, 1986; *Huang et al.*, 2000; *Chiu*, 1975; *Ho*, 1988] and our own observations. In the description of the structure that follows, the map area is divided into the Changhua, Chelungpu, and Shuangtung thrust sheets forming a linked thrust system. Cross sections have been constructed in several orientations in order to better illustrate the 3-D variation of the structures (Figures 4 and 5). The cross sections were constructed using standard techniques in which the location of faults in the shallow subsurface (~5 km) is determined using the geometric controls provided by the observed outcropping and borehole stratigraphic contacts and the bedding dips [e.g., *Dahlstrom*, 1969; *Hossack*, 1979]. Boreholes HM-3, MLN-1, and SKH-1 provide further constraints on the frontal part of some cross sections, in the Changhua and Chelungpu thrust sheets. Two of the sections have been line length and area balanced, and restored (Figure 6). We stress, however, that errors may have been introduced into the cross sections because of the uncertainties in the stratigraphic thicknesses [e.g., *Judge and Allmendinger*, 2011; *Allmendinger and Judge*, 2013]. Therefore, fault contour and branch line maps with hanging wall and footwall stratigraphic cutoff lines are used to maintain consistency between all sections (Figure 7). These maps, together with the two restored sections, provide minimum estimates of shortening and displacement directions.

3.2. The Changhua Thrust Sheet

The Changhua thrust sheet is bound to the west by the Changhua thrust and to the east by the Chelungpu thrust. In the southernmost part of the map area the Changhua thrust interacts in some indeterminate way with the Meishan fault (Figure 3). In our interpretation the Meishan fault acts as a lateral tear fault to the Changhua thrust. Some map interpretations [e.g., *CPC*, 1986; *Liu et al.*, 2004; *Mouthereau and Lacombe*, 2006; *Yang et al.*, 2007; *Rodriguez-Roa and Wiltschko*, 2010] extend the Changhua thrust (with a different name) farther southward, but we have not found any evidence for this in our surface mapping. Although we interpret the buried Changhua thrust to be at ~1000 m depth in borehole HM-3 (Figures 2 and 4). In the northern part of the map area it is also buried, but has been imaged by reflection seismic data along the Choshui River (Figure 3) and intersected in borehole MLN-1 (Figure 2) [*Wang et al.*, 2002]. Only two outcrops of the Changhua thrust were found during our mapping; both in the central part of the map area where it places Toukoshan Formation sandstones on top of Holocene gravels. The Neilin anticline, in the hanging wall of the Changhua thrust, plunges between 5° and 25° both northward and southward. It is cored by rocks of the Cholan Formation and locally has a steep to overturned forelimb and a gently dipping backlimb. Northward, it plunges beneath the Holocene gravels along the Choshui River (Figure 3).

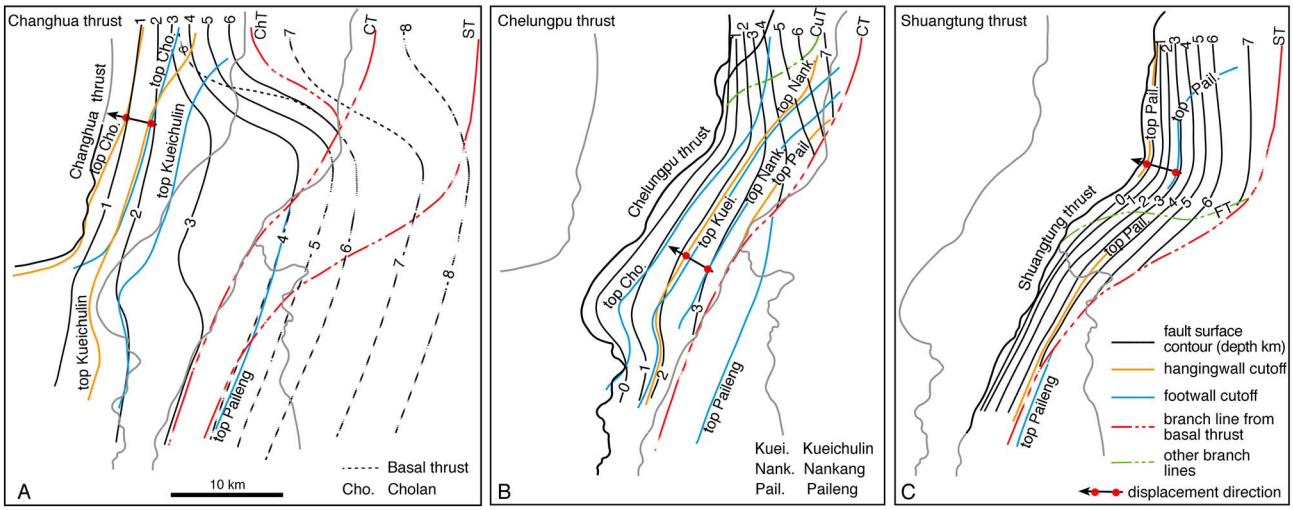

Figure 7. Maps of (a) the contours of the basal thrust surface with the branch lines of the Changhua, Chelungpu, and Shuangtung thrusts. Various hanging wall and footwall stratigraphic cutoffs in the Changhua thrust sheet. The contours for the Changhua thrust are shown as solid lines beginning at the branch line. The displacement direction of the Changhua thrust is shown by the arrow. (b) Contours of the Chelungpu thrust, its branch line from the basal thrust, and various hanging wall and footwall stratigraphic cutoffs. The branch line of the Chusiang thrust is also shown. The displacement direction of the Chelungpu thrust is shown by the arrow. (c) Contours of the Shuangtung thrust and its branch line from the basal thrust. The displacement direction of the Shuangtung thrust is shown by the arrow. The branch line of the Fengshan thrust is also shown. A general displacement direction of about N70°W can be determined from these reconstructions. Thrust abbreviations are the same as those in Figure 4. Numbers represent depth of contour in km.

Southward, the Neilin anticline disappears and immediately below the Chelungpu thrust there is an area with widely dispersed, shallow bedding dips that form the open Chunglun anticline (Figure 3).

We could not find outcrops of the Meishan fault, although there is a topographic expression left from the 1906 7.1 M_L Meishan earthquake. Based on fault plane solutions of recent earthquakes the Meishan fault is interpreted to be a dextral strike slip fault [e.g., *Wu et al.*, 2010], which is in keeping with different map interpretations in the area [*CPC*, 1986; *Liu et al.*, 2004]. The Meishan fault appears to form part of the eastern extension of the B and Yichu faults (Figure 1) and is interpreted to be so in what follows.

In the cross sections shown in Figure 4, the Changhua thrust is the frontal expression of the basal thrust, extending from the branch points of the Chelungpu thrust to the surface, except in section A-A′ where it ramps from the basal thrust. The Changhua thrust has been interpreted to be predominately within the synorogenic sediments (Figures 4 and 5) before ramping gently down into the Miocene formations toward the east and south (except in section A-A′). There is a significant change in depth of the Changhua thrust along strike, from ~7 km deep in the north to about 3 km in the south (compare the branch points of Chelungpu thrust (CT) between sections A-A′ and E-E′ in Figure 4, as well as section G-G′ in Figure 5b), as it climbs progressively up the stratigraphic section in its footwall. The hanging wall and footwall cutoff maps (Figure 7a) of the top Cholan and Kueichulin Formations indicate that the displacement along the Changhua thrust was overall toward the west-northwest. By restoring these cutoffs along the displacement direction the horizontal displacement of the Changhua thrust is estimated to be approximately 5 km in section A-A′ and lessening southward to about 2.5 km (Figure 6). Note that in cross sections A-A′, D-D′, and E-E′, the tip line is buried by the synorogenic sediments, as shown in the seismic line farther north [*Wang et al.*, 2002] (Figure 3). Our interpretation of the shallowing of the Changhua thrust southward from the Choshui River is in agreement with other cross sections through the area [e.g., *Mouthereau and Lacombe*, 2006; *Yang et al.*, 2007; *Rodriguez-Roa and Wiltschko*, 2010], although our estimations of displacement vary.

3.3. The Chelungpu Thrust Sheet

The Chelungpu thrust sheet is bound to the west by the Chelungpu thrust and to the east by the Shuangtung thrust. It includes the Chusiang thrust to the north and displays important changes southward. North of the Choshui River it carries only rocks of the Cholan and Toukoshan Formations, whereas southward the Chelungpu thrust merges with the Chusiang thrust and cuts down the stratigraphic section to involve the

Kueichulin and Nanchuang Formations (Figure 3). The hanging wall of the Chusiang thrust comprises the northeast plunging Lugu syncline. Immediately southward, the Kueichulin Formation has a number of minor thrusts within it, although it is often not possible to trace these faults for long distances. Nevertheless, they appear to form a thrust system that may significantly thicken the Kueichulin Formation (borehole SHK-1 intersects some 1500 m of Kueichulin Formation in this area). The base of the Cholan Formation in this part of the Chelungpu thrust sheet is at greater than 1400 m above sea level, indicating a large change in elevation of this contact with respect to its depth of ~7 km below sea level along the Choshui River (Figure 5b) [see also, *Yue et al.*, 2005; *Yang et al.*, 2007; *Rodriguez-Roa and Wiltschko*, 2010; *Brown et al.*, 2012].

In cross section, the Chelungpu thrust is interpreted to be at the base of the Cholan Formation in the north (section A-A′), whereas southward it ramps down section to form a flat near the top of the Nanchuang Formation (Figure 4). This interpretation is in keeping with others in this area [e.g., *Yang et al.*, 2007; *Rodriguez-Roa and Wiltschko*, 2010], although some authors interpret it to cut steeply down into the Miocene and older rocks along the Choshui River [e.g., *Yue et al.*, 2005; *Mouthereau and Lacombe*, 2006]. Despite ramping down the stratigraphic section southward, the depth of the Chelungpu thrust and its branch line shallows along strike from ~7 km deep along the Choshui River (section A-A′) to ~3 km farther south (sections D-D′ and E-E′): a roughly 4 km change in elevation (Figure 5b). Hanging wall and footwall stratigraphic cutoffs indicate that the displacement direction was overall northwestward (Figure 7b). The amount of displacement along the Chelungpu thrust is difficult to determine because of the change in stratigraphic thicknesses that take place across it. Nevertheless, we estimate that the horizontal displacement is ~7 km throughout the Alishan area (Figure 6), which is in keeping with other cross-section interpretations in the area [e.g., *Yang et al.*, 2007; *Rodriguez-Roa and Wiltschko*, 2010]. Because of the increase in thickness of the Miocene stratigraphy across the Chelungpu thrust (Figure 2b), we interpret it to have reactivated a previous extensional fault (Figure 6).

3.4. The Shaungtung Thrust Sheet

The Shuangtung thrust sheet is bound to the west by the Shuangtung thrust and to the east by the Shuilikeng fault. The thrust sheet widens significantly from less than 5 km along the Choshui River to ~25 km in the central part of the Alishan Ranges (Figure 3). As it does, the Miocene stratigraphic sequence thickens and the Nanchuang Formation becomes an important stratigraphic unit. The Shuangtung thrust sheet comprises two regional-scale fault panels that are separated by the Fengshan thrust. The eastern part of the Shaungtung thrust sheet is dominated by the Hoshe anticlinorium (and the smaller Tungfushan syncline). The Hoshe anticlinorium comprises a system of northwest verging, variably plunging folds that terminate northward against the Shuilikeng fault [*Camanni et al.*, 2014] and can be traced southward for several kilometers before they are lost in an area without access (Figure 3). A number of mostly northwest verging thrusts (there is one significant exception to this) have been mapped, but their along-strike continuity is difficult to constrain. The Hoshe anticlinorium is flanked to the west by the broad, flat-bottomed Lukushan syncline. Access to much of the area occupied by the Lukushan syncline is restricted, and the area is heavily forested, making field and remote sensing observations difficult. The Lukushan syncline is bound to the west by the Fengshan thrust. The thrust panel below the Fengshan thrust is comprised by the Fenchihu anticlinorium, a system of northwest verging, variably plunging folds developed in the Nanchuang and Kueichulin Formations. The Fengshan thrust appears to be a splay off the Shuangtung thrust, but difficulty in accessing the area in the steep topography where the two merge makes the interpretation of how these two faults interact somewhat uncertain.

In cross section, at the surface the Shuangtung thrust is a steep reverse fault, dipping ~80° (this is well-constrained in sections C-C′, D-D′, and E-E′). The regional-scale structure of the Shaungtung thrust sheet in the Alishan area is that of a dome consisting of two anticlinoria separated by the Lukushan syncline. Pervasive, km-scale folding in the Shuangtung thrust sheet is indicative of significant horizontal shortening. While it is not possible to quantify the shortening because of uncertainties in the stratigraphy, we estimate the horizontal shortening across the Shuangtung thrust to be less than 5 km and the displacement direction is toward the west-northwest (Figures 6 and 7c). Using the stratigraphic template given in Figure 2 there does, however, appear to be an important amount of vertical displacement (see, for example, the elevation of the Takeng Formation in the Takeng anticline). This can be interpreted based on two points. First, in the northern part of the map area the involvement of the Takeng Formation (the base of the Miocene) in the

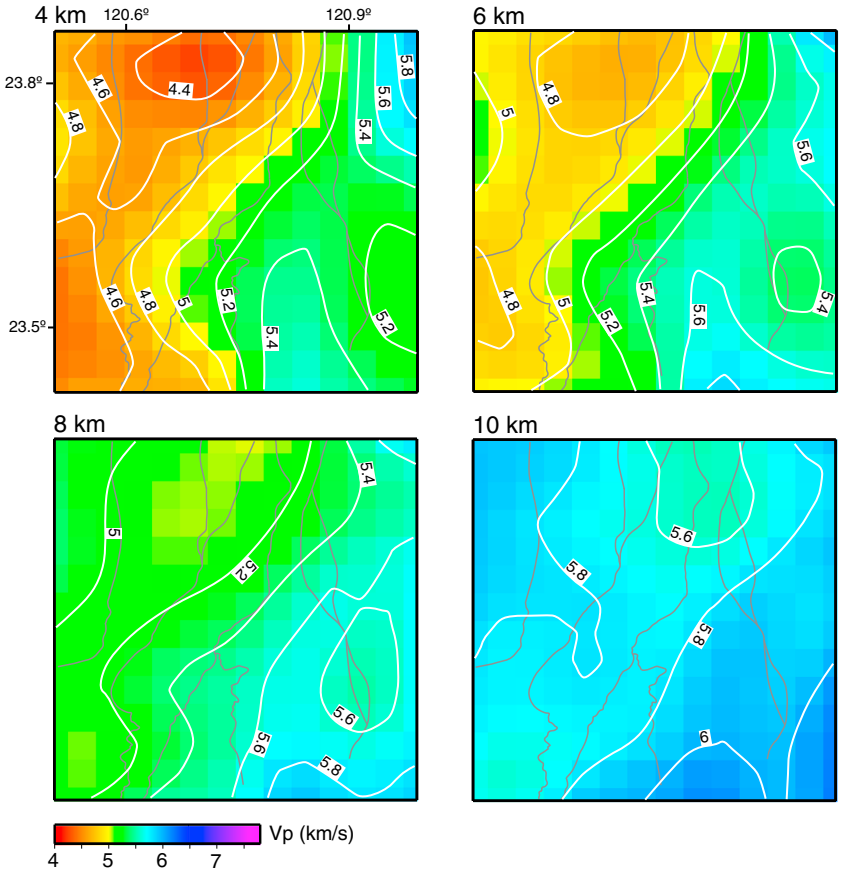

Figure 8. Horizontal cuts at 4, 6, 8, and 10 km depth through the *P* wave velocity model with various isovelocity lines shown.

thrusting indicates that the Shuangtung thrust penetrates to at least this level in the stratigraphy and perhaps deeper. Second, in our interpretation, the branch points of the Shaungtung thrust is interpreted to mark the location in which the basal thrust ramps down eastward into the Eocene synrift and, we think, the basement rocks (Figures 4, 6, and 7) (see section 5). The branch line of the Shuangtung thrust indicates that it changes from southeast to east dipping as it deepens toward the northeast (Figure 7c).

4. Tomography Data

4.1. Methodology

To further constrain the structure at a depth greater than 5 km, especially within and beneath the Shuangtung thrust sheet, we use the *P* wave (*Vp*) velocity model derived from the TAIGER "local" tomography [*Kuo-Chen et al.*, 2012]. The horizontal resolution of the model in the Alishan area is 4 km by 4 km, and the vertical resolution is 2 km. See *Kuo-Chen et al.* [2012] for an overview of the model setup and the data handling. Horizontal slices were cut at various depths through the Alishan area (Figure 8), and vertical sections (Figure 9) were cut along the line of the west-east geological cross sections shown in Figure 4.

4.2. *P* Wave Velocity Model

Within the upper 8 km of the crust in the Alishan area there is a marked change in *Vp* from less than 4.4 km/s in the northwest and west to greater than 5.6 km/s in the southeast (Figure 8). This is outlined by the change in strike of the 4.6 through to 5.4 km/s isovelocity lines from roughly north-south in the north to a northeast-southwest across the Alishan area. This change in strike roughly coincides with similar changes in the strikes of the Chelungpu and Shuangtung thrusts at the surface (shown in gray in Figure 8). The *Vp* model clearly indicates the presence of a shallow velocity high in the southeast part of the area, especially in the area of the Shuangtung thrust sheet. At a depth of 10 km the velocities range between 5.6 and 5.8 km/s, indicating that rocks with similar

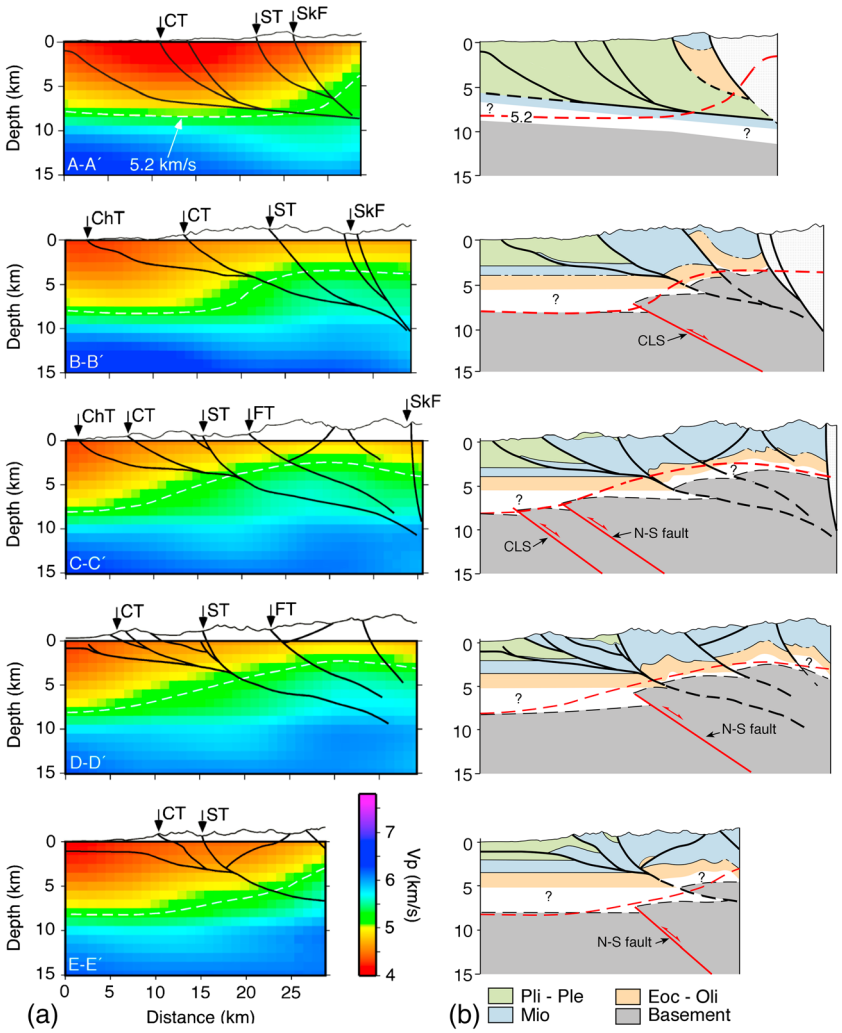

Figure 9. (a) Vertical sections through the *P* wave velocity model with the fault interpretations taken from Figure 3 plotted on them. The locations are shown in Figure 3. The 5.2 km/s isovelocity line is shown. Thrust abbreviations are the same as those in Figure 4. (b) Simplified geological cross sections from Figure 4 with an interpretation of the basement constrained by the *Vp* model. Note that we do not interpret the structure east of the Shuilikeng fault (SkF). CLS = Choshui lateral structure. CLS and the N-S fault are shown in Figure 10.

physical properties are widespread at this depth. We interpret these velocities to image the presence of basement rocks everywhere at this depth within the Alishan area (Figure 9) (also see section 5).

In the vertical sections, low velocities (<4.6 km/s) in the west and northwest correspond to the Miocene and younger sediments (Figure 9). The pronounced west to east shallowing of higher velocities starts beneath the Chelungpu thrust sheet and takes on a dome-shape in the area of the Shuangtung thrust sheet. This is particularly well-illustrated by the 5.2 km/s isovelocity line as it shallows from ~8 km depth in the west to about 3 km depth in the Shuangtung thrust sheet (Figures 4 and 8). We interpret this feature as a shallowing of the basement rocks as it is uplifted by reverse activation of two deep faults, one striking N-E that we name the Choshui lateral structure (CLS) (see Figure 5), and another striking approximately N-S (Figure 9b) (also see section 5).

5. Discussion

The Alishan area of Taiwan provides new data on the importance of the morphological and structural architecture in the early convergent history of a rifted continental margin. It encompasses the shelf-slope break (or necking zone), which is known to be an area of change in the amount of extension, from low β factors on the platform to increasingly higher β factors on the slope and with, commonly, a corresponding

change in fault style from high angle to listric [e.g., *Manatschal*, 2004; *Reston*, 2009; *Reston and Manatschal*, 2011; *Mohn et al.*, 2012]. The structure of the Alishan area presented in this paper shows that the change in basement structure from the platform to the slope, together with changes in the postrift sedimentary carapace all play a significant role early on in the structural history of the thrust belt evolution. In many orogens worldwide, the involvement of the platform or slope in the deformation can be shown to have taken place, but it is not always straightforward from the final rock record exactly how or when this happened [e.g., *Flöttmann and James*, 1997; *Faulds and Varga*, 1998; *Smith*, 1999; *Butler et al.*, 2006; *Zanchi et al.*, 2006; *Yagupsky et al.*, 2008]. This makes the Alishan area of considerable importance in placing more precise constraints on the early stages of development of a thrust belt within the complex structural and sedimentological context that is the shelf-slope break of a continental margin.

The new surface geological data and velocity models presented above confirm that there are significant changes that take place in the structure from north to south across the Alishan area. These observations coincide with interpretations by *Rodriguez-Roa and Wiltschko* [2010], *Yang et al.* [2006, 2007], and *Mouthereau and Lacombe* [2006], but adding more data to, for example, the change in strike and detachment level of the fault and fold systems. The location and geometry of the basal thrust to the east of the branch line with the Chelungpu thrust is not well constrained. But interpolating geometries in 3-D of hanging wall and footwall stratigraphic cutoffs and the fault contours (Figures 4–6) from those of the better constrained Changhua and Chelungpu thrusts to the basal thrust provides the model with consistency. One of the important results of our study is that the estimated minimum shortening across the Alishan area is about 15 km. As stated in section 3.1, we realize that there are uncertainties in this estimation, but they are overall in keeping with the shortening calculated by *Rodriguez-Roa and Wiltschko* [2010]. *Mouthereau and Lacombe* [2006] and *Yang et al.* [2007] do not provide shortening for all of Alishan. Another of the important results is that while the Changhua and Chelungpu thrusts cut down the hanging wall stratigraphic section toward the south, they also display a 4 km shallowing in elevation. This change in elevation is perhaps best visualized by comparing the location of the contact between the Cholan and Kueichulin formations in the southern limb of the Lugu syncline, which shows a ~7 km change in elevation from north to south (Figures 3 and 5b). In their cross sections, *Yang et al.* [2007] also interpret (but do not explicitly say) that there is a shallowing of the Changhua and Chelungpu thrusts southward from the Choshui River to the Alishan area, whereas *Rodriguez-Roa and Wiltschko* [2010] do not interpret this to happen. *Mouthereau and Lacombe* [2006] have both thrusts ramping continuously down section. Finally, while we make certain assumptions about the changes in thickness of sediments of all ages, the appearance of the Nanchuang Formation in the Miocene and its increasing importance southward across the Alishan area is obvious and significant. We interpret the changes in strike of the faults and fold axial traces, the change in elevation of the Changhua and Chelungpu thrusts, the change in elevation of stratigraphic contacts, and the growing importance of the Nanchuang Formation, all of which take place from north to south across the Alishan area, to be associated with a roughly northeast striking feature that we call the Choshui lateral structure (Figure 10).

Many of the structural and stratigraphic changes that we outline above have been attributed to the Alishan area being located along the southern flank of the Peikang High [e.g., *Mouthereau et al.*, 2002; *Cheng et al.*, 2003; *Wu et al.*, 2007; *Byrne et al.*, 2011], which comprises a number of approximately east-northeast trending extensional faults in the footwall to the exposed thrust system. Many of these are buried beneath synorogenic sediments but have been either imaged in reflection seismic data or sampled in boreholes [*Yang et al.*, 1991; *Chen and Yang*, 1996; *Lin et al.*, 2003]. The Meishan fault (Figure 3) is a notable exception to this. In map view, a number of these faults are often grouped and represented by two major faults called the "B" and Yichu faults [e.g., *Chen and Yang*, 1996; *Lin et al.*, 2003] (Figure 1). Most known faults along the southern flank of the Peikang High are thought to be Miocene in age [*Lin et al.*, 2003, 2008; *Ding et al.*, 2008], although Eocene-age extensional faults have also been interpreted to occur in this area [*Lin et al.*, 2003, 2008; *Li et al.*, 2007; *Tang and Zheng*, 2010]. The Peikang High itself is interpreted as an Eocene-age feature with the Taishi and Hsuehshan basins to the north and east, respectively [e.g., *Lin et al.*, 2003]. To the south of it are the shelf-slope break (Alishan), the slope, and finally the ocean-continent transition of the Eurasian margin. We therefore interpret some of the faults affecting the basement along the southern flank of the Peikang High to be Eocene in age, and that this area formed the shelf-slope transition (or necking zone) of the Eurasian margin at the time of continental break up in the Early Oligocene. The present day shelf-slope break is farther south (Figure 3) due to the progradation of the Miocene to recent sediments onto the slope [*Ho*, 1988; *Yu and Lin*, 1991]. Other features, such

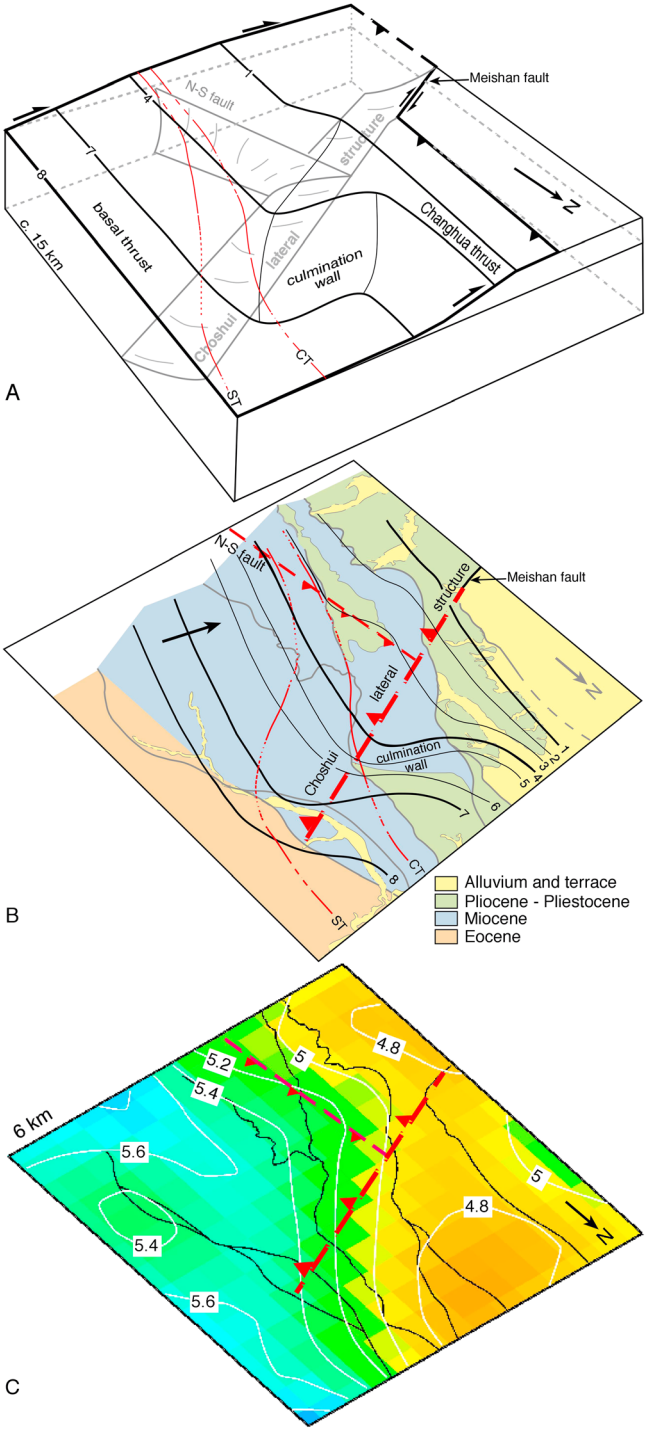

Figure 10. (a) Schematic diagram showing the interpreted 3-D hanging wall and footwall structure to the basal thrust system across the Alishan area. Numbers represent depth of contours in km. The terminology used in the text is explained. Note that the footwall structure is shown in gray, whereas the basal thrust surface is shown by contours in black. The Meishan fault, which is part of the B and Yichu fault system, is interpreted to be related to the Choshui lateral structure. Fault abbreviations are as in Figure 4. (b) Simplified geological map rotated into the same orientation as Figure 10a. The basal thrust contours, the Shuangtung and Chelungpu cut-off lines, the Choshui lateral structure, and the lateral culmination wall are shown. Black arrow indicates the general transport direction of thrusts and is oblique to both the N-S fault and the CLS. Fault abbreviations are as in Figure 4. (c) Horizontal cut at 6 km depth through the *P* wave velocity model with the location of the N-S fault and the CLS. It is rotated into a similar orientation as Figures 10a and 10b.

as the changes in thickness of the Miocene sediments, and the increasing importance of the Nanchuang Formation southward can be attributed to the widespread Middle to Late Miocene-age extension that affected the area [e.g., *Lin et al.*, 2003; *Yang et al.*, 2006; *Rodriguez-Roa and Wiltschko*, 2010]. Changes in thickness of the Miocene stratigraphy across, for example, the Chelungpu thrust indicate that reactivation of the Miocene-age faults is also taking place. This may, in part, account for changes in strike of the various thrusts in the Alishan area. Direct evidence for the reactivation of Eocene-aged extensional faults is difficult to infer from the surface geology alone. The *P* wave velocity model presented in Figures 7 and 8 may, however, provide key insights into this important question.

The *P* wave velocity model indicates that rocks with relatively high velocities are close to the surface beneath the Shuangtung thrust sheet as it widens southward through the Alishan area (Figures 8 and 9). We interpret a *Vp* of ≥ 5.2 km/s to be indicative of the presence of the Mesozoic clastic sedimentary basement rocks intersected in boreholes in western Taiwan [*Chiu*, 1975; *Ho*, 1988; *Shaw*, 1996]. While *Chen and Yang* [1996] and *Tang and Zheng* [2010] give these rocks a slightly lower *Vp* (≤ ~5 km/s), 5.2 km/s is in agreement with laboratory measurements of *Vp* of weakly metamorphosed polymictic clastic sediments (the bulk of the Cretaceous rocks found in boreholes in western Taiwan is arkosic sandstone, slate, and graywacke [*Chiu*, 1975]) at depths of 5 to 10 km [*Christensen*, 1989; *Christensen and Mooney*, 1995]. We suggest, then, that the 5.2 km/s isovelocity line (Figures 8 and 9) marks the approximate location of the contact between the Mesozoic basement and the overlying Eocene rocks. We stress, though, that 5.2 km/s provides only an estimate for the location of the top of the basement, as it is not possible to differentiate between it and the overlying Eocene rocks (of similar composition) on the basis of *Vp*. Nevertheless, if we accept that a *Vp* of 5.2 km/s is near the basement-synrift contact, then basement rocks are at a relatively shallow level in the crust beneath the Shuangtung thrust sheet (Figure 9b). This interpretation is different from that of *Yang et al.* [2007] and *Tsai et al.* [2012] who put large thicknesses of Miocene and younger rocks at depth in the Shunagtung thrust sheet, and more in agreement with *Rodriguez-Roa and Wiltschko* [2010] who put Paleogene and older rocks. As can be seen from Figures 7 and 8, the Miocene and younger rocks have a much lower *Vp* than do the rocks under the Shuangtung thrust sheet, suggesting that they are not present there [see also, *Rau and Wu*, 1995; *Kim et al.*, 2005, 2010; *Wu et al.*, 2007; *Kuo-Chen et al.*, 2012] (Figure 9).

Although we can interpret the uplift of basement rocks in the Shuangtung thrust sheet, this uplift does not account for the change in elevation of the Changhua and Chelungpu thrusts, and the stratigraphic contacts in their hanging walls (Figure 5). We therefore propose that there is reactivation and inversion of a NE striking extensional fault system (i.e., B and Yichu faults in Figure 1) that is resulting in the formation of the NE striking Choshui lateral structure (Figure 10). Inversion of this fault system is resulting in basement rocks (with velocities > 5.2) being uplifted, forming what is structurally termed a basement culmination. In this interpretation, the N-S fault (Figure 10) is a feature that is needed at depth to accommodate the uplift of these basement rocks. The basement culmination is developing in such a way that the Changhua-Chelungpu thrusts are being folded over the culmination wall developed in the hanging wall of the Choshui lateral structure (Figure 10). In this way, the basement culmination accounts for the north-south changes in elevation of structures (including branch lines) and stratigraphic contacts, as well as the change in strike and shallowing of the *Vp* isovelocity lines (which coincide with the change in strike of thrusts and with the southward change in elevation of stratigraphic contacts). The folding of the Changhua-Chelungpu thrusts above the basement culmination suggests that the sequence of thrusting initiated with the emplacement of the Shuantung thrust followed by the Chelungpu thrust, then the Changua thrust and later the development of the basement culmination. Today, all appear to be active at the same time. Based on the amount of uplift that can be determined from the change in elevation of stratigraphic contacts and the faults in our cross sections, we estimate that there is a minimum of 3 km of vertical displacement across this culmination wall (Figure 10a). It appears that there is displacement transferred westward along a deeper detachment level in the region to the south of the culmination wall. It is not possible to determine the horizontal displacement with the current data set.

6. Conclusions

In this paper we have mapped important changes in structure, stratigraphy, and seismic velocities across the Alishan area of Taiwan. Our new geological mapping, together with the geological cross sections, fault contour, stratigraphic cutoff, and branch line maps provide an estimate of a minimum amount of horizontal

shortening of about 15 km. Displacement directions along the Changhua, Chelungpu, and Shuangtung thrusts are, overall, roughly northwest directed. There is a several kilometer change in elevation of the location of the Changhua and Chelungpu thrusts, and stratigraphic contacts as they shallow southward. The *P* wave velocity model shows an increase in *Vp* from northwest to southeast across the area, with a *Vp* of ≥ 5.2 km/s coming to within 3 km of the surface within the Shuangtung thrust sheet. This higher *Vp* is interpreted to indicate the presence of basement rocks in the shallow subsurface throughout much of the southeastern part of the Alishan area.

The change in elevation of the thrust surfaces and stratigraphic contacts, taken together with the presence of higher *Vp* rocks (>5.2 km/s) in the shallow subsurface, suggests that there is a basement culmination forming beneath the Alishan area. This basement culmination can, in part, be explained by the uplift of rocks with these physical properties along the Shuangtung thrust. There are, however, changes in the Changhua and Chelungpu thrust surfaces and stratigraphic contacts in their hanging walls that suggest that there is uplift of rocks beneath the basal thrust that must account for a change of greater than 7 km in elevation of the base of the Cholan Formation. We interpret this to be the result of reactivation of preexisting northeast striking faults that affected the basement, folding the thrust system above it. We furthermore interpret it to be related to the B and Yichu group of faults found in the foreland and possibly their northeast extension into the Western Foothills. In this scenario, the changes in strike and elevation of fault surfaces and stratigraphic contacts that take place from north to south are associated with a feature that we call the Choshui lateral structure, which we interpret to reactivate the northeast striking basement faults (Figure 10).

Acknowledgments

This research was carried out with the aid of grants by CSIC—Proyectos Intramurales 2006 3 01 010 and MICINN: CGL2009-11843-BTE. The TAIGER local tomography data can be found at H. Kuo-Chen's personal web page at Taiwan's National Central University: http://www.cc.ncu.edu.tw/~kuochen/data/taiger_local.xyzv. All structural geological data presented in Figure 3 can be obtained from the lead author. The help and guidance provided by M.-M. Chen, H.-T. Chu, and C.-Y Huang have been invaluable in our work in Taiwan. Reviews by J. Malaveille, T. Bryne, and P. Vannucchi helped clarify a number of points in the manuscript.

References

Allmendinger, R. W., and P. A. Judge (2013), Stratigraphic uncertainty and errors in shortening from balanced sections in the North American Cordillera, *Geol. Soc. Am. Bull.*, *125*, 1569–1579.

Brown, D., J. Alvarez-Marron, M. Schimmel, Y.-M. Wu, and G. Camanni (2012), The structure and kinematics of the central Taiwan mountain belt derived from geological and seismicity data, *Tectonics*, *31*, TC5013, doi:10.1029/2012TC003156.

Butler, R. W. H., E. Tavarnelli, and M. Grasso (2006), Structural inheritance in mountain belts: An Alpine – Apennine perspective, *J. Struct. Geol.*, *28*, 1893–1908.

Byrne, T., Y.-C. Chan, R.-J. Rau, C.-Y. Lu, Y.-H. Lee, and Y.-J. Wang (2011), The arc-continent collision in Taiwan, in *Arc-Continent Collision*, *Front. Earth Sci. Ser.*, edited by D. Brown and P. D. Ryan, pp. 213–245, Springer, Berlin Heidelberg.

Camanni, G., D. Brown, J. Alvarez-Marron, Y.-M. Wu, and H.-A. Chen (2014), The Shuilikeng fault in central Taiwan mountain belt, *J. Geol. Soc.*, *171*, 117–130.

Chen, A. T., and Y.-L. Yang (1996), Lack of compressional overprint on the extensional structure in offshore Tainan and the tectonic implications, *Terr. Atmos. Ocean*, *4*, 505–522.

Chen, C.-H., et al. (2000), Geological Map of Taiwan. 1:500,000 scale, Central Geol. Sur., Taiwan.

Chen, W.-S., K. D. Ridgway, C.-S. Horng, Y.-G. Chen, K.-S. Shea, and M.-G. Yeh (2001), Stratigraphic architecture, magnetostratigraphy, and incised-valley systems of the Pliocene-Pleistocene collisional marine foreland basin of Taiwan, *Geol. Soc. Am. Bull.*, *113*, 1249–1271.

Chen, W.-S., et al. (2007), Late Holocene paleoearthquake activity in the middle part of the Longitudinal Valley Fault, eastern Taiwan, *Earth Planet. Sci. Lett.*, *264*, 420–437.

Cheng, W.-B., H.-C. Huang, C. Wang, M.-S. Wu, and T.-H. Hsiuan (2003), Velocity structure, seismicity, and fault structure in the Peikang High area of western Taiwan, *Terr. Atmos. Ocean*, *14*, 63–83.

Ching, K.-E., R.-J. Rau, K. M. Johnson, J.-C. Lee, and J.-C. Hu (2011), Present-day kinematics of active mountain building in Taiwan from GPS observations during 1995–2005, *J. Geophys. Res.*, *116*, B09405, doi:10.1029/2010JB008058.

Chiu, H.-T. (1975), Miocene stratigraphy and its relation to the Palaeogene rocks in west-central Taiwan, *Pet. Geol. Taiwan*, *12*, 51–80.

Christensen, N. I. (1989), Seismic velocities, in *CRC Practical Handbook of Physical Properties of Rocks and Minerals*, edited by R. S. Carmichael, pp. 429–546, CRC Press, Boca Raton.

Christensen, N. I., and W. D. Mooney (1995), Seismic velocity structure and composition of the continental crust: A global view, *J. Geophys. Res.*, *100*, 9761–9788, doi:10.1029/95JB00259.

Covey, M. (1984), Lithofacies analysis and basin reconstruction, Plio-Pleistocene Western Taiwan foredeep, *Pet. Geol. Taiwan*, *20*, 53–83.

Covey, M. (1986), The evolution of foreland basins to steady state: Evidence from the western Taiwan foreland basin, in *Foreland Basins*, *Int. Assoc. Sedimentol. Spec. Publ.*, vol. 8, edited by P. A. Allen and P. Homewood, pp. 77–90, Blackwell, Oxford, U. K.

Chinese Petroleum Company (CPC) (1986), Geologic Map No. 5, Chiayi. Scale: 1:100000. Taiwan Petroleum, Exploration Division, Chinese Petroleum Company, Taipei, Taiwan.

Dahlstrom, C. D. A. (1969), Balanced cross sections, *Can. J. Earth Sci.*, *6*, 743–757.

Ding, W.-W., J.-B. Li, M.-B. Li, X.-L. Qiu, Y.-X. Fang, and Y. Tang (2008), A Cenozoic tectono-sedimentary model of the Tainan Basin, the South China Sea: Evidence from multi-channel seismic profile, *J. Zhejiang Univ. Sci. A.*, *9*, 702–713.

Eakin, D. H., K. D. McIntosh, H. J. A. van Avendonk, L. Lavier, R. Lester, C.-S. Liu, and C.-S. Lee (2014), Crustal-scale seismic profiles across the Manila subduction zone: The transition from intraoceanic subduction to incipient collision, *J. Geophys. Res. Solid Earth*, *119*, 1–17, doi:10.1002/2013JB010395.

Faulds, J. E., and R. J. Varga (1998), The role of accommodation zones and transfer zones in the regional segmentation of extended terranes, in *Accommodation Zones and Transfer Zones; the Regional Segmentation of the Basin and Range Province*, *Geol. Soc. Am. Spec. Pap.*, *323*, 1–45, doi:10.1130/0-8137-2323-X.1.

Flöttmann, T., and P. James (1997), Influence of basin architecture on the style of inversion and fold-thrust belt tectonics – The southern Adelaide Fold-Thrust Belt, South Australia, *J. Struct. Geol.*, *19*, 1093–1110.
Hall, R. (1996), Reconstructing Cenozoic SE Asia, in *Tectonic Evolution of Southeast Asia*, edited by R. Hall and D. Blundell, *Geol. Soc. London Spec. Publ.*, *106*, 153–184.
Hall, R. (2001), Cenozoic reconstructions of SE Asia and the SW Pacific: Changing patterns of land and sea, in *Faunal and Floral Migrations and Evolution in SE Asia-Australasia*, edited by I. Metcalfe, pp. 35–56, Swets and Zeitlinger, Lisse.
Ho, C.-S. (1988), *An Introduction to the Geology of Taiwan: Explanatory Text of the Geological Map of Taiwan*, Central Geol. Sur, Taipei, Taiwan.
Hong, E. (1997), Evolution of Pliocene to Pleistocene sedimentary environments in an arc-continent collision zone: Evidence from analyses of lithofacies and ichnofacies in the southwestern foothills of Taiwan, *J. Asian Earth Sci.*, *15*, 381–392.
Hossack, J. R. (1979), The use of balanced cross-sections in the calculation of orogenic contraction: A review, *J. Geol. Soc. London*, *136*, 705–711.
Hsu, S.-K., Y.-C. Yeh, W.-B. Doo, and C.-H. Tsai (2004), New bathymetry and magnetic lineations identifications in the northernmost South China Sea and their tectonic implications, *Mar. Geophys. Res.*, *25*, 29–44.
Huang, C.-S., K.-S. Shea, and M.-M. Chen (2000), Geological map of Taiwan: Sheet 32, Puli, Central Geol. Sur. Taiwan.
Huang, C.-Y., W.-Y. Wu, C.-P. Chang, S. Tsao, P.-B. Yuan, C.-W. Lin, and K.-Y. Xia (1997), Tectonic evolution of accretionary prism in the arc-continent collision terrane of Taiwan, *Tectonophysics*, *281*, 31–51.
Huang, C.-Y., K. Xia, P. B. Yuan, and P.-G. Chen (2001), Structural evolution from Paleogene extension to Latest Miocene-Recent arc-continent collision offshore Taiwan: Comparison with on land geology, *J. Asian Earth Sci.*, *19*, 619–639.
Jahn, B.-M., W.-R. Chi, and T.-F. Yui (1992), A Late Permian formation of Taiwan (marbles from Chia-Li well No.1): Pb-Pb isochron and Sr isotopic evidence, and its regional geological significance, *J. Geol. Soc. China*, *35*, 193–218.
Judge, P. A., and R. W. Allmendinger (2011), Assessing uncertainties in balanced cross sections, *J. Struct. Geol.*, *33*, 458–467.
Kim, K.-H., J.-M. Chiu, J. Pujol, K.-C. Chen, B.-S. Huang, Y.-H. Yeh, and P. Shen (2005), Three-dimensional VP and VS structural models associated with the active subduction and collision tectonics in the Taiwan region, *Geophys. J. Int.*, *162*, 204–220.
Kim, K.-H., K.-C. Chen, J.-H. Wang, and J.-M. Chiu (2010), Seismogenic structures of the 1999 Mw 7.6 Chi-Chi, Taiwan, earthquake and its aftershocks, *Tectonophysics*, *489*, 119–127.
Kuo-Chen, H., F. T. Wu, and S. W. Roecker (2012), Three-dimensional P velocity structures of the lithosphere beneath Taiwan from the analysis of TAIGER and related seismic data sets, *J. Geophys. Res.*, *117*, B06306, doi:10.1029/2011JB009108.
Lee, T.-Y., and L. A. Lawver (1994), Cenozoic plate reconstruction of the South China Sea region, *Tectonophysics*, *235*, 149–180.
Li, C.-F., Z. Zhou, J. Li, H. Hao, and J. Geng (2007), Structures of the northeasternmost South China Sea continental margin and ocean basin: Geophysical constraints and tectonic implications, *Mar. Geophys. Res.*, *28*, 59–79.
Lin, A. T.-S., and A. Watts (2002), Origin of the west Taiwan basin by orogenic loading and flexure of a rifted continental margin, *J. Geophys. Res.*, *107*(B9), 2185, doi:10.1029/2001JB000669.
Lin, A., A. Watts, and P. Hesselbo (2003), Cenozoic stratigraphy and subsidence history of the South China Sea margin in the Taiwan region, *Basin Res.*, *15*, 453–478, doi:10.1046/j.1365-2117.2003.00215.x.
Lin, A. T., C.-S. Liu, C.-C. Lin, P. Schnurle, G.-Y. Chen, W.-Z. Liao, L. S. Teng, H.-J. Chuang, and M.-S. Wu (2008), Tectonic features associated with the overriding of an accretionary wedge on top of a rifted continental margin: An example from Taiwan, *Mar. Geol.*, *255*, 186–203.
Liu, H.-C., J.-F. Lee, and C.-C. Chi (2004), Geological map of Taiwan: Sheet 38, Yulin, Central Geol. Sur. Taiwan.
Malavielle, J., S. E. Lallemand, S. Dominguez, A. Deschamps, C.-Y. Lu, C. A. Liu, P. Schnürle, and ACT Scientific Crew (2002), Arc-continent collision in Taiwan: New marine observations and tectonic evolution, in *Geology and Geophysics of an Arc-Continent Collision, Taiwan*, edited by T. B. Byrne and C.-S. Liu, *Geol. Soc. Am. Spec. Pap.*, *358*, 187–211.
Manatschal, G. (2004), New models for the evolution of magma-poor rifted margins based on a review of data and concepts from West Iberia and the Alps, *Int. J. Earth Sci.*, *93*, 432–466.
Mohn, G., G. Manatschal, M. Beltrando, E. Masini, and N. Kusnir (2012), Necking of the continental crust in magma-poor rifted margins: Evidence from fossil Alpine Tethys margins, *Tectonics*, *31*, doi:10.1029/2011TC002961.
Mouthereau, F., and O. Lacombe (2006), Inversion of the Paleogene Chinese continental margin and thick-skinned deformation in the Western Foreland of Taiwan, *J. Struct. Geol.*, *28*, 1977–1993.
Mouthereau, F., O. Lacombe, B. Deffontaines, J. Angelier, and S. Brusset (2001), Deformation history of the southwestern Taiwan foreland thrust belt: Insights from tectono-sedimentary analyses and balanced cross-sections, *Tectonophysics*, *333*, 293–322.
Mouthereau, F., B. Deffontaines, O. Lacombe, and J. Angelier (2002), Variations along the strike of the Taiwan thrust belt: Basement control on structural style, wedge geometry, and kinematics, in *Geology and Geophysics of an Arc-Continent Collision, Taiwan*, edited by T. B. Byrne and C.-S. Liu, *Geol. Soc. Am. Spec. Pap.*, *358*, 31–54.
Nagel, S., S. Castelltort, A. Wetzel, S. D. Willett, F. Mouthereau, and A. T. Lin (2013), Sedimentology and foreland basin paleogeography during Taiwan arc continent collision, *J. Asian Earth Sci.*, *62*, 180–204.
Rau, R.-J., and F. T. Wu (1995), Tomographic imaging of lithospheric structures under Taiwan, *Earth Planet. Sci. Lett.*, *133*, 517–532.
Reston, T. J. (2009), The structure, evolution and symmetry of the magma poor rifted margins of the North and Central Atlantic: A synthesis, *Tectonophysics*, *468*, 6–27.
Reston, T. J., and G. Manatschal (2011), Rifted margins: Building blocks of later collision, in *Arc-Continent Collision*, *Front. Earth Sci. Ser.*, edited by D. Brown and P. D. Ryan, pp. 3–21, Springer, Berlin Heidelberg.
Rodriguez-Roa, F. A., and D. V. Wiltschko (2010), Thrust belt architecture of the central and southern Western Foothills of Taiwan, in *Hydrocarbons in Contractional Belts*, edited by G. P. Goffey et al., *Geol. Soc. London Spec. Publ.*, *348*, 137–168.
Shaw, C.-L. (1996), Stratigraphic correlation and isopach maps of the Western Taiwan Basin, *TAO*, *7*, 333–360.
Shea, K.-S., H.-C. Chang, T.-Y. Huang, H.-C. Ho, W.-H. Lin, C.-W. Lin, and H.-W. Chen (2003), *Geological Column in Taiwan*, Central Geological Survey of Taiwan, Taiwan.
Shyu, J. B. H., K. Sieh, Y.-G. Chen, R.-Y. Chuang, Y. Wang, and L.-H. Chung (2008), Geomorphology of the southernmost Longitudinal Vally Fault: Implications for evolution of the active suture of eastern Taiwan, *Tectonics*, *27*, TC1019, doi:10.1029/2006TC002060.
Sibuet, J. C., and S.-K. Hsu (1997), Geodynamic of the Taiwan arc-continent collision, *Tectonophysics*, *274*, 221–252.
Sibuet, J. C., and S.-K. Hsu (2004), How was Taiwan created?, *Tectonophysics*, *379*, 159–181.
Smith, N. T. (1999), Variscan inversion within the Cheshire Basin, England: Carboniferous evolution north of the Variscan Front, *Tectonophysics*, *309*, 211–225.
Suppe, J. (1980), A retrodeformable cross section of northern Taiwan, *Proc. Geol. Soc. China*, *23*, 46–55.
Suppe, J. (1984), Kinematics of arc-continent collision, flipping of subduction, and back-arc spreading near Taiwan, *Mem. Geol. Soc. China*, *6*, 21–33.

Tang, Q., and C. Zheng (2010), Seismic velocity structure and improved seismic image of the Southern Depression of the Tainan Basin from pre-stack depth migration, *Terr. Atmos. Ocean. Sci.*, *21*, 807–816.
Teng, L. S. (1987), Stratigraphic records of the Late Cenozoic Penglai Orogeny of Taiwan, *Acta Geol. Taiwanica*, *25*, 205–224.
Teng, L.-S. (1990), Geotectonic evolution of the late Cenozoic arc-continent collision in Taiwan, *Tectonophysics*, *183*, 57–76.
Teng, L.-S. (1992), Geotectonic evolution of Tertiary continental margin basins of Taiwan, *Pet. Geol. Taiwan*, *27*, 1–19.
Teng, L.-S., and A.-T. Lin (2004), Cenozoic tectonics of the China continental margin; Insights from Taiwan, in *Aspects of the Tectonic Evolution of China*, edited by J. Malpas et al., *Geol. Soc. London Spec. Publ.*, *226*, 313–332.
Tensi, J., F. Mouthereau, and O. Lacombe (2006), Lithospheric bulge in the West Tainan Basin, *Basin Res.*, *18*, 277–299.
Tsai, M.-C., S.-B. Yu, Y.-J. Hsu, H.-Y. Chen, and H.-W. Chen (2012), Interseismic crustal deformation of frontal thrust fault system in the Chiayi-Tainan area, Taiwan, *Tectonophysics*, *554-557*, 169–184.
Wang, C.-Y., C.-L. Li, F.-C. Su, M.-T. Leu, M.-S. Wu, S.-H. Lai, and C.-C. Chern (2002), Structural mapping of the 1999 Chi-Chi earthquake fault, Taiwan, by seismic reflection methods, *Terr. Atmos. Ocean. Sci.*, *13*, 211–226.
Wu, Y.-M., C.-H. Chang, L. Zhao, J. B. H. Shyu, Y.-G. Chen, K. Sieh, and J. P. Avouac (2007), Seismic tomography of Taiwan: Improved constraints from a dense network of strong motion stations, *J. Geophys. Res.*, *112*, B08312, doi:10.1029/2007JB004983.
Wu, Y.-M., Y.-J. Hsu, C.-H. Chang, L.-S. Teng, and M. Nakamura (2010), Temporal and spatial variation of stress field in Taiwan from 1991 to 2007: Insights from comprehensive first motion focal mechanism catalog, *Earth Planet. Sci. Lett.*, *298*, 306–316, doi:10.1016/j.epsl.2010.07.047.
Yagupsky, D. L., E. O. Cristallini, J. Fantín, G. Z. Valcarce, G. Bottesi, and R. Varadé (2008), Oblique half-graben inversion of the Mesozoic Neuquén Rift in the Malargüe Fold and Thrust Belt, Mendoza, Argentina: New insights from analogue models, *J. Struct. Geol.*, *30*, 839–853.
Yang, K.-M., H.-H. Ting, and J. Yuan (1991), Structural styles and tectonic modes of Neogene extensional tectonics in southwestern Taiwan: Implication for hydrocarbon exploration, *Pet. Geol. Taiwan*, *26*, 1–31.
Yang, K.-M., S.-T. Huang, J.-C. Wu, H.-H. Ting, and W.-W. Mei (2006), Review and insights on foreland tectonics in western Taiwan, *Int. Geol. Rev.*, *48*, 910–941.
Yang, K.-M., S.-T. Huang, J.-C. Wu, H.-H. Ting, W.-W. Mei, M. Lee, H.-H. Hsu, and C.-J. Lee (2007), 3D geometry of the Chelungpu thrust system in Central Taiwan: Its implications for active tectonics, *Terr. Atmos. Ocean. Sci.*, *18*, 143–181.
Yeh, Y.-C., and S.-K. Hsu (2004), Crustal structure of the northernmost South China Sea: Seismic reflection and gravity modeling, *Mar. Geophys. Res.*, *25*, 45–61.
Yu, H.-S. (2004), Nature and distribution of the deformation front in the Luzon arc-Chinese continental margin collision zone at Taiwan, *Mar. Geophys. Res.*, *25*, 109–122.
Yu, H.-S., and Y.-W. Chou (2001), Characteristics and development of the flexural forebulge and basal unconformity of western Taiwan foreland basin, *Tectonophysics*, *333*, 277–291.
Yu, H.-S., and S.-J. Lin (1991), A preliminary study of seismic stratigraphy of the Late Cenozoic sequences in the Tainan Basin off southwestern Taiwan, *Terr. Atmos. Ocean. Sci.*, *2*, 75–94.
Yu, S.-B., and L. C. Kuo (2001), Present day crustal motion along the Longitudinal Valley Fault, eastern Taiwan, *Tectonophysics*, *333*, 199–217.
Yu, S.-B., H. Y. Chen, and L. C. Kuo (1997), Velocity field of GPS stations in the Taiwan area, *Tectonophysics*, *274*, 41–60.
Yue, L.-F., J. Suppe, and J.-H. Hung (2005), Structural geology of a classic thrust belt earthquake: the 1999 Chi-Chi earthquake Taiwan (Mw = 7.6), *J. Struct. Geol.*, *27*, 2058–2083.
Zanchi, A., F. Berra, M. Mattei, M. R. Ghassemi, and J. Sabouri (2006), Inversion tectonics in the central Alboraz, Iran, *J. Struct. Geol.*, *28*, 2023–2037.

Article 5 - The deep structure of south-central Taiwan illuminated by seismic tomography, earthquake hypocentre, and gravity data

Giovanni Camanni[1], Joaquina Alvarez-Marron[1], Dennis Brown[1], Conxi Ayala[2], Yih-Min Wu[3], and Hsien-Hsiang Hsieh[4]

[1]Institute of Earth Sciences Jaume Almera, ICTJA-CSIC, Lluis Sole i Sabaris s/n, 08028 Barcelona, Spain
[2]Instituto Geológico y Minero de España - IGME (Spanish Geological Survey), La Calera n. 1, 28760 Tres Cantos, Madrid, Spain. Currently visiting at ICTJA-CSIC
[3]Department of Geosciences, National Taiwan University, Taipei, 106, Taiwan
[4]Lamont-Doherty Earth Observatory, Earth Institute at Columbia University, Palisades, New York, USA

Status of publication: under review in "**Geological Society of America Bullettin**", MS number: B31138

Contributions of the Ph.D. student to the article:

- Manuscript conception and writing;
- Analysis of earthquake hypocentre data;
- Analysis of P-wave velocity data

Abstract

The Taiwan mountain belt is generally thought to develop above a shallow, through-going basal detachment confined to within the sedimentary cover of the Eurasian continental margin. A number of datasets, however, such as surface geology, earthquake hypocenter, and seismic tomography data among others, suggest that crustal levels below the interpreted location of the detachment are also currently being involved in the deformation. In this paper, we combine seismic tomography, earthquake hypocenter, and gravity inversion data to investigate the deformation that is taking place at depth beneath south-central Taiwan. We found that beneath the Coastal Plain and the Western Foothills most of the deformation is taking place near the basement-cover interface that is acting as an extensive level of detachment. This level of detachment is located at ≥10 km depth, below the basal detachment proposed from surface geology for this part of the mountain belt, and extends westward of the deformation front of the mountain belt as defined by geological structures at the surface. Beneath this level of detachment, inherited extensional faults appear, locally, to maintain the bulk of their extensional displacement. However, across the Shuilikeng and the Chaochou faults, earthquake hypocenters define steeply dipping clusters that extend to greater than 20 km depth. We interpret these clusters to be related to deformation that is taking place along a deep-penetrating, east-dipping ramp that joins westward with the detachment at the basement-cover interface. Basement rocks are uplifted along this ramp to form a basement culmination beneath the Hsuehshan and Central ranges.

1. Introduction

The Taiwan mountain belt has been forming since the Late Miocene as a result of the oblique collision between the southeast continental margin of Eurasia and the Luzon volcanic arc on the Philippine Sea Plate (Byrne et al., 2011; Huang et al., 2006; Sibuet and Hsu, 2004; Suppe, 1981, 1984; Teng, 1990) (Fig. 1). Studies of the structure of the western flank of the Taiwan mountain belt have led many authors to suggest that it is evolving by thrusting above a shallowly east-dipping basal detachment that extends all the way eastward beneath the orogen (Carena et al., 2002; Ding et al., 2001; Malavieille and Trullenque, 2009; Suppe, 1980, 1981; Suppe and Namson, 1979; Yue et al., 2005). Although both along- and across-strike variations in the depth and stratigraphic location of the basal detachment have been proposed, it is generally thought to be confined to within the sedimentary cover of the margin, either at the base of the syn-orogenic sediments or within the older platform and slope sediments (Brown et al., 2012; Suppe, 1976, 1980, 1981; Suppe and Namson, 1979; Yue et al., 2005).

There are, however, a number of pieces of evidence in the surface geology (Alvarez-Marron et al., in Press; Brown et al., 2012; Camanni et al., 2014a), as well as in magnetotelluric (Bertrand et al., 2009, 2012), GPS (Chuang et al., 2013), earthquake hypocentre (Gourley et al., 2007; Lacombe and Mouthereau, 2002; Lacombe et al., 2001; Mouthereau and Petit, 2003; Wu et al., 1997, 2004, 2014; Wu et al., 2008; Yue et al., 2005) and seismic tomography data (Camanni et al., 2014b; Huang et al., 2014; Kim et al., 2005, 2010; Kuo-Chen et al., 2012; Lin, 2007; Rau and Wu, 1995; Wu et al., 2007) which suggest that rocks below the interpreted detachment, an even the basement (here we define it as any pre-Eocene rifting rocks, but it is often defined by others as any pre-Miocene rocks) may also be involved in the deformation in much of Taiwan. For example, combining surface geological and borehole data, Hickman et al. (2002); Hung et al. (1999) interpret the basal detachment to cut down section to lie near the basement-cover interface. Similarly, seismic activity beneath the interpreted location of the basal detachment in west-central and southwestern Taiwan also led Mouthereau and Petit (2003) and Yue et al. (2005) to postulate the presence of a second, deeper detachment surface that lies either near the basement-cover interface or within the basement. Furthermore, on the basis of surface geological, borehole and seismicity data, Mouthereau et al. (2002), Mouthereau et al. (2001), Lacombe and Mouthereau (2002), and Mouthereau and Lacombe (2006), interpret the basement (note that they call basement any pre-Miocene rocks) to be involved in the deformation along much of westernmost Taiwan. Eastward, Brown et al. (2012), Camanni et al. (2014a,b), and Chuang et al. (2013) use either surface geology, seismicity, or GPS data to interpret the basal detachment to ramp down into the middle crust and to involve basement in the deformation. These latter observations are further corroborated by the presence of high P-wave velocities close to the surface, suggesting that basement rocks are being uplifted (e.g., Alvarez-Marron et al., in Press; Camanni et al., 2014b). Furthermore, in much of Taiwan Wu et al. (1997, 2004, 2014) and Gourley et al. (2007) have used earthquake hypocenter data to suggest that there are a number of steeply dipping faults that penetrate into the middle and perhaps even the lower crust.

These observations suggest that deformation that is taking place near the basement-cover interface and within the basement may be playing a more significant role in the structural development of the Taiwan orogeny than predicted by the model with a detachment confined to within the sedimentary cover. To help place further constraints on the structural architecture of the Taiwan mountain belt, in this paper we use a P-wave tomography model together with a three-dimensional gravity inversion to define a proxy for the basement-cover interface in south-central Taiwan (Figs. 1 and 2). We then use earthquake hypocenter data to evaluate the location and the geometry of deep-seated faults that are contributing to the deformation that is taking place in this part of Taiwan.

2. Geological setting

The outcropping geology of the south-central part of the Taiwan mountain belt (Figs. 1 and 2) is made up of Eocene to Miocene sediments of the continental margin overlain by Pliocene to Holocene syn-orogenic sediments of the foreland basin (Brown et al., 2012; Hickman et al., 2002; Hung et al., 1999; Lacombe et al., 1999; Mouthereau et al., 2001; Rodriguez-Roa and Wiltschko, 2010; Yue et al., 2005). Basement rocks do not crop out within the study area, although they have been intersected in a number of boreholes (Chiu, 1975; Jahn et al., 1992; Mouthereau et al., 2002; Shaw, 1996). This basement predominantly comprises clastic sediments of Jurassic and Cretaceous age (Chiu, 1975; Shaw, 1996). Only in one borehole in the southern part of the study area (CLI-1, Fig. 2) has marble been found, from which a Pb-Pb isochron age of 242 ± 22 Ma, or Triassic, has been determined (Jahn et al., 1992).

In this part of Taiwan, the mountain belt can be roughly divided in four tectonostratigraphic zones separated by major faults (Figs. 1 and 2). From west to east these zones are: the Coastal Plain, the Western Foothills, the Hsuehshan Range, and the Central Range. The Coastal Plain is made up of weakly deformed Pliocene to Holocene syn-orogenic sediments of the foreland basin, while the Western Foothills comprise a west-verging thrust system that imbricates the Miocene pre-orogenic and the younger syn-orogenic sediments (Alvarez-Marron et al., in Press; Brown et al., 2012; Hickman et al., 2002; Hung et al., 1999; Lacombe et al., 1999; Rodriguez-Roa and Wiltschko, 2010; Yue et al., 2005). The boundary between the Coastal Plain and the Western Foothills is generally thought to coincide with the tip line of the Changua Thrust (Ching et al., 2011b; Hsu et al., 2009; Yu et al., 1997) (Fig. 2), which is usually presented as the deformation front of the Western Foothills thrust system. Although, in the southwestern part of the study area, some authors place it farther west (Lin and Watts, 2002; Shyu et al., 2005; Yang et al., 2007). The Western Foothills thrust system appears to be linked to an east-dipping basal detachment that, in the northern part of the map area, is located at the base of the syn-orogenic sediments (Brown et al., 2012; Carena et al., 2002; Suppe, 1981; Yue et al., 2005), while in the south it cuts down section into Miocene sediments (Alvarez-Marron et al., in Press; Hickman et al., 2002; Lacombe et al., 1999; Mouthereau et al., 2001; Suppe, 1976; Suppe and Namson, 1979) and, locally, lies within undifferentiated pre-Miocene rocks (Hickman et al., 2002; Hung et al., 1999).

In the north of the study area, the Western Foothills is juxtaposed against the Hsuehshan Range across the Shuilikeng Fault (Brown et al., 2012; Camanni et al., 2014a) (Fig. 2). The Hsuehshan Range is made up of variably metamorphosed (Beyssac et al., 2007; Sakaguchi et al., 2007; Simoes et al., 2012) Eocene and Oligocene clastic sediments that were deposited in the so-called Hsuehshan Basin (Ho, 1988; Huang et al., 1997; Teng and Lin, 2004). The Hsuehshan Range is juxtaposed against the Central Range in the east across the Lishan Fault (Brown et al., 2012; Camanni et al., 2014b; Clark et al., 1993; Lee et al., 1997). Southward, the Central Range is juxtaposed against the Western Foothills along the Chaochou Fault (Mouthereau et al., 2002; Tang et al., 2011; Wiltschko et al., 2010). The outcropping geology of the Central Range within the study area is made up of Miocene rocks of the Lushan Formation (Beyssac et al., 2007; Brown et al., 2012; Lee et al., 2006; Simoes et al., 2007; Tillman and Byrne, 1995; Wiltschko et al., 2010) which comprises variably metamorphosed slates with a well-developed cleavage (Brown et al., 2012; Fisher et al., 2002; Stanley et al., 1981; Wiltschko et al., 2010).

3. Methodologies used

3.1. Tomography and earthquake hypocenter data

In what follows in Section 4, we use the 3D P-wave velocity model of Wu et al. (2007) in combination with earthquake hypocentre data to investigate the deep structure of south-central Taiwan and, in particular, the location and geometry of the basement-cover interface. The reader is referred to Wu et al. (2007) for the

data, the methodology used in the tomogaphy inversion, and the resolution testing. Importantly for this study, the horizontal resolution of the model in the study area is 7.5 km in the WNW-ESE direction by 12.5 km in the NNE-SSW direction, whereas the depth resolution is 2 km from 0 to 6 km depth, 3 km from 6 to 9 km depth, 4 km from 9 to 25 km depth, and then 5 km to the base of our data set at 30 km depth. Earthquake hypocenter data from 1990 to 2011 are located in the 3D P-wave velocity model using the methodology of Wu et al. (2008). Hypocentres were subsequently collapsed (relocated) using the methodology of Jones and Stewart (1997).

In the description of the velocity model that follows in Section 4.2, vertical and horizontal slices were cut through the volume and the collapsed hypocenters were projected on to them. The vertical sections were cut perpendicular to the strike of the surface geological structures and perpendicular to the strike of the extensional fault systems imaged offshore southwest Taiwan and beneath its western Coastal Plain (e.g., Lin et al., 2003). Horizontal slices were cut through the nodal points of the velocity model grid.

Since defining an accurate location and geometry for the top of the basement is of primary importance in this study, we use a P-wave velocity of 5.2 km/s as a proxy for this surface. Tests made using P-wave velocities between 5 km/s and 5.5 km/s have overall a similar geometry and plot in a similar location (see Fig. DR 3). However, we choose a velocity of 5.2 km/s since it is consistent with laboratory measurements of Vp of weakly metamorphosed polymictic clastic sediments at a depth of between 5 and 15 km (Christensen, 1989; Christensen and Mooney, 1995) and with the temperatures thought to occur at these depths in Taiwan (Wu et al., 2013; Zhou et al., 2003). It is also consistent with estimates of Lester et al. (2013) and Eakin et al. (2014) who interpret the basement offshore of southwestern Taiwan to have a P-wave velocity above 5.0 km/s. It is, however, slightly higher than the c. $\leq$ 5 km/s given to basement by Chen and Yang (1996) and Tang and Zheng (2010). Finally, we stress that a P-wave velocity of 5.2 km/s provides only a proxy for the location and geometry of the basement-cover interface and may not correspond to it everywhere.

3.2. Three-dimensional gravity modeling

In order to test the validity of the interpretation that the top of the basement may coincide with the 5.2 km/s P-wave velocity surface, we carried out a three-dimensional stochastic gravity inversion of the Bouguer anomaly data (Fig 3 A). The data and its distribution can be found in Yen et al. (1995) and Yen and Hsieh (2010). The stochastic inversion was done using Geomodeller software (Gibson et al., 2013). The model was discretized in voxels of 1000 m x 1000 m x 250 m to obtain smooth interfaces. In order to filter the noise from the short wavelength component of the calculated Bouguer anomaly introduced by the topography we continued the observed anomaly upward to 4000 m. The inversion was set to run for $15x10^6$ iterations. The RMS of the inversion ranges from 28 mGal in the first iteration to 0.6 mGal in the last.

The starting densities used in the model were obtained from the conversion of the P-wave velocities derived from the tomography data using the method of Barton (1986). From these starting densities, a four-layer input density model was built and the modeling program was allowed to modify the densities and the surfaces between the layers until a close match between the observed and the calculated anomaly was obtained (Fig. 3). The model comprises a sedimentary cover with a density of 2.4 g/cm^3 with its base located at the 5.2 km/s isovelocity surface; a middle crustal layer with a density of c. 2.7 g/cm^3 with its bottom located at the 6.2 km/s; a lower crustal layer with a density of 2.9 g/cm^3; and a basal, upper mantle layer with a density of 3.25 g/cm^3 down to 60 km depth. The depth distribution of the layer interfaces are given in Fig. DR 1. The location of the Moho was chosen to lie between the c. 7.5 to 7.8 km/s isovelocity surfaces. This is in agreement with other interpretations of the Moho in Taiwan by Wu et al. (2007) and Ustaszewski et al. (2012). Its depth and shape are also in agreement with that derived from travel time inversion of PmP phases (Hsu et al., 2011), receiver functions (Wang et al., 2010a,b), and two-dimensional gravity modeling (Yen et al., 1998).

4. Results

4.1. The basement-cover interface

After the gravity inversion, the main features of the observed Bouguer anomaly are recovered in the calculated model, with a RMS misfit of 0.6 mGal, which is less than the 2% of the total amplitude of the Bouguer anomaly (Figs. 3 B and C). Finally, the location and geometry of the 5.2 km/s isovelocity surface can

be modeled using the Bouguer data, with vertical misfits that are mostly less than ± 3 km (Fig. 4), well within the vertical resolution of the tomography model being used. The close coincidence between the input and the modeled surfaces suggests that using the 5.2 km/s isovelocity surface as a proxy for the basement-cover interface is reasonable in the interpretation of the tomography data that follows.

The basement-cover interface as defined by the 5.2 km/s isovelocity surface (Fig. 4 A) deepens southward beneath the Coastal Plain and the Western Foothills from c. 8-10 km to c. 15 km, whereas it shallows eastward to less than 4 km depth beneath the Hsuehshan and Central ranges. An exception to this overall trend occurs in the central part of the map area where, immediately to the west of the Changhua thrust, it begins to shallow defining a basement high that we call the Alishan Uplift (Alvarez-Marron et al., in Press) (AU, Fig. 4 A). The depth of the basement-cover interface determined in this way is overall deeper than that previously proposed from beneath the Coastal Plain, where its location is derived from borehole and seismic reflection data (Lin et al., 2003). The differences in depth between the two interpretations is on the order of several kilometers (see Fig. DR 2 for comparison and a misfit calculation). These differences can be related to a number of factors, including; 1) the vertical resolution of the P-wave velocity model used here, 2) the depth conversion of time-migrated seismic reflection data by Lin et al. (2003) and, 3) the choice of 5.2 km/s as marking top basement. Mouthereau et al. (2002) also produce a top-basement contour map, but in their case this implies any pre-Miocene rocks so it is not possible to do a direct comparison with our results. There are also significant differences between the top of the basement presented here and that intersected in the seven boreholes within the western part of the study area (Fig. 2) (WG-1 at -3054m; PK-2 and PK-3 at -1467m and -1962, respectively; LC-1 at -2320m; HP-1 at -4023m; PCC-1 at -3373m; and CLI-1 at -4612) (e.g., Chiu, 1975; Jahn et al., 1992; Shaw, 1996). Despite these inconsistencies in the depth between interpretations, the overall geometry of the top of the basement obtained by the 5.2 km/s isovelocity surface, especially its southward deepening, is consistent between models. Note that the interpretation presented here extends into the Western Foothills, Hsuehshan, and Central ranges whereas those of Lin et al. (2003) and Mouthereau et al. (2002) do not.

4.2. The basement-cover interface and earthquake hypocenters

Having established our working definition for the basement-cover interface as well as its geometry, we now proceed with the descriptions of the velocity and hypocenter data using this interface as a reference. In the P-wave velocity sections oriented perpendicular to the strike of the surface structures, the basement-cover interface (the 5.2 km/s isovelocity line) shows a marked shallowing from west to east (Fig. 5 A), with the change taking place approximately at the Shuilikeng fault in the north (sections A-A′, B-B′, and C-C′) and the Chaochou fault in the south (sections D-D′, E-E′, and F-F′). West of the Shuilikeng and Chaochou faults, earthquake hypocenters form a well-defined, sub-horizontal cluster near the basement-cover interface. As the basement-cover interface deepens to the south, however, there is a significant reduction in the number of events (i.e., in sections E-E′ and F-F′) (see also Fig. 6). In sections B-B′ through to E-E′ the hypocenter cluster extends several kilometers west of the deformation front defined by the Changhua Thrust (see also Fig. 6). Section A-A′ is a notable exception to this. Furthermore, in the collapsed data set it is not possible to make a direct correlation between any fault mapped at the surface and the hypocenter data forming this sub-horizontal cluster, although other authors have attempted this with un-collapsed data (e.g., Wu et al., 2003). From approximately the Shuilikeng and Chaochou faults to the east, hypocenters form a moderately east-dipping cluster that locally extends to a depth of more than 20 km. This feature is particularly well developed in sections A-A′, E-E′, and F-F′ (Fig. 5 A). Farther east, seismicity is diffuse. This deepening of the seismicity coincides with a marked shallowing of the basement-cover interface (Figs. 5 and 6). An exception to this relationship between the basement-cover interface and the seismicity is a well-defined cluster that begins near the Shuilikeng fault and extends westward in sections B-B′, C-C′ and G-G′. This cluster (named TF in Figs. 5 and 6) is related to a series of earthquakes that began after the 1999 Chi-Chi event (Wu et al., 2004) that, in 3D, has a tubular shape, and in which strike-slip focal mechanisms dominate (Wu et al., 2010). To date we are unable to correlate this cluster of events with any structure.

In the sections cut perpendicular to the extensional faults imaged offshore southwest Taiwan and beneath the Coastal Plain, the southward deepening of the basement-cover interface is particularly well-defined in sections J-J′ and K-K′ (Fig. 5 B). In the sections that cross the Shuilikeng and Chaochou faults (G-G′ through to J-J′) the marked shallowing of the basement-cover interface is also imaged. In sections G-G′ to I-I′, hypocenters form sub-horizontal clusters near the basement-cover interface, although in section H-H′ a weakly developed vertical cluster can also be identified; it extends down to a little over 15 km depth. Section

J-J′ displays moderately SSE-dipping, tight to open clusters of hypocenters together with the sub-horizontal events. Together they define an overall deepening of the basement-cover interface with a rugose or step-like geometry. Section K-K′ shows very clearly the SE-deepening of the basement-cover interface and, where it is at its deepest, the almost complete absence of seismicity (Figs. 5 B and 6).

Throughout the study area, there is a notable difference between the location of the deformation front defined by the Changhua thrust tip line and the western limit of the seismicity (as defined by a significant reduction in the number of earthquakes). To demonstrate this, all hypocenters from 0 to 30 km depth are projected onto a map of the surface geology of the Coastal Plain and the Western Foothills within the study area (Fig. 7). In the northern part of the map area (coinciding with section A-A′) the majority of the seismicity is east of the deformation front, whereas southward it is far to the west and even extends into the offshore. In the southwest, where the sedimentary package of the Tainan Basin is thickest, there are also very few events. The distribution of hypocenters suggests that the Changhua thrust does not everywhere coincide with the western limit of the deformation. This observation is also corroborated by other studies of seismicity, GPS, and geomorphology data which place the deformation front farther to the west in the southwestern part of the map area (Lin and Watts, 2002; Shyu et al., 2005; Yang et al., 2007).

5. Discussion

One of the basic tenets in the geometric, mechanical, numerical, and analogue modeling of mountain belts is that at shallow depths beneath their flanks there is a through-going, gently-dipping basal detachment above which a fold-and-thrust belt develops (e.g., Poblet and Lisle, 2011; Rodgers, 1990). In this model, the sedimentary cover of a continental margin is detached above a basement that is not extensively involved in the deformation (Buiter, 2012; Chapple, 1978; Dahlen et al., 1984; Dahlstrom, 1970; Davis et al., 1983; Fitz-Diaz et al., 2011; Pérez-Estaún et al., 1988, 1994; Price, 1981). This level of detachment is often located in a zone of weakness in the crust that, in a number of thrust belts, coincides with the interface between the basement and the sedimentary cover (Chapple, 1978; Dahlstrom, 1970; Price, 1981; Rodgers, 1990; Srivastava and Mitra, 1994). While this simplified view of thrust belt architecture is widely accepted, how a continental margin deforms during collision depends to a large degree on its prior morphological and structural architecture. In particular, that of the basement, the structure of its platform and slope, and of its post-rift sedimentary carapace (e.g., Brown et al., 2011; Thomas, 2006). Below we will discuss how the evolving structure of south-central Taiwan appears to be controlled by a number of these factors.

The Eurasian continental margin that is entering into the collision currently taking place in Taiwan has been extensively studied, in particular in the offshore to the southwest (Ding et al., 2008; Eakin et al., 2014; Huang et al., 2004; Lester et al., 2014; Li et al., 2007; Lin et al., 2003; McIntosh et al., 2013; Tang and Zheng, 2010; Yang et al., 2006). This area of the margin comprises the platform (full thickness of the continental crust), the slope (starting at the 200 m bathymetry contour, Figs. 1 and 2), and the continent-ocean transition. On the outer platform to slope areas of the margin Miocene extension resulted in the development of the deep Tainan Basin offshore southwest Taiwan (Figs. 1 and 2) (Ding et al., 2008; Huang et al., 2004; Lester et al., 2014; Li et al., 2007; Lin et al., 2003; Tang and Zheng, 2010; Yang et al., 2006). The Tainan Basin comprises two fault-bound depocentres called the Northern and Southern depressions, separated by a structural high called the Central Uplift (Fig. 8, section X-X′). The thickness of the Oligocene and Miocene sediments in the Tainan Basin offshore reaches up to 6 km, and these are overlain by up to 7 km (in the Southern Depression) of Pliocene to Holocene syn-orogenic sediments (Lin et al., 2003). The Tainan Basin is bound to the north by a system of SSE-dipping extensional faults that have been grouped together and called “B” (Lin et al., 2003) or Meishan (Yang et al., 2007) and Yichu faults (Fig. 2) (Lin et al., 2003). Although there are a number of very different structural interpretations for the extensional fault geometries of the Tainan Basin (e.g., Chen and Yang, 1996; Huang et al., 2004; Lin et al., 2003), the overall regional-scale architecture can be interpreted to project onshore where it appears to be imaged by the step-like geometry of the hypocenter cluster and overall southward deepening of the basement-cover interface in section J-J′ (Fig. 8).

While this rugose geometry of the hypocenter cluster is not well-developed everywhere (in the offshore Lester et al. (2013) and Eakin et al. (2014) have imaged a similar rugose detachment at the basement-cover interface), from the Shuilikeng and Chaochou faults to the west there is nevertheless a well-defined clustering of hypocenters near the basement-cover interface as we define (Fig. 5). The clustering of hypocenters at the basement-cover interface suggests that it is acting as a detachment surface (Fig. 8). This, taken together with the rugose nature of the hypocenter cluster imaged in section J-J′ may indicate that the

original basement structure of the continental margin (i.e., section X-X´ in Fig. 8) is preserved in the southwestern part of the Taiwan mountain belt. It may also indicate that the extensional fault systems developed on the outer platform to slope maintain at least some of their original extensional displacement in this part of the mountain belt (Fig. 8). However, the development of the Alishan Uplift in the central part of the map area appears to indicate that these faults are locally being reactivated (Alvarez-Marron et al., in Press). This interpretation is similar to that of other authors that suggest that pre-existing extensional faults in the Coastal Plain and Western Foothills of south-central Taiwan are being reactivated (e.g., Lacombe and Mouthereau, 2002; Mouthereau et al., 2002; Mouthereau and Lacombe, 2006; Mouthereau and Petit, 2003; Suppe, 1986).

In the northern, western, and southern part of the study area the limits of this detachment are defined by the seismicity front (as defined in Section 4.2). In the north, it has an overall northeast trend, similar to the outcropping structural trend (e.g., Alvarez-Marron et al., in Press) and to the interpreted location of the north-western flank of the Tainan Basin as defined by the "B" and Yichu faults (Fig. 7). In the south, however, it appears to be related to thickening of the sedimentary package in the Southern Depression of the Tainan Basin. Furthermore, the deep level (≥10 km) of the hypocenter cluster along the basement-cover interface make it difficult to link the geometry of the thrust systems developed at the surface (Alvarez-Marron et al., in Press; Hickman et al., 2002; Lacombe et al., 1999; Mouthereau et al., 2001; Suppe, 1976; Suppe and Namson, 1979) to a detachment at this depth (see also Yue et al. (2005) for a discussion of this point). This suggests that there might be a deeper, active level of detachment near the basement-cover interface that is located beneath the basal thrust of the upper thrust system throughout a large part of south-central Taiwan. The basal thrust of the upper thrust system is at the base of the syn-orogenic sediments in the north and southwards cuts down section into Miocene sediments. The deformation front of the upper thrust system is located at the tip line of the Changhua Thrust, whereas that of the lower detachment is defined by the seismicity front (Fig. 7). Both appear to be active at the same time, although seismicity seems to be largely taking place along the deeper of the two.

There is a considerable change in the surface geology across the Shuilikeng, Lishan, and Chaochou faults (Fig. 8) that is clearly expressed in the P-wave velocity, density, and hypocenter data (Figs. 4, 5, and 6). To the west of these faults the deformation is confined to shallow crustal levels, whereas to the east the hypocenter cluster deepens to greater than 20 km depth and coincides with higher P-wave velocity and denser material close to the surface. In the northern part of the study area, Brown et al. (2012) and Camanni et al. (2014b) suggest that this is related to inversion of the Hsuehshan Basin and the uplift of basement rocks between the Shuilikeng and Lishan faults (sections A-A´ in Figs. 5 A and 8). With the current data set we can interpret this same process (uplift of basement rocks) to extend southward along the Chaochou Fault, where the sub-horizontal cluster imaged to the west takes on an eastward dip and extends to 20 km or more depth (sections E-E´ and F-F´ in Figs. 5 A and 8). In this interpretation the sub-horizontal hypocenter cluster located at the basement-cover interface beneath the Coastal Plain and the Western Foothills ramps down section to merge with the Chaochou Fault that uplift the higher velocity, denser basement rocks in the east to near the surface. This interpretation implies that the Shuilikeng, Lishan, and Chaochou faults are linked together and in some way are rooted into the middle or even lower crust along this east-dipping hypocenter cluster (Fig. 8). This interpretation is in keeping with those of Ching et al. (2011a), Mouthereau et al. (2002), Tang et al. (2011), and Wiltschko et al. (2010) who also interpret the Chaochou fault to be rooted deep in the crust. This type of feature is common to many mountain belts where the basal detachment of the foreland fold-and-thrust belt ramps down into the middle or lower crust, resulting in the development of a regional-scale basement culmination (e.g., Cook et al., 1979; Coward, 1983; Hatcher and Williams, 1986; Pérez-Estaún et al., 1988). A corollary to this is that, in south-central Taiwan, to the west of these faults the basement-cover interface appears to be acting as a detachment, whereas to the east it is not. Unlike in the examples of the fossil orogens referred to above, with the current data set from south-central Taiwan it is not possible to determine how (or even if) the detachment extends eastward into the internal part of the mountain belt that is the Central Range.

6. Conclusions

The combination of seismic tomography, earthquake hypocenter, and gravity inversion data presented in this paper help define the deep structure of the south-central Taiwan mountain belt. In this paper we define the basement-cover interface to coincide with a P-wave velocity of 5.2 km/s. This interpretation is further validated by the inversion of the Bouguer anomaly data. These data suggest that in the west, beneath the

Coastal Plain and the Western Foothills, the mountain belt is evolving above a southward deepening level of detachment that is illuminated by sub-horizontal clusters of earthquake hypocenters located near this basement-cover interface. This detachment appears to be below the basal thrust of the thrust system mapped at the surface. In much of south-central Taiwan, the western limit of the seismicity that defines the detachment does not coincide with the deformation front as defined by the tip line of the Changhua thrust. Eastward, the detachment at the basement-cover interface joins with an east-dipping hypocenter cluster that is interpreted to form a ramp that extends to greater than 20 km depth, into the middle crust. Above this ramp, basement rocks (P-wave > 5.2 km/s) are uplifted to near the surface, forming a basement culmination beneath the Hsuehshan and Central ranges. The uplift of these basement rocks, together with the juxtaposition of higher metamorphic grade rocks across the Shuilikeng, Lishan and Chaochou faults suggests that these faults form a linked fault system that extends downward into the middle crust at the location of the ramp.

Acknowledgements

Discussions with E. Casciello, M.-M. Chen, H.-T. Chu, and A. Pérez-Estaún are acknowledged, as is the help of C.-H. Chen and H.-A. Chen in the collapsing of the earthquake hypocenters. The earthquake hypocenter database is available from authors or at http://seismology.gl.ntu.edu.tw/download_04.htm. The P-wave velocity model is available from authors or at http://seismology.gl.ntu.edu.tw/data/02.%203D%20Vp%20VpVs%20model.txt. The Bouguer Anomaly dataset is available from authors. This research was carried out with the aid of grants by Consejo Superior de Investigaciones Científicas (CSIC) Proyectos Intramurales 2006 301010, Ministerio de Ciencia y Innovación CGL2009-11843-BTE, and the CSIC predoctoral program Junta para la Ampliación de Estudios (JAE-Predoc). The Generic Mapping Tools (GMT) were used to produce some of the figures.

References

Alvarez-Marron, J., Brown, D., Camanni, G., Wu, Y. M., and Kuo-Chen, H., in Press, Structural complexities in a foreland thrust belt inherited from the shelf-slope transition: Insights from the Alishan area of Taiwan: Tectonics.

Barton, P. J., 1986, The relationship between seismic velocity and density in the continental crust - a useful constraint?: Geophysical Journal of the Royal Astronomical Society, v. 87, no. 1, p. 195-208.

Bertrand, E. A., Unsworth, M. J., Chiang, C.-W., Chen, C.-S., Chen, C.-C., Wu, F. T., Türkoğlu, E., Hsu, H.-L., and Hill, G. J., 2009, Magnetotelluric evidence for thick-skinned tectonics in central Taiwan: Geology, v. 37, no. 8, p. 711-714.

-, 2012, Magnetotelluric imaging beneath the Taiwan orogen: An arc-continent collision: Journal of Geophysical Research, v. 117, no. B1.

Beyssac, O., Simoes, M., Avouac, J. P., Farley, K. A., Chen, Y.-G., Chan, Y.-C., and Goffé, B., 2007, Late Cenozoic metamorphic evolution and exhumation of Taiwan: Tectonics, v. 26, no. 6.

Brown, D., Alvarez-Marron, J., Schimmel, M., Wu, Y.-M., and Camanni, G., 2012, The structure and kinematics of the central Taiwan mountain belt derived from geological and seismicity data: Tectonics, v. 31, no. 5.

Brown, D., Ryan, P. D., Afonso, J. C., Boutelier, D., Burg, J. P., Byrne, T., Calvert, A., Cook, F., DeBari, S., Dewey, J. F., Gerya, T. V., Harris, R., Herrington, R., Konstantinovskaya, E., Reston, T., and Zagorevski, A., 2011, Arc–Continent Collision: The Making of an Orogen, *in* Brown, D., and Ryan, P. D., eds., Arc-Continent Collision: New York, Springer Berlin Heidelberg, p. 477-493.

Buiter, S. J. H., 2012, A review of brittle compressional wedge models: Tectonophysics, v. 530-531, p. 1-17.

Byrne, T., Chan, Y. C., Rau, R. J., Lu, C. Y., Lee, Y. H., and Wang, Y. J., 2011, The Arc–Continent Collision in Taiwan, *in* Brown, D., and Ryan, P. D., eds., Arc-Continent Collision: New York, Springer Berlin Heidelberg, p. 213-245.

Camanni, G., Brown, D., Alvarez-Marron, J., Wu, Y.-M., and Chen, H.-A., 2014a, The Shuilikeng fault in the central Taiwan mountain belt: Journal of the Geological Society, v. 171, p. 117-130.

Camanni, G., Chen, C.-H., Brown, D., Alvarez-Marron, J., Wu, Y.-M., Chen, H.-A., Huang, H.-H., Chu, H.-T., Chen, M.-M., and Chang, C.-H., 2014b, Basin inversion in central Taiwan and its importance for seismic hazard: Geology, v. 42, no. 2, p. 147-150.

Carena, S., Suppe, J., and Kao, H., 2002, Active detachment of Taiwan illuminated by small earthquakes and its control of first-order topography: Geology, v. 30, no. 10, p. 935-938.

Chapple, W. M., 1978, Mechanics of thin-skinned fold-and-thrust belts: Geological Society of America Bulletin, v. 89, no. 8, p. 1189-1198.

Chen, A., and Yang, Y.-L., 1996, Lack of Compressional Overprint on the Extensional Structure in Offshore Tainan and the Tectonic Implications: Terrestrial, Atmospheric and Oceanic Sciences, v. 7, no. 4, p. 505-522.

Ching, K.-E., Johnson, K. M., Rau, R.-J., Chuang, R. Y., Kuo, L.-C., and Leu, P.-L., 2011a, Inferred fault geometry and slip distribution of the 2010 Jiashian, Taiwan, earthquake is consistent with a thick-skinned deformation model: Earth and Planetary Science Letters, v. 301, no. 1–2, p. 78-86.

Ching, K.-E., Rau, R.-J., Johnson, K. M., Lee, J.-C., and Hu, J.-C., 2011b, Present-day kinematics of active mountain building in Taiwan from GPS observations during 1995–2005: Journal of Geophysical Research: Solid Earth, v. 116, no. B9.

Chiu, H.-T., 1975, Miocene stratigraphy and its relation to the Palaeogene rocks in west-central Taiwan: Petroleum Geology of Taiwan, v. 12, p. 51-80.

Christensen, N. I., 1989, Reflectivity and seismic properties of the deep continental crust: Journal of Geophysical Research: Solid Earth, v. 94, no. B12, p. 17793-17804.

Christensen, N. I., and Mooney, W. D., 1995, Seismic velocity structure and composition of the continental crust: A global view: Journal of Geophysical Research: Solid Earth, v. 100, no. B6, p. 9761-9788.

Chuang, R. Y., Johnson, K. M., Wu, Y.-M., Ching, K.-E., and Kuo, L.-C., 2013, A midcrustal ramp-fault structure beneath the Taiwan tectonic wedge illuminated by the 2013 Nantou earthquake series: Geophysical Research Letters, v. 40, no. 19, p. 2013GL057779.

Clark, M. B., Fisher, D. M., Lu, C.-Y., and Chen, C.-H., 1993, Kinematic analyses of the Hsüehshan Range, Taiwan: A large-scale pop-up structure: Tectonics, v. 12, no. 1, p. 205-217.

Cook, F. A., Albaugh, D. S., Brown, L. D., Kaufmann, S., Oliver, J. E., and Hatcher Jr, R. D., 1979, Thin-skinned tectonics in the crystalline southern Appalachians: COCORP seismic- reflection profiling of the Blue Ridge and Piedmont: Geology, v. 7, no. 12, p. 563-567.

Coward, M. P., 1983, Thrust tectonics, thin skinned or thick skinned, and the continuation of thrusts to deep in the crust: Journal of Structural Geology, v. 5, no. 2, p. 113-123.

Dahlen, F. A., Suppe, J., and Davis, D., 1984, Mechanics of fold-and-thrust belts and accretionary wedges: Cohesive Coulomb Theory: Journal of Geophysical Research, v. 89, no. B12, p. 10087-10101.

Dahlstrom, C. D. A., 1970, Structural geology in the eastern margin of the canadian rocky mountains: Bulletin of Canadian Petroleum Geology, v. 18, no. 3, p. 332-406.

Davis, D., Suppe, J., and Dahlen, F. A., 1983, Mechanics of fold-and- thrust belts and accretionary wedges: Journal of Geophysical Research, v. 88, no. B2, p. 1153-1172.

Ding, W.-W., Li, J.-B., Li, M.-B., Qiu, X.-L., Fang, Y.-X., and Tang, Y., 2008, A Cenozoic tectono-sedimentary model of the Tainan Basin, the South China Sea: evidence from a multi-channel seismic profile: Journal of Zhejiang University SCIENCE A, v. 9, no. 5, p. 702-713.

Ding, Z. Y., Yang, Y. Q., Yao, Z. X., and Zhang, G. H., 2001, A thin-skinned collisional model for the Taiwan orogeny: Tectonophysics, v. 332, no. 3, p. 321-331.

Eakin, D. H., McIntosh, K. D., Van Avendonk, H. J. A., Lavier, L., Lester, R., Liu, C.-S., and Lee, C.-S., 2014, Crustal-scale seismic profiles across the Manila subduction zone: The transition from intraoceanic subduction to incipient collision: Journal of Geophysical Research: Solid Earth, v. 119, no. 1, p. 2013JB010395.

Fisher, D. M., Lu, C.-Y., and Chu, H.-T., 2002, Taiwan slate belt: Insights into the ductile interior of an arc-continent collision: Geological Society of America Special Papers, v. 358, p. 93-106.

Fitz-Diaz, E., Hudleston, P., and Tolson, G., 2011, Comparison of tectonic styles in the Mexican and Canadian Rocky Mountain Fold-Thrust Belt: Geological Society, London, Special Publications, v. 349, no. 1, p. 149-167.

Gibson, H., Sumpton, J., Fitzgerald, D., and Seikel, R., 3D Modelling of Geology and Gravity Data: Summary Workflows for Minerals Exploration, *in* Proceedings 2013: East Asia: Geology, Exploration Technologies and Mines - Bali2013, p. 24-26.

Gourley, J. R., Byrne, T., Chan, Y.-C., Wu, F., and Rau, R.-J., 2007, Fault geometries illuminated from seismicity in central Taiwan: Implications for crustal scale structural boundaries in the northern Central Range: Tectonophysics, v. 445, no. 3-4, p. 168-185.

Hatcher, R. D., and Williams, R. T., 1986, Mechanical model for single thrust sheets Part I: taxonomy of crystalline thrust sheets and their relationships to the mechanical behavior of orogenic belts: Geological Society of America Bulletin, v. 97, no. 8, p. 975-985.

Hickman, J. B., Wiltschko, D. V., Hung, J.-H., Fang, P., and Bock, Y., 2002, Structure and evolution of the active fold-and-thrust belt of southwestern Taiwan from Global Positioning System analysis: Geological Society of America Special Papers, v. 358, p. 75-92.

Ho, C.-S., 1988, An introduction to the geology of Taiwan: Explanatory text of the geological map of Taiwan, Taipei, Central Geological Survey

Hsu, H.-J., Wen, S., and Chen, C.-H., 2011, 3D topography of the Moho discontinuity in the Taiwan area as extracted from travel time inversion of PmP phases: Journal of Asian Earth Sciences, v. 41, no. 3, p. 335-343.

Hsu, Y.-J., Yu, S.-B., Simons, M., Kuo, L.-C., and Chen, H.-Y., 2009, Interseismic crustal deformation in the Taiwan plate boundary zone revealed by GPS observations, seismicity, and earthquake focal mechanisms: Tectonophysics, v. 479, no. 1–2, p. 4-18.

Huang, C.-Y., Wu, W.-Y., Chang, C.-P., Tsao, S., Yuan, P. B., Lin, C.-W., and Xia, K.-Y., 1997, Tectonic evolution of accretionary prism in the arc-continent collision terrane of Taiwan: Tectonophysics, v. 281, no. 1–2, p. 31-51.

Huang, C.-Y., Yuan, P. B., and Tsao, S. J., 2006, Temporal and spatial records of active arc-continent collision in Taiwan: A synthesis: Geological Society of America Bulletin, v. 118, no. 3-4, p. 274-288.

Huang, H.-H., Wu, Y.-M., Song, X., Chang, C.-H., Lee, S.-J., Chang, T.-M., and Hsieh, H.-H., 2014, Joint Vp and Vs tomography of Taiwan: Implications for subduction-collision orogeny: Earth and Planetary Science Letters, v. 392, no. 0, p. 177-191.

Huang, S.-T., Yang, K.-M., Hung, J.-H., Wu, J.-C., Ting, H.-H., Mei, W.-W., Hsu, S.-H., and Lee, M., 2004, Deformation Front Development at the Northeast Margin of the Tainan Basin, Tainan–Kaohsiung Area, Taiwan: Marine Geophysical Researches, v. 25, no. 1-2, p. 139-156.

Hung, J.-H., Wiltschko, D., Lin, H.-C., Hickman, J., B., Fang, P., and Bock, Y., 1999, Structure and Motion of the Southwestern Taiwan Fold and Thrust Belt: Terrestrial, Atmospheric and Oceanic Sciences, v. 10, no. 3, p. 543-568.

Jahn, B.-M., Chi, W.-R., and Yui, T.-F., 1992, A Late Permian formation of Taiwan (marbles from Chia-Li well No. 1): Pb-Pb isochron and Sr isotope evidence, and its regional geological significance: Journal of the Geological Society of China, v. 35, p. 193-218.

Jones, R. H., and Stewart, R. C., 1997, A method for determining significant structures in a cloud of earthquakes: Journal of Geophysical Research: Solid Earth, v. 102, no. B4, p. 8245-8254.

Kim, K.-H., Chen, K.-C., Wang, J.-H., and Chiu, J.-M., 2010, Seismogenic structures of the 1999 Mw 7.6 Chi-Chi, Taiwan, earthquake and its aftershocks: Tectonophysics, v. 489, no. 1-4, p. 119-127.

Kim, K.-H., Chiu, J.-M., Pujol, J., Chen, K.-C., Huang, B.-S., Yeh, Y.-H., and Shen, P., 2005, Three-dimensional VP and VS structural models associated with the active subduction and collision tectonics in the Taiwan region: Geophysical Journal International, v. 162, no. 1, p. 204-220.

Kuo-Chen, H., Wu, F. T., and Roecker, S. W., 2012, Three-dimensional P velocity structures of the lithosphere beneath Taiwan from the analysis of TAIGER and related seismic data sets: Journal of Geophysical Research, v. 117, no. B6.

Lacombe, O., and Mouthereau, F., 2002, Basement-involved shortening and deep detachment tectonics in forelands of orogens: Insights from recent collision belts (Taiwan, Western Alps, Pyrenees): Tectonics, v. 21, no. 4, p. 12-11-12-22.

Lacombe, O., Mouthereau, F., Angelier, J., and Deffontaines, B., 2001, Structural, geodetic and seismological evidence for tectonic escape in SW Taiwan: Tectonophysics, v. 333, no. 1–2, p. 323-345.

Lacombe, O., Mouthereau, F., Deffontaines, B., Angelier, J., Chu, H. T., and Lee, C. T., 1999, Geometry and Quaternary kinematics of fold-and-thrust units of southwestern Taiwan: Tectonics, v. 18, no. 6, p. 1198-1223.

Lee, J.-C., Angelier, J., and Chu, H.-T., 1997, Polyphase history and kinematics of a complex major fault zone in the northern Taiwan mountain belt: the Lishan Fault: Tectonophysics, v. 274, no. 1–3, p. 97-115.

Lee, Y.-H., Chen, C.-C., Liu, T.-K., Ho, H.-C., Lu, H.-Y., and Lo, W., 2006, Mountain building mechanisms in the Southern Central Range of the Taiwan Orogenic Belt — From accretionary wedge deformation to arc–continental collision: Earth and Planetary Science Letters, v. 252, no. 3-4, p. 413-422.

Lester, R., McIntosh, K., Van Avendonk, H. J. A., Lavier, L., Liu, C. S., and Wang, T. K., 2013, Crustal accretion in the Manila trench accretionary wedge at the transition from subduction to mountain-building in Taiwan: Earth and Planetary Science Letters, v. 375, no. 0, p. 430-440.

Lester, R., Van Avendonk, H. J. A., McIntosh, K., Lavier, L., Liu, C. S., Wang, T. K., and Wu, F., 2014, Rifting and magmatism in the northeastern South China Sea from wide-angle tomography and seismic reflection imaging: Journal of Geophysical Research: Solid Earth, v. 119, no. 3, p. 2305-2323.

Li, C.-F., Zhou, Z., Li, J., Hao, H., and Geng, J., 2007, Structures of the northeasternmost South China Sea continental margin and ocean basin: geophysical constraints and tectonic implications: Marine Geophysical Researches, v. 28, no. 1, p. 59-79.

Lin, A. T., Liu, C.-S., Lin, C.-C., Schnurle, P., Chen, G.-Y., Liao, W.-Z., Teng, L. S., Chuang, H.-J., and Wu, M.-S., 2008, Tectonic features associated with the overriding of an accretionary wedge on top of a rifted continental margin: An example from Taiwan: Marine Geology, v. 255, no. 3–4, p. 186-203.

Lin, A. T., and Watts, A. B., 2002, Origin of the West Taiwan basin by orogenic loading and flexure of a rifted continental margin: Journal of Geophysical Research: Solid Earth, v. 107, no. B9, p. 2185.

Lin, A. T., Watts, A. B., and Hesselbo, S. P., 2003, Cenozoic stratigraphy and subsidence history of the South China Sea margin in the Taiwan region: Basin Research, v. 15, no. 4, p. 453-478.

Lin, C.-H., 2007, Tomographic image of crustal structures across the Chelungpu fault: Is the seismogenic layer structure- or depth-dependent?: Tectonophysics, v. 443, no. 3-4, p. 271-279.

Malavieille, J., and Trullenque, G., 2009, Consequences of continental subduction on forearc basin and accretionary wedge deformation in SE Taiwan: Insights from analogue modeling: Tectonophysics, v. 466, no. 3-4, p. 377-394.

McIntosh, K., van Avendonk, H., Lavier, L., Lester, W. R., Eakin, D., Wu, F., Liu, C.-S., and Lee, C.-S., 2013, Inversion of a hyper-extended rifted margin in the southern Central Range of Taiwan: Geology.

Mouthereau, F., Deffontaines, B., Lacombe, O., and Angelier, J., 2002, Variations along the strike of the Taiwan thrust belt: Basement control on structural style, wedge geometry, and kinematics, *in* Byrne, T., and Liu, C. S., eds., Geology and Geophysics of an Arc-Continent Collision, Taiwan, Volume 358, Geological Society of America Special Papers, p. 31-54.

Mouthereau, F., and Lacombe, O., 2006, Inversion of the Paleogene Chinese continental margin and thick-skinned deformation in the Western Foreland of Taiwan: Journal of Structural Geology, v. 28, no. 11, p. 1977-1993.

Mouthereau, F., Lacombe, O., Deffontaines, B., Angelier, J., and Brusset, S., 2001, Deformation history of the southwestern Taiwan foreland thrust belt: insights from tectono-sedimentary analyses and balanced cross-sections: Tectonophysics, v. 333, no. 1–2, p. 293-318.

Mouthereau, F., and Petit, C., 2003, Rheology and strength of the Eurasian continental lithosphere in the foreland of the Taiwan collision belt: Constraints from seismicity, flexure, and structural styles: Journal of Geophysical Research: Solid Earth, v. 108, no. B11.

Pérez-Estaún, A., Bastida, F., Alonso, J. L., Marquinez, J., Aller, J., Alvarez-Marron, J., Marcos, A., and Pulgar, J. A., 1988, A thin-skinned tectonics model for an arcuate fold and thrust belt: The Cantabrian Zone (Variscan Ibero-Armorican Arc): Tectonics, v. 7, no. 3, p. 517-537.

Pérez-Estaún, A., Pulgar, J. A., Banda, E., and Alvarez-Marrón, J., 1994, Crustal structure of the external variscides in northwest spain from deep seismic reflection profiling: Tectonophysics, v. 232, no. 1–4, p. 91-118.

Poblet, J., and Lisle, R. J., 2011, Kinematic evolution and structural styles of fold-and-thrust belts, *in* Poblet, J., and Lisle, R. J., eds., Kinematic evolution and structural styles of fold-and-thrust belts, Volume 349, Geological Society, London, Special Publications, p. 1-24.

Price, R. A., 1981, The Cordilleran foreland thrust and fold belt in the southern Canadian Rocky Mountains: Geological Society, London, Special Publications, v. 9, no. 1, p. 427-448.

Rau, R.-J., and Wu, F. T., 1995, Tomographic imaging of lithospheric structures under Taiwan: Earth and Planetary Science Letters, v. 133, no. 3–4, p. 517-532.

Rodgers, J., 1990, Fold-and-thrust belts in sedimentary rocks; Part 1, Typical examples: American Journal of Science, v. 290, no. 4, p. 321-359.

Rodriguez-Roa, F. A., and Wiltschko, D. V., 2010, Thrust belt architecture of the central and southern Western Foothills of Taiwan: Geological Society, London, Special Publications, v. 348, no. 1, p. 137-168.

Sakaguchi, A., Yanagihara, A., Ujiie, K., Tanaka, H., and Kameyama, M., 2007, Thermal maturity of a fold–thrust belt based on vitrinite reflectance analysis in the Western Foothills complex, western Taiwan: Tectonophysics, v. 443, no. 3–4, p. 220-232.

Shaw, C.-L., 1996, Stratigraphic correlation and isopach maps of the Western Taiwan Basin: Terrestrial, Atmospheric and Oceanic Sciences, v. 7, p. 333-360.

Shyu, J. B. H., Sieh, K., Chen, Y.-G., and Liu, C.-S., 2005, Neotectonic architecture of Taiwan and its implications for future large earthquakes: Journal of Geophysical Research: Solid Earth, v. 110, no. B8, p. B08402.

Sibuet, J.-C., and Hsu, S.-K., 2004, How was Taiwan created?: Tectonophysics, v. 379, no. 1-4, p. 159-181.

Simoes, M., Avouac, J. P., Beyssac, O., Goffé, B., Farley, K. A., and Chen, Y.-G., 2007, Mountain building in Taiwan: A thermokinematic model: Journal of Geophysical Research, v. 112, no. B11.

Simoes, M., Beyssac, O., and Chen, Y.-G., 2012, Late Cenozoic metamorphism and mountain building in Taiwan: A review: Journal of Asian Earth Sciences, v. 46, no. 0, p. 92-119.

Srivastava, P., and Mitra, G., 1994, Thrust geometries and deep structure of the outer and lesser Himalaya, Kumaon and Garhwal (India): Implications for evolution of the Himalayan fold-and-thrust belt: Tectonics, v. 13, no. 1, p. 89-109.

Stanley, R. S., Hill, L. B., Chang, H. C., and Hu, H. N., 1981, A transect through the metamorphic core of the central mountains, southern Taiwan: Memoir of the Geological Society of China, v. 4, p. 443-473.

Suppe, J., 1976, Decollement Folding in Southwestern Taiwan: Petroleum Geology of Taiwan, v. 13, p. 25-35.

-, 1980, A retrodeformable cross section of northern Taiwan: Proceedings Geological Society of China, v. 23, p. 46-55.

-, 1981, Mechanics of mountain building and metamorphism in Taiwan: Memoir of the Geological Society of China, v. 4, p. 67-89.

-, 1984, Kinematics of arc-continent collision, flipping of subduction, and back-arc spreading near Taiwan: Memoir of the Geological Society of China, v. 6, p. 21-33.

-, 1986, Reactivated normal faults in the Western Taiwan fold-and-thrust belt: Memoir of the Geological Society of China, v. 7, p. 187-200.

Suppe, J., and Namson, J., 1979, Fault-Bend Origin of Frontal Folds of the Western Taiwan Fold-and-Thrust Belt: Petroleum Geology of Taiwan, v. 16, p. 1-18.

Tang, C.-C., Zhu, L., Chen, C.-H., and Teng, T.-L., 2011, Significant crustal structural variation across the Chaochou Fault, southern Taiwan: New tectonic implications for convergent plate boundary: Journal of Asian Earth Sciences, v. 41, no. 6, p. 564-570.

Tang, Q., and Zheng, C., 2010, Seismic Velocity Structure and Improved Seismic Image of the Southern Depression of the Tainan Basin from Pre-Stack Depth Migration: Terrestrial, Atmospheric and Oceanic Sciences, v. 21, no. 5, p. 807-816.

Teng, L. S., 1990, Geotectonic evolution of late Cenozoic arc-continent collision in Taiwan: Tectonophysics, v. 183, no. 1–4, p. 57-76.

Teng, L. S., and Lin, A. T., 2004, Cenozoic tectonics of the China continental margin: insights from Taiwan, *in* Malpas, J., Fletcher, C. J. N., Ali, J. R., and Aitchison, J. C., eds., Aspects of the Tectonic Evolution of China, Volume 226, Geological Society, London, Special Publications, p. 313-332.

Thomas, W. A., 2006, Tectonic inheritance at a continental margin: GSA Today, v. 16, no. 2, p. 4-11.

Tillman, K. S., and Byrne, T. B., 1995, Kinematic analysis of the Taiwan Slate Belt: Tectonics, v. 14, no. 2, p. 322-341.

Ustaszewski, K., Wu, Y.-M., Suppe, J., Huang, H.-H., Chang, C.-H., and Carena, S., 2012, Crust–mantle boundaries in the Taiwan–Luzon arc-continent collision system determined from local earthquake tomography and 1D models: Implications for the mode of subduction polarity reversal: Tectonophysics, v. 578, no. 0, p. 31-49.

Wang, H.-L., Chen, H.-W., and Zhu, L., 2010a, Constraints on average Taiwan Reference Moho Discontinuity Model-receiver function analysis using BATS data: Geophysical Journal International, v. 183, no. 1, p. 1-19.

Wang, H.-L., Zhu, L., and Chen, H.-W., 2010b, Moho depth variation in Taiwan from teleseismic receiver functions: Journal of Asian Earth Sciences, v. 37, no. 3, p. 286-291.

Wiltschko, D. V., Hassler, L., Hung, J.-H., and Liao, H.-S., 2010, From accretion to collision: Motion and evolution of the Chaochou Fault, southern Taiwan: Tectonics, v. 29, no. 2.

Wu, F. T., Chang, C.-H., and Wu, Y.-M., 2004, Precisely relocated hypocentres, focal mechanisms and active orogeny in Central Taiwan, *in* Malpas, J., Fletcher, C. J. N., Ali, J. R., and Aitchison, J. C., eds., Aspects of the Tectonic Evolution of China, Volume 226, Geological Society, London, Special Publications, p. 333-354.

Wu, F. T., Kuo-Chen, H., and McIntosh, K. D., 2014, Subsurface Imaging, TAIGER Experiments and Tectonic Models of Taiwan: Journal of Asian Earth Sciences, no. 0.

Wu, F. T., Rau, R.-J., and Salzberg, D., 1997, Taiwan orogeny: Thin-skinned or lithospheric collision?: Tectonophysics, v. 274, no. 1-3, p. 191-220.

Wu, S.-K., Chi, W.-C., Hsu, S.-M., Ke, C.-C., and Wang, Y., 2013, Shallow Crustal Thermal Structures of Central Taiwan Foothills Region: Terrestrial, Atmospheric and Oceanic Sciences, v. 24, no. 4, p. 659-707.

Wu, Y.-M., Chang, C.-H., Zhao, L., Shyu, J. B. H., Chen, Y.-G., Sieh, K., and Avouac, J.-P., 2007, Seismic tomography of Taiwan: Improved constraints from a dense network of strong motion stations: Journal of Geophysical Research, v. 112, no. B8.

Wu, Y.-M., Chang, C.-H., Zhao, L., Teng, T. L., and Nakamura, M., 2008, A Comprehensive Relocation of Earthquakes in Taiwan from 1991 to 2005: Bulletin of the Seismological Society of America, v. 98, no. 3, p. 1471-1481.

Wu, Y.-M., Hsu, Y.-J., Chang, C.-H., Teng, L. S.-y., and Nakamura, M., 2010, Temporal and spatial variation of stress field in Taiwan from 1991 to 2007: Insights from comprehensive first motion focal mechanism catalog: Earth and Planetary Science Letters, v. 298, no. 3-4, p. 306-316.

Wu, Y. M., Chang, C. H., Hsiao, N.-C., and Wu, F., 2003, Relocation of the 1998 Rueyli, Taiwan, earthquake sequence using three-dimensions velocity structure with stations corrections: Terrestrial, Atmospheric and Oceanic Sciences, v. 14, no. 4, p. 421-430.

Yang, C.-C. B., Chen, W.-S., Wu, L.-C., and Lin, C.-W., 2007, Active deformation front delineated by drainage pattern analysis and vertical movement rates, southwestern Coastal Plain of Taiwan: Journal of Asian Earth Sciences, v. 31, no. 3, p. 251-264.

Yang, K.-M., Huang, S.-T., Wu, J.-C., Ting, H.-H., and Mei, W.-W., 2006, Review and New Insights on Foreland Tectonics in Western Taiwan: International Geology Review, v. 48, no. 10, p. 910-941.

Yeh, Y.-C., Hsu, S.-K., Doo, W.-B., Sibuet, J.-C., Liu, C.-S., and Lee, C.-S., 2012, Crustal features of the northeastern South China Sea: insights from seismic and magnetic interpretations: Marine Geophysical Research, v. 33, no. 4, p. 307-326.

Yen, H.-Y., and Hsieh, H.-H., 2010, A study on the compatibility of 3-D seismic velocity structures with gravity data of Taiwan: Terrestrial, Atmospheric and Oceanic Sciences, v. 21, no. 6, p. 897-904.

Yen, H.-Y., Yeh, Y.-H., Lin, C.-H., Chen, K.-J., and Tsai, Y.-B., 1995, Gravity Survey of Taiwan: Journal of Physics of the Earth, v. 43, no. 6, p. 685-696.

Yen, H.-Y., Yeh, Y.-H., and Wu, F. T., 1998, Two-dimensional crustal structures of Taiwan from gravity data: Tectonics, v. 17, no. 1, p. 104-111.

Yu, S.-B., Chen, H.-Y., and Kuo, L.-C., 1997, Velocity field of GPS stations in the Taiwan area: Tectonophysics, v. 274, no. 1–3, p. 41-59.

Yue, L.-F., Suppe, J., and Hung, J.-H., 2005, Structural geology of a classic thrust belt earthquake: the 1999 Chi-Chi earthquake Taiwan (Mw=7.6): Journal of Structural Geology, v. 27, no. 11, p. 2058-2083.

Zhou, D., Yu, H.-S., Xu, H.-H., Shi, X.-B., and Chou, Y.-W., 2003, Modeling of thermo-rheological structure of lithosphere under the foreland basin and mountain belt of Taiwan: Tectonophysics, v. 374, no. 3-4, p. 115-134.

Figure captions

Figure 1. Tectonic setting and major tectonostratigraphic zones of the Taiwan mountain belt. The -200 m isobath marks the current location of the shelf-slope break in the Eurasian margin. The structures on the Eurasian margin and the location of the deformation front offshore southwestern Taiwan are from Lin et al. (2008); Lin et al. (2003) and Yeh et al. (2012). The location of Fig. 2 is shown.

Figure 2. Major geological features of the study area. Fault traces are from our own field data. The structure offshore south-central Taiwan is from Lin et al. (2003), as are the contours representing the top of the basement. Fault abbreviations: BF, "B" Fault; ChF, Chaochou Fault; ChT, Changhua Thrust; LF, Lishan Fault; SkF, Shuilikeng Fault; YF, Yichu Fault. The locations of the boreholes discussed in the text are shown, as is the location of Figs. 3, 4, 6, and 7.

Figure 3. (A) Map of the observed and (B) calculated Bouguer anomaly data, and (C) the misfit map showing the difference between them. The observed Bouguer anomaly data are from Yen et al. (1995) and Yen and Hsieh (2010). Fault abbreviations are as in Fig. 2. Location of the maps is given in Fig. 2.

Figure 4. (A) Depth distribution of the 5.2 km/s isovelocity surface which we interpreted to be at or near the basement-cover interface, (B) depth distribution of the calculated basement-cover interface modeled from the gravity data, and (C) misfit map showing the difference between them. Note the coincidence between the major features in A and B. Fault abbreviations are as in Fig. 2. AU, Alishan Uplift. Location of the maps is given in Fig. 2.

Figure 5. (A) Vertical sections through the 3D P-wave velocity model (Wu et al., 2007) and the relocated (Wu et al., 2008) and collapsed seismicity dataset. These sections are orthogonal to the structural grain of the mountain belt, and (B) orthogonal to the strike of basin-bounding faults located on the margin and imaged beneath the Coastal Plain. Hypocenters were collapsed using the methodology of Jones and Stewart (1997). Collapsing involves the determination of statistical measurements for standard errors in the depth, latitude and longitude for each event (ERH and ERZ in the database of Wu et al. (2008)) and the clustering of events with overlapping error spheroids. A 3D spatial uncertainty of 4 standard deviations was used to truncate confidence ellipsoid and estimated variance in the data. Hypocenter movements were compared with χ^2 distribution and repeated until a minimum misfit was reached. For comparison between the un-collapsed and collapsed hypocenter locations see Fig. DR 3. Hypocenters (which are shown as black dots) are projected from 4.99 km on either side of the sections. Seismic events range up to >7 M_L. Dashed white line indicates the 5.2 km/s isovelocity line. The surface location of the major faults (fault abbreviations are as in Fig. 2) and the points of intersection between sections are shown. The location of the sections is indicated in Fig. 2.

Figure 6. Horizontal slices through the 3D P-wave velocity model (Wu et al., 2007) and the relocated (Wu et al., 2008) and collapsed seismicity dataset used in this study. The depth intervals are dependent on the vertical resolution of the 3D P-wave velocity model. Hypocenters (shown as black dots) are projected from 0.99 km on either side of the horizontal slices. Seismic events range up to >7 M_L. Dashed white line indicates the 5.2 km/s isovelocity line. Fault abbreviations are as in Fig. 2. Location of the maps is given in Fig. 2.

Figure 7. Geological map of the Coastal Plain and Western Foothills within the study area, and the collapsed earthquake hypocenters from 0 to 30 km depth. The blue line marks the seismicity front that is defined by a marked reduction in the number of earthquakes. Note how the seismicity front does not coincide with the Changhua Thrust tip line, which is often presented as the deformation front of the mountain belt. Colors and location of the map are given in Fig. 2.

Figure 8. Schematic block diagram showing the interpreted deep structure beneath the study area. Section X-X′ is drawn using the sedimentary thicknesses offshore southwest Taiwan proposed by Lin et al. (2003). Note how the deepening of the basement shown in section X-X′ can be interpreted to project onshore to section J-J′, where the large-scale structural architecture appears to be preserved. Eastward, the basement shallows across the Shuilikeng and Chaochou faults. The basement cover interface beneath the Coastal Plain and the Western Foothills appears to be acting as an extensive zone of detachment (DT) that, eastward, merges with the deep trace of the Shuilikeng and Chaochou faults. Fault abbreviations are as in Fig. 2.

Figure 1
Click here to download Figure: Fig. 1.pdf

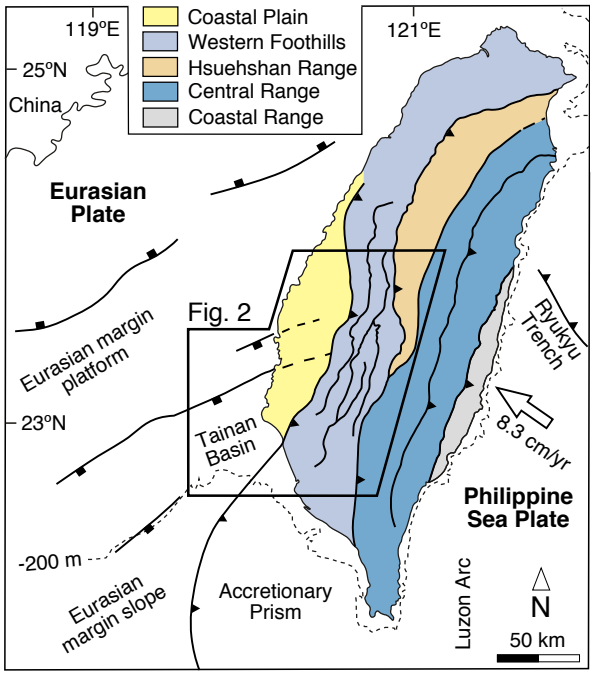

Fig. 1. Camanni et al.

Figure 2
Click here to download Figure: FIG. 2.pdf

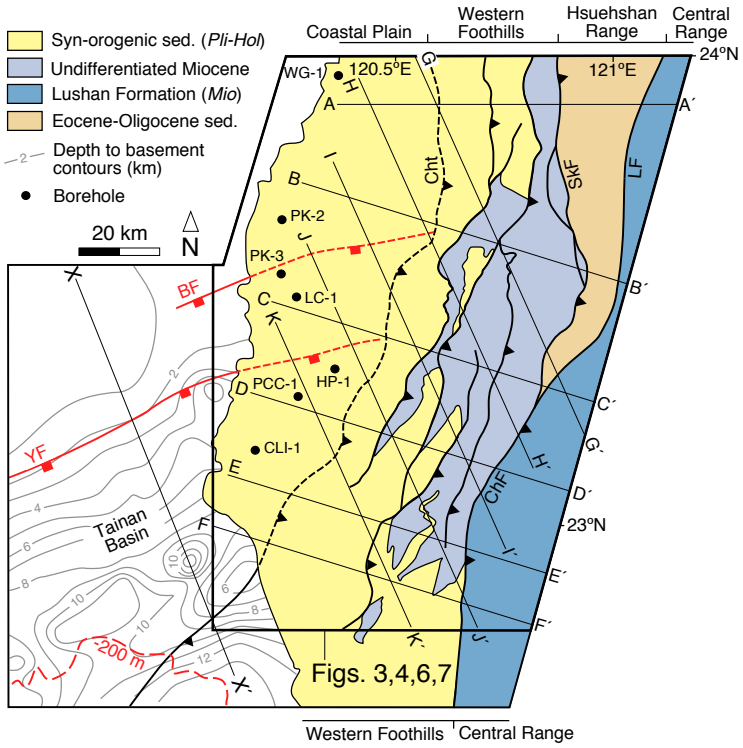

Fig. 2. Camanni et al.

Figure 3
Click here to download Figure: Fig. 3.pdf

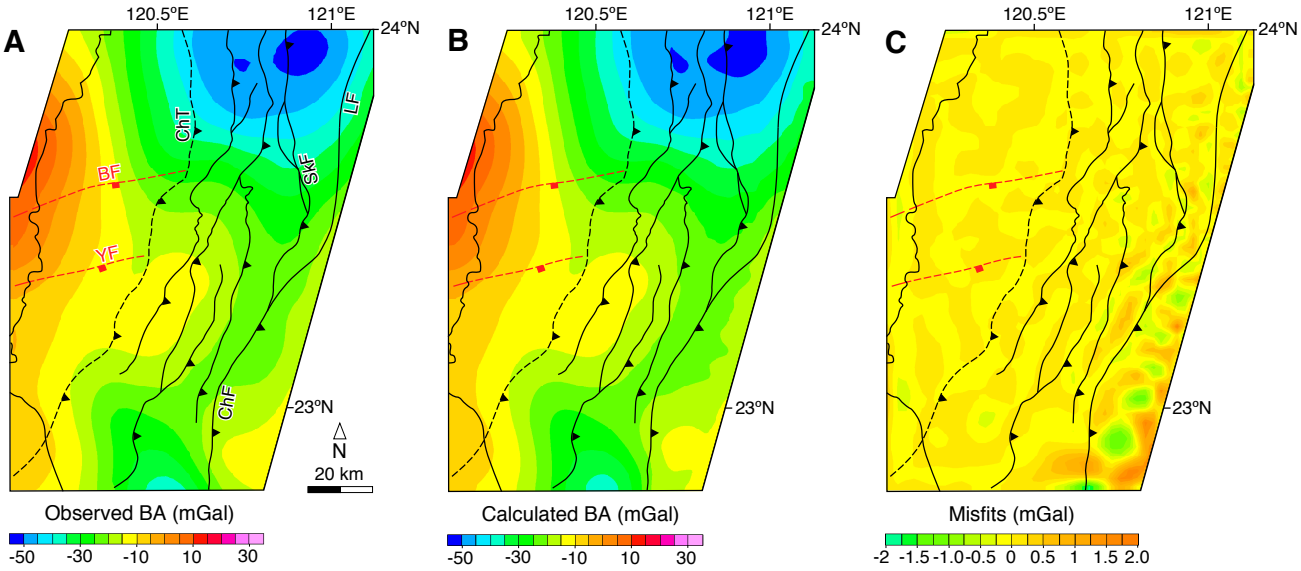

Fig. 3. Camanni et al.

Figure 4
Click here to download Figure: Fig. 4.pdf

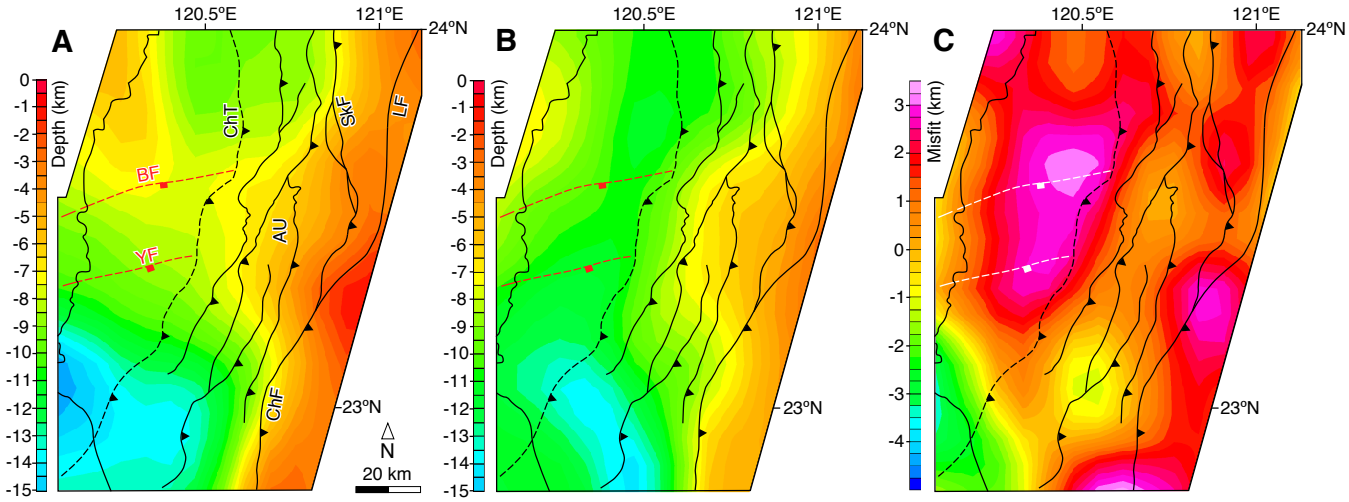

Fig. 4. Camanni et al.

Figure 5
Click here to download Figure: FIG. 5.pdf

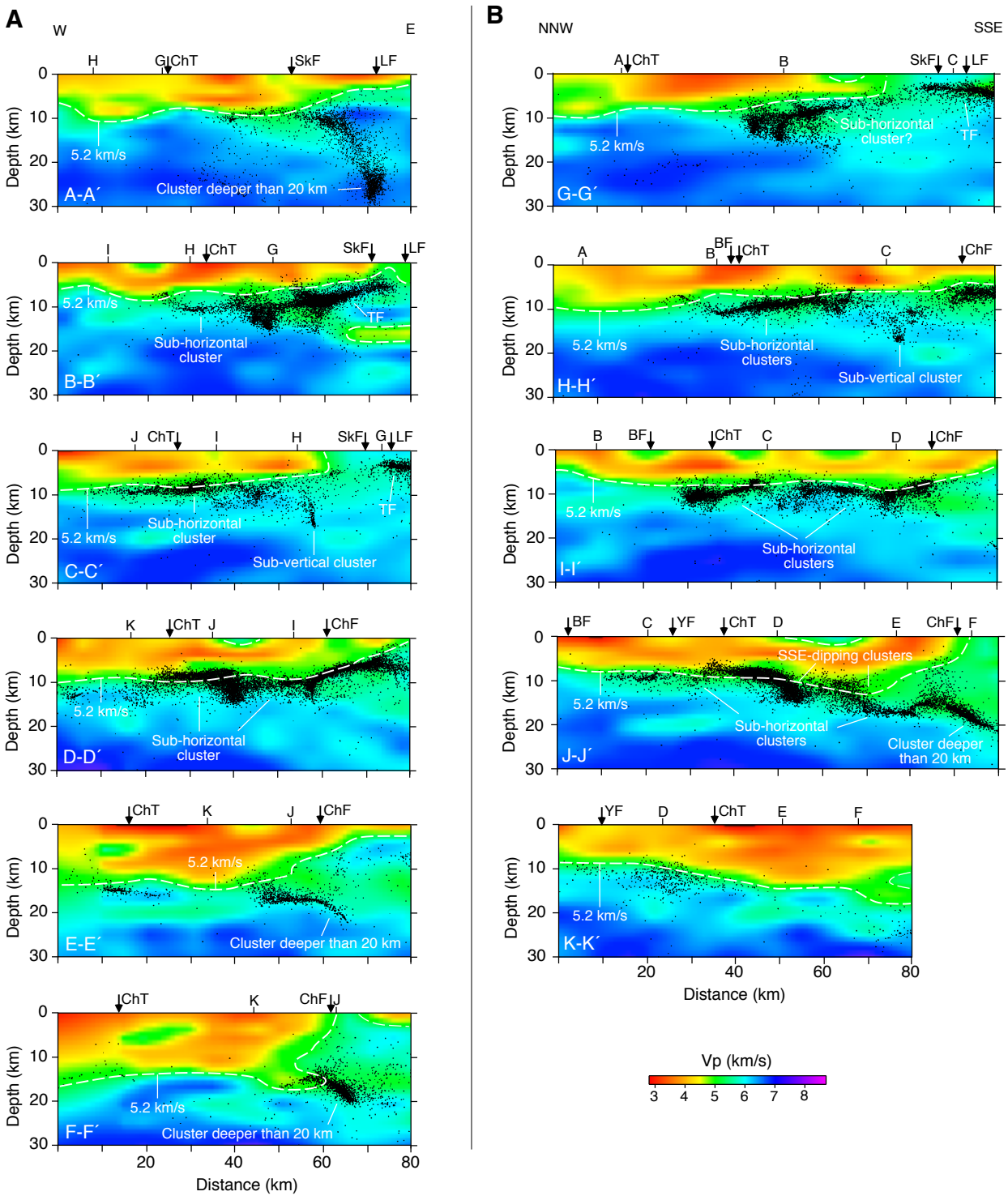

Fig. 5. Camanni et al.

Figure 6
Click here to download Figure: Fig. 6.pdf

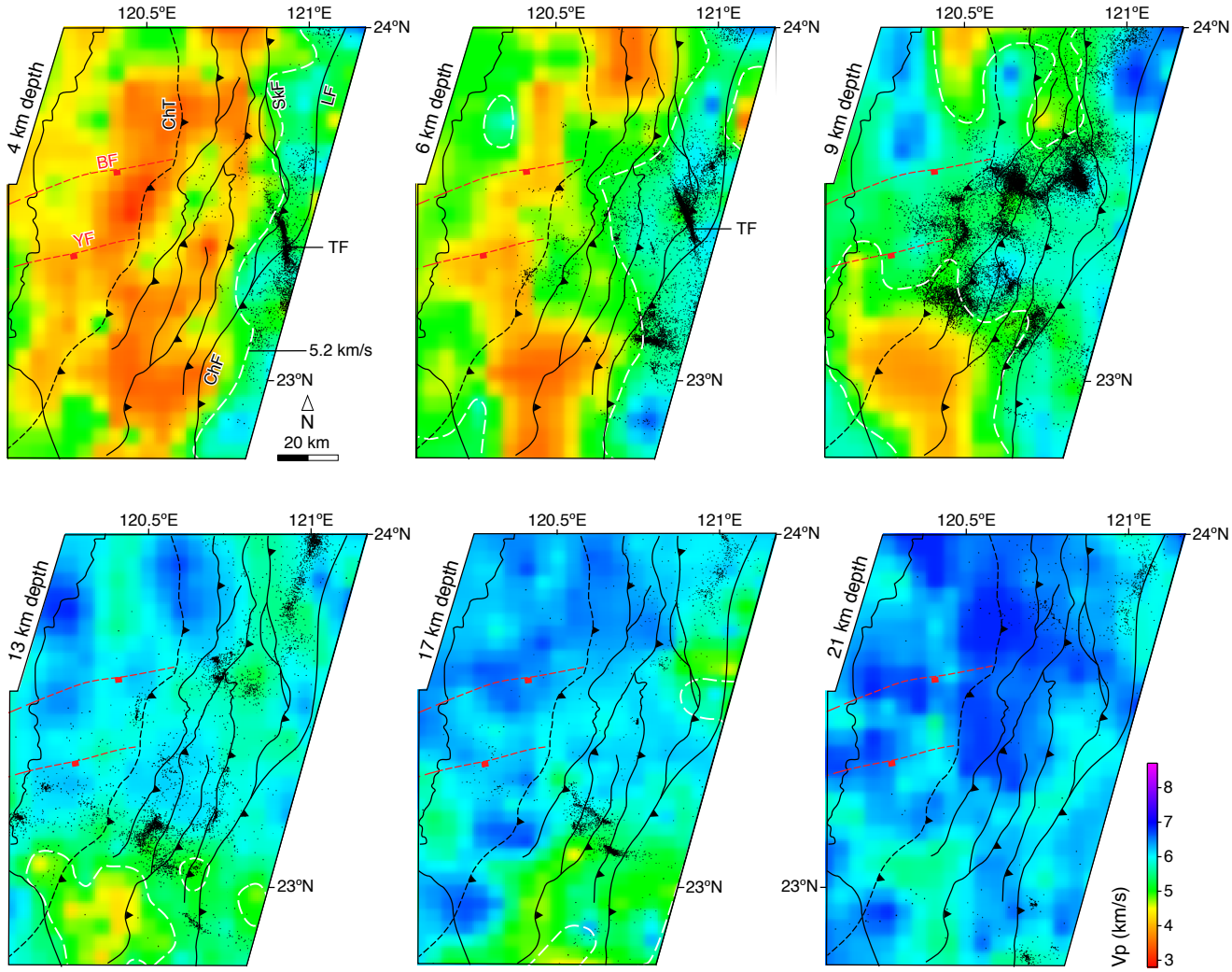

Fig. 6. Camanni et al.

Figure 7
Click here to download Figure: FIG. 7.pdf

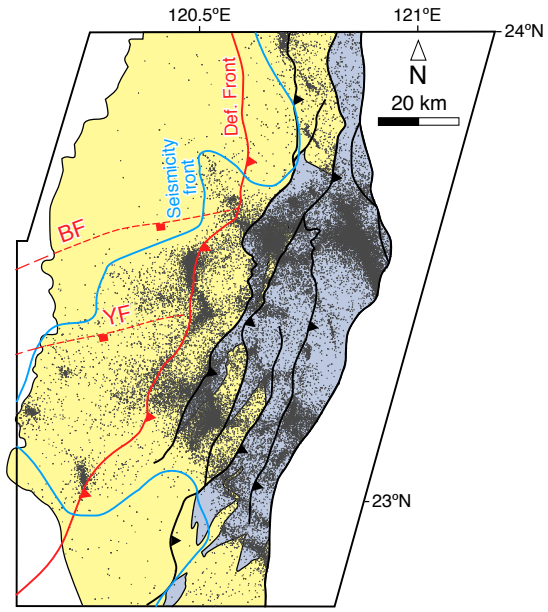

Fig. 7. Camanni et al.

Figure 8
Click here to download Figure: FIG. 8.pdf

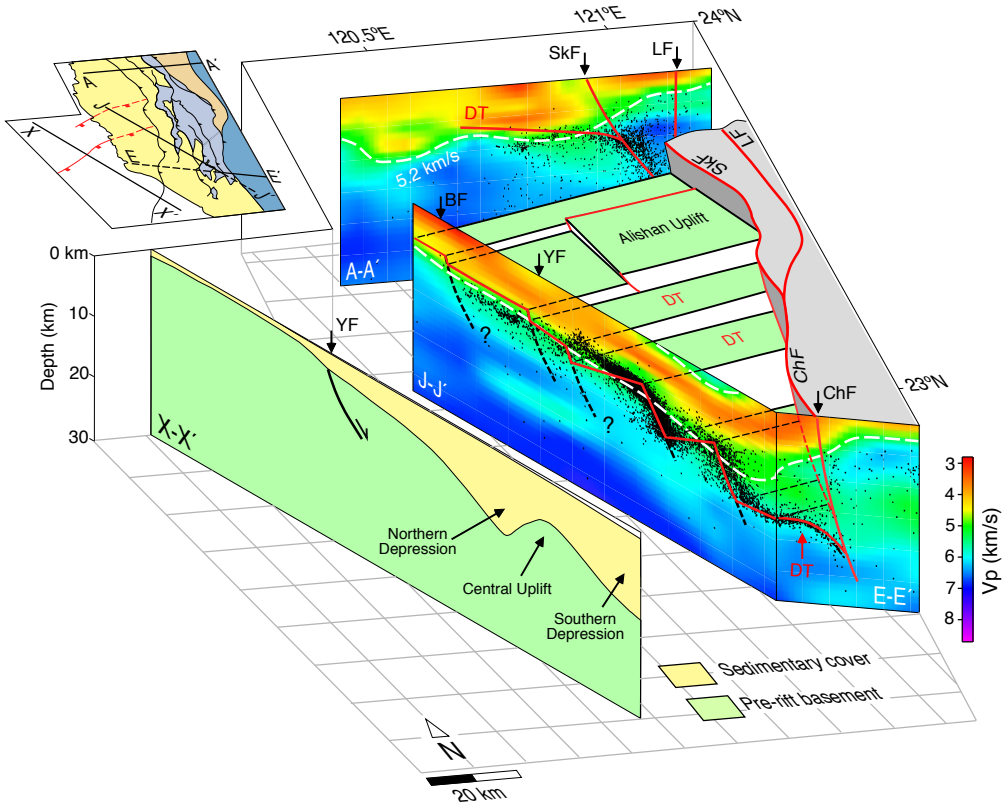

Fig. 8. Camanni et al.

Chapter 3 - Overall summary

3.1. Summary of results

3.1.1. The structure and kinematics of the Shuilikeng Fault

3.1.1.1. The Shuilikeng Fault at the surface

The Shuilikeng Fault at the surface clearly demarcates the contact between the Miocene rocks of the Western Foothills and the Eocene to Oligocene rocks of the Hsuehshan Range (Geological maps 1 and 2). In particular, results of the mapping indicate that, rather than being a single discrete feature, the Shuilikeng Fault is defined by a fault system with faults and folds that splay off the main fault in both its hanging wall and footwall (such as, for example, the Guaosing and Alenkeng faults; Geological map 2). Results of the mapping also indicate that there are notable changes in the map pattern of the fault that take place, from north to south, across the Choshui River (Geological map 2). To the north of the Choshui River, the Shuilikeng Fault has a rectilinear map pattern in which its trace cuts roughly straight across the topography, suggesting that it has a steep dip at the surface. South of the Choshui River, the Shuilikeng Fault displays an anastomosing map pattern in which two fault-bound lenses of steeply west dipping to locally overturned Miocene rocks can be identified (Geological map 2). In this area, the Tili Thrust approaches and is cut by the Shuilikeng Fault. This is especially apparent along the Zhuogun River (Geological map 2) where the cleavage in the hanging wall of the Tili Thrust is folded into an anticline whose forelimb directly abuts the Shuilikeng fault, suggesting that the Tili Thrust and the cleavage in its hangingwall are older features that likely pre-dated the emplacement of the Shuilikeng Fault.

Where observed in the field, the Shuilikeng Fault is everywhere a brittle feature composed of a fault core of breccia and fault gouge, bound by an up to several hundreds metre wide damage zone of intense faulting and folding. Fault and slickenfibre orientation data collected within the fault core from a number of locations along the Shuilikeng Fault indicate senses of slip that range from thrusting, to strike-slip, to extension. In several localities, slickenfibres developed on slip surfaces, small bedding displacements across discrete faults, and minor fold vergence indicate all three different senses of movement have taken place at different times in the same outcrop. Despite these local complexities, the averaged fault plane solutions indicate a nearly NW-SE to E-W average shortening direction (P axis). The T axes, however, range from steeply plunging to sub-horizontal, resulting in average fault plane solutions for individual outcrops that go from thrusting through to strike-slip. For further details on the kinematics of the Shuilikeng Fault at the surface see Figure 9 of Article 2 included in this thesis.

The damage zone of the Shuilikeng Fault comprises a high strain zone in which rocks in both the hanging wall and footwall are intensely deformed. A good example of this damage zone can be found along the Chenyulan River immediately south of the village of Dongpu, in the southern part of the mapped area in central Taiwan (Geological map 2). Here, the Eocene Shihpachungchi Formation in the hanging wall of the Shuilikeng Fault can be observed to directly overlie the Middle Miocene Shimen Formation. The Eocene rocks are strongly sheared and tightly folded into a west-verging anticline. The structure of the Miocene rocks in the footwall comprises a several hundred metre wide zone of intense brittle faulting and folding (Fig. 3.1). The majority of the faults are east-dipping and kinematic indicators such as slickenfibres on slip surfaces and small bedding displacements indicate an overall top-to-the-west sense of movement. Fold geometries in this area are often very complex, as thick-bedded sandstone units display various degrees of brecciation and boudinage, whereas more thin-bedded sandstone and shale units show disharmonic folding (Fig. 3.1).

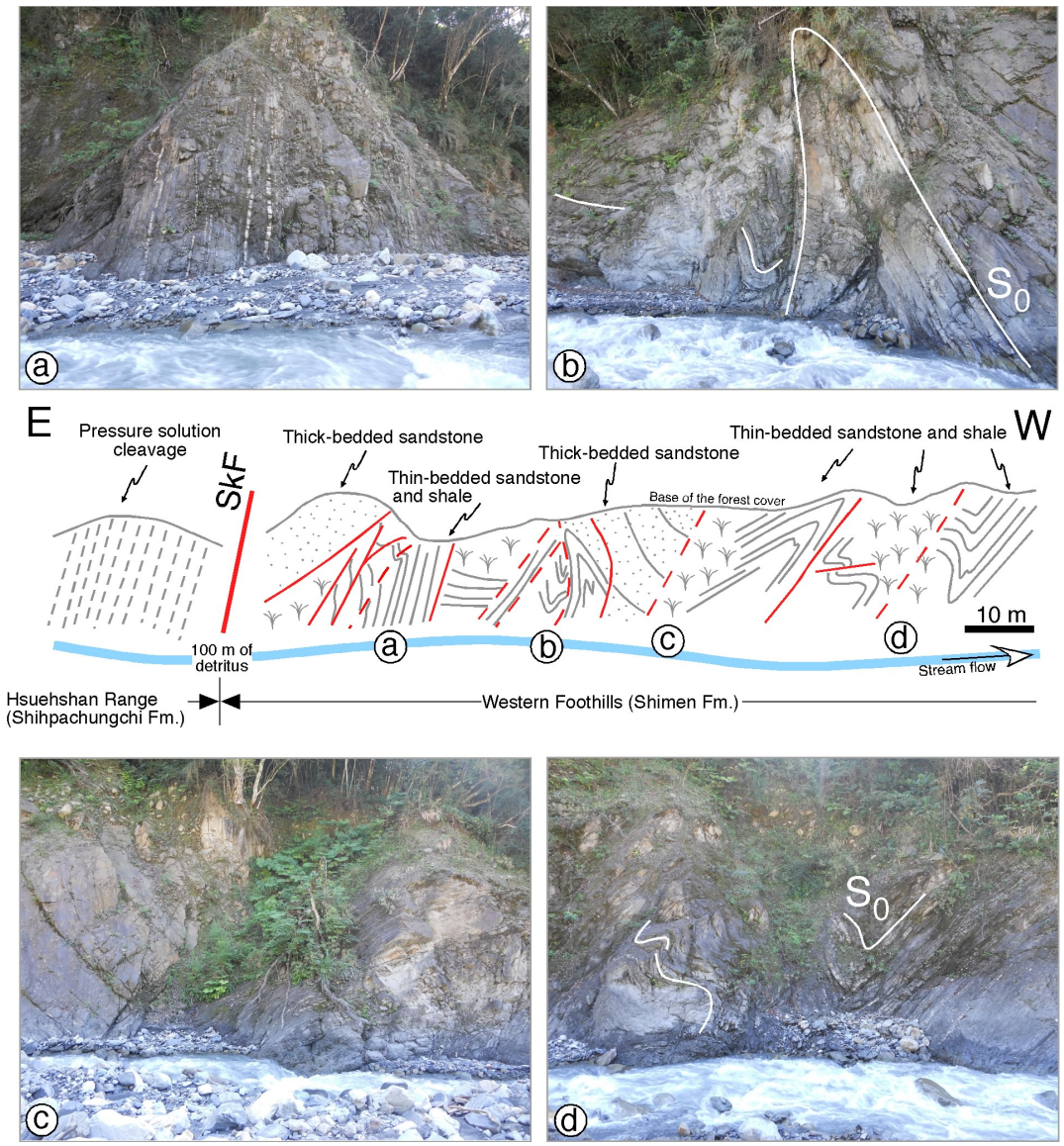

Fig. 3.1. Sketch and photographs of the damage zone developed within the Miocene that defines the Shuilikeng Fault in the southernmost part of the map area along the Chenyulan River. Note the disharmonic folding of the thin-bedded sandstone and shale units and the brecciation of the thick-bedded sandstone units. Figure from Article 2 included in this thesis.

3.1.1.2. The Shuilikeng Fault at depth

On the basis of the surface geology data, the Shuilikeng Fault can be interpreted to be steeply east-dipping and to extend deeply into the crust. Earthquake hypocentres helped to place constraints on the location and geometry of the Shuilikeng Fault at depth. In particular, earthquake hypocentres from beneath the surface trace of the Shuilikeng Fault are mainly distributed in an east-dipping cluster of seismicity (Fig. 3.2). This east-dipping cluster of seismicity, that starts at nearly 10 km and extends to c. 20 km depth, can be interpreted to illuminate the Shuilikeng Fault at depth. Earthquake focal mechanisms from within this east-dipping cluster of seismicity, and in particular the average principal strain axes derived from them, indicate that the average shortening direction is nearly NW-SE-oriented in consistence with the fault-slip data collected in the field. For further details on the kinematics of the Shuilikeng Fault at depth see Figure 11 of Article 2 included in this thesis. Furthermore, high P-wave

velocities shallow across the Shuilikeng Fault and clearly define a culmination beneath the Hsuehshan Range (Fig. 3.2).

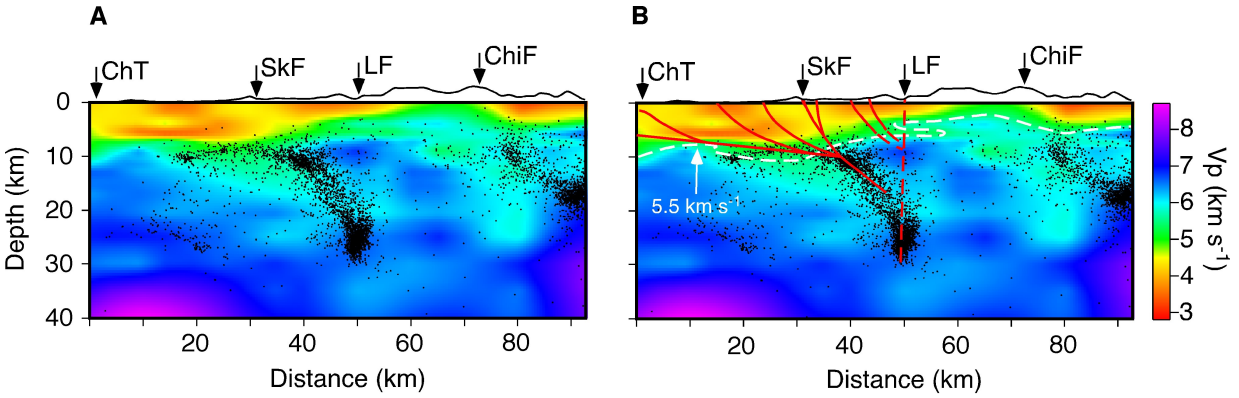

*Fig. 3.2. **A**, Uninterpreted, and **B**, interpreted vertical section through the P-wave velocity model of Wu et al. (2007). Hypocentres are projected from 4.99 km on either side of the sections. The dashed white line indicates the 5.5 km/s isovelocity line, which was used as a reference for the top of the basement. Location of the section is given in Geological map 1. Figure modified after Article 3 included in this thesis.*

The Shuilikeng Fault was highly active in central Taiwan during the 27 March 2013 6.2 M_L Nantou earthquake (e.g., Chuang et al., 2013) (Fig. 3.3). In particular, a number of the hypocentres associated with this seismic event, including the main shock, plot along the deep trace of the Shuilikeng Fault and have thrust focal mechanisms. The coincidence of the Nantou earthquake hypocentres with the location of the Shuilikeng Fault indicates that this fault is a significant structure contributing to mountain building in central Taiwan. It also indicates that a good knowledge of this fault was required not only for better understanding how the Taiwan mountain belt is evolving, but also for identifying fault source when assessing seismic hazard, as well as for correctly developing risk models and management protocols for seismic risk in this part of the orogen.

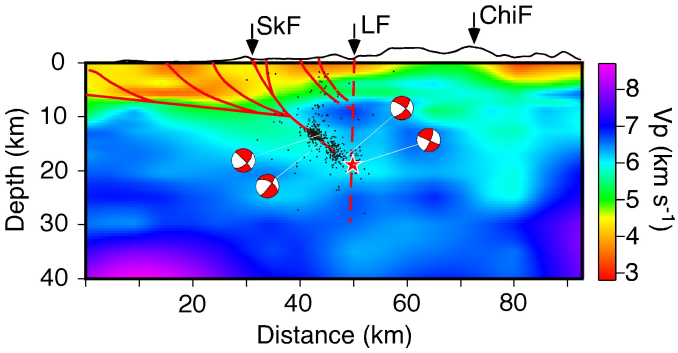

Fig. 3.3. P-wave velocity model from Fig. 3.2 with the geologically determined faults and the collapsed March 27th to April 15th 2013 Nantou sequence hypocentres. The red star indicates the location of the 6.2 M_L main shock. Hypocentres have been projected from 4.99 km on either side of the section for a total of 418 events. Figure from Article 3 included in this thesis.

3.1.2. Deep structure beneath south-central Taiwan

3.1.2.1. Basement-cover interface

A key for understanding the deep structure of south-central Taiwan is the location and geometry of the basement-cover interface because it provides information on basement involvement and on the possible reactivation of pre-existing structures. The trend of the basement-cover interface as defined by P-wave isovelocity surfaces comprised between 5.2 and 5.5 km/s, and tested using Bouguer anomaly inversion data, shows significant changes beneath the study area in south-central Taiwan (Fig. 3.4). Beneath the Coastal Plain and the Western Foothills the basement-cover interface appears to deepen from c. 8-10 km in the northern part of the map area, to c. 15 km depth in its southern part. An

exception to this overall southward deepening is represented by the Alishan area of the Western Foothills in the central part of the study area. Here, the basement-cover interface shallows to less than 5 km depth defining a basement culmination, here called the Alishan uplift (AU in Fig. 3.4). The shallowing of the basement-cover interface in this location within the study area appears to be taking place across the onshore projection of the northern bounding fault of the Tainan Basin, the "B" Fault, and across a nearly north-south-oriented feature that bound this basement culmination in the west.

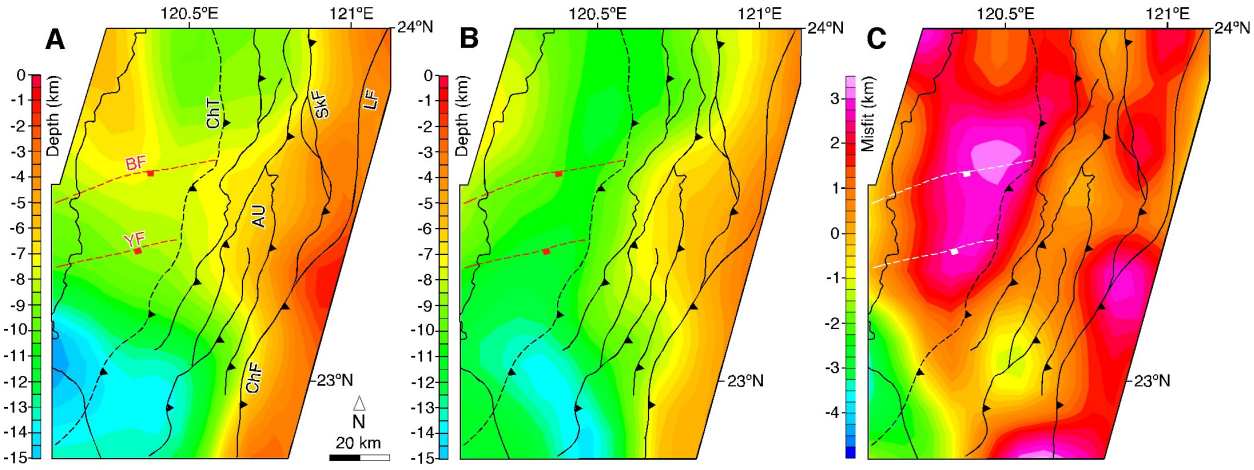

*Fig. 3.4. **A**, Depth distribution of the 5.2 km/s isovelocity surface in south-central Taiwan from the P-wave velocity model of Wu et al. (2007) which is interpreted to be at or near the basement-cover interface, **B**, depth distribution of the calculated basement-cover interface modelled from the gravity data, and **C**, misfit map showing the difference between them. Note the coincidence between the major features in **A** and **B**. AU, Alishan Uplift. Figure from Article 5 included in this thesis.*

However, the most prominent features that can be recognized throughout the study area is that across the Shuilikeng and the Chaochou faults there is a significant eastward shallowing of the basement-cover interface (Fig. 3.4). This shallowing of the basement-cover interface results in the occurrence of basement rocks at less than 4 km depth beneath the Hsuehshan Range in the northern half of the map area, and beneath the Central Range in its southern half. This shallow high velocity material beneath the Hsuehshan and Central ranges is a robust feature that has been recognized in a number of other studies, regardless of the tomographic inversion used (e.g., Kim et al., 2010; Kim et al., 2005; Lin, 2007; Rau and Wu, 1995).

3.1.2.2. Deep-seated fault systems

The locations and geometries of deep-seated faults show significant changes from beneath the Coastal Plain and the Western Foothills, to beneath the tectonostratigraphic zones in the east. Beneath the Coastal Plain and the Western Foothills, earthquake hypocentres form a well-defined, sub-horizontal cluster near the basement-cover interface as defined in the previous paragraph (Fig. 3.5). Earthquake hypocentres concentrated in this location of the crust suggest that in this part of the study area the basement-cover interface is acting as an extensive fault zone along which rocks of the sedimentary cover are being detached from the underlying basement. The earthquake hypocentre data also indicate that this detachment is roughly horizontal to moderately SSE-dipping, and locally has a rugose, or step-like, geometry (Fig. 3.5). This rugose geometry appears to reflect the large-scale structure of the Tainan Basin imaged offshore to the west (Fig. 3.5). Furthermore, seismic activity at the basement-cover interface appears to extend westward of the Changhua Thrust, which forms the surface deformation

front of the imbricate thrust system that defines the shallow structure of the Coastal Plain and Western Foothills, suggesting that deformation at depth in this location of the thrust belt might extend more to the west than at the surface (see, for example, Figure 7 of Article 5 included in this thesis).

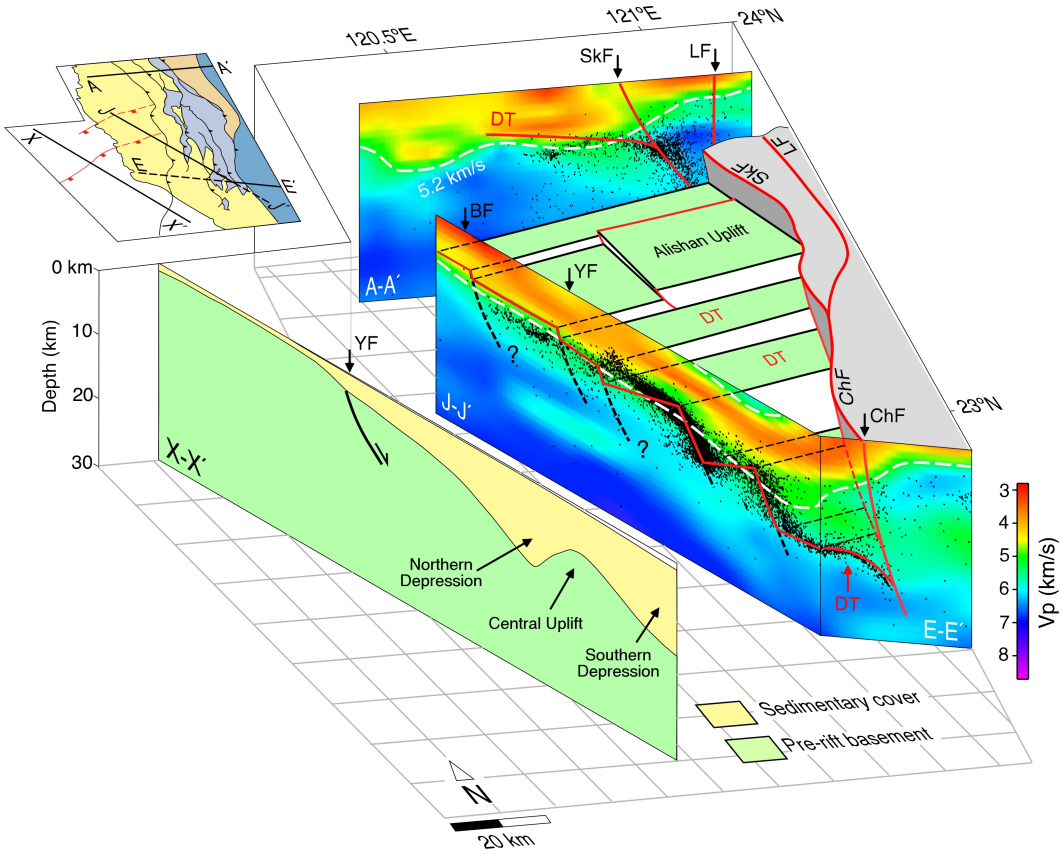

Fig. 3.5. Schematic block diagram showing the interpreted deep structure beneath the study area in south-central Taiwan. The locations of the sections are given in the small map of south-central Taiwan at the top on the left. Section X-X´ is drawn using the sedimentary thicknesses offshore southwest Taiwan proposed by Lin et al. (2003). Note how the deepening of the basement shown in section X-X´ can be interpreted to project onshore to section J-J´, where the large-scale structural architecture appears to be preserved. Eastward, the basement shallows across the Shuilikeng and Chaochou faults. The basement-cover interface beneath the Coastal Plain and the Western Foothills appears to be acting as an extensive zone of detachment (DT) that, eastward, merges with the deep trace of the Shuilikeng and Chaochou faults. Figure from Article 5 included in this thesis.

From approximately the Shuilikeng and Chaochou faults to the east, however, hypocentres form a moderately east-dipping cluster that locally extends to a depth of more than 20 km. In the northern part of the map area, as already described in the paragraph on the deep structure of the Shuilikeng Fault, this east-dipping cluster extends downward from the location of the Shuilikeng Fault (Fig. 3.2). Similarly, in the southern part of the map area, it appears to extend downward from the shallow location of the Chaochou Fault (Fig. 3.5). For further details on the distribution of earthquake hypocentres beneath this part of the study area see Figure 5 of Article 5 included in this thesis.

In central Taiwan, the deep part of the Shuilikeng Fault appears also to join, at nearly 20 km depth, a steeply west-dipping to sub-vertical elliptical cluster of hypocentres (Fig. 3.2). This cluster of hypocentres extends from 20 to 30 km depth downward from the shallow location of the Lishan Fault, which bounds the Hsuehshan Range in the east. Finally, farther east (Fig. 3.2), an open to tight east-dipping cluster of hypocentres, extending from 5 to 15 km depth, appears to illuminate the Chinma Fault, which places basement rocks on top of Eocene and younger slope-derived sediments that constitute the western part of the Central Range within the study area.

3.2. Discussion: the influence of variously oriented extensional basement faults inherited from the Eurasian margin on the structural development of the south-central Taiwan thrust belt

3.2.1. Introduction to the discussion

It is a common feature in a number of thrust belts worldwide that develop on a rifted continental margin that their structure is variably influenced by extensional basement faults inherited from the continental margin (e.g., Thomas, 2006). A distinction has been made in the literature between the influence of inherited extensional faults sub-parallel to the structural grain of a developing thrust belt, and that of those at an angle to it (e.g., Brown et al., 1999; Butler et al., 2006). Inherited extensional basement faults sub-parallel to the structural grain of a developing thrust belt are those that are better documented. During the structural development of a thrust belt, such faults can be fully or partially inverted often resulting in the uplift of basement rocks (e.g., Bonini et al., 2012; Coward et al., 1999; Coward et al., 1991; De Paola et al., 2006; Di Domenica et al., 2014; Jackson, 1980; Madritsch et al., 2008; Molinaro et al., 2005; Noguera and Rea, 2000; Sibson, 1995). In addition, they can determine the localization of the deformation within the sedimentary cover in their hanging walls causing the development of compressive structures such as buttresses and back-thrusts (e.g., Casciello et al., 2013; de Graciansky et al., 1989; Gillcrist et al., 1987), and can be truncated by newly-formed thrusts resulting in the development of footwall shortcuts displacing lenses of basement rocks (e.g., Calamita et al., 2010; Cooper et al., 1989; Hayward and Graham, 1989; McClay, 1989). On the other hand, the influence of inherited extensional basement faults at an angle to the structural grain of a developing thrust belt is less well-studied. Such oriented faults are generally thought to be reactivated as strike-slip faults during the structural evolution of a thrust belt, often resulting in the development of lateral structures (Brown et al., 1999; Butler et al., 2006; Turner et al., 2010), or wide strike-slip deformation zones (Dooley and Schreurs, 2012; Naylor et al., 1986) within the deforming sedimentary cover above them. It has been also shown that this interpretation in which inherited faults at an angle to the orientation of a developing thrust belt are reactivated as strike-slip faults is particularly valid for inherited faults with significant extensional displacements (Turner et al., 2010). Conversely, minor variations in sediment thickness across inherited extensional faults can cause the development of a through-going detachment at the basement-cover interface above which several closely spaced newly-formed thrusts are developed within the sedimentary cover (Turner et al., 2010).

Although the south-central Taiwan thrust belt is developing over the Eurasian continental margin, which has been shown to contain a number of fault-bound rift-related basins (e.g., Lin et al., 2003), early studies on its structure (Suppe, 1976, 1980b, 1981; Suppe and Namson, 1979), and interpretations based on earthquake hypocentres and analogue modelling data (Carena et al., 2002; Malavieille and Trullenque, 2009; Yue et al., 2005), led a number of authors to suggest that the south-central part of the orogen is evolving by thrusting above a shallowly east-dipping basal detachment (i.e., Taiwan main detachment of Carena et al., 2002) located within the sedimentary cover of the margin (Carena et al., 2002; Ding et al., 2001; Malavieille and Trullenque, 2009; Suppe, 1976, 1980b, 1981; Suppe and Namson, 1979; Yue et al., 2005). This structural interpretation implies that deformation throughout south-central Taiwan is confined to within the sedimentary cover of the Eurasian margin, and that the inherited extensional basement structure of the margin has not influenced the structure of the thrust belt.

There are, however, a number of other pieces of evidence in magnetotelluric (Bertrand et al., 2009, 2012), GPS (Chuang et al., 2013), earthquake hypocentre (Gourley et al., 2007; Lacombe and Mouthereau, 2002; Lacombe et al., 2001; Mouthereau and Petit, 2003; Wu et al., 2004; Wu et al., 2014; Wu et al., 1997; Wu et al., 2008a; Yue et al., 2005) and seismic tomography data (Huang et al., 2014; Kim et al., 2010; Kim et al., 2005; Kuo-Chen et al., 2012; Lin, 2007; Rau and Wu, 1995; Wu et al., 2007) which suggest that rocks below the interpreted detachment, and even the basement may also be involved in the deformation in much of south-central Taiwan. Results of this thesis not only support this idea, but also add new data that provide further constraints on this structural interpretation. The location of the recognized deep-seated faults within deep crustal levels suggests that these deep-seated faults might be somehow reusing segments of extensional basement faults inherited from the Eurasian continental margin. In the following two paragraphs, an interpretation of the relationships between the recognized deep-seated fault systems and extensional basement faults inherited from the Eurasian margin is provided in relation to their orientation with respect to the overall north-south structural grain of the thrust belt, as well as to their location within the thrust belt.

3.2.2. Inherited faults sub-parallel to the structural grain of south-central Taiwan

The deep-seated fault systems sub-parallel to the structural grain of south-central Taiwan recognized in this study are located beneath the Hsuehshan and Central ranges and appear to extend downward from the shallow location of major mapped faults such as, for example, the Shuilikeng and the Lishan faults in the central part of the study area, and the Chaochou Fault in the southern part of it. This suggests that deep-seated faults and faults mapped at the surface are likely linked to form deep-penetrating through-going faults that extend from the surface to the middle to lower crust (Fig. 3.5). In the central part of the study area, the Shuilikeng and the Lishan faults coincide with the bounding faults of the Hsuehshan Range, which is largely made up of Eocene syn-rift rocks that were deposited within the Hsuehshan Basin, which was located on the Eurasian continental margin prior to the Taiwan orogeny (Ho, 1988; Huang et al., 1997; Teng, 1990; Teng and Lin, 2004; Teng et al., 1991). These Eocene rocks now structurally overlie Miocene post-rift sediments, and have been exhumed from nearly 10 km depth (Sakaguchi et al., 2007). These evidences, together with the shallowing of the basement-cover interface across the Shuilikeng Fault, suggest that the Shuilikeng and the Lishan faults likely coincided with the basin-bounding faults of the Hsuehshan Basin (for an interpretation of the Lishan Fault as coinciding with the eastern bounding fault of the Hsuehshan Basin see also Huang et al. (1997); Lee et al. (1997); Lin et al. (2003); Teng and Lin (2004)) and that they are currently being inverted causing the inversion of the Hsuehshan Basin (see also Clark et al., 1993, for discussion of the Hsuehshan Range as a "pop-up" structure).

Results of this thesis indicate, furthermore, that a similar process in which basement rocks are uplifted can be interpreted to extend southward to the Central Range in the hanging wall of the Chaochou Fault. Although the Chaochou Fault was interpreted to be rooted deep into the crust (Ching et al., 2011; Mouthereau et al., 2002; Tang et al., 2011; Wiltschko et al., 2010), further studies are needed to determine whether it coincides or not with an inherited extensional fault which is being currently inverted. However, the uplifting of basement rocks in its hanging wall, together with its deep extension, suggest that the Shuilikeng, Lishan, and Chaochou faults are likely linked together to form a fault system in some way rooted into the middle or even the lower crust.

This deep-penetrating fault system appears to join westward with the detachment at the basement-cover interface, suggesting that it might form a ramp of it. However, with the datasets presented in this

study, no constraints can be placed on the possible deep continuation of this detachment in the east, beneath the Hsuehshan and Central ranges.

3.2.3. Inherited faults at an angle to the structural grain of south-central Taiwan

Beneath the Coastal Plain and the Western Foothills deformation at depth appears to be concentrated along a deep-seated detachment located at the basement-cover interface. This detachment is made up of SSE-dipping steps forming an angle to the structural grain of south-central Taiwan, alternated with sub-horizontal segments. The orientation of the SSE-dipping steps is similar to that of the extensional basement fault systems located on the Eurasian margin as derived using seismic reflection data from offshore of southwest Taiwan (e.g., Lin et al., 2003; Figs. 1.1 and 3.5), suggesting that SSE-dipping steps may coincide with segments of pre-existing extensional fault systems inherited from the Eurasian margin. Such inherited extensional faults at an angle to the structural grain of south-central Taiwan appear to be active (i.e., illuminated by earthquake hypocentres) in their upper parts where they juxtapose basement rocks in their footwalls against rocks of the sedimentary cover in their hanging walls. This evidence suggests that seismicity along SSE-dipping inherited faults beneath the study area is likely related to the detachment of the sedimentary cover from the basement rather than due to their inversion. This is further corroborated by the southward deepening of the basement-cover interface across these SSE-dipping faults, which suggests that they likely maintain the bulk of their extensional displacements.

Nevertheless, inherited faults at an angle to the structural grain of the thrust belt appear to have a significant control on the structural development of the Coastal Plain and Western Foothills in south-central Taiwan. In particular, they determine the geometry of the detachment at the basement-cover interface, which appears to have a number of steps coinciding with inherited extensional faults that define a step-like geometry for it. This rugose geometry for the detachment at the basement-cover interface differs significantly from that often suggested in other foreland thrusts belts worldwide such as, for example, the southern Canadian Rocky Mountains (e.g., Price, 1981), the Valley and Ridge province of the central and southern Appalachians (Rodgers, 1990), and the central Himalayan thrust belt (Srivastava and Mitra, 1994), where the detachment at the basement-cover interface is often presented as a nearly flat surface. However, this rugose geometry for the detachment appears to be confined to its westernmost part. Eastward, for example, it appears to be smoother (see, for example, Figure 5 of Article 5 included in this thesis). This can be related to the different amount of deformation in these two areas, as well as to the lack of extensional faults in the internal part of the Western Foothills. Furthermore, the rugose geometry for the detachment can be an artefact in earthquake hypocentre data, and more data are needed to definitively prove this geometry.

While this model in which pre-existing extensional fault systems at an angle to the structural grain of the thrust belt appear to maintain their original displacement may explain local structures within the Coastal Plain and Western Foothills in south-central Taiwan, the Alishan area represents a notable exception to this. In this area, there is a significant shallowing of the basement-cover interface across the northern bounding fault of the Tainan Basin, the “B” Fault. This can be interpreted to be developing as the result of the inversion of this fault, which appears to be reactivating together with a nearly north-south oriented basement fault. This interpretation is similar to that of other authors that suggest that pre-existing extensional faults within the Coastal Plain and Western Foothills of south-central Taiwan

are being inverted (e.g., Lacombe and Mouthereau, 2002; Mouthereau et al., 2002; Mouthereau and Lacombe, 2006; Mouthereau and Petit, 2003; Suppe, 1986).

3.2.4. Implications for the interpretation of the structure of south-central Taiwan

The new structural interpretation derived from this study in which the Shuilikeng, Lishan, and Chaochou faults appear to be deep-penetrating through-going features that extend from the surface to the middle to lower crust, has significant implications for how the south-central part of the Taiwan thrust belt is interpreted. In particular, it implies that these features would cut across the suggested basal detachment (e.g., Carena et al., 2002; Ding et al., 2001; Malavieille and Trullenque, 2009; Suppe, 1976, 1980b, 1981; Suppe and Namson, 1979; Yue et al., 2005) and would extend below it. There might not be, therefore, a structural linkage in the form of a shallow detachment between the Western Foothills, the Hsuehshan Range, and the Central Range that cut across, respectively, the Shuilikeng and the Lishan Fault in central Taiwan, and between the Western Foothills and the Central Range across the Chaochou Fault in the south. A consequence to this is that there might not be transfer of material between the Western Foothills, the Hsuehshan and Central ranges in central Taiwan, and that the outcropping syn-rift sediments of the Hsuehshan Basin and the underlying basement were uplifted along deep-penetrating faults rather than transported as thrust sheets from internal parts of the orogen above a shallow detachment as implied by previous structural interpretations of south central Taiwan (e.g., Carena et al., 2002; Suppe, 1976, 1980b, 1981; Suppe and Namson, 1979; Yue et al., 2005).

A large part of the deformation beneath the Coastal Plain and the Western Foothills in south-central Taiwan is taking place at the southward deepening basement-cover interface, which is acting as a regional level of detachment. Because of its overall location at ≥10 km depth (in particular in the southern part of the map area where the basement-cover interface appears to be located at c. 15 km depth), this detachment is difficult to relate with the imbricate thrust system developed at the surface (e.g., Alvarez-Marron et al., 2014; Brown et al., 2012; Suppe, 1976, 1981; Suppe and Namson, 1979; Yue et al., 2005). Furthermore, deformation along the detachment at the basement-cover interface extending westward of the deformation front of the shallow imbricate thrust system (i.e., the Changhua Thrust) further indicates the difficulty of relating the detachment at the basement-cover interface with the imbricate thrust system developed at the surface. The possibility of the frontal part of the mountain belt in this region evolving above two different detachment levels (a deeper level of detachment near the basement-cover interface, and the shallower, east-dipping basal thrust of the upper thrust system) could be an option that should be further investigated. A similar model in which the external part of the thrust belt is evolving above two levels of detachment was previously proposed by a number of authors, such as, for example, Lacombe and Mouthereau (2002), Rodriguez-Roa and Wiltschko (2010), Yue et al. (2005). Most of them, however, suggest that the deeper level of detachment is located somewhere into the basement, rather than at the basement-cover interface.

3.3. Conclusions

The multidisciplinary methodological approach adopted in this study, in which surface geology, earthquake hypocentres, focal mechanisms, and P-wave velocity data were combined together, has proven to be a valuable tool for investigating how the active Taiwan mountain belt is deforming. In particular, the integration of structural data collected in the field with earthquake hypocentre and focal mechanism data, revealed the location, linkage, structure and kinematics of active fault systems. P-wave velocity data helped place constraints on the trend of the basement-cover interface beneath the study area from which insights on the degree and mode of basement involvement in the deformation were derived.

Although the Taiwan mountain belt is often presented as evolving above a shallow basal thrust located within the sedimentary cover of the Eurasian margin, results of this study indicate that the structure of the south-central part of the mountain belt may differ significantly from this structural model. In particular, they indicate that the Coastal Plain and the Western Foothills of the mountain belt are evolving above a detachment, which coincides with the basement-cover interface. Locally, beneath this detachment, pre-existing basement extensional fault systems inherited from the Eurasian margin appear to preserve their extensional displacements. In the east, however, the Shuilikeng, Lishan, and Chaochou faults appear to form a through-going linked fault system that extend from the surface to at least the middle crust. In the hangingwall of the Shuilikeng and the Chaochou faults, the Hsuehshan Range and the western portion of the Central Range are defined by a notable shallowing of the basement-cover interface with the development of a regional basement culmination in which basement rocks are uplifted to near the surface. While for the Hsuehshan Range this structure can be interpreted as the result of the inversion of a basin that was located on the Eurasian continental margin prior to the Taiwan orogeny (i.e., the Hsuehshan Basin), more studies are needed to determine the mode of basement involvement beneath the Central Range.

Furthermore, observing the relationships between the angle that fault systems inherited from the Eurasian margin form with the structural grain of south-central Taiwan and their structural response when they become involved in the deformation, an example for how variously oriented inherited faults influence the structural development of south-central Taiwan was provided. In particular, inherited basement faults sub-parallel to the structural grain of south-central Taiwan, such as the Shuilikeng and the Lishan faults (and, likely, also the Chaochou Fault), are being inverted when they become involved in the deformation. On the contrary, most of the inherited basement faults at an angle to the structural grain of south-central Taiwan appear not to invert but do have, however, a significant control on the geometry of the detachment at the basement-cover interface beneath the external part of the mountain belt.

Acknowledgements

I am infinitely grateful to Dennis and Joaquina, my supervisors, for having closely supervised me through all the phases of this thesis, for their enthusiasm in helping me to improve my knowledge of geology and, above all, for having taught me (with a lot of patience) the craft of doing and communicating research. I also thank them for believing in me since the beginning and up to the end of this thesis, which gave me the confidence for proposing and defending new ideas. A big thanks also to Yih-Min, who always helped me sympathetically during my stays in Taiwan.

I'd like to thank colleagues from ICTJA, Alba, Alberto, Andrés, Bea, Conxi, David, Eduard, Emilio, Fulvio, Flavia, Guiomar, Helena, Ignacio, Israel, Jan, Juan, Juan Diego, Lavinia, Mar, Marcel, Maria Jesús, Martin, Massimiliano, Noemi, Olga, Paolo, Raquel, Riccardo, Siddique, Stefania, Stephanie, and Vinyet. I'd also like to thank the students of Yih-Min, Chi-Hsuan, Chung-Han, Han-Fang, Hsin-Hua, and his assistant and singer Ling-Mei. Hao-Tsu, Mien-Ming, 陳柏村 (Oden), and 姜彥麟 (wild pig Black) from the Central Geological Survey of Taiwan also deserve a big thank.

I'd like to thank my family, in particular my parents and my sister Stefania, as well as my friends scattered around the world, Agnese, Albi F., Albi M., Andrea, Enrica, Fred, Gabri, Gianlu, Giovanni, Giulia A., Giulia C., Giulia P., Irene, Isacco, Liuc, Luca, Luisa, Marco S., Marco T., Matteo, Mauro, Melissa, Maik, Sara, Serena, Silvia, Steo, and Virginia. Although geographically distant, I always felt you close to me over the last four years.

A huge thank to you, Sofia. You enlightened me a street also when there was no path. Thanks for sharing with me (with a lot of patience, you too!) the last four years.

A last welcome to Sally, who meanwhile has joined us.

References cited in the text

Alvarez-Marron, J., Brown, D., Camanni, G., Wu, Y.M., Kuo-Chen, H., 2014. Structural complexities in a foreland thrust belt inherited from the shelf-slope transition: Insights from the Alishan area of Taiwan. Tectonics 33, 1322–1339.

Angelier, J., 1986. Preface, in: Angelier, J., Blanchet, R., Ho, C.S., Le Pichon, X. (Eds.), Geodynamics of the Eurasia-Philippine Sea Plate Boundary. Tectonophysics, pp. IX-X.

Barton, P.J., 1986. The relationship between seismic velocity and density in the continental crust — a useful constraint? Geophysical Journal of the Royal Astronomical Society 87, 195-208.

Bertrand, E.A., Unsworth, M.J., Chiang, C.-W., Chen, C.-S., Chen, C.-C., Wu, F.T., Türkoğlu, E., Hsu, H.-L., Hill, G.J., 2009. Magnetotelluric evidence for thick-skinned tectonics in central Taiwan. Geology 37, 711-714.

Bertrand, E.A., Unsworth, M.J., Chiang, C.-W., Chen, C.-S., Chen, C.-C., Wu, F.T., Türkoğlu, E., Hsu, H.-L., Hill, G.J., 2012. Magnetotelluric imaging beneath the Taiwan orogen: An arc-continent collision. Journal of Geophysical Research 117.

Beyssac, O., Simoes, M., Avouac, J.P., Farley, K.A., Chen, Y.-G., Chan, Y.-C., Goffé, B., 2007. Late Cenozoic metamorphic evolution and exhumation of Taiwan. Tectonics 26.

Bonini, M., Sani, F., Antonielli, B., 2012. Basin inversion and contractional reactivation of inherited normal faults: A review based on previous and new experimental models. Tectonophysics 522–523, 55-88.

Briais, A., Patriat, P., Tapponnier, P., 1993. Updated interpretation of magnetic anomalies and seafloor spreading stages in the south China Sea: Implications for the Tertiary tectonics of Southeast Asia. Journal of Geophysical Research: Solid Earth 98, 6299-6328.

Brown, D., Alvarez-Marron, J., Perez-Estaun, A., Puchkov, V., Ayala, C., 1999. Basement influence on foreland thrust and fold belt development: an example from the southern Urals. Tectonophysics 308, 459-472.

Brown, D., Alvarez-Marron, J., Schimmel, M., Wu, Y.-M., Camanni, G., 2012. The structure and kinematics of the central Taiwan mountain belt derived from geological and seismicity data. Tectonics 31.

Butler, R.W.H., Tavarnelli, E., Grasso, M., 2006. Structural inheritance in mountain belts: An Alpine–Apennine perspective. Journal of Structural Geology 28, 1893-1908.

Byrne, T., Chan, Y.C., Rau, R.J., Lu, C.Y., Lee, Y.H., Wang, Y.J., 2011. The Arc–Continent Collision in Taiwan, in: Brown, D., Ryan, P.D. (Eds.), Arc-Continent Collision. Springer Berlin Heidelberg, New York, pp. 213-245.

Calamita, F., Satolli, S., Scisciani, V., Esestime, P., Pace, P., 2010. Contrasting styles of fault reactivation in curved orogenic belts: Examples from the Central Apennines (Italy). Geological Society of America Bulletin 123, 1097-1111.

Carena, S., Suppe, J., Kao, H., 2002. Active detachment of Taiwan illuminated by small earthquakes and its control of first-order topography. Geology 30, 935-938.

Casciello, E., Esestime, P., Cesarano, M., Pappone, G., Snidero, M., Vergés, J., 2013. Lower plate geometry controlling the development of a thrust-top basin: the tectonosedimentary evolution of the Ofanto basin (Southern Apennines). Journal of the Geological Society 170, 147-158.

Castelltort, S., Nagel, S., Mouthereau, F., Lin, A.T.-S., Wetzel, A., Kaus, B., Willett, S., Chiang, S.-P., Chiu, W.-Y., 2011. Sedimentology of early Pliocene sandstones in the south-western Taiwan foreland: Implications for basin physiography in the early stages of collision. Journal of Asian Earth Sciences 40, 52-71.

Chen, A., Yang, Y.-L., 1996. Lack of Compressional Overprint on the Extensional Structure in Offshore Tainan and the Tectonic Implications. Terrestrial, Atmospheric and Oceanic Sciences 7, 505-522.

Chen, M.-M., Yu, N.-T., Chu, H.-T., Shea, K.-S., Hsieh, Y.-C., 2009. Larger Foraminifera in the So-called 'Meichi Sandstone' of Wujie Area, Sothern Hsuehshan Range. Central Geological Survey Special Publication 22, 227–242.

Chen, W., Yen, I., Fengler, K., Rubin, C., Yang, C., Yang, H., Chang, H., Lin, C., Lin, W., Liu, Y., 2007. Late Holocene paleoearthquake activity in the middle part of the Longitudinal Valley fault, eastern Taiwan. Earth and Planetary Science Letters 264, 420-437.

Ching, K.-E., Johnson, K.M., Rau, R.-J., Chuang, R.Y., Kuo, L.-C., Leu, P.-L., 2011. Inferred fault geometry and slip distribution of the 2010 Jiashian, Taiwan, earthquake is consistent with a thick-skinned deformation model. Earth and Planetary Science Letters 301, 78-86.

Chuang, R.Y., Johnson, K.M., Wu, Y.-M., Ching, K.-E., Kuo, L.-C., 2013. A midcrustal ramp-fault structure beneath the Taiwan tectonic wedge illuminated by the 2013 Nantou earthquake series. Geophysical Research Letters 40.

Clark, M.B., Fisher, D.M., Lu, C.-Y., Chen, C.-H., 1993. Kinematic analyses of the Hsüehshan Range, Taiwan: A large-scale pop-up structure. Tectonics 12, 205-217.

Cooper, M.A., Williams, G.D., de Graciansky, P.C., Murphy, R.W., Needham, T., de Paor, D., Stoneley, R., Todd, S.P., Turner, J.P., Ziegler, P.A., 1989. Inversion tectonics — a discussion, in: Cooper, M.A., Williams, G.D. (Eds.), Inversion Tectonics. Geological Society, London, Special Publications, pp. 335-347.

Covey, M., 2009. The Evolution of Foreland Basins to Steady State: Evidence from the Western Taiwan Foreland Basin, Foreland Basins. Blackwell Publishing Ltd., pp. 77-90.

Coward, M.P., De Donatis, M., Mazzoli, S., Paltrinieri, W., Wezel, F.-C., 1999. Frontal part of the northern Apennines fold and thrust belt in the Romagna-Marche area (Italy): Shallow and deep structural styles. Tectonics 18, 559-574.

Coward, M.P., Gillcrist, R., Trudgill, B., 1991. Extensional structures and their tectonic inversion in the Western Alps. Geological Society, London, Special Publications 56, 93-112.

de Graciansky, P.C., Dardeau, G., Lemoine, M., Tricart, P., 1989. The inverted margin of the French Alps and foreland basin inversion, in: Cooper, M.A., Williams, G.D. (Eds.), Inversion Tectonics. Geological Society, London, Special Publications, pp. 87-104.

De Paola, N., Mirabella, F., Barchi, M.R., Burchielli, F., 2006. Early orogenic normal faults and their reactivation during thrust belt evolution: the Gubbio Fault case study, Umbria-Marche Apennines (Italy). Journal of Structural Geology 28, 1948-1957.

Deng, J.-M., Wang, T., Yang, B., Lee, C.-S., Liu, C.-S., Chen, S.-C., 2012. Crustal velocity structure off SW Taiwan in the northernmost South China Sea imaged from TAIGER OBS and MCS data. Mar Geophys Res 33, 327-349.

Di Domenica, A., Bonini, L., Calamita, F., Toscani, G., Galuppo, C., Seno, S., 2014. Analogue modeling of positive inversion tectonics along differently oriented pre-thrusting normal faults: An application to the Central-Northern Apennines of Italy. Geological Society of America Bulletin.

Ding, W.-W., Li, J.-B., Li, M.-B., Qiu, X.-L., Fang, Y.-X., Tang, Y., 2008. A Cenozoic tectono-sedimentary model of the Tainan Basin, the South China Sea: evidence from a multi-channel seismic profile. Journal of Zhejiang University SCIENCE A 9, 702-713.

Ding, Z.Y., Yang, Y.Q., Yao, Z.X., Zhang, G.H., 2001. A thin-skinned collisional model for the Taiwan orogeny. Tectonophysics 332, 321-331.

Dooley, T.P., Schreurs, G., 2012. Analogue modelling of intraplate strike-slip tectonics: A review and new experimental results. Tectonophysics 574-575, 1-71.

Fisher, D.M., Lu, C.-Y., Chu, H.-T., 2002. Taiwan slate belt: Insights into the ductile interior of an arc-continent collision. Geological Society of America Special Papers 358, 93-106.

Fisher, D.M., Willett, S., En-Chao, Y., Clark, M.B., 2007. Cleavage fronts and fans as reflections of orogen stress and kinematics in Taiwan. Geology 35, 65-68.

Gibson, H., Sumpton, J., Fitzgerald, D., Seikel, R., 2013. 3D Modelling of Geology and Gravity Data: Summary Workflows for Minerals Exploration, 2013: East Asia: Geology, Exploration Technologies and Mines - Bali, pp. 24-26.

Gillcrist, R., Coward, M.P., Mugnier, J., 1987. Structural inversion and its controls: examples from the Alpine foreland and the French Alps. Geodinamica Acta 1, 5-34.

Gourley, J.R., Byrne, T., Chan, Y.-C., Wu, F., Rau, R.-J., 2007. Fault geometries illuminated from seismicity in central Taiwan: Implications for crustal scale structural boundaries in the northern Central Range. Tectonophysics 445, 168-185.

Hayes, D.E., Nissen, S.S., 2005. The South China sea margins: Implications for rifting contrasts. Earth and Planetary Science Letters 237, 601-616.

Hayward, A.B., Graham, R.H., 1989. Some geometrical characteristics of inversion, in: Cooper, M.A., Williams, G.D. (Eds.), Inversion Tectonics. Geological Society, London, Special Publications, pp. 17-39.

Hickman, J.B., Wiltschko, D.V., Hung, J.-H., Fang, P., Bock, Y., 2002. Structure and evolution of the active fold-and-thrust belt of southwestern Taiwan from Global Positioning System analysis. Geological Society of America Special Papers 358, 75-92.

Ho, C.-S., 1988. An introduction to the geology of Taiwan: Explanatory text of the geological map of Taiwan. Central Geological Survey Taipei.

Hong, E., 1997. Evolution of Pliocene to Pleistocene sedimentary environments in an arc-continent collision zone: Evidence from the analyses of lithofacies and ichnofacies in the southwestern foothills of Taiwan. Journal of Asian Earth Sciences 15, 381-392.

Hsu, S.-K., Yeh, Y.-c., Doo, W.-B., Tsai, C.-H., 2004. New Bathymetry and Magnetic Lineations Identifications in the Northernmost South China Sea and their Tectonic Implications. Mar Geophys Res 25, 29-44.

Hsu, Y.-J., Yu, S.-B., Simons, M., Kuo, L.-C., Chen, H.-Y., 2009. Interseismic crustal deformation in the Taiwan plate boundary zone revealed by GPS observations, seismicity, and earthquake focal mechanisms. Tectonophysics 479, 4-18.

Huang, C.-Y., Chi, W.-R., Yan, Y., Yang, K.-M., Liew, P.-M., Wu, M.-S., Wu, J.-C., Zhang, C., 2013. The first record of Eocene tuff in a Paleogene rift basin near Nantou, Western Foothills, central Taiwan. Journal of Asian Earth Sciences 69, 3-16.

Huang, C.-Y., Wu, W.-Y., Chang, C.-P., Tsao, S., Yuan, P.B., Lin, C.-W., Xia, K.-Y., 1997. Tectonic evolution of accretionary prism in the arc-continent collision terrane of Taiwan. Tectonophysics 281, 31-51.

Huang, C.-Y., Yuan, P.B., Lin, C.-W., Wang, T.K., Chang, C.-P., 2000. Geodynamic processes of Taiwan arc–continent collision and comparison with analogs in Timor, Papua New Guinea, Urals and Corsica. Tectonophysics 325, 1-21.

Huang, C.-Y., Yuan, P.B., Tsao, S.J., 2006. Temporal and spatial records of active arc-continent collision in Taiwan: A synthesis. Geological Society of America Bulletin 118, 274-288.

Huang, H.-H., Wu, Y.-M., Song, X., Chang, C.-H., Lee, S.-J., Chang, T.-M., Hsieh, H.-H., 2014. Joint Vp and Vs tomography of Taiwan: Implications for subduction-collision orogeny. Earth and Planetary Science Letters 392, 177-191.

Huang, S.-T., Yang, K.-M., Hung, J.-H., Wu, J.-C., Ting, H.-H., Mei, W.-W., Hsu, S.-H., Lee, M., 2004. Deformation Front Development at the Northeast Margin of the Tainan Basin, Tainan–Kaohsiung Area, Taiwan. Mar Geophys Res 25, 139-156.

Hung, J.-H., Wiltschko, D., Lin, H.-C., Hickman, J., B., Fang, P., Bock, Y., 1999. Structure and Motion of the Southwestern Taiwan Fold and Thrust Belt. Terrestrial, Atmospheric and Oceanic Sciences 10, 543-568.

Jackson, J.A., 1980. Reactivation of basement faults and crustal shortening in orogenic belts. Nature 283, 343-346.

Jones, R.H., Stewart, R.C., 1997. A method for determining significant structures in a cloud of earthquakes. Journal of Geophysical Research: Solid Earth 102, 8245-8254.

Kim, K.-H., Chen, K.-C., Wang, J.-H., Chiu, J.-M., 2010. Seismogenic structures of the 1999 Mw 7.6 Chi-Chi, Taiwan, earthquake and its aftershocks. Tectonophysics 489, 119-127.

Kim, K.-H., Chiu, J.-M., Pujol, J., Chen, K.-C., Huang, B.-S., Yeh, Y.-H., Shen, P., 2005. Three-dimensional VP and VS structural models associated with the active subduction and collision tectonics in the Taiwan region. Geophysical Journal International 162, 204-220.

Kuo-Chen, H., Wu, F.T., Roecker, S.W., 2012. Three-dimensional P velocity structures of the lithosphere beneath Taiwan from the analysis of TAIGER and related seismic data sets. Journal of Geophysical Research 117.

Lacombe, O., Mouthereau, F., 2002. Basement-involved shortening and deep detachment tectonics in forelands of orogens: Insights from recent collision belts (Taiwan, Western Alps, Pyrenees). Tectonics 21, 12-11-12-22.

Lacombe, O., Mouthereau, F., Angelier, J., Deffontaines, B., 2001. Structural, geodetic and seismological evidence for tectonic escape in SW Taiwan. Tectonophysics 333, 323-345.

Lee, C.-S., 1979. Paleogene Rocks Of The Yushan-Shuili Area, Nantou, Central Taiwan. Memoir of the Geological Society of China 3, 237-247.

Lee, J.-C., Angelier, J., Chu, H.-T., 1997. Polyphase history and kinematics of a complex major fault zone in the northern Taiwan mountain belt: the Lishan Fault. Tectonophysics 274, 97-115.

Lee, Y.-H., Chen, C.-C., Liu, T.-K., Ho, H.-C., Lu, H.-Y., Lo, W., 2006. Mountain building mechanisms in the Southern Central Range of the Taiwan Orogenic Belt — From accretionary wedge deformation to arc–continental collision. Earth and Planetary Science Letters 252, 413-422.

Lester, R., Lavier, L.L., McIntosh, K., Van Avendonk, H.J.A., Wu, F., 2012. Active extension in Taiwan's precollision zone: A new model of plate bending in continental crust. Geology 40, 831-834.

Lester, R., Van Avendonk, H.J.A., McIntosh, K., Lavier, L., Liu, C.S., Wang, T.K., Wu, F., 2014. Rifting and magmatism in the northeastern South China Sea from wide-angle tomography and seismic reflection imaging. Journal of Geophysical Research: Solid Earth 119, 2305-2323.

Li, C.-F., Zhou, Z., Li, J., Hao, H., Geng, J., 2007. Structures of the northeasternmost South China Sea continental margin and ocean basin: geophysical constraints and tectonic implications. Mar Geophys Res 28, 59-79.

Liao, W.-Z., Lin, A.T., Liu, C.-S., Oung, J.-N., Wang, Y., 2014. Heat flow in the rifted continental margin of the South China Sea near Taiwan and its tectonic implications. Journal of Asian Earth Sciences 92, 233-244.

Lin, A.T., Liu, C.-S., Lin, C.-C., Schnurle, P., Chen, G.-Y., Liao, W.-Z., Teng, L.S., Chuang, H.-J., Wu, M.-S., 2008. Tectonic features associated with the overriding of an accretionary wedge on top of a rifted continental margin: An example from Taiwan. Marine Geology 255, 186-203.

Lin, A.T., Watts, A.B., 2002. Origin of the West Taiwan basin by orogenic loading and flexure of a rifted continental margin. Journal of Geophysical Research: Solid Earth 107, 2185.

Lin, A.T., Watts, A.B., Hesselbo, S.P., 2003. Cenozoic stratigraphy and subsidence history of the South China Sea margin in the Taiwan region. Basin Research 15, 453-478.

Lin, C.-H., 2007. Tomographic image of crustal structures across the Chelungpu fault: Is the seismogenic layer structure- or depth-dependent? Tectonophysics 443, 271-279.

Madritsch, H., Schmid, S.M., Fabbri, O., 2008. Interactions between thin- and thick-skinned tectonics at the northwestern front of the Jura fold-and-thrust belt (eastern France). Tectonics 27.

Malavieille, J., Trullenque, G., 2009. Consequences of continental subduction on forearc basin and accretionary wedge deformation in SE Taiwan: Insights from analogue modeling. Tectonophysics 466, 377-394.

Marrett, R., Allmendinger, R.W., 1990. Kinematic analysis of fault-slip data. Journal of Structural Geology 12, 973-986.

McClay, K.R., 1989. Analogue models of inversion tectonics, in: Cooper, M.A., Williams, G.D. (Eds.), Inversion Tectonics. Geological Society, London, Special Publications, pp. 41-59.

McIntosh, K., van Avendonk, H., Lavier, L., Lester, W.R., Eakin, D., Wu, F., Liu, C.-S., Lee, C.-S., 2013. Inversion of a hyper-extended rifted margin in the southern Central Range of Taiwan. Geology 41, 871-874.

Molinaro, M., Leturmy, P., Guezou, J.C., Frizon de Lamotte, D., Eshraghi, S.A., 2005. The structure and kinematics of the southeastern Zagros fold-thrust belt, Iran: From thin-skinned to thick-skinned tectonics. Tectonics 24.

Mouthereau, F., Deffontaines, B., Lacombe, O., Angelier, J., 2002. Variations along the strike of the Taiwan thrust belt: Basement control on structural style, wedge geometry, and kinematics, in: Byrne, T., Liu, C.S. (Eds.), Geology and Geophysics of an Arc-Continent Collision, Taiwan. Geological Society of America Special Papers, pp. 31-54.

Mouthereau, F., Lacombe, O., 2006. Inversion of the Paleogene Chinese continental margin and thick-skinned deformation in the Western Foreland of Taiwan. Journal of Structural Geology 28, 1977-1993.

Mouthereau, F., Petit, C., 2003. Rheology and strength of the Eurasian continental lithosphere in the foreland of the Taiwan collision belt: Constraints from seismicity, flexure, and structural styles. Journal of Geophysical Research: Solid Earth 108.

Naylor, M.A., Mandl, G., Supesteijn, C.H.K., 1986. Fault geometries in basement-induced wrench faulting under different initial stress states. Journal of Structural Geology 8, 737-752.

Nissen, S.S., Hayes, D.E., Bochu, Y., Zeng, W., Chen, Y., Nu, X., 1995. Gravity, heat flow, and seismic constraints on the processes of crustal extension: Northern margin of the South China Sea. Journal of Geophysical Research: Solid Earth 100, 22447-22483.

Noguera, A.M., Rea, G., 2000. Deep structure of the Campanian–Lucanian Arc (Southern Apennine, Italy). Tectonophysics 324, 239-265.

Pin, Y., Di, Z., Zhaoshu, L., 2001. A crustal structure profile across the northern continental margin of the South China Sea. Tectonophysics 338, 1-21.

Price, R.A., 1981. The Cordilleran foreland thrust and fold belt in the southern Canadian Rocky Mountains, in: McClay, K., Price, N.J. (Eds.), Thrust and Nappe Tectonics. Geological Society, London, Special Publications, pp. 427-448.

Rau, R.-J., Wu, F.T., 1995. Tomographic imaging of lithospheric structures under Taiwan. Earth and Planetary Science Letters 133, 517-532.

Rodgers, J., 1990. Fold-and-thrust belts in sedimentary rocks; Part 1, Typical examples. American Journal of Science 290, 321-359.

Rodriguez-Roa, F.A., Wiltschko, D.V., 2010. Thrust belt architecture of the central and southern Western Foothills of Taiwan. Geological Society, London, Special Publications 348, 137-168.

Sakaguchi, A., Yanagihara, A., Ujiie, K., Tanaka, H., Kameyama, M., 2007. Thermal maturity of a fold–thrust belt based on vitrinite reflectance analysis in the Western Foothills complex, western Taiwan. Tectonophysics 443, 220-232.

Seno, T., 1977. The instantaneous rotation vector of the Philippine sea plate relative to the Eurasian plate. Tectonophysics 42, 209-226.

Shyu, J.B.H., Sieh, K., Chen, Y.-G., Chuang, R.Y., Wang, Y., Chung, L.-H., 2008. Geomorphology of the southernmost Longitudinal Valley fault: Implications for evolution of the active suture of eastern Taiwan. Tectonics 27.

Sibson, R.H., 1995. Selective fault reactivation during basin inversion: potential for fluid redistribution through fault-valve action, in: Buchanan, J.G., Buchanan, P.G. (Eds.), Basin Inversion. Geological Society, London, Special Publications, pp. 3-19.

Sibuet, J.-C., Hsu, S.-K., 2004. How was Taiwan created? Tectonophysics 379, 159-181.

Sibuet, J.-C., Hsu, S.-K., Le Pichon, X., Le Formal, J.-P., Reed, D., Moore, G., Liu, C.-S., 2002. East Asia plate tectonics since 15 Ma: constraints from the Taiwan region. Tectonophysics 344, 103-134.

Simoes, M., Avouac, J.P., Beyssac, O., Goffé, B., Farley, K.A., Chen, Y.-G., 2007. Mountain building in Taiwan: A thermokinematic model. Journal of Geophysical Research: Solid Earth 112.

Simoes, M., Beyssac, O., Chen, Y.-G., 2012. Late Cenozoic metamorphism and mountain building in Taiwan: A review. Journal of Asian Earth Sciences 46, 92-119.

Srivastava, P., Mitra, G., 1994. Thrust geometries and deep structure of the outer and lesser Himalaya, Kumaon and Garhwal (India): Implications for evolution of the Himalayan fold-and-thrust belt. Tectonics 13, 89-109.

Stanley, R.S., Hill, L.B., Chang, H.C., Hu, H.N., 1981. A transect through the metamorphic core of the central mountains, southern Taiwan. Memoir of the Geological Society of China 4, 443-473.

Suppe, J., 1976. Decollement Folding in Southwestern Taiwan. Petroleum Geology of Taiwan 13, 25-35.

Suppe, J., 1980a. Imbricated structure of Western Foothills Belt, Southcentral Taiwan. Petroleum Geology of Taiwan 17, 1-16.

Suppe, J., 1980b. A retrodeformable cross section of northern Taiwan. Proceedings Geological Society of China 23, 46-55.

Suppe, J., 1981. Mechanics of mountain building and metamorphism in Taiwan. Memoir of the Geological Society of China 4, 67-89.

Suppe, J., 1984. Kinematics of arc-continent collision, flipping of subduction, and back-arc spreading near Taiwan. Memoir of the Geological Society of China 6, 21-33.

Suppe, J., 1986. Reactivated normal faults in the Western Taiwan fold-and-thrust belt. Memoir of the Geological Society of China 7, 187-200.

Suppe, J., 1987. The active Taiwan mountain belt, in: Schaer, J.P., Rodgers, J. (Eds.), The Anatomy of Mountain Ranges. Princeton University Press, Princeton, pp. 277-293.

Suppe, J., Namson, J., 1979. Fault-Bend Origin of Frontal Folds of the Western Taiwan Fold-and-Thrust Belt. Petroleum Geology of Taiwan 16, 1-18.

Tang, C.-C., Zhu, L., Chen, C.-H., Teng, T.-L., 2011. Significant crustal structural variation across the Chaochou Fault, southern Taiwan: New tectonic implications for convergent plate boundary. Journal of Asian Earth Sciences 41, 564-570.

Tang, Q., Zheng, C., 2010. Seismic Velocity Structure and Improved Seismic Image of the Southern Depression of the Tainan Basin from Pre-Stack Depth Migration. Terrestrial, Atmospheric and Oceanic Sciences 21, 807-816.

Teng, L.S., 1987. Stratigraphic records of the Late Cenozoic Penglai Orogeny of Taiwan. Acta Geologica Taiwanica 25, 205-224.

Teng, L.S., 1990. Geotectonic evolution of late Cenozoic arc-continent collision in Taiwan. Tectonophysics 183, 57-76.

Teng, L.S., Lin, A.T., 2004. Cenozoic tectonics of the China continental margin: insights from Taiwan, in: Malpas, J., Fletcher, C.J.N., Ali, J.R., Aitchison, J.C. (Eds.), Aspects of the Tectonic Evolution of China. Geological Society, London, Special Publications, pp. 313-332.

Teng, L.S., Wang, Y., Tang, C.H., Huang, C.Y., Huang, T.C., Yu, M.S., Ke, A., 1991. Tectonic aspects of the Paleogene depositional basin of Northern Taiwan. Proceedings Geological Society of China 34, 313-336.

Thomas, W.A., 2006. Tectonic inheritance at a continental margin. GSA Today 16, 4-11.

Tillman, K.S., Byrne, T.B., 1995. Kinematic analysis of the Taiwan Slate Belt. Tectonics 14, 322-341.

Turner, S.A., Cosgrove, J.W., Liu, J.G., 2010. Controls on lateral structural variability along the Keping Shan Thrust Belt, SW Tien Shan Foreland, China, in: Goffey, G.P., Craig, J., Needham, T., Casp, R.S. (Eds.), Hydrocarbons in Contractional Belts. Geological Society, London, Special Publications, pp. 71-85.

Wiltschko, D., Hassler, L., Hung, J.-H., Liao, H.-S., 2010. From accretion to collision: Motion and evolution of the Chaochou Fault, southern Taiwan. Tectonics 29.

Wu, F.T., Chang, C.-H., Wu, Y.-M., 2004. Precisely relocated hypocentres, focal mechanisms and active orogeny in Central Taiwan, in: Malpas, J., Fletcher, C.J.N., Ali, J.R., Aitchison, J.C. (Eds.), Aspects of the Tectonic Evolution of China. Geological Society, London, Special Publications, pp. 333-354.

Wu, F.T., Kuo-Chen, H., McIntosh, K.D., 2014. Subsurface Imaging, TAIGER Experiments and Tectonic Models of Taiwan. Journal of Asian Earth Sciences 90, 173-208.

Wu, F.T., Rau, R.-J., Salzberg, D., 1997. Taiwan orogeny: Thin-skinned or lithospheric collision? Tectonophysics 274, 191-220.

Wu, Y.-M., Chang, C.-H., Zhao, L., Shyu, J.B.H., Chen, Y.-G., Sieh, K., Avouac, J.-P., 2007. Seismic tomography of Taiwan: Improved constraints from a dense network of strong motion stations. Journal of Geophysical Research: Solid Earth 112.

Wu, Y.-M., Chang, C.-H., Zhao, L., Teng, T.L., Nakamura, M., 2008a. A Comprehensive Relocation of Earthquakes in Taiwan from 1991 to 2005. Bulletin of the Seismological Society of America 98, 1471-1481.

Wu, Y.-M., Hsu, Y.-J., Chang, C.-H., Teng, L.S.-y., Nakamura, M., 2010. Temporal and spatial variation of stress field in Taiwan from 1991 to 2007: Insights from comprehensive first motion focal mechanism catalog. Earth and Planetary Science Letters 298, 306-316.

Wu, Y.-M., Zhao, L., Chang, C.-H., Hsiao, N.-C., Chen, Y.-G., Hsu, S.-K., 2009. Relocation of the 2006 Pingtung Earthquake sequence and seismotectonics in Southern Taiwan. Tectonophysics 479, 19-27.

Wu, Y.-M., Zhao, L., Chang, C.-H., Hsu, Y.-J., 2008b. Focal-Mechanism Determination in Taiwan by Genetic Algorithm. Bulletin of the Seismological Society of America 98, 651-661.

Yamato, P., Mouthereau, F., Burov, E., 2009. Taiwan mountain building: insights from 2-D thermomechanical modelling of a rheologically stratified lithosphere. Geophysical Journal International 176, 307-326.

Yang, C.-C.B., Chen, W.-S., Wu, L.-C., Lin, C.-W., 2007. Active deformation front delineated by drainage pattern analysis and vertical movement rates, southwestern Coastal Plain of Taiwan. Journal of Asian Earth Sciences 31, 251-264.

Yang, K.-M., Huang, S.-T., Wu, J.-C., Ting, H.-H., Mei, W.-W., 2006. Review and New Insights on Foreland Tectonics in Western Taiwan. International Geology Review 48, 910-941.

Yeh, Y.-C., Hsu, S.-K., Doo, W.-B., Sibuet, J.-C., Liu, C.-S., Lee, C.-S., 2012. Crustal features of the northeastern South China Sea: insights from seismic and magnetic interpretations. Mar Geophys Res 33, 307-326.

Yen, H.-Y., Hsieh, H.-H., 2010. A study on the compatibility of 3-D seismic velocity structures with gravity data of Taiwan. Terrestrial, Atmospheric and Oceanic Sciences 21, 897-904.

Yen, H.-Y., Yeh, Y.-H., Lin, C.-H., Chen, K.-J., Tsai, Y.-B., 1995. Gravity Survey of Taiwan. Journal of Physics of the Earth 43, 685-696.

Yu, H.-S., Chou, Y.-W., 2001. Characteristics and development of the flexural forebulge and basal unconformity of Western Taiwan Foreland Basin. Tectonophysics 333, 277-291.

Yu, S.-B., Chen, H.-Y., Kuo, L.-C., 1997. Velocity field of GPS stations in the Taiwan area. Tectonophysics 274, 41-59.

Yu, S.-B., Kuo, L.-C., 2001. Present-day crustal motion along the Longitudinal Valley Fault, eastern Taiwan. Tectonophysics 333, 199-217.

Yue, L.-F., Suppe, J., Hung, J.-H., 2005. Structural geology of a classic thrust belt earthquake: the 1999 Chi-Chi earthquake Taiwan (Mw=7.6). Journal of Structural Geology 27, 2058-2083.

Zoback, M.L., 1992. First- and second-order patterns of stress in the lithosphere: The World Stress Map Project. Journal of Geophysical Research: Solid Earth 97, 11703-11728.

Appendices

Appendix 1 - Geological maps

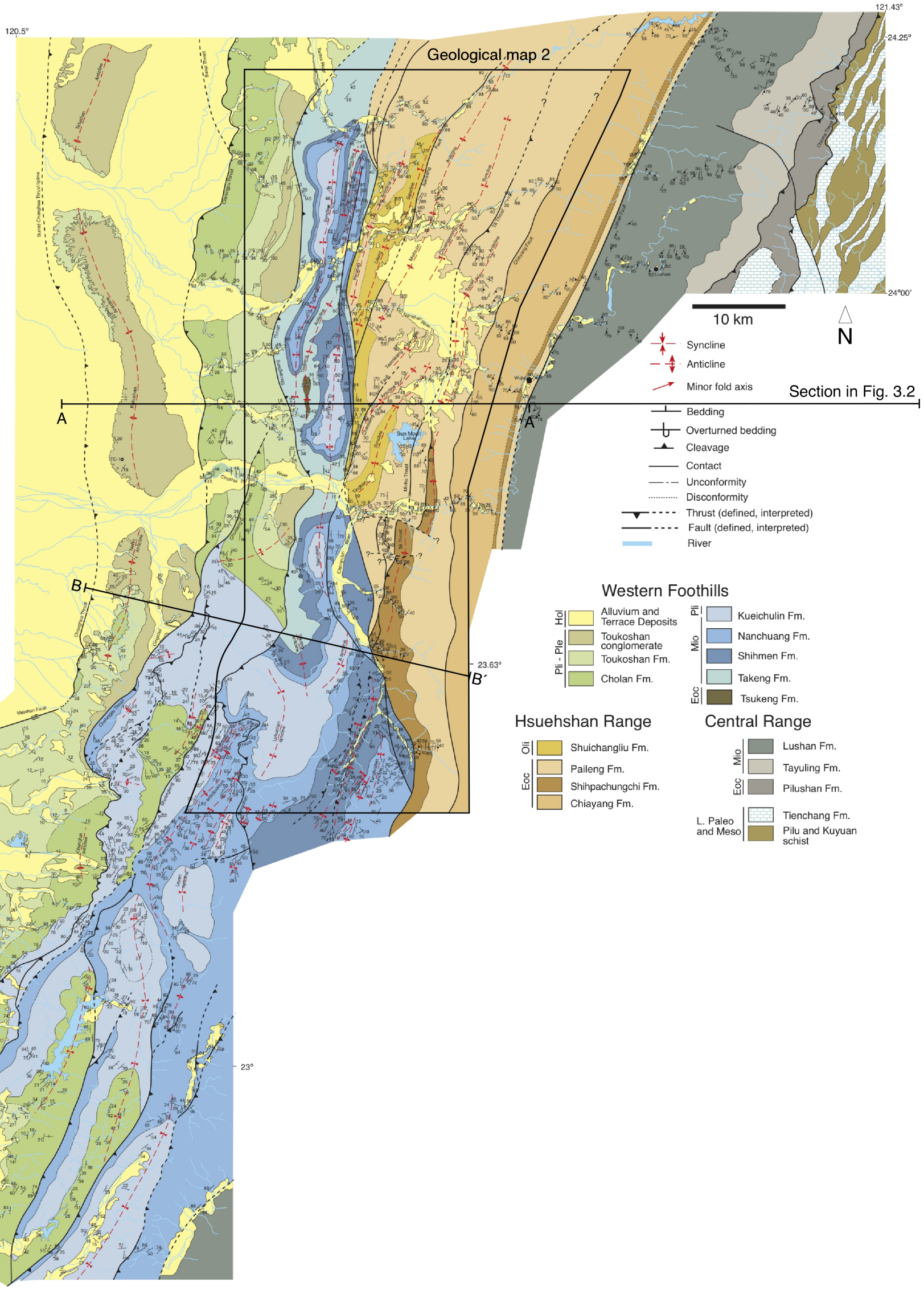

Geological map 1. Geological map of the study area in south-central Taiwan. This map is, in part, the result of fieldwork carried out by colleagues from ICTJA before the beginning of this Ph.D. thesis and, in part, the result of the fieldwork the Ph.D. student carried out in collaboration with them during this thesis. The exact extension of the area mapped during this thesis is given in the paragraph on the methodology of this thesis. The location of the cross-sections A-A´ and B-B´ in Fig. 1.8 is given, as it is the location of Geological map 2 and of the section in Fig. 3.2. The location of the map is given in Fig. 1.4.

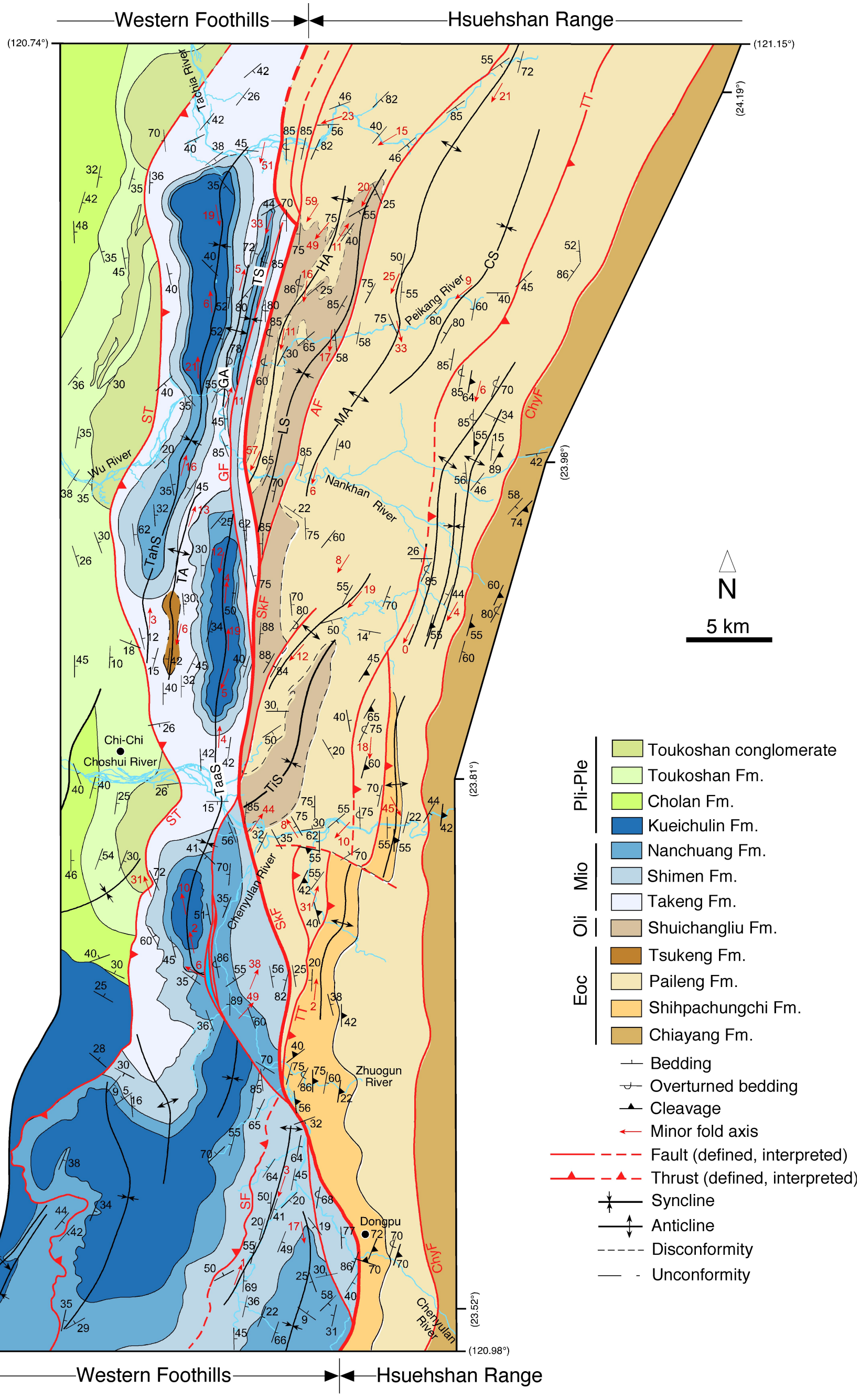

Geological map 2. Geological map of the study area across the Shuilikeng Fault in central Taiwan. The location of the map is given in Geological map 1. Geological map modified after Article 2 included in this thesis.

Appendix 2 - Conference abstracts related to the thesis

Abstract 1 - Strain partitioning along the Shuilikeng Transpressive Fault System (Central Taiwan fold-and-thrust belt)

Giovanni Camanni[1], Dennis Brown[1], Joaquina Alvarez-Marron[1], Martin Schimmel[1], and Yih-Min Wu[2]

[1]Institute of Earth Sciences Jaume Almera, ICTJA-CSIC, Lluis Sole i Sabaris s/n, 08028 Barcelona, Spain
[2]Department of Geosciences, National Taiwan University, Taipei, 106, Taiwan

Presented at: 2011 EGU General Assembly. Vienna (Austria)

Type of presentation: poster

Abstract:

The Shuilikeng Fault, in the Central Taiwan fold-and-thrust belt, is a roughly north-south striking zone comprised of a number of high-angle faults and fault splays that juxtaposes the Miocene rocks of the Western Foothills against the Eocene and Oligocene rocks of the Hsuehshan Range. Geomorphologically, it coincides with a pronounced system of valleys that clearly demarcates the contact between these two tectonostratigraphic units in Central Taiwan. Using river incision, channel morphology, and stream gradient along the Wu and Peikang rivers, YANITES *et al*. (2010) and SUNG *et al*. (2000) suggest that the Shuilikeng Fault is currently active, and has been throughout the Holocene. However, because of the absence of Pleistocene and Pliocene sediments they are unable to put any constraints on older activity. The Shuilikeng Fault is poorly imaged in reflection seismic data, where it has been interpreted to dip steeply eastward and extend to deep in the middle crust (i.e., the Shuichangliu Fault of WANG *et al*., 2002). YUE *et al*. (2005) interpret the Shuilikeng Fault to be the westward-dipping displaced upper part of a pre-existing Miocene-age extensional fault whose lower part, they suggest, coincides with an area of high seismic activity below their detachment. On the basis of new surface geological mapping we suggest that the Shuilikeng Fault, rather than being a single discrete feature, consists of a main fault zone with a linked system of associated faults that affect much of the Hsuehshan Range. All faults (from west to east, Alenkeng Fault, Checheng Fault, Tili Fault) and folds that have been so far mapped in the Hsuehshan Range merge southward with the Shuilikeng Fault, resulting in a regional map pattern that is strongly suggestive of a strike-slip or transpressive fault system. Bending of folds into the Shuilikeng Fault System in, e.g., the Tingkan Syncline and the Tsukeng Anticline, suggests a left lateral (top-to-the-northwest) sense of displacement along it. Focal mechanisms are in keeping with field observations and suggest shallow oblique to strike-slip faulting (e.g., northern sector) and deeper thrust faulting (e.g., southern sector).

SUNG Q., CHEN Y.C., TSAI H., CHEN Y.G. & CHEN W.S. (2000) - *Comparison Study on the Coseismic Deformation of the 1999 Chi-Chi Earthquake and Long-term Stream Gradient Changes Along the Chelungpu Fault in Central Taiwan.* Terrestrial Atmospheric and Oceanic Sciences, 11: 735-750

WANG C.Y., LI C.L., SU F.C., LEU M.T., WU M.S., LAI S.H. & CHERN C.C. (2002) - *Structural Mapping of the 1999 Chi-Chi Earthquake Fault, Taiwan, by Seismic Reflection Methods*. Terrestrial Atmospheric and Oceanic Sciences, 13: 211-226

YANITES B.J., TUCKER G.E., MUELLER K.J., CHEN Y.G., WILCOX T., HUANG S.Y. & SHI K.W. (2010) - *Incision and channel morphology across active structures along the Peikang River, central Taiwan: Implications for the importance of channel width*. Geological Society of America Bulletin, 122: 1192-1208

YUE L.F., SUPPE J. & HUNG J.H. (2005) - *Structural geology of a classic thrust belt earthquake: the 1999 Chi-Chi earthquake Taiwan (Mw = 7.6)*. Journal of Structural Geology, 27: 2058-2083

Abstract 2 - Deformation partitioning in Central Taiwan: new insights from surface geology, earthquake focal mechanisms, seismic energy release, and GPS measurements along the Shuilikeng Transpressive Fault System

Giovanni Camanni[1], Dennis Brown[1], Joaquina Alvarez-Marron[1], Martin Schimmel[1], and Yih-Min Wu[2]

[1]Institute of Earth Sciences Jaume Almera, ICTJA-CSIC, Lluis Sole i Sabaris s/n, 08028 Barcelona, Spain
[2]Department of Geosciences, National Taiwan University, Taipei, 106, Taiwan

Presented at: 2011 Annual Meeting of the Italian Group of Structural Geology. Cagliari (Italy)

Type of presentation: poster

Abstract (extended):

INTRODUCTION

The Shuilikeng Fault System (SKFS), in the Central Taiwan mountain belt, is a roughly N-S striking fault zone comprised of a number of high-angle faults and fault splays mostly E-dipping that juxtaposes the Miocene rocks of the Western Foothills (i.e. platform sediments of the Shuangtung Unit) against the Eocene and Oligocene rocks of the Hsuehshan Range (i.e. platform sediments of the Sun-Moon Lake Unit). We present a new surface geological mapping integrated with earthquake seismic energy release and focal mechanisms data as well as with GPS data to better constrain the structural architecture and kinematics of the SKFS in Central Taiwan.

BACKGROUND

The Shuilikeng Fault marks a "jump" in the crustal level of involvement of the platform margin between its two sides; SAKAGUCHI *et alii* (2007) on the basis of vitrinite reflectance data have recently suggested an increase in temperature of ~90 °C from the Shuangtung Unit to the Sun-Moon Lake Unit, across the Shuilikeng Fault. Using river incision, channel morphology, and stream gradient along the Wu and Peikang rivers, YANITES *et alii* (2010) and SUNG *et alii* (2000) suggest that the Shuilikeng Fault is currently active, and has been throughout the Holocene. However, because of the absence of Pleistocene and Pliocene sediments they are unable to put any constraints on older activity. The Shuilikeng Fault is poorly imaged in reflection seismic data, where it has been interpreted to dip steeply eastward and extend to deep in the middle crust (i.e. the Shuichangliu Fault of WANG *et alii*, 2002). YUE *et alii* (2005) interpret the Shuilikeng Fault to be the westward-dipping displaced upper part of a pre-existing Miocene-age extensional fault whose lower part, they suggest, coincides with an area of high seismic activity below their detachment.

REMARKABLE OBSERVATIONS

Surface geology

On the basis of new surface geological mapping we suggest that the Shuilikeng Fault, rather than being a single discrete feature, consists of a system of associated faults and folds that affect much of the Hsuehshan Range (Sun-Moon Lake Unit) and the eastern part of the Western Foothills (Shuangtung Unit). Geomorphologically, it coincides with a pronounced system of valleys that clearly demarcates the contact between these two tectonostratigraphic units along nearly its entire length in Central Taiwan.

All faults (from north to south, Alenkeng Fault and Checheng Fault) and folds (mostly related to the kinematics of the SKFS) that have been so far mapped in the Sun-Moon Lake Unit merge southward with the SKFS, resulting in a regional map pattern that is strongly suggestive of a strike-slip or transpressive fault system. The roughly NNE-SSW striking Tili Thrust marks the western limit of cleavage development (cleavage front) in the Taiwan mountain belt and juxtaposes the Tili Unit against the Sun-Moon Lake Unit; its truncation by the SKFS suggests that it is an older feature. Bending of fold traces into the SKFS as well as its overall framework suggest a top-to-the-NW sense of displacement along it.

The surface geology of the Shuangtung Unit is mostly comprised of folds with axial traces at high angle to the Shuilikeng Fault that appear to be cut by it. To the north the eastern flank of the unit is tightly folded into the N-S

trending Kuohsing Anticline and Tachiwei Syncline. The eastern limb of the Tachiwei Syncline is cut by the Kuohsing Fault that merge southward with the SKFS and should be part of it. At the southern edge of the map area a map scale weakly ESE-dipping duplex with a top-to-the-WNW direction of tectonic transport and related NNE-SSW trending folds have been recognized.

Earthquake focal mechanisms

Earthquake focal mechanisms are updated from the database of WU *et alii* (2010) to cover the period from 1991 to 2009. They suggest that the strain to the E of the Shuilikeng Fault (i.e. Hsuehshan Range) is mostly partitioned in shallow (~0-15 km depth) highly oblique to strike-slip faulting (northern sector) and deeper (~15-30 km depth) thrust faulting (central-southern sector).

Seismic energy release

The SKFS beneath the Hsuehshan Range is highlighted by and coincides with an abrupt increase in the density and depth (up to ~30 km) of cumulative seismic energy release along a steeply eastward dipping zone. The western bound of the zone projects to the surface at the location of the map trace of the Shuilikeng Fault.

GPS data

Horizontal velocity components of continuous GPS measurements for the years 2005 through 2009 (courtesy of Yu Shui-Beih) are mainly NW-directed and show a general increase going from NW to SE; all the GPS stations in each unit in Central Taiwan provide similar velocities and the main velocity variations coincide with the bounding faults between the units, thus demonstrating that they are active. Across the Shuilikeng Fault GPS data show an increase of horizontal velocity from ~22,8 mm/yr (Shuangtung Unit) to ~24,2 mm/yr (Sun-Moon Lake Unit). Horizontal velocity components in the Sun-Moon Lake Unit illustrate the overall obliquity between the present surface velocity field and the surface trace of the Shuilikeng Fault.

GPS vertical velocity components show a general uplift to the east of the Shuangtung Fault (western boundary of the Shuangtung Unit) and a general subsidence to the west of it.

REFERENCES

SAKAGUCHI A., YANAGIHARA A., UJIIE K., TANAKA H. & KAMEJAMA M. (2007) - *Thermal maturity of a fold-thrust belt based on vitrinite reflectance analysis in the Western Foothills complex, Taiwan*. Tectonophysics, 443, 220-232.

SUNG Q., CHEN Y.C., TSAI H., CHEN Y.G. & CHEN W.S. (2000) - *Comparison Study on the Coseismic Deformation of the 1999 Chi-Chi Earthquake and Long-term Stream Gradient Changes Along the Chelungpu Fault in Central Taiwan*. Terrestrial Atmospheric and Oceanic Sciences, 11, 735-750.

WANG C.Y., LI C.L., SU F.C., LEU M.T., WU M.S., LAI S.H. & CHERN C.C. (2002) - *Structural Mapping of the 1999 Chi-Chi Earthquake Fault, Taiwan, by Seismic Reflection Methods*. Terrestrial Atmospheric and Oceanic Sciences, 13, 211-226.

WU Y. M., HSU Y. J., CHANG C. H., TENG L. S. & NAKAMURA M. (2010) - *Temporal and spatial variation of stress field in Taiwan from 1991 to 2007: Insights from comprehensive first motion focal mechanism catalog*. Earth and Planetary Science Letters, 298, 306–316.

YANITES B.J., TUCKER G.E., MUELLER K.J., CHEN Y.G., WILCOX T., HUANG S.Y. & SHI K.W. (2010) - *Incision and channel morphology across active structures along the Peikang River, central Taiwan: Implications for the importance of channel width*. Geological Society of America Bulletin, 122, 1192-1208.

YUE L.F., SUPPE J. & HUNG J.H. (2005) - *Structural geology of a classic thrust belt earthquake: the 1999 Chi-Chi earthquake Taiwan (Mw = 7.6)*. Journal of Structural Geology, 27, 2058-2083.

Abstract 3 - The structure and kinematics of the central Taiwan mountain belt derived from geological, GPS, and seismicity data

Joaquina Alvarez-Marron[1], Dennis Brown[1], Martin Schimmel[1], Yih-Min Wu[2], Shui-Beih Yu[3], and Giovanni Camanni[1]

[1]Institute of Earth Sciences Jaume Almera, ICTJA-CSIC, Lluis Sole i Sabaris s/n, 08028 Barcelona, Spain
[2]Department of Geosciences, National Taiwan University, Taipei, 106, Taiwan
[3]Institute of Earth Sciences, Academica Sinica, Nankang, Taipei, Taiwan

Presented at: 2011 AGU Fall Meeting, Abstract T43J-03. San Francisco (USA)

Type of presentation: oral

Abstract:

The structure of the Taiwan mountain belt is thought to be that of an imbricate thrust and fold belt developed above a shallowly dipping basal detachment. In recent years, however, a growing amount of seismicity data from the internal part of the mountain belt indicates the existence of widespread fault activity in the middle and lower crust, suggesting that deeper levels of the crust must be involved in the deformation than is predicted by the imbricate thrust belt model. To address this issue, we present new geological mapping, long-term GPS, earthquake focal mechanism, and seismic energy release data from the central part of Taiwan. We suggest that the foreland basin part of the Western Foothills comprises an imbricate thrust system that is structurally and kinematically linked to a basal detachment at between 7 and 10 km depth. To the east of the foreland basin, in the Hsuehshan Range, our data show the presence of major faults that are steeply dipping and which penetrate 25 to 30 km depth, or more. This indicates that much deeper levels of the crust are involved in the deformation, and that a structural and kinematic model in which this part of the mountain belt forms a zone of transpression with a structural architecture similar to that of a crustal-scale positive flower structure better fits the available data. Eastward, in the Central Range, deep-water sediments appear to form an allochthon that is being overthrust by Mesozoic basement rocks. The involvement of such deep crustal levels and Mesozoic basement in the deformation if suggestive of the reactivation of pre-existing basin-bounding faults that where located on the Eurasian continental margin.

Abstract 4 - The structure and kinematics of the central Taiwan mountain belt derived from geological, GPS, and seismicity data

Dennis Brown[1], Joaquina Alvarez-Marron[1], Martin Schimmel[1], Giovanni Camanni[1], Yih-Min Wu[2], and Shui-Beih Yu[3]

[1]Institute of Earth Sciences Jaume Almera, ICTJA-CSIC, Lluis Sole i Sabaris s/n, 08028 Barcelona, Spain
[2]Department of Geosciences, National Taiwan University, Taipei, 106, Taiwan
[3]Institute of Earth Sciences, Academica Sinica, Nankang, Taipei, Taiwan

Presented at: 2012 Annual Meeting of the Geological Association of Canada and Mineralogical Association of Canada. St. John's (Canada)

Type of presentation: oral

Abstract:

The structure of the Taiwan mountain belt is thought to be that of an imbricate thrust and fold belt developed above a shallowly dipping basal detachment. In recent years, however, a growing amount of seismicity data from the internal part of the mountain belt indicates the existence of widespread fault activity in the middle and lower crust, suggesting that deeper levels of the crust must be involved in the deformation than is predicted by the imbricate thrust belt model. To address this issue, we present new geological mapping, long-term GPS, earthquake focal mechanism, and seismic energy release data from the central part of Taiwan. We suggest that the foreland basin part of the Western Foothills comprises an imbricate thrust system that is structurally and kinematically linked to a basal detachment at between 7 and 10 km depth. To the east of the foreland basin, in the Hsuehshan Range, our data show the presence of major faults that are steeply dipping and which penetrate 25 to 30 km depth, or more. This indicates that much deeper levels of the crust are involved in the deformation, and that a structural and kinematic model in which this part of the mountain belt forms a zone of transpression with a structural architecture similar to that of a crustal-scale positive flower structure better fits the available data. Eastward, in the Central Range, deep-water sediments appear to form an allochthon that is being overthrust by Mesozoic basement rocks. The involvement of such deep crustal levels and Mesozoic basement in the deformation if suggestive of the reactivation of pre-existing basin-bounding faults that where located on the Eurasian continental margin.

Abstract 5 - Structural styles of the Shuilikeng fault system in the central Taiwan mountain belt

Giovanni Camanni[1], Dennis Brown[1], and Joaquina Alvarez-Marron[1]

[1]Institute of Earth Sciences Jaume Almera, ICTJA-CSIC, Lluis Sole i Sabaris s/n, 08028 Barcelona, Spain

Presented at: 2012, 8th Geological Congress of Spain. Oviedo (Spain)

Type of presentation: poster

Abstract (extended):

INTRODUCTION

The structural architecture of the central part of the Taiwan orogen has been classically interpreted as a west-verging fold-and-thrust belt developed above a shallowly east-dipping detachment (Suppe, 1981; Ding et al., 2001; Carena et al., 2002). Nevertheless, earthquake seismicity (Brown et al., in review; Wu et al., 1997), magnetotelluric (Bertrand et al., 2009) and geological (Brown et al., in review) data suggest that a transpressive, thick-skinned style of deformation, that is reactivating pre-existing basement faults (Mouthereau et al., 2002), may better describe the evolving structure of the interior of the central Taiwan mountain belt. In the study area, the change from one structural style to the other takes place across the Shuilikeng fault system. Therefore, determining its structure and kinematics has important implications for understanding how the entire Taiwan mountain belt is growing. Here, we present the results of new structural mapping along the Shuilikeng fault system which is then combined with earthquake focal mechanism data to better resolve its structure and kinematics.

GEOLOGICAL BACKGROUND

In the study area, the western part of the central Taiwan mountain belt can be divided into two tectonostratigraphic zones separated by the Shuilikeng fault system; the Western Foothills to the west, and the Hsuehshan Range to the east. The Western Foothills comprises unmetamorphosed Eocene to Miocene platform sediments that are thrust over Late Miocene to Recent synorogenic sediments of the foreland basin. The Hsuehshan Range is made up of weakly metamorphosed Eocene and Oligocene clastics that, eastward and southward reach lower greenschist facies and have a penetrative pressure solution cleavage in the hangingwall to the Tili thrust. The juxtaposition of these two zones across the Shuilikeng fault, together with its structural architecture, kinematics, and seismicity suggest that it is a steeply east-dipping transpressive fault system, with linked splays and fault zone bifurcations, that appears to extend into the middle and perhaps even the lower crust (Brown et al., in review, Wang et al., 2002). River channel incision and morphology (Yanites et al., 2010), as well as changes in the stream gradient (Sung et al., 2000) along the main rivers in the interior of the mountain belt, show that the Shuilikeng fault system has been active throughout the Holocene.

FIELD DATA

Throughout the study area, the Shuilikeng fault system is defined by the structural juxtaposition of the Eocene and Oligocene rocks against the Miocene. The main fault zone has a marked geomorphological signature defined by a series of roughly N-S-sriking valleys. While it crops out poorly, it can be an up to kilometre-wide zone of intense brecciation, or a several kilometre-wide area of complex faulting and folding. The structural style of the Shuilikeng fault system changes from north to south.

To the north, it is defined by steeply dipping diverging splays and by non-cylindrical folds branching off the Shuilikeng fault. In the Hsuehshan Range these diverging features are north-northeast-striking with the folds being largely asymmetric and west-northwest-verging. In the Western Foothills they are north-striking and roughly parallel to the surface trace of the Shuilikeng fault. For example, the easternmost margin of the Western Foothills is deformed by the steeply dipping nearly north-striking Guaosing fault splaying off the Shuilikeng fault and by the associated north-trending Tachiwei-Guaosing syncline-anticline pair. Minor faults related to the Guaosing fault show a composite kinematics with left-lateral transpressive senses of movement being dominant.

To the south, the structure of the Hsuehshan Range is dominated by right-lateral east-striking strike-slip faults while that of the Western Foothills is defined by a rejoining splay branching off the Shuilikeng fault and isolating a lens-shaped horse of Miocene rocks. For most of its length the rejoining splay is defined by a wide north-striking

breccia zone developed into a very thick-bedded sandstone unit. Kinematic indicators such as slickenfibres show a complex kinematic pattern, with a slight dominance of right- and left-lateral strike-slip senses of movement.

In its southernmost part, the Shuilikeng fault is defined by a several hundred meters-wide high strain zone of intense faulting and folding. The resultant geometries are very complex with the thick-bedded sandstone units being largely brecciated and the thin-bedded sandstone and shale units undergoing very disharmonic folding. In that part of the map area, the structure of the Western Foothills is defined by a north-northeast-oriented horsetail fanlike map pattern branching off the Shuilikeng fault comprising a km-wavelength regional anticlinorium highly folded and faulted along its limbs.

ACKNOWLEDGMENTS

G. Camanni acknowledges the grant JAE-Predoc (CSIC). This research was carried out with the aid of the grant MICINN: CGL2009-11843-BTE.

REFERENCES

Bertrand, E., Unsworth, M., Chiang, C.-W., Chen, C.-S., Chen, C.-C., Wu, F., Türkoglu, E., Hsu, H.-L, and Hill, G. (2009): Magnetotelluric evidence for thick- skinned tectonics in central Taiwan. *Geology*, 37: 711-714.

Brown, D., Alvarez-Marron, J., Schimmel, M., Wu, Y-M., Yu, S-B., and Camanni, G. (in review): The structure and kinematics of the central Taiwan mountain belt derived from geological, GPS, and seismicity data. Submitted to *Tectonics*.

Carena, S., Suppe, J., and Kao, H. (2002): Active detachment of Taiwan illuminated by small earthquakes and its control of first-order topography. *Geology*, 30: 935- 938.

Ding, Z.-Y., Yang, Y.-Q.,Yao, Z.-X., and Zhang, G.-H. (2001): A thin-skinned collisional model for the Taiwan orogeny. *Tectonophysics*, 332: 321-331.

Mouthereau, F., Deffontaines, B., Lacombe, O., and Angelier, J. (2002): Variations along the strike of the Taiwan thrust belt: basement control on structural style, wedge geometry, and kinematics. In *Geology and Geophysics of an Arc-Continent Collision, Taiwan* (T.B. Byrne and C.-S. Liu, eds.). GSA Special Paper, Boulder, USA, 358: 31-54.

Sung, Q.-C., Chen, Y.-C., Tsai, H., Chen, Y.-G., and Chen, W-.S. (2000): Comparison study on the coseismic deformation of the 1999 Chi-Chi earthquake and long-term stream gradient changes along the Chelungpu fault in central Taiwan. *Terr. Atmos. Ocean. Sci*., 11: 735–750.

Suppe, J. (1981): Mechanics of mountain building and metamorphism in Taiwan. *Geol. Soc. China Mem*., 4: 67-89.

Wang, C.-Y., Li, C.-L., Su, F.-C., Leu, M.-T., Wu, M.-S., Lai, S.-H., and Chern C.-C. (2002): Structural mapping of the 1999 Chi-Chi earthquake fault, Taiwan, by seismic reflection methods. *Terr. Atmos. Ocean. Sci.*, 13: 211–226.

Wu, Y.-M., Chang, C.-H. , Zhao, L., Shyu, J.B.H., Chen, Y.-G., Sieh, K., and Avouac, J.P. (2007): Seismic tomography of Taiwan: Improved constraints from a dense network of strong motion stations. *J. Geophys. Res.*, 112, doi: 10.1029/2007JB004983.

Yanites, B.J., Tucker, G.E., Mueller, K.J., Chen, Y.-G., Wilcox, T., Huang, S.-Y., and Shi, K.-W. (2010): Incision and channel morphology across active structures along the Peikang River, central Taiwan: implications for the importance of channel width. Geol. Soc. Am. Bull.,122: 1192-1208.

Abstract 6 - The structure of the central Taiwan mountain belt

Dennis Brown[1], Joaquina Alvarez-Marron[1], and Giovanni Camanni[1]

[1]Institute of Earth Sciences Jaume Almera, ICTJA-CSIC, Lluis Sole i Sabaris s/n, 08028 Barcelona, Spain

Presented at: 2012, 8th Geological Congress of Spain. Oviedo (Spain)

Type of presentation: poster

Abstract (extended):

INTRODUCTION

The structure of the faulted and folded rocks of the Eurasian continental margin involved in the Taiwan mountain belt is often presented as an imbricate thrust and fold belt developed above a shallowly eastward-dipping basal detachment (e.g., Suppe, 1980, 1981). The bulk of the data for this interpretation of the structure comes from surface geological observations, shallow reflection seismics, and borehole data along the western flank of the mountain belt, in what is known as the Western Foothills. The more internal parts of the mountain belt are less well understood because of difficult access in the areas of high rugged topography and heavy forest cover. Nevertheless, collapsing and selective picking of relocated small magnitude (between ML 1 and 4) earthquake hypocenter data appears to validate the interpretation of extending a detachment from beneath the Western Foothills across the entire mountain belt. Combining these seismicity data with surface geological data from published geological maps from the Western Foothills and the western part of the Hsuehshan Range, others have also interpreted the basal detachment to extend eastward, with ramps and flats, beneath the entire mountain belt. In this latter interpretation, the more internal units are structurally linked to the basal detachment, forming three imbricate thrust sheets with the largest of these, the Tili thrust sheet, transporting nearly the entire Taiwan mountain belt at least several 10's of kilometres westward.

There is, however, a growing amount of geophysical data from the internal part of the mountain belt that indicates widespread fault activity in the middle and lower crust, well below the level of the proposed detachment (e.g., Wu et al., 1997, 2004). For example, recent magnetotelluric experiments show a prominent electrical conductor that extends into the middle crust, crossing the proposed detachment. Similarly, analyses of seismicity data also indicate that there are several steeply dipping faults that penetrate into the middle and perhaps even the lower crust. On the basis of these data, it has been suggested that any model for the structural architecture of the Taiwan mountain belt needs to incorporate a number of steeply dipping faults that involve nearly the entire crust. A corollary to this is that these faults would have to cut the basal detachment proposed in the imbricate fold and thrust belt model. This proposal therefore has significant implications for the geometric, mechanical and kinematic evolution of the Taiwan mountain belt that are very different from what has so far been presented on the basis of the imbricate thrust belt model.

While geophysical and thermochronological data can provide significant insights into the geometry, kinematics, and mechanics of the Taiwan mountain belt, in order to further advance our understanding of the structures that provide first order controls on these types of data much more surface geology data is needed from its interior. In this paper we present new geological mapping in the central part of Taiwan which spans nearly the entire width of the mountain belt.

STRUCTURE AND KINEMATICS

Our surface geological mapping presented here indicates that in Central Taiwan, from the buried Changhua thrust in the west to the Tananao Unit in the east, the mountain belt can be divided into six distinct, roughly northeast-southwest trending fault bounded units.

These data corroborate the previous interpretations of a gently eastward-dipping detachment at about 7 to 10 km depth below the Western Foothills. Like the previous interpretations, to the north of the Choshui River we place the detachment to the Changhua- Chelungpu imbricate thrust system within the Chinshui shale member of Cholan Formation synorogenic sediments. South of the Choshui River, however, there is a significant change in the location of this basal detachment as it ramps down section into the older Miocene rocks, placing them on top of Pleistocene rocks in the Neilin anticline. Rare kinematic indicators found in the field indicate a top-to-the-northwest (oblique) sense of movement is taking place.

Unlike previous interpretations, we suggest that the detachment beneath the Changhua-Chelungpu imbricate thrust system does not continue eastward beneath the Hsuehshan and Central ranges. Instead, it appears to be truncated by, or is perhaps somehow linked with, the Shuilikeng fault. We recognise that there are problems in interpreting the geometry of the Shuangtung thrust at depth. In this study, we suggest that since it cuts down section through the Miocene and into Eocene-aged Paileng Formation rocks it is more likely to be structurally and kinematically linked to the Sun-Moon Lake Unit, although its eastern flank has been cut by the Shuilikeng fault. With the current data, however, it is not possible to determine the nature of this linkage. In the surface geology, the Shuangtung thrust places Miocene rocks on top of the upper part of the Toukoshan Formation, indicating that is was active during the late Pleistocene to Holocene.

We suggest that the Shuilikeng fault, rather than being a single discrete feature, comprises a system of faults and folds that splay off the main fault, resulting in a regional map pattern that is strongly suggestive of a transpressive or strike-slip system fault. This Shuilikeng fault "system" dominates the structure of the Sun-Moon Lake Unit in the map area. The bending of folds (e.g., the Tingkan syncline or the Tsukeng anticline), together with the bending and truncation of the Tili Unit, against the Shuilikeng fault indicates that it has a sinistral component of displacement.

The Tili thrust marks a clear structural and metamorphic boundary in the Hsuehshan Range. It juxtaposes lower metamorphic grade rocks of the Sun- Moon Lake Unit against higher grade rocks with a well-developed cleavage of the Tili Unit. It also represents an abrupt change in structural style from the Sun-Moon Lake Unit, with fault propagation folding becoming dominant and a well-developed axial planar cleavaged being developed.

We confirm, for the first time, the presence of a clearly defined zone of intense ductile strain that coincides with the location of the Lishan fault. This high strain zone, together with the recent finding of large foraminifera that are assigned to the NP14 biozone in rocks along the western side of the Lishan fault confirm that it juxtaposes Early to Middle Eocene higher metamorphic grade rocks of the Tili Unit against Middle Miocene lower metamorphic grade rocks of the Lushan Unit.

To the east of the Lishan fault, the Lushan Unit displays highly nonclyndrical folding. In general, the structure displays an overall northwest vergence, which we can determine from the well developed, moderately southeast-dipping cleavage. Nevertheless, it is not possible to determine the deep subsurface structure in this part of the Central Range because of the lack of seismicity. There is only a minor increase in both the horizontal and vertical components of GPS velocity vector from the Tili Unit to the Lushan Unit.

We have very little geological data from the Tananao Unit, which is being thrust westward over the Lushan Unit along the Chinma fault. This fault outcrops very well along the Central Cross Island Highway, where it clearly dips ca. 60o to the southeast.

RELATIVE DEFORMATION SEQUENCE

We interpret the earliest deformation associated with the Taiwan orogeny in our map area to be the development and emplacement of the Tili and Lushan units. It is not possible to accurately constrain the age and timing of emplacement of these units, but the first appearance of lithic clasts containing a cleavage in the forearc region of the Coastal Range and in the Western Foothills foreland basin sediments occurred during the Early Pliocene, or some 3.5 to 4 My ago. This indicates that these rocks were above sea level and being eroded by this time. Further indications that this is one of the earliest events recorded in the map area is given by the geometric relationships between faults. For example, the Tili Unit is cut by the Shuilikeng fault system in the southwest and appears to be cut by the Lishan fault in the northeast (out of the current map area). Similarly, along its western flank the Lushan Unit is cut by the Lishan fault and, in the east, by the Chinma fault. These geometric relationships indicate that activity along the Shuilikeng, Lishan, and Chinma faults must post-date the emplacement of the Tili and Lushan units. We therefore suggest that, despite the different metamorphic conditions undergone by the Tili and Lushan units, that there is a close enough similarity in the structural style and in the orientations of bedding and cleavage between the two to interpret that they developed at the same time, early on in the history of the Taiwan orogeny, and that they were both being emplaced by at least the Early Pliocene. These units were subsequently juxtaposed along the Lishan fault at some unknown time.

The second phase of deformation related to the Taiwan orogeny that we see in the current study area is the in-sequence development of the Shuangtung, Chelungpu, and Changhua units, respectively. On the basis of foreland basin sedimentation, geomorphic structures, and magnetostratigraphy, it has been estimated that the Shuangtung thrust became active at ca. 1.1 Ma, the Chelungpu thrust at 0.7 to 0.9 Ma., and the Changhua at 0.62 to 0.65 Ma.

The last fault activity to start in the study area is related to the Shuilikeng fault system, and possibly the Lishan fault. The Shuilikeng fault system is active and has been so throughout the Holocene. Our mapping clearly shows that it affects the eastern margin of the Shuangtung Unit and therefore post-dates its emplacement. At the moment, it is not possible to place any constraints on the age of activity along the Lishan fault. Although, within our map area, seismic activity along its southern part indicates that it is active.

ACKNOWLEDGEMENTS

This research was carried out with the aid of grants by CSIC –Proyectos Intramurales 2006 3 01 010, and MICINN: CGL2009-11843-BTE.

REFERENCES

Suppe, J. (1980): A retrodeformable cross section of northern Taiwan, Proc. Geol. Soc. China, 23, 46- 55.

Suppe, J. (1981): Mechanics of mountain building and metamorphism in Taiwan, Geol. Soc. China Mem. 4: 67-89

Wu, F., R.-J. Rau, and D. Salzberg (1997): Taiwan Orogeny; thin-skinned or lithospheric collision? An introduction to active tectonics in Taiwan. Tectonophysics, 274: 191-220.

Wu, F., C-S. Chang, and Y.M. Wu (2004): Precisely relocated hypocentres, focal mechamisms and active orogeny in Central Taiwan, In Aspects of the Tectonic Evolution of China, (J. Malpas, C.J.N. Fletcher, J.R. Ali, and J.C. Aitchison, eds.), Geol. Soc. of London, Spec. Pub. 226, pp. 333-354, London, UK.

Abstract 7 - Is there a detachment beneath the Taiwan thrust belt? A view from seismic energy release

Dennis Brown[1], Martin Schimmel[1], Joaquina Alvarez-Marron[1], Giovanni Camanni[1], and Yih-Min Wu[2]

[1]Institute of Earth Sciences Jaume Almera, ICTJA-CSIC, Lluis Sole i Sabaris s/n, 08028 Barcelona, Spain
[2]Department of Geosciences, National Taiwan University, Taipei, 106, Taiwan

Presented at: 2012, 8th Geological Congress of Spain. Oviedo (Spain)

Type of presentation: poster

Abstract (extended):

INTRODUCTION

One of the basic tenets in the geometric, mechanical, numerical, and analog modeling of mountain belts is that there is a through-going, gently dipping basal detachment at shallow depths beneath their flanks, above which a foreland thrust and fold belt develops. The Taiwan mountain belt is often cited as an example par excellence of this sort of thrust and fold belt (Suppe, 1980, 1981; Carena et al., 2002), and it has consequently served as an important example for the development of the critical wedge model (Davis et al., 1983; Dahlen et al., 1984). But, does this through- going detachment model indeed apply to the Taiwan thrust belt?

The Taiwan thrust belt has been forming since the Late Miocene as the result of the collision of the Luzon arc with the southeast Eurasian margin. In the surface geology, the Taiwan orogen can be divided into four N-S oriented tectonostratigraphic zones that are separated by major faults. From west to east these zones are; the Western Foothills, the Hsuehshan Range, the Central Range, and the Coastal Range. The Western Foothills, Hsuehshan Range, and the Central Range are comprised of the rocks from the imbricated continental margin of Eurasia and the foreland basin. It is these three zones, and the structures that mark the boundaries between them, in particular the Shuili-Keng and Lishan faults, that are of interest to this paper. The Coastal Range is comprised of volcanic rocks and sediments of the Luzon arc, which is being thrust over the Eurasian margin along the Longitudinal Valley Fault.

By far, the bulk of the data for constructing the structural architecture of the Taiwan thrust belt, including its basal detachment, has come from surface geological observations and shallow reflection seismic data along the western flank of the thrust belt. On a geometric basis for geological cross-section construction, the shallow basal detachment determined from there was then extrapolated eastward beneath the whole thrust belt. Recently, selective picking of relocated earthquake hypocenter data has been presented as a validation of the shallow detachment model (Carena et al., 2002). Nevertheless, with a growing amount of seismicity data indicating widespread activity in the middle and lower crust, particularly beneath the central part of the thrust belt, researchers have begun to challenge the shallow detachment model (Wu et al., 1997, 2004). These authors suggest that any model for the structural architecture of the Taiwan thrust belt needs to incorporate nearly the entire crust and include a number of steeply dipping faults that penetrate to the lower crust, where they possibly link with a deep detachment. This interpretation has significant implications for the geometrical, mechanical and kinematic evolution of the thrust belt that is different from what has so far been predicted by the wedge- shaped shallow detachment model.

Here we present an imaging approach that uses cumulative seismic energy release data to resolve the crustal-scale structure in central Taiwan. By using this approach we are able to determine the locations of the major structures at depth beneath much of the Taiwan thrust belt. We show that a model in which the deep crust of Taiwan is being deformed may be more appropriate than the shallow detachment model.

SEISMIC ENERGY RELEASE APPROACH

Earthquake hypocenter maps and sections with a large number of seismic events can provide important information about the geometry of fault systems. There are, however, several disadvantages. For example, clustering of events may be misleading in the visual inspection of these maps and sections, since small magnitude events cannot be distinguished from large ones. With an energy increase of about a factor of 30 for each unit increase in magnitude, the cumulative energy released by many small events may not reach the energy of a single large event, and this can mask the important structures along which major earthquakes occur. Also, in hypocenter

cross-sections events are generally projected over distances of 10's of km's onto the plane of section. Many of these events may be related to structures that are not present in the plane of the section, or which intersect it in a completely different place from where the events are projected. The advantages of using the cumulative energy release method are that zones of high magnitude earthquakes are readily distinguished and imaged in-situ. Following this, we assume that the highs in cumulative energy release are related to earthquakes taking place along the major structures. A limitation of the cumulative energy release modelling is the recurrence time of earthquakes, which can significantly bias the results locally and may account for areas of low energy release such as in the western part of the Central Range. Nevertheless, the large number of events recorded in the study area over the 15 year period used here provides an important new view of the crustal structure.

For our modelling in central Taiwan, we extracted 34,818 events (>ML = 2) from the 1991 to 2008 database of relocated earthquakes. In accordance with the Taiwan Central Weather Bureau Seismic Network Earthquake Catalogue, the local magnitude ML is used to compute the seismic energy release (E, units are in ergs) for each event using the empirical relation

logE=9.4+2.14ML -0.054ML**2

In this study, cumulative seismic energy release was determined in a 3D volume using a discretized 100m grid in which the energy is summed for all events that are located within a sphere of 2 km diameter centred at each grid point. Horizontal and vertical slices were then cut through the volume.

SEISMIC ENERGY RELEASE IN CENTRAL TAIWAN

The seismic energy being released by earthquakes in the Western Foothills of central Taiwan is largely scattered throughout the upper 30 km of crust, with minor amounts being released to a depth of at least 40 km. There is a relatively higher amount of energy being released along its eastern flank, and a marked high occurs in the central and southern part of the map area that is centred at about 10 km depth. The subhorizontal cumulative energy release high located at ca. 10 km depth beneath the Western Foothills can be interpreted to image a basal detachment. This detachment coincides with the one that has been inferred from earthquake hypocenter locations, but is several kilometres deeper than that determined from geological cross-section balancing techniques. The relative increase in cumulative energy release in the upper 10 km of crust along the eastern flank of the Western Foothills seems to be related to earthquakes occuring along faults within the zone.

There is an abrupt deepening in the zone of cumulative energry release beneath the Hsuehshan Range that reaches a depth of ca. 30 km. Along its western flank, there is a steeply eastward dipping zone of high energy release that projects to the surface at the location of the Shuilikeng fault. Along its eastern flank, a steeply westward dipping to vertical truncation of energy release projects to the surface at the location of the Lishan fault. This zone coincides very well with the area of high conductivity imaged by Bertrand et al. (2009). In the southeastern part of the map area, from ca. 20 to 35 km depth, there is a near vertical high in the cumulative energy release that projects to the Lishan fault at the surface. The high energy release in the central part of the Hsuehshan Range is likely due to faults that have been mapped within it.

In the western part of the Central Range, the seismic energy release is relatively low and is scattered throughout the crust to a depth of at least 40 km. With the present dataset we are unable to determine any relationship between cumulative seismic energy release and geological structures in the western part of the Central Range. Eastward, there is an abrupt increase in the amount of energy being released in the upper 20 to 30 km of crust. At the surface, however, the western margin of this high coincides with the location of the Chinma Tunnel fault, a moderately east-dipping thrust that is uplifting Mesozoic and older crystalline basement rocks and placing them on top of Paleogene and younger rocks to the west.

The cumulative seismic energy release data corroborates the previous interpretations of a detachment at about 10 km depth beneath the Western Foothills, but it also suggests that this detachment does not continue eastward at this shallow level beneath the Hsuehshan and Central ranges. Instead, the Western Foothills detachment appears to ramp steeply down into the lower crust beneath the Hsuehshan Range where it either continues eastward at this deep level, or is truncated by the Lishan fault. Recently, modeling approaches have suggested that the basal detachment beneath the Hsuehshan and Central ranges is steeply dipping and located somewhere in the middle to lower crust. It is not possible to resolve this with the data set presented here, however, since the cumulative seismic energy release beneath the western part of the Central Range is too low to allow faults to be illuminated and a structural linkage to be established between it and the structure of the Hsuehshan Range.

We suggest that a model in which the Western Foothills and Hsuehshan Range is a zone of transpression with a structural architecture similar to that of a crustal-scale positive flower structure better fits the available data than the shallow through-going detachment model. In this transpression model, there is a suite of linked, active faults whose kinematics range from oblique thrusting through to strike-slip and extensional faulting, all of which respond to the same regional geodynamic stress field. The Western Foothills detachment ramps down into the lower crust along the western flank of the Hsuehshan Range and is truncated by the Lishan fault. This implies that there is no,

or very limited material transfer across the Lishan fault and therefore no structural linkage in the form of a fault between the Hsuehshan and Central ranges. The western part of the Central Range is, therefore, acting as a steeply west-dipping backstop to the transpressional thrust belt that is developing in the Hsuehshan Range and Western Foothills. With the current available data sets it is not possible to resolve what is happening at depth in the Central Range, although the east-dipping Chinma Tunnel fault is clearly active and important.

ACKNOWLEDGEMENTS

This research was carried out with the aid of grants by CSIC –Proyectos Intramurales 2006 3 01 010, and MICINN: CGL2009-11843-BTE.

REFERENCES

Bertrand, E., M. Unsworth, C.-W. Chiang, C.-S. Chen, C.-C. Chen, F. Wu, E. Türkoglu, H.-L Hsu, G. Hill (2009), Magnetotelluric evidence for thick-skinned tectonics in central Taiwan, Geology, 37: 711-714.

Carena, S., J. Suppe, H. Kao, (2002), Active detachment of Taiwan illuminated by small earthquakes and its control of first-order topography, Geology, 30: 935-938.

Dahlen, F.A, Suppe, J., Davis, D., (1984): Mechanics of fold- and-thrust belts and accrectionary wedges: Cohesive Coulomb Theory, Journal of Geophysical Research, 89: 10,087-10,101.

Davis, D., Suppe, J., Dahlen, F.A, (1983): Mechanics of fold- and-thrust belts and accretionary wedges, Journal of Geophysical Research, 88: 1153-1172.

Suppe, J. (1980): A retrodeformable cross section of northern Taiwan, Proc. Geol. Soc. China, 23, 46-55.

Suppe, J. (1981): Mechanics of mountain building and metamorphism in Taiwan, Geol. Soc. China Mem. 4: 67- 89.

Wu, F., R.-J. Rau, and D. Salzberg (1997): Taiwan Orogeny; thin-skinned or lithospheric collision? An introduction to active tectonics in Taiwan. Tectonophysics, 274: 191- 220.

Wu, F., C-S. Chang, and Y.M. Wu (2004): Precisely relocated hypocentres, focal mechamisms and active orogeny in Central Taiwan, In Aspects of the Tectonic Evolution of China, (J. Malpas, C.J.N. Fletcher, J.R. Ali, and J.C. Aitchison, eds.), Geol. Soc. of London, Spec. Pub. 226, pp. 333-354, London, UK.

Abstract 8 - Basement-involved shortening in the Central Part of the Taiwan Mountain Belt

Giovanni Camanni[1], Dennis Brown[1], Joaquina Alvarez-Marron[1], Martin Schimmel[1], Yih-Min Wu[2], and Hsin-Hua Huang[2]

[1]Institute of Earth Sciences Jaume Almera, ICTJA-CSIC, Lluis Sole i Sabaris s/n, 08028 Barcelona, Spain
[2]Department of Geosciences, National Taiwan University, Taipei, 106, Taiwan

Presented at: 2012 AGU Fall Meeting, Abstract T53B-2705. San Francisco (USA)

Type of presentation: poster

Abstract:

New surface geological mapping in the central part of the Taiwan mountain belt indicates that the structure of the Western Foothills is that of an imbricate thrust system developed above a shallowly dipping basal detachment. On the contrary, the Hsuehshan Range appears to form a zone of transpression, deeply rooted into the crust, bounded by the Shuilikeng fault to the west and by the Lishan fault to the east. Seismicity data help to place constraints on this composite scenario. In a W-E section, the Hsuehshan Range is juxtaposed against the Western Foothills across a zone of intense seismic activity that penetrates into the middle crust and projects to the Shuilikeng fault at the surface. Tomography data suggest that high Vp material, that is thought to represent the Mesozoic crystalline basement, is progressively uplifted eastward to form a basement culmination beneath the Hsuehshan Range and the western portion of the Central Range. Basement involvement in the deformation reaches its peak in the Tananao Complex of the eastern Central Range where it is thrust over the Miocene slope sediments along the Chinma fault.

Abstract 9 - The Shuilikeng fault in central Taiwan: the transpressional reactivation of a basement fault

Giovanni Camanni[1], Dennis Brown[1], Joaquina Alvarez-Marron[1], Yih-Min Wu[2], and Hsi-An Chen[2]

[1]Institute of Earth Sciences Jaume Almera, ICTJA-CSIC, Lluis Sole i Sabaris s/n, 08028 Barcelona, Spain
[2]Department of Geosciences, National Taiwan University, Taipei, 106, Taiwan

Presented at: 2013 Taiwan Geosciences Assembly (TGA) - Tectonics of Taiwan: an International Conference. Taoyuan (Taiwan)

Type of presentation: oral

Abstract:

The Taiwan orogen is forming as the result of oblique convergence between the Eurasian and Philippine Sea plates. Part of the oblique component of the convergence is taken up along the suture zone between the two, but stress is translated westward into the mountain belt in a very complex way. How these stresses are resolved at the frontal part of the orogen to form individual faults is, in many cases, conditioned by pre-collisional structures in the Eurasian margin basement. In central Taiwan, the Shuilikeng fault system bounds the eastern flank of the Western Foothills imbricate thrust system, marking the eastward transition from a thin-skinned to a thick-skinned deformational style. At the surface, it comprises a brittle, steeply dipping fault system with a series of splays and bifurcations and variable kinematics. Seismicity data suggest that it dips moderately to steeply eastward and can be traced to greater than 20 km depth. Individual earthquake focal mechanisms, together with mean principal stress axes and fault plane solutions, indicate predominately strike-slip fault mechanisms. The Shuilikeng fault appears to be reactivating a pre-existing, basin-bounding fault to the east of which a basement-cored culmination is developing in the Hsuehshan Range.

Abstract 10 - Imaging basement involvement in the Hsuehshan Range of central Taiwan

Giovanni Camanni[1], Dennis Brown[1], Martin Schimmel[1], Joaquina Alvarez-Marron[1], Yih-Min Wu[2], Hsin-Hua Huang[2], and Hsi-An Chen[2]

[1]Institute of Earth Sciences Jaume Almera, ICTJA-CSIC, Lluis Sole i Sabaris s/n, 08028 Barcelona, Spain
[2]Department of Geosciences, National Taiwan University, Taipei, 106, Taiwan

Presented at: 2013 Taiwan Geosciences Assembly (TGA) - Tectonics of Taiwan: an International Conference. Taoyuan (Taiwan)

Type of presentation: oral

Abstract:

New geological mapping in the central Taiwan mountain belt, together with a new collapsed data set of relocated seismicity, indicate that the basal detachment beneath the thin-skinned Western Foothills possibly ramps down in the crystalline basement along their eastern flank. Consequently, the basement appears to be involved in the deformation in the more internal Hsuehshan Range. Furthermore, seismic tomography data indicate a shallowing of high Vp velocity material beneath the Hsuehshan Range. Therefore, we propose that the crystalline basement is possibly being uplifted along the eastern flank of the Western Foothills to form a basement-cored culmination beneath the Hsuehshan Range in which basement rocks appear to be located at shallower structural level than the basement rocks beneath the Western Foothills. This structural architecture is similar to that in other orogens worldwide, where the thin-skinned foreland fold-and-thrust belt ends hinterlandward with a ramp down into the middle to lower crust and, subsequently, the involvement of basement rocks in the deformation. However, we are uncertain if this basement culmination is somehow linked to the outcropping basement rocks of the Tananao Complex in the Central Range or if two different types of basement rocks are juxtaposed across the Lishan fault.

Abstract 11 - Structure of central Taiwan: integrating geological and geophysical data

Dennis Brown[1], Joaquina Alvarez-Marron[1], Giovanni Camanni[1], Martin Schimmel[1], and Yih-Min Wu[2]

[1]Institute of Earth Sciences Jaume Almera, ICTJA-CSIC, Lluis Sole i Sabaris s/n, 08028 Barcelona, Spain
[2]Department of Geosciences, National Taiwan University, Taipei, 106, Taiwan

Presented at: 2013 Taiwan Geosciences Assembly (TGA) - Tectonics of Taiwan: an International Conference. Taoyuan (Taiwan)

Type of presentation: oral

Abstract:

The structure of the Taiwan mountain belt is thought to be that of an imbricate thrust and fold belt developed in a forward-breaking sequence above a shallowly dipping basal detachment. In recent years, however, a growing amount of seismicity data from the internal part of the mountain belt indicates the existence of widespread fault activity in the middle and lower crust, suggesting that deeper levels of the crust must be involved in the deformation than is predicted by the shallow detachment, imbricate thrust belt model. To address this issue, we present new geological mapping, together seismicity and local tomography data from the central part of Taiwan. We concur with the interpretation that the foreland basin part of the Western Foothills comprises an imbricate thrust system that is developing as a forward breaking sequence that is structurally and kinematically linked to a basal detachment at between 7 and 10 km depth. To the east of the foreland basin, however, in the Hsuehshan and Central ranges, our data show the presence of two fault systems; an earlier, inactive thrust system with a well-developed cleavage that is cut by a system of steeply dipping active faults that penetrate to a depth of 25 to 30 km or more. In the Hsuehshan Range, the second fault system is best represented by a structural and kinematic model in which this part of the mountain belt forms a zone of transpression with a structural architecture similar to that of a crustal-scale positive flower structure. The shallowing of higher velocities beneath the Hsuehshan Range suggests that basement rocks are closer to the surface than beneath the Western Foothills. Eastward, in the Central Range, Mesozoic basement rocks are over thrusting strongly folded and cleaved deep water sediments of the first, now inactive, thrust system. The involvement of deep crustal levels and Mesozoic basement in the second fault system is suggestive of the reactivation of pre-existing basin-bounding faults that where located on the Eurasian continental margin.

Abstract 12 - Geological interpretation of the Bouguer anomaly data in Central Taiwan

Conxi Ayala[1], Giovanni Camanni[2], Dennis Brown[2], Joaquina Alvarez-Marron[2], and Hsien-Hsiang Hsieh[3]

[1]Instituto Geológico y Minero de España - IGME (Spanish Geological Survey), La Calera n. 1, 28760 Tres Cantos, Madrid, Spain. Currently visiting at ICTJA-CSIC
[2]Institute of Earth Sciences Jaume Almera, ICTJA-CSIC, Lluis Sole i Sabaris s/n, 08028 Barcelona, Spain
[3]Lamont-Doherty Earth Observatory, Earth Institute at Columbia University, Palisades, New York, USA.

Presented at: 2013 Taiwan Geosciences Assembly (TGA) - Tectonics of Taiwan: an International Conference. Taoyuan (Taiwan)

Type of presentation: poster

Abstract:

Gravity data from the central part of the Taiwan mountain belt define an approximately 60 km E-W by 100 km N-S area of negative Bouguer anomaly (from -25 to -60 mGal) roughly coinciding with an expanse of low relief in the central part of the study area. This minimum appears to be divided into two well-defined lows, separated by the Shuilikeng fault. The western low correlates with the location of the Pliocene-Pleistocene, synorogenic sediments of the Western Foothills, whereas the eastern one appears at the location of the Puli Basin in the Hsuehshan Range. The boundaries of this low in the gravity anomaly are well-defined in the vertical derivative of the Bouguer anomaly. In this region, the contours have an approximately N-S trend. To the north, there is a slight increase in the Bouguer anomaly and also a change in its strike as it becomes NE-SW. This is consistent with the structure fabrics in the mountain belt, which also shows a change from a north-south strike towards a northeast-southeast strike. To the east, the zone of negative Bouguer anomaly shows a steep gradient across the Lishan fault, which separates the Hsuehshan Range from the Central Range. There is also a notable change in the vertical derivative of the Bouguer anomaly across this fault. The gradient in the Bouguer anomaly becomes steeper in the eastern flank of the mountain belt.

Preliminary results of the 2D gravity models across selected transects in Central Taiwan are; 1) the depth change of the top of the basement from deeper in the Western Foothills to shallower in the Hsuehshan and Central ranges that appears in the seismic velocity models can be modeled and, 2) there is a change in the density of the basement across the Lishan fault. The modeling is compatible with a higher density Mesozoic basement on the eastern side of the fault. We stress, however, that modeling of these data need to be further constrained by analyses and comparison with seismic velocity models and surface geology data.

Abstract 13 - How the structure of the Eurasian continental margin predetermines the development of the Taiwan orogen: a view from surface geology, seismic tomography, earthquake hypocenter, and gravity data

Dennis Brown[1], Giovanni Camanni[1], Joaquina Alvarez-Marron[1], Conxi Ayala[2], Yih-Min Wu[3], Hao Kuo-Chen[4], and Hsien-Hsiang Hsieh[5]

[1]Institute of Earth Sciences Jaume Almera, ICTJA-CSIC, Lluis Sole i Sabaris s/n, 08028 Barcelona, Spain
[2]Instituto Geológico y Minero de España - IGME (Spanish Geological Survey), La Calera n. 1, 28760 Tres Cantos, Madrid, Spain. Currently visiting at ICTJA-CSIC
[3]Department of Geosciences, National Taiwan University, Taipei, 106, Taiwan
[4]Institute of Geophysics, National Central University, Jhongli, Taiwan
[5]Lamont-Doherty Earth Observatory, Earth Institute at Columbia University, Palisades, New York, USA

To be presented at: 2014 16th Edition of the Deep SEISMIX International Symposium. Barcelona (Spain)

Abstract:

Because of the oblique nature of the collision that is taking place between the southeastern margin of Eurasia and the western limit of the Philippine Sea Plate (the Luzon Arc), Taiwan provides and ideal laboratory to study what influence the differing morphological parts of the margin (platform and slope) have on the structural development of a thrust belt. The Taiwan mountain belt is generally thought to develop above a shallow, through-going basal detachment confined to within the sedimentary cover of the Eurasian continental margin. A number of datasets, such as surface geology, earthquake hypocenter, and seismic tomography data suggest, however, that crustal levels below the interpreted location of the detachment are also involved in the deformation. Here, we combine these data sets with gravity data to investigate the deformation that is taking place at depth beneath south-central Taiwan. We find that beneath the Coastal Plain and the Western Foothills most of the deformation is taking place near the basement-cover interface that is acting as an extensive level of detachment. This level of detachment is located at ≥10 km depth, below the basal detachment proposed from surface geology for this part of the mountain belt, and extends westward of the deformation front of the mountain belt as defined by geological structures at the surface. Beneath this level of detachment, inherited extensional faults appear, locally, to maintain the bulk of their extensional displacement. However, across the Shuilikeng and the Chaochou faults, earthquake hypocenters define steeply dipping clusters that extend to greater than 20 km depth. We interpret these clusters to be related to deformation that is taking place along a deep-penetrating, east-dipping ramp that joins westward with the detachment at the basement-cover interface. Basement rocks are uplifted along this ramp to form a basement culmination beneath the Hsuehshan and Central ranges.